IMPROVEMENT OF GENETICALLY DETERMINED CHRONIC KIDNEY DISEASE BY DIETARY FLAX OIL- THE CYCLOOXYGENASE-2 CONNECTION

BY

DEEPA SANKARAN

A Thesis

Submitted to the Faculty of Graduate Studies of

The University of Manitoba

in Partial Fulfillment of the Requirements

for the Degree of

DOCTOR OF PHILOSOPHY

Foods and Nutritional Sciences

University of Manitoba

Winnipeg, Manitoba

© August 2006

THE UNIVERSITY OF MANITOBA

FACULTY OF GRADUATE STUDIES

*****

COPYRIGHT PERMISSION

IMPROVEMENT OF GENETICALLY DETERMINED CHRONIC KIDNEY DISEASE BY DIETARY FLAX OIL- THE CYCLOOXYGENASE-2 CONNECTION

BY

DEEPA SANKARAN

A Thesis/Practicum submitted to the Faculty of Graduate Studies of The University of Manitoba in partial fulfillment of the requirement of the degree

OF

DOCTOR OF PHILOSOPHY

DEEPA SANKARAN © 2006

Permission has been granted to the Library of the University of Manitoba to lend or sell copies of this thesis/practicum, to the National Library of Canada to microfilm this thesis and to lend or sell copies of the film, and to University Microfilms Inc. to publish an abstract of this thesis/practicum.

This reproduction or copy of this thesis has been made available by authority of the copyright owner solely for the purpose of private study and research, and may only be reproduced and copied as permitted by copyright laws or with express written authorization from the copyright owner.

TABLE OF CONTENTS

ACKNOWLEDGEMENTS

I would like to express my sincerest gratitude to all those who have made this six-year-journey a truly unforgettable one and it's only befitting that I begin with the person who started this whole saga.

Dr. Harold Aukema has been a supervisor and mentor par excellence. I cannot overstate my gratitude for his constant encouragement, his infectious enthusiasm, his friendship and support, his good teaching, his constructive criticism, his gargantuan pool of patience and for his steadfast belief in me.

I would also like to express my heartfelt thanks to my co-supervisor, Dr. Malcolm Ogborn for his expert scientific guidance and for giving me the opportunity to get acquainted with the colorful world of renal histology.

Many thanks also are due to the other members of my graduate committee, Dr. Ranjana Bird and Dr. Grant Hatch, for their sound advice and constant support through the years. In addition to serving on my graduate committee, Dr. Ranjana Bird has been a wonderful mentor and a good friend and I owe her my sincerest gratitude.

I would like to thank Dr. Neda Bankovic-Calic and John Tutt for their assistance with all the histology and immunohistochemistry and for helping me learn to love the microscope.

I wish to recognize the support of the Kidney Foundation of Canada, the University of Manitoba, the Manitoba Institute of Child Health and the Manitoba Health Research Council for their generous graduate fellowships.

Marilyn Latta and Dennis Laboissiere deserve a special mention for always being around to handle equipment and other technical malfunctions and for trying to make lab

work less frustrating. I'd like to thank Pat Parish, the staff of the Human Ecology General Office and Vernelle Mirosh and Shannon McAteer for helping me with all the administrative kinks that came my way.

I would not have been able to conduct my experiments without the assistance of the staff at the Animal Holding Facility of the University of Manitoba.

The assistance of all the summer students and undergraduate students that have worked in the Aukema lab has been monumental in the completion of this thesis and a simple thank-you definitely does not suffice.

I certainly would not have made it through grad school without (Tim Hortons' coffee and) the friendship and support of all my lab mates and my fellow grad students in the Department of Human Nutritional Sciences. Thank you for sharing the frustrations of being a graduate student and ensuring that I had fun anyway!

To my friends outside of the department (and University) who have made this journey more enjoyable, thank you for always being there for me and for the cherished memories of social craziness!

To my parents, S. V. Sankaran and Lalitha Sankaran, your unwavering and unconditional support has brought me this far. My educational goals have had no boundaries, geographical or otherwise, solely because of your support and encouragement.

Finally, to the person that held it all together and helped me make it through this journey without losing my sanity, my husband, Suresh Jayaraman ; you made the failures less painful and the successes more rewarding.

ABSTRACT

Polycystic kidney disease (PKD) is the most commonly inherited chronic kidney disease (CKD) affecting 1 in 1000 individuals worldwide. Despite a paucity of treatment options to combat disease progression, dietary intervention studies in animal models of PKD have obtained promising results. Of note, dietary flaxseed and flax oil (rich in 18:3n-3) ameliorate early renal injury in the Han:SPRD-*cy* rat model of PKD as well as other models of CKD. The present research sought to further characterize this reno-protective effect of dietary flax oil by investigating 1) the effect of a flax oil diet on disease progression in another model of PKD, the *pcy* mouse model, 2) the effects of such an intervention when given during pregnancy and lactation, as well as 3) in advanced stages of renal injury. Cyclooxygenase-2 (COX-2) is a key enzyme involved in 20C fatty acid metabolism and previous studies have demonstrated altered renal COX-2 expression and activity in animal models of PKD. Thus, this research also investigated 4) *in vivo* regulation of COX-2 expression by dietary oils containing n-3 fatty acids, and 5) selective COX-2 inhibition in cystic rat kidneys. The main findings of this research were that 1) dietary flax oil slows early renal disease progression in weanling *pcy* mice with PKD, consistent with previous studies using the Han:SPRD-*cy* rat model, 2) prenatal exposure to flax-oil based diets attenuates renal histologic injury in Han:SPRD-*cy* rat offspring, 3) flax oil diets retard further pathologies associated with renal injury when introduced in adult Han:SPRD-*cy* rats with advanced kidney disease, 4) dietary oils rich in 20:5n-3 and 22:6n-3, specifically up-regulate COX-2 mRNA and protein levels in diseased rodent kidneys with PKD, while flax oil diets rich in 18:3n-3 do not exert this effect and 5) selective COX-2 inhibition by NS398 significantly ameliorates renal injury

and disease-associated elevations in prostanoid production in Han:SPRD-*cy* rats. The findings of this research may impact treatment options, both dietary and pharmaceutical, in those afflicted with PKD as well as other chronic renal diseases and contribute to the current knowledge of pathogenesis of this inherited cystic disease.

LIST OF TABLES

LIST OF FIGURES

LIST OF ABBREVIATIONS

6-ketoPGF$_{1\alpha}$	6-keto prostaglandin F$_{1\alpha}$
AA	Arachidonic Acid
ALA	Alpha-linolenic acid
cAMP	Adenosine 3',5'-cyclic phosphate
CKD	Chronic kidney disease
CO	Corn oil diet
COX	Cyclooxygenase
cPLA$_2$	cytosolic phospholipase A$_2$
CSO	Cottonseed oil diet
DHA	Docosahexaenoic acid
DO	DHASCO diet
EET	Epoxyeicosatrienoic acid
EPA	Eicosapentaenoic acid
ESRD	End stage renal disease
FO	Flax oil diet
GFR	Glomerular Filtration Rate
HETE	Hydroxy eicosatetraenoic acid
LA	Linoleic Acid
LOX	Lipoxygenase
LT	Leukotriene
LX	Lipoxin
MGV	Mean Glomerular Volume

MO	Menhaden oil diet
NFκB	Nuclear Factor kappa B
OxLDL	Oxidized Low Density Lipoprotein
PCNA	Proliferating cell nuclear antigen
PGE_2	Prostaglandin E_2
PGEM	Prostaglandin E Metabolite
PGI_2	Prostaglandin I_2
PKD	Polycystic Kidney Disease
PPAR	Peroxisome Proliferator-Activated Receptor
PUFA	Polyunsaturated fatty acid
SUN	Serum Urea Nitrogen
TXA_2	Thromboxane A_2

1. INTRODUCTION

Chronic kidney disease (CKD) is a gradual irreversible loss of kidney function that eventually leads to end-stage renal disease and the need for expensive renal replacement therapies. It is now recognized as a worldwide pandemic, with over 1.9 million Canadians (1) and 19 million Americans (2) suffering from CKD. Despite considerable gains that have been made in retarding CKD progression, the increasing prevalence (>50% rise in 10 years in the U.S and about 19% rise in 5 years in Canada) and associated healthcare costs of end-stage renal disease warrant further inquiry into treatment options that slow or prevent the progression of CKD. It is widely acknowledged that irrespective of the initiating cause of renal injury, substantial loss of functioning nephrons results in a common progressive pathway of decline characterized by structural damage to the kidney, proteinuria, a decrease in glomerular filtration rate (GFR) as well as systemic hypertension (3). One such leading cause of chronic renal injury is polycystic kidney disease (PKD).

1.1 Polycystic Kidney Disease

PKD is the most common inherited nephropathy affecting 1 in 1000 individuals and comprises of a number of cystic diseases that share the characteristic presence of renal cysts. Autosomal dominant PKD is more prevalent than Huntington disease, sickle cell disease, hemophilia, cystic fibrosis, myotonic dystrophy and Down syndrome combined and is the fourth most common cause of end stage renal disease worldwide (4). Autosomal dominant PKD is genetically heterogenous with 2 common disease loci on chromosome 16 (*PKD1*) and chromosome 4 (*PKD2*). Mutations in *PKD1* account for a majority of PKD cases (85-90%), while mutations in *PKD2* account for about 10-15% of

all cases (4). Polycystin 1, the gene product of *PKD1*, is a large (>460kD) membrane protein involved in multi-protein complexes at the cell membrane and is thought to function in cell-cell and cell-matrix interactions, signal transduction, and in mechanosensation (5). The C-terminal region of polycystin 1 interacts and regulates the function of polycystin 2, the gene product of *PKD2*. Polycystin 2 is also a membrane protein and functions primarily as a divalent cation (such as calcium) channel (6). Although the physiologic location of polycystin 2 is still controversial, having been identified both in the plasma membrane and the endoplasmic reticulum, either location is consistent with its regulation of intracellular calcium. Polycystins and other proteins involved in renal cystic disorders have recently been identified in primary cilia of renal epithelial cells (7) suggesting that abnormalities in ciliary formation and function likely play a role in pathogenesis of PKD.

Currently there are no known specific therapeutic interventions for this disease with treatment of PKD patients being confined to alleviation of secondary disorders. Despite a paucity of comprehensive strategies to combat the disease progression a number of studies involving dietary interventions have been conducted on animal models of PKD and have obtained promising results. Reduction of dietary protein to a low yet growth-maintaining level, substitution of soy protein for casein, supplementation with soyasaponins, adding flaxseed, flax oil and conjugated linoleic acid to the diet (8-16) are some of the dietary alterations that were found to have beneficial effects on the disease progression in animal models of PKD.

1.2 Dietary fat modulation of progressive renal disease

Dietary fat manipulation, in general, has been shown to influence the progression of chronic renal disease due to a variety of etiologies. The effects of polyunsaturated fatty acids (PUFA) on progressive renal disease have been explored in both humans as well as animal models.

1.2.1 Dietary fish oil

The n-3 fatty acids, eicosapentaenoic acid (EPA, 20:5n-3) and docosahexaenoic acid (DHA, 22:6n-3), have long been identified as essential elements of human nutrition. The primary dietary sources of these fatty acids are aquatic in nature, with fish, fish oils and certain algae being the major sources. The immunomodulating and anti-inflammatory properties of fish oil have resulted in a plethora of fish-oil supplementation studies, the ones of interest being those that examine its effects on various renal pathologies.

Animal models of inflammatory renal diseases (17-20), reduced renal mass (21-25), immune-related nephropathy (26,27) and hypertension (28) revealed that dietary n-3 PUFA alleviated renal disease and improved kidney function. Several human studies also demonstrate a potential therapeutic benefit of dietary n-3 PUFA supplementation in patients with renal disease (26).

Although a majority of the reports indicate an improvement in kidney function with dietary fish oil, a few studies suggest otherwise. Eberhard and co-workers (29) demonstrated that in Milan normotensive rats that spontaneously developed progressive glomerulosclerosis, short term fish oil supplementation resulted in elevated renal blood flow with a concomitant increase in prostaglandin E_2 (PGE_2). However, in the long term there was a faster progression of proteinuria and a reduction in renal blood flow after 32 weeks, in rats given fish oil concentrate. Also, accelerated development of

nephrosclerosis with sclerotic lesions in about 60% of the glomeruli was observed with chronic dietary fish oil supplementation (29). Similar deleterious effects of chronic fish oil feeding on renal structure and function were observed in normal rats (30) and in mice with immune complex nephritis (31).

Studies on n-3 PUFA supplementation in animal models of PKD have resulted in conflicting observations. No protective effect of dietary fish oil on early progression of PKD was noted when weanling DBA/2FG-*pcy* mice were fed either a normal or a low protein diet, with 10% of either sunflower seed oil or fish oil (32). In fact, replacing sunflower oil with fish oil reduced survival time in male, but not female *pcy* mice. Fish oil supplementation resulted in significantly lower levels of n-6 fatty acids and higher amounts of n-3 fatty acids in renal phospholipids.

On the contrary, an earlier study (33) showed that in adult male (but not female) *pcy* mice, fish oil concentrate (MaxEPA) had beneficial effects on renal morphology compared to sunflower oil. Male *pcy* mice given fish oil diets had less severe tubular dilatation and lower cyst areas compared to their counterparts given n-6 enriched sunflower oil diets. Also, renal enrichment of n-3 fatty acids (in phospholipid and triglyceride fractions) was observed in mice given MaxEPA.

Recent studies observing the effects of dietary fat supplementation in weaning Han-SPRD-*cy* rats demonstrated that a high fat diet accelerates progression of renal disease compared to a low fat diet (34,35). Han-SPRD-*cy* rats fed high fat (20g fat/100g diet) diets had larger kidneys, greater cystic expansion and worsened renal function as reflected in higher serum creatinine levels and lower creatinine clearances, than rats fed low fat diets. Interestingly, fish oil supplementation mitigated the detrimental renal

effects of the high fat diet (35) when given to weanling Han:SPRD-*cy* rats with renal cystic disease.

1.2.2 Dietary flaxseed and flax oil

Numerous health benefits such as reduction of inflammation in rheumatic disease (36), anti-atherosclerotic effects (37) and modification of hormone-dependent tumor growth (38) have been attributed to the consumption of flaxseed. Components of flaxseed that are likely responsible for these reported health benefits include the high α-linolenic acid (ALA, 18:3n-3) content (39,40) and the mammalian lignan, secoisolariciresinol diglycoside (41). Both these components also are potentially reno-protective as indicated in a number of reports. Earlier studies in mice (42) and humans with lupus nephritis (43) revealed a reduction in proteinuria and increased creatinine clearance in flaxseed supplemented groups. Flaxseed supplementation conferred benefit with regards to renal function as well as inflammatory and atherogenic mechanisms which are important in the pathogenesis of lupus nephritis. Another study conducted by Ingram and coworkers assessed the effects of flaxseed and flax oil in the rat renal ablation model (44). Both flax diets were found to attenuate the nephrectomy-associated increases in blood pressure and proteinuria as well as the decrease in GFR. Also, both diets prevented glomerulosclerosis and mesangial expansion. Renal ALA (18:3n-3) levels were elevated in rats given both diets (with flax oil having a greater effect than flaxseed) while elevated EPA (20:5n-3) levels were observed in the flax oil group only. Elevated urinary prostanoid excretion was attenuated by both flax-containing diets. Thus the study showed that benefits of flax-derived ALA in the rat 5/ 6 renal ablation model can be noted with and without lignans.

Similarly, Ogborn and coworkers reported the effects of flaxseed (13,45) as well as flax oil (15) consumption in Han:SPRD-*cy* rats that manifest PKD. Partial dietary substitution of ground flaxseed (10%) into a standard laboratory rodent diet reduced renal cyst expansion and renal interstitial fibrosis as well renal inflammation in Han:SPRD-*cy* rats (13). A decrease in the n-6:n-3 PUFA ratio in the renal tissue of flaxseed-fed animals was observed, suggesting that there was likely a direct inhibition of n-6 PUFA metabolism by the n-3 fatty acids, thereby promoting the synthesis of the less inflammatory trienoic prostanoids. However, since the study utilized whole flaxseed (ground) containing lignans in addition to the ALA-containing fractions, a clear role for the ALA-containing fraction in ameliorating renal injury could not be ascribed. In a follow-up study where dietary flax oil was substituted at a level of 5% into a standard AIN76 rodent diet (15), Han:SPRD-*cy* rats given flax oil diets had less cyst expansion and renal interstitial fibrosis as well as reduced renal cell proliferation, inflammation and oxidant injury compared to those given control diets (containing 5% corn oil rich in n-6 PUFA).

Thus, studies with various experimental models of renal disease, including PKD, have suggested that diets containing fats with varying fatty acid composition differentially modulate the progression of kidney disease. Dietary flaxseed, flax oil and fish oil ameliorate early renal injury in the Han:SPRD-*cy* rat model of PKD (13,15,35). In the *pcy* mouse model of PKD, diets containing fish oil concentrate (enriched in the long chain n-3 fatty acids-EPA and DHA) worsen disease progression, with the adult male mice showing a marked deterioration of renal architecture and function (32). It is not known, however, if dietary flax oil alters early disease progression in the mouse model of

PKD. The beneficial effects of diets containing fish oil (EPA+DHA) in early renal injury in the Han:SPRD-*cy* rat, but not *pcy* mouse, model of PKD and the reno-protective effects of flaxseed and flax oil (rich in ALA) in weanling Han:SPRD-*cy* rats, compel an investigation into whether diets containing flax oil will attenuate renal disease progression in weanling *pcy* mice. A comparison of the effects produced by dietary flaxseed oil (rich in ALA) and corn oil (rich in n-6 linoleic acid), therefore, would provide evidence as to whether dietary flax oil does have a significant effect on early disease progression in *pcy* mice. Chapter two focuses on the effects of diets containing flax oil, compared to those containing corn oil, on markers of renal injury and renal fatty acid proportions in weanling *pcy* mice. In this study, weanling *pcy* mice were also given diets rich in 22:6n-3 DHA to further probe the effects of diets rich in n-3 fatty acids of differing lengths on early renal disease progression.

1.3 Maternal Diet and Renal Function

Barker and his colleagues first proposed the developmental (or fetal) origins hypothesis which states that the 'first' environment, namely the intrauterine, influences the risk of chronic diseases such as coronary heart disease, type 2 diabetes and hypertension in later life (46). During development, the organs and their systems pass through critical periods where they are 'plastic' and sensitive to the environment. For most organs, including the kidney, this period occurs *in utero* (46). Since the fetal environment is largely impacted by the maternal diet, numerous studies have attempted to re-create a milieu favoring intrauterine growth restriction via changes in the maternal diet. Impaired fetal nephrogenesis and reduced glomerular and nephron numbers can

result from maternal protein restriction and are associated with adult hypertension in humans (47) as well as experimental models of developmental programming (48-54).

On the other hand, increased maternal saturated fat intake has been linked to hyperinsulinemic, hyperglycemic, pro-atherogenic and hypertensive phenotypes in offspring (55-59), while a study with high maternal n-3 fatty acids intake failed to show such deleterious fetal programming effects (60). These reports demonstrate that renal organogenesis is susceptible to changes in the fetal environment which further modulates development of chronic diseases later in life.

Based on the earlier studies, flaxseed (13,42,45), flaxseed meal (61) and flax oil diets (15,44) appear to have protective effects on the kidney when given to adult or weanling animals with renal disease. Although dietary flaxseed and flax oil, when administered in the post-weaning period of life, have previously been shown to reduce renal interstitial fibrosis, cystic growth and renal macrophage infiltration in this model of chronic kidney disease (13,15,45), we do not know the effects of this intervention when given prenatally. Therefore, the focus of chapter three is to determine whether flax oil supplementation during pregnancy and lactation would slow renal disease progression in offspring of Han:SPRD-*cy* rats.

1.4 Diet and Advanced CKD

There is ample evidence to indicate that dietary interventions initiated at the early stages of deterioration of renal function reduce chronic renal injury in subtotally nephrectomized rats (62), mice with type II diabetic nephropathy (63), rats with chronic nephritic syndrome (64,65), rats with early diabetic nephropathy (66) and rat and mouse models of PKD (8,11,12,14,35,67,68). Particularly, flaxseed and flax oil-based diets are

reno-protective in rats with 5/6 nephrectomy(44), and rats with polycystic kidney disease (13,15,45).

However, individuals with CKD often do not become aware of their condition, until injury to the kidney is extensive (69). In addition, prevalence of decreased kidney function increases with age (2). Thus, most individuals diagnosed with CKD are more likely to be older and have established renal disease.

In animal models of advanced chronic renal injury, pharmacologic interventions such as anti-hypertensives (70), cyclooxygenase-2 (COX-2) inhibitors (71), angiotensin-II receptor antagonists in combination with COX-2 inhibitors (72) as well as dietary interventions such as low protein diets (73), soy protein supplementation (62) and flaxseed based diets (42) are beneficial in retarding renal disease progression. Similar protective effects of soy protein (74,75) and flaxseed (43) have also been demonstrated in humans with advanced nephropathies.

Whether dietary flax oil ameliorates established renal injury in adult Han:SPRD-*cy* rats remains unknown. Thus, the research objective in chapter four is to determine whether flax oil supplementation can alter further progression of renal injury in Han:SPRD-*cy* rats with advanced polycystic kidney disease. In this study, adult Han:SPRD-*cy* rats were also given soy protein-based diets to compare and contrast the effects of diets supplemented with soy protein with those rich in flax oil.

1.5 Prostanoids and Renal Disease

The mechanisms underlying the effects produced by dietary fat in PKD have not yet been elucidated. It has however, been established that dietary fat modulates

arachidonate metabolism. Renal pathophysiologic states are often accompanied by an upregulation of arachidonate metabolism (76).

Prostanoids are biologically active molecules derived from the enzymatic transformation of arachidonic acid (AA) and other 20-carbon fatty acids, as a result of incorporation of oxygen atoms at various sites of the fatty acid backbone and subsequent cyclisation. Twenty carbon fatty acids, incorporated into tissue phospholipids, are released by phospholipases and can be converted to prostanoids by three enymatic pathways present in the kidney (Figs.1-1 and 1-2)

- the COX pathway that results in the formation of PGs and thromboxanes (TXA_2)
- the lipoxygenase (LOX) pathway that results in the formation of mono-, di- and tri-hydroxy eicosatetraenoic acids (HETEs), leukotrienes (LT) and lipoxins (LXs) and
- the cytochrome P450-mediated oxygenation (CYP450) pathways that leads to formation of epoxyeicosatrienoic acids (EETs) (76).

Although all these pathways of arachidonate metabolism co-exist in the kidney and have significant roles in the maintenance of normal kidney function, the focus of this thesis is the COX pathway. Aberrant COX-2 expression and activity in animal models of PKD (77,78) as well as the increased affinity of COX-2 for n-3, compared to n-6 PUFA, make the COX-2 pathway a logical focus of this thesis.

1.5.1 Phospholipase A_2

Among the several classes of mammalian PLA_2s, the cytosolic PLA_2s ($cPLA_2$) are ubiquitously present forms of the enzyme with higher molecular weight (~85 Kda) and are tightly regulated by calcium ions and phosphorylation. Based on the relative specificity of $cPLA_2$ for AA in the sn-2 position of phospholipids, it has been proposed

that the primary role of $cPLA_2$ is to release AA for synthesis of prostanoids (79). Since prostanoids play important physiological roles in the kidney, the regulation of $cPLA_2$ would have important implications in the kidney (80). Consistent with this premise, elevated steady state renal levels of $cPLA_2$ have been demonstrated in *pcy* mice with PKD compared to controls (78).

1.5.2 Cyclooxygenases

COX or prostaglandin H_2 synthase (PGHS) is the enzyme that catalyzes the first two steps in the biosynthesis of prostanoids from AA, namely oxidation of AA to the hydroperoxy endoperoxide PGG_2 and its subsequent reduction to the hydroperoxy endoperoxide $PGH_{2(81)}$. PGH_2 is then transformated enzymatically as well as non-enzymatically into the primary prostanoids PGE_2, $PGF_{2\alpha}$, PGD_2, PGI_2, and TXA_2 (see Fig.1.1).

Three known isoforms of this prostanoid-forming enzyme have been identified, COX-1, -2, and a recently identified splice variant of the COX-1 gene, COX-3 (82,83). Initial evidence showed COX-1 to be constitutively expressed in most tissues, while COX-2 was considered to be primarily inducible. Thus, the two isoforms were thought to have mutually exclusive roles, with prostanoids derived from COX-1 appearing to exert diverse homeostatic or "housekeeping" effects while those produced by COX-2 being intimately involved in the induction of pain and inflammation and hence could be therapeutically targeted. These premises formed the basis for the development of COX-2 selective inhibitors, drugs that block formation of the pro-inflammatory COX-2 derived prostanoids, while maintaining the housekeeping effects of COX-1 metabolites.

However, studies in the kidney contradicted this classification, as they indicated that in certain cells of the kidney COX-2, but not COX-1, is constitutively expressed. Harris et al (84) were the first to demonstrate constitutive expression of COX-2 in the rat macula densa, juxtaglomerular apparatus, cortical thick ascending limb of the loop of henle and medullary interstitial cells. Knock-out mouse studies indicate that COX-2 is necessary for the postnatal development of the rat kidney (85). In concordance with observations in rats, Nantel and co-workers (86) detected the presence of COX-1 in the collecting ducts, thin loops of Henle and portions of renal vasculature in humans of all age-groups, while COX-2 was detected in the renal vasculature (afferent arterioles), medullary interstitial cells, and the macula densa, and this was more evident in the kidneys of elderly subjects (86). While the expression of COX-1 and -2 in the kidney is widely acknowledged, the presence of COX-3 in the kidney remains to be determined.

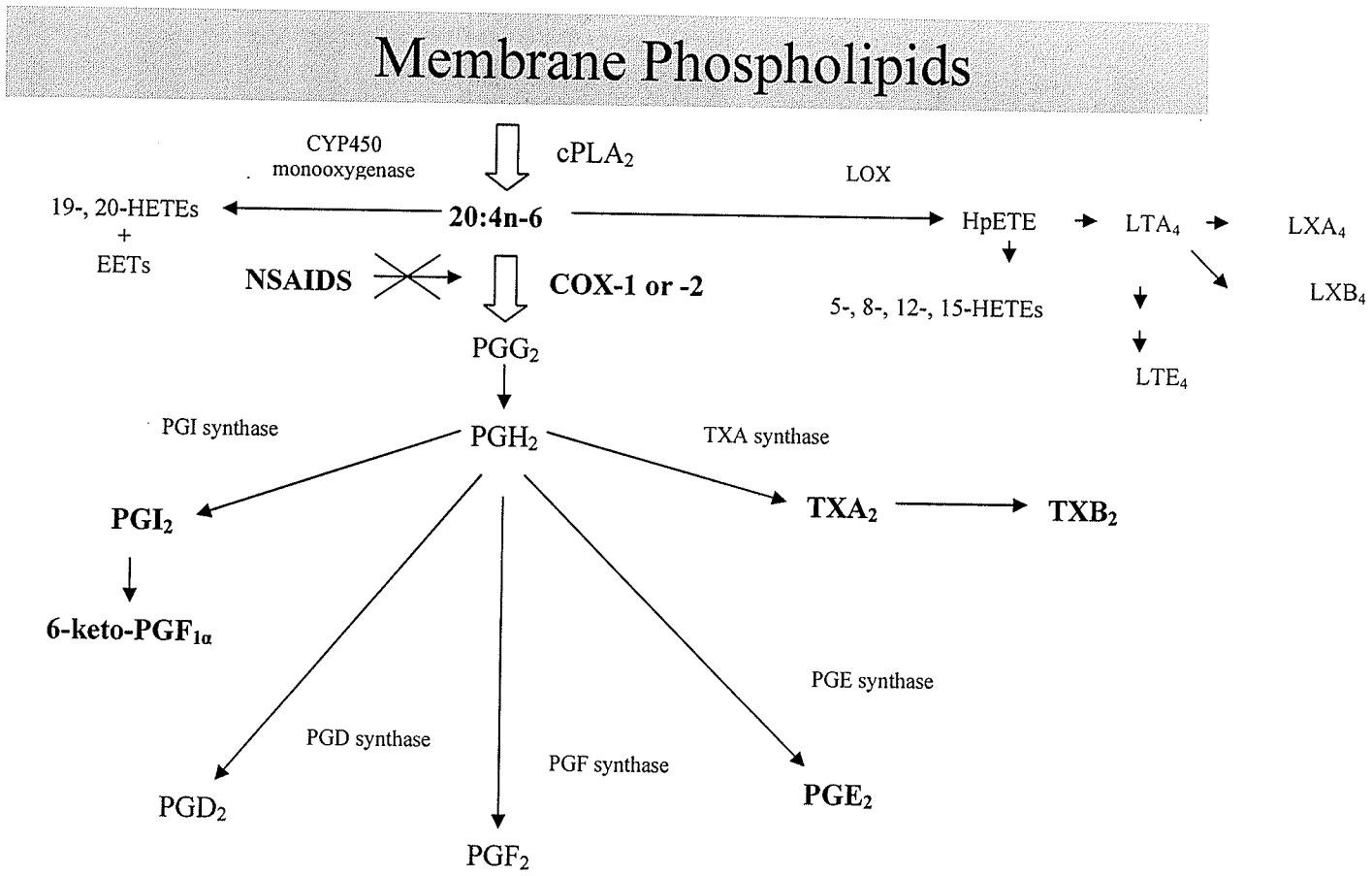

Figure 1-1. Prostanoid Synthetic Pathway. Adapted from (87,88)

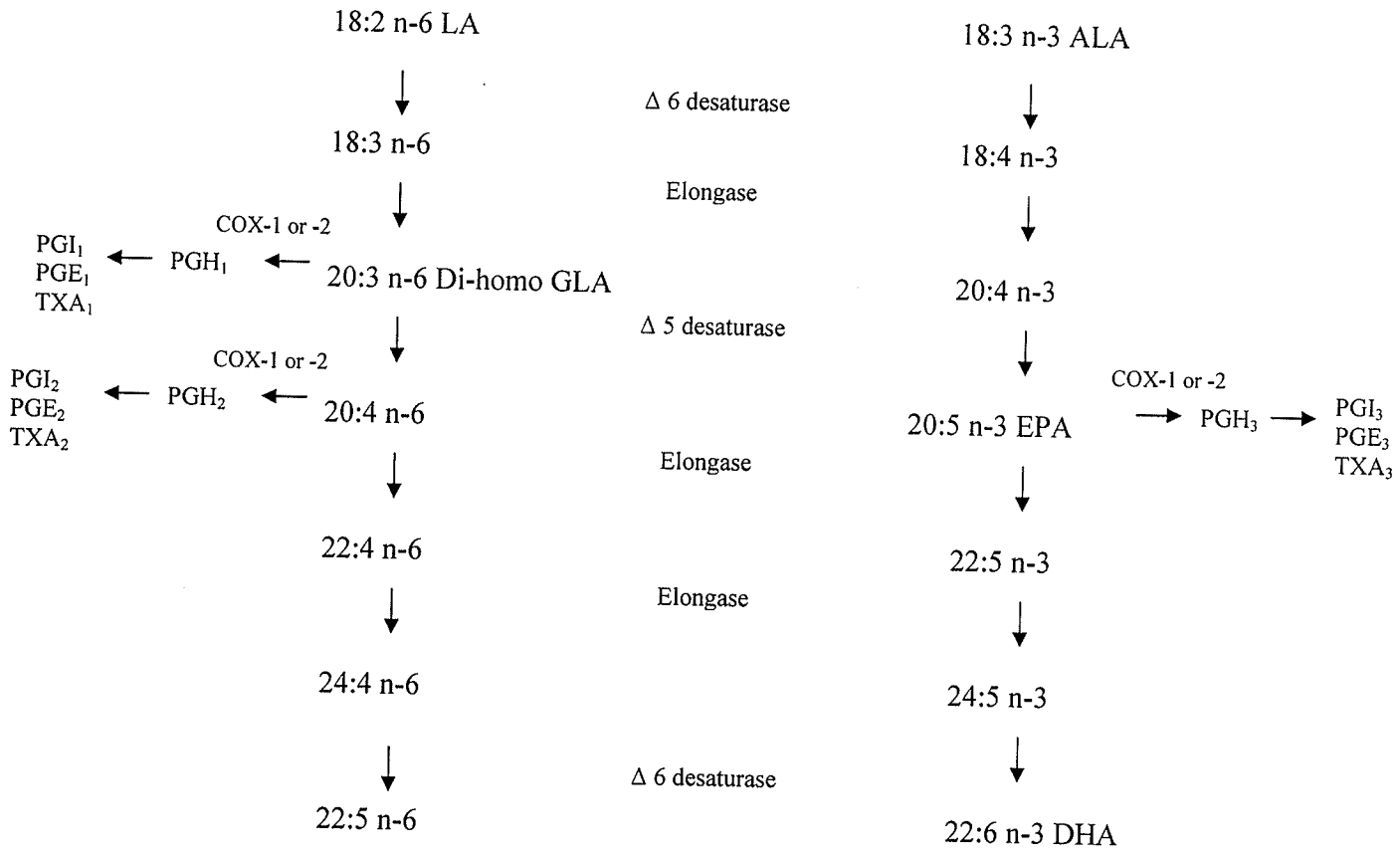

Figure 1-2. Long Chain PUFA synthesis. Adapted from (89,90)

The presence of COX-2 in the macula densa implies a role in renin release which in turn is involved with the renin-angiotensin-aldosterone system. In the mammalian kidney, macula densa is involved in regulating afferent arteriole tone and renin release, in response to alterations in luminal Cl^-, via changes in Na^+, K^+ and Cl^- co-transport (91,92). High renin states, associated with salt deficiency, angiotensin converting enzyme inhibitors or angiotensin receptor blockers, diuretic administration or experimental renovascular hypertension, lead to increased COX-2 expression in the macula densa/ cortical thick ascending limb of the loop of henle region (84,93-97). Most (93,97-100), but not all experimental studies (99,101) have indicated a role for COX-2 in the macula densa-mediated renin release. Modulation of the renin-angiotensin system by renocortical COX-2 metabolites has been demonstrated in models of COX-2 deletion (94,100) as well as in studies using COX-2 inhibitors (99,102). These interactions of COX-2 derived prostanoids and the renin–angiotensin system may underlie the physiological and patho-physiological regulation of renal function.

Both COX-1 and -2 proteins are about 600 amino acids in size (COX-1=70 kDa, COX-2=72 kDa) and share ~60% homology in their amino-acid compositions (87). The structures of COX-1 and -2 predict that both enzymes are located in the lumen of the nuclear envelope and endoplasmic reticulum. COX-1 and COX-2 molecules consist of several major domains, including an NH_2-terminal epidermal growth factor-like domain, a membrane-binding domain (which forms the mouth of a narrow hydrophobic channel that is the cyclooxygenase active site), and the COOH-terminal catalytic domain (87). The catalytic center is highly conserved (87%), while the amino acid sequences of other domains of COX-1 and COX-2 molecules are largely different (87). A significant

structural difference between the active sites of COX-1 and -2 is a substitution of isoleucine 523 in COX-1 for a valine in COX-2. This single difference opens a hydrophobic out-pocketing in COX-2 which can be accessed by some COX-2-selective drugs (103).

1.5.3 COX and PKD

COX-2 expression is generally up-regulated with disease, as seen in inflammatory conditions (104) and cancer (105). Of note, COX-2 up-regulation has been described in nephritic models (106,107), sclerotic-hypertensive (108) as well as renal ablation (71,109) models. Alterations in the enzyme levels of $cPLA_2$ as well as COX-1 and -2 in PKD have been demonstrated using the *pcy* mouse in which decline in renal function begins in adulthood, and the Han:SPRD-*cy* rat in which decline in renal function occurs during the growth phase (77,78). $cPLA_2$ and COX-1 protein expression were elevated in diseased kidneys in both rodent models of PKD by 34-131% and 87-110% respectively. On the other hand, COX-2 levels were below the detection limit in the *pcy* mice and 58% lower in diseased Han:SPRD-*cy* rat kidneys as compared with normals. These alterations were associated with disease progression, with few changes being detected in the early stages of the disease. Also, we have recently demonstrated that these changes in protein expression in diseased cystic kidneys are reflected in mRNA expression (77).

1.5.4 N-3 fatty acids and COX-2

The role of n-3 fatty acids in the modulation of COX-2 expression *in vivo* as well as *in vitro* has been studied in a number of experimental models of disease. Both long chain ALA (18:3n-3) and very long chain EPA (20:5n-3) and DHA (22:6n-3) n-3 fatty

acids attenuate elevated COX-2 levels and activity in various cancer cell-lines as well as animal models (110-116), in mice with mycotoxin-induced IgA nephropathy (117,118) and in Long-Evans Cinnamon rats with acute hepatitis (119). In these models, attenuation of the disease-induced COX-2 elevation by n-3 fatty acids is associated with slower disease progression.

However, since animal models of renal cystic disease exhibit reduced COX-2 expression with disease, these models offer a unique opportunity to examine the regulation of COX-2 gene and protein expression by dietary n-3 fatty acids *in vivo*. This research question has been explored in chapter five using both rodent models of renal cystic disease given diets containing n-3 fatty acids of differing lengths.

1.5.5 COX-2 activity and renal prostanoid profiles in renal disease

Elevated COX-2 enzyme activity has been reported in a number of renal disorders and nephritic models (93,106,109,120-123) including the rat model of PKD (77). In animal models of renal disease as well as in humans with elevated COX-2 activity, COX-2 inhibition appears to have beneficial effects (71,121,123-129). On the contrary, pharmacologic blockade of COX-2 was detrimental in a rat model of glomerulonephritis (130) and decreased GFR in salt-depleted and elderly subjects(131,132). Diseased Han:SPRD-*cy* rats exhibit elevated renal COX-1 and lower renal COX-2 protein and mRNA expression (77,78). In contrast, COX-2 (and COX-1) enzyme activities were significantly higher in diseased compared to normal kidneys, as measured by increased relative levels of renal PGE_2, TXB_2 and 6-ketoPGF$_{1\alpha}$ production (77). However, the effect of selectively blocking COX-2 in cystic kidneys has not yet been tested.

In diseased kidneys, the TXB_2 to PG ratios were higher than in normals, suggesting that the presence of cystic kidney disease shifts the balance towards a greater vasoconstrictory effect which may contribute to disease progression. In addition, among the vasodilatory prostanoids, prostacyclin was altered to a greater extent than PGE_2 by renal disease. Although renal COX-2 activity was the predominant COX activity in normal and diseased Han:SPRD-*cy* rats, a clear role of the independent COX isoforms in the disease process failed to emerge since both renal COX-1 and COX-2 activities were elevated in diseased rats. The study also failed to identify the relative importance of each COX isoform for basal prostanoid production in renal cystic disease. However, the study provided evidence that renal COX-2 activity is predominantly responsible for the overall renal COX activity in normal and diseased Han:SPRD-*cy* rats and that diseased rat kidneys exhibit elevated COX-2 activity (77). Chapter six outlines the effect of a selective COX-2 inhibitor on renal disease progression in Han:SPRD-*cy* rats as well as disease-associated alterations in prostanoid production in these rats.

1.6 General Hypotheses and Objectives

The objectives of the various studies in this thesis were defined based on the following general hypotheses

Hypothesis # 1 Diets containing flax oil (rich in ALA), compared to those rich in n-6 PUFA, will attenuate the progress of early polycystic kidney disease in male and female CD1 *pcy/pcy* mice.

Based on this hypothesis, the main objective for the study presented in chapter 2 was to determine the effects of diets containing flax oil (enriched in 18:3n-3), compared to those containing corn oil (rich in 18:2n-6), on the early stages of PKD progression in weanling *pcy* mice by assessing markers of renal function as well renal pathology. In addition, weanling male and female *pcy* mice also were given diets containing the long chain 22:6n-3 DHA to further probe the effects of diets rich in n-3 fatty acids of differing lengths on early renal disease progression.

Hypothesis # 2 Dietary flax oil, given during pregnancy and lactation, will slow the progression of renal disease in offspring of rats with genetically determined chronic kidney disease.

The objective of the study in chapter 3 was to assess the effects of dietary flax oil given during the maternal as well as post-weaning period on renal disease progression in offspring of Han:SPRD-*cy* rats by measuring parameters of renal function and pathology in the rat offspring.

Hypothesis # 3 Diets containing flax oil will attenuate the progression of renal disease in rats with established inherited cystic kidney disease.

In chapter 4, the main objective of the study was to determine the effects of dietary flax oil on established renal disease in adult Han:SPRD-*cy* rats. In addition, adult male Han:SPRD-*cy* rats with established CKD were given soy protein-based diets as well in order to compare and contrast the effects of dietary soy protein with dietary flax oil. Hypothesis # 4 The effects of diets containing different n-3 fatty acids on renal disease progression in rodent models of cystic disease are associated with alterations in the key enzymes involved in 20-carbon fatty acid metabolism, particularly COX-1 and -2.

The objective of the research in chapter 5 was to determine the effects of diets rich in n-3 fatty acids of varying length on disease-associated alterations in renal COX-1 and -2 protein and gene expression in weanling *pcy* mice as well as Han:SPRD-*cy* rats. Hypothesis # 5 Selective COX-2 inhibition will ameliorate progression of renal disease as well as disease-associated up-regulation of COX-2 activity in Han:SPRD-*cy* rats with PKD.

Based on this hypothesis, the main objective of the study in chapter 6 was to examine the impact of selective COX-2 inhibition on early renal disease progression as well as disease-associated elevation in prostanoid production in weanling Han:SPRD-*cy* rats.

1.7 References

1. Chauhan T. End-stage renal disease patients up nearly 19%. Cmaj 2004; 170:1087.

2. Coresh J, Astor BC, Greene T, Eknoyan G, Levey AS. Prevalence of chronic kidney disease and decreased kidney function in the adult US population:Third National Health and Nutrition Examination Survey. Am J Kidney Dis 2003; 41:1-12.

3. Remuzzi G, Ruggenenti P, Benigni A. Understanding the nature of renal disease progression. Kidney Int 1997; 51:2-15.

4. Schrier RW. Optimal care of autosomal dominant polycystic kidney disease patients. Nephrology (Carlton) 2006; 11:124-30.

5. Wilson PD. Polycystic kidney disease. N Engl J Med 2004; 350:151-64.

6. Torres VE. Therapies to slow polycystic kidney disease. Nephron Exp Nephrol 2004; 98:e1-7.

7. Yoder BK, Hou X, Guay-Woodford LM. The polycystic kidney disease proteins, polycystin-1, polycystin-2, polaris, and cystin, are co-localized in renal cilia. J Am Soc Nephrol 2002; 13:2508-16.

8. Aukema HM, Housini I, Rawling JM. Dietary soy protein effects on inherited polycystic kidney disease are influenced by gender and protein level. J Am Soc Nephrol 1999; 10:300-8.

9. Tomobe K, Philbrick D, Aukema HM, Clark WF, Ogborn MR, Parbtani A, Takahashi H, Holub BJ. Early dietary protein restriction slows disease progression and lengthens survival in mice with polycystic kidney disease. J Am Soc Nephrol 1994; 5:1355-60.

10. Tomobe K, Philbrick DJ, Ogborn MR, Takahashi H, Holub BJ. Effect of dietary soy protein and genistein on disease progression in mice with polycystic kidney disease. Am J Kidney Dis 1998; 31:55-61.

11. Ogborn MR, Bankovic-Calic N, Shoesmith C, Buist R, Peeling J. Soy protein modification of rat polycystic kidney disease. Am J Physiol 1998; 274:F541-9.

12. Philbrick DJ, Bureau DP, Collins FW, Holub BJ. Evidence that soyasaponin Bb retards disease progression in a murine model of polycystic kidney disease. Kidney Int 2003; 63:1230-9.

13. Ogborn MR, Nitschmann E, Weiler H, Leswick D, Bankovic-Calic N. Flaxseed ameliorates interstitial nephritis in rat polycystic kidney disease. Kidney Int 1999; 55:417-23.

14. Ogborn MR, Nitschmann E, Weiler HA, Bankovic-Calic N. Modification of polycystic kidney disease and fatty acid status by soy protein diet. Kidney Int 2000; 57:159-66.

15. Ogborn MR, Nitschmann E, Bankovic-Calic N, Weiler HA, Aukema H. Dietary flax oil reduces renal injury, oxidized LDL content, and tissue n-6/n-3 FA ratio in experimental polycystic kidney disease. Lipids 2002; 37:1059-65.

16. Ogborn MR NE, Bankovic-Calic N, Weiler H, Aukema H. Flax and soy phytoestrogen effects on renal injury and lipid content in experimental polycystic kidney disease. J Am Nutraceut Assoc 2005.

17. Prickett JD, Robinson DR, Steinberg AD. Dietary enrichment with the polyunsaturated fatty acid eicosapentaenoic acid prevents proteinuria and prolongs survival in NZB x NZW F1 mice. J Clin Invest 1981; 68:556-9.

18. Barcelli UO, Beach DC, Thompson B, Weiss M, Pollak VE. A diet containing n-3 and n-6 fatty acids favorably alters the renal phospholipids, eicosanoid synthesis and plasma lipids in nephrotic rats. Lipids 1988; 23:1059-63.

19. Ito Y, Barcelli U, Yamashita W, Weiss M, Glas-Greenwalt P, Pollak VE. Fish oil has beneficial effects on lipids and renal disease of nephrotic rats. Metabolism 1988; 37:352-7.

20. Robinson DR, Tateno S, Patel B, Hirai A. Dietary marine lipids after the course of autoimmune disease. Prog Clin Biol Res 1988; 282:295-303.

21. Scharschmidt LA, Gibbons NB, McGarry L, Berger P, Axelrod M, Janis R, Ko YH. Effects of dietary fish oil on renal insufficiency in rats with subtotal nephrectomy. Kidney Int 1987; 32:700-9.

22. Barcelli U, Pollak VE. Is there a role for polyunsaturated fatty acids in the prevention of renal disease and renal failure? Nephron 1985; 41:209-12.

23. Logan JL, Michael UF, Benson B. Effects of dietary fish oil on renal growth and function in uninephrectomized rats. Kidney Int 1990; 37:57-63.

24. Clark WF, Parbtani A, Philbrick DJ, Holub BJ, Huff MW. Chronic effects of omega-3 fatty acids (fish oil) in a rat 5/6 renal ablation model. J Am Soc Nephrol 1991; 1:1343-53.

25. Brown SA, Brown CA, Crowell WA, Barsanti JA, Kang CW, Allen T, Cowell C, Finco DR. Effects of dietary polyunsaturated fatty acid supplementation in early renal insufficiency in dogs. J Lab Clin Med 2000; 135:275-86.

26. Donadio JV. The emerging role of omega-3 polyunsaturated fatty acids in the management of patients with IgA nephropathy. J Ren Nutr 2001; 11:122-8.

27. Grande JP, Donadio JV. Role of dietary fish oil supplementation in IgA nephropathy. Mechanistic implications. Minerva Urol Nefrol 2001; 53:201-9.

28. Miyazaki M, Takemura N, Watanabe S, Hata N, Misawa Y, Okuyama H. Dietary docosahexaenoic acid ameliorates, but rapeseed oil and safflower oil accelerate renal injury in stroke-prone spontaneously hypertensive rats as compared with soybean oil, which is associated with expression for renal transforming growth factor-beta, fibronectin and renin. Biochim Biophys Acta 2000; 1483:101-10.

29. Eberhard OK, Potschick H, Neumann KH, Kliem V, Brunkhorst R. Short- and long-term effects of fish oil on proteinuria, morphology and renal hemodynamics in the Milan normotensive rat model of spontaneous glomerulosclerosis. Kidney Blood Press Res 1999; 22:128-34.

30. Logan JL, Michael UF, Benson B. Dietary fish oil interferes with renal arachidonic acid metabolism in rats:correlations with renal physiology. Metabolism 1992; 41:382-9.

31. Tateno S, Kobayashi Y, Robinson DR. Dietary fish oil supplementation exacerbates serum sickness nephritis in mice. Nephron 1997; 77:86-92.

32. Aukema HM, Yamaguchi T, Takahashi H, Philbrick DJ, Holub BJ. Effects of dietary fish oil on survival and renal fatty acid composition in murine polycystic kidney disease. Nutrition Research 1992; 12:1383-92.

33. Yamaguchi T, Valli VE, Philbrick D, Holub B, Yoshida K, Takahashi H. Effects of dietary supplementation with n-3 fatty acids on kidney morphology and the fatty acid composition of phospholipids and triglycerides from mice with polycystic kidney disease. Res Commun Chem Pathol Pharmacol 1990; 69:335-51.

34. Jayapalan S, Saboorian MH, Edmunds JW, Aukema HM. High dietary fat intake increases renal cyst disease progression in Han:SPRD-cy rats. J Nutr 2000; 130:2356-60.

35. Lu J, Bankovic-Calic N, Ogborn M, Saboorian MH, Aukema HM. Detrimental effects of a high fat diet in early renal injury are ameliorated by fish oil in Han:SPRD-cy rats. J Nutr 2003; 133:180-6.

36. Kurzer MS, Xu X. Dietary phytoestrogens. Annu Rev Nutr 1997; 17:353-81.

37. Prasad K. Dietary flax seed in prevention of hypercholesterolemic atherosclerosis. Atherosclerosis 1997; 132:69-76.

38. Tou JC, Thompson LU. Exposure to flaxseed or its lignan component during different developmental stages influences rat mammary gland structures. Carcinogenesis 1999; 20:1831-5.

39. Caughey GE, Mantzioris E, Gibson RA, Cleland LG, James MJ. The effect on human tumor necrosis factor alpha and interleukin 1 beta production of diets enriched in n-3 fatty acids from vegetable oil or fish oil. Am J Clin Nutr 1996; 63:116-22.

40. Mozaffarian D. Does alpha-linolenic acid intake reduce the risk of coronary heart disease? A review of the evidence. Altern Ther Health Med 2005; 11:24-30; quiz 1, 79.

41. Velasquez MT, Bhathena SJ. Dietary phytoestrogens:a possible role in renal disease protection. Am J Kidney Dis 2001; 37:1056-68.

42. Hall AV, Parbtani A, Clark WF, Spanner E, Keeney M, Chin-Yee I, Philbrick DJ, Holub BJ. Abrogation of MRL/lpr lupus nephritis by dietary flaxseed. Am J Kidney Dis 1993; 22:326-32.

43. Clark WF, Parbtani A, Huff MW, Spanner E, de Salis H, Chin-Yee I, Philbrick DJ, Holub BJ. Flaxseed:a potential treatment for lupus nephritis. Kidney Int 1995; 48:475-80.

44. Ingram AJ, Parbtani A, Clark WF, Spanner E, Huff MW, Philbrick DJ, Holub BJ. Effects of flaxseed and flax oil diets in a rat-5/6 renal ablation model. Am J Kidney Dis 1995; 25:320-9.

45. Ogborn MR, Nitschmann E, Bankovic-Calic N, Buist R, Peeling J. The effect of dietary flaxseed supplementation on organic anion and osmolyte content and excretion in rat polycystic kidney disease. Biochem Cell Biol 1998; 76:553-9.

46. Barker DJ. The fetal and infant origins of disease. Eur J Clin Invest 1995; 25:457-63.

47. Keller G, Zimmer G, Mall G, Ritz E, Amann K. Nephron number in patients with primary hypertension. N Engl J Med 2003; 348:101-8.

48. Vehaskari VM, Aviles DH, Manning J. Prenatal programming of adult hypertension in the rat. Kidney Int 2001; 59:238-45.

49. Woods LL, Weeks DA, Rasch R. Programming of adult blood pressure by maternal protein restriction:role of nephrogenesis. Kidney Int 2004; 65:1339-48.

50. Langley-Evans SC, Langley-Evans AJ, Marchand MC. Nutritional programming of blood pressure and renal morphology. Arch Physiol Biochem 2003; 111:8-16.

51. Lisle SJ, Lewis RM, Petry CJ, Ozanne SE, Hales CN, Forhead AJ. Effect of maternal iron restriction during pregnancy on renal morphology in the adult rat offspring. Br J Nutr 2003; 90:33-9.

52. Sahajpal V, Ashton N. Renal function and angiotensin AT1 receptor expression in young rats following intrauterine exposure to a maternal low-protein diet. Clin Sci (Lond) 2003; 104:607-14.

53. Welham SJ, Riley PR, Wade A, Hubank M, Woolf AS. Maternal diet programs embryonic kidney gene expression. Physiol Genomics 2005; 22:48-56.

54. Armitage JA, Khan IY, Taylor PD, Nathanielsz PW, Poston L. Developmental programming of the metabolic syndrome by maternal nutritional imbalance:how strong is the evidence from experimental models in mammals? J Physiol 2004; 561:355-77.

55. Khan I, Dekou V, Hanson M, Poston L, Taylor P. Predictive adaptive responses to maternal high-fat diet prevent endothelial dysfunction but not hypertension in adult rat offspring. Circulation 2004; 110:1097-102.

56. Khan IY, Dekou V, Douglas G, Jensen R, Hanson MA, Poston L, Taylor PD. A high-fat diet during rat pregnancy or suckling induces cardiovascular dysfunction in adult offspring. Am J Physiol Regul Integr Comp Physiol 2005; 288:R127-33.

57. Taylor PD, McConnell J, Khan IY, Holemans K, Lawrence KM, Asare-Anane H, Persaud SJ, Jones PM, Petrie L, Hanson MA, Poston L. Impaired glucose homeostasis and mitochondrial abnormalities in offspring of rats fed a fat-rich diet in pregnancy. Am J Physiol Regul Integr Comp Physiol 2005; 288:R134-9.

58. Palinski W, D'Armiento FP, Witztum JL, de Nigris F, Casanada F, Condorelli M, Silvestre M, Napoli C. Maternal hypercholesterolemia and treatment during pregnancy influence the long-term progression of atherosclerosis in offspring of rabbits. Circ Res 2001; 89:991-6.

59. Armitage JA, Lakasing L, Taylor PD, Balachandran AA, Jensen RI, Dekou V, Ashton N, Nyengaard JR, Poston L. Developmental programming of aortic and renal structure in offspring of rats fed fat-rich diets in pregnancy. J Physiol 2005; 565:171-84.

60. Siemelink M, Verhoef A, Dormans JA, Span PN, Piersma AH. Dietary fatty acid composition during pregnancy and lactation in the rat programs growth and glucose metabolism in the offspring. Diabetologia 2002; 45:1397-403.

61. Velasquez MT, Bhathena SJ, Ranich T, Schwartz AM, Kardon DE, Ali AA, Haudenschild CC, Hansen CT. Dietary flaxseed meal reduces proteinuria and ameliorates nephropathy in an animal model of type II diabetes mellitus. Kidney Int 2003; 64:2100-7.

62. Williams AJ, Walls J. Metabolic consequences of differing protein diets in experimental renal disease. Eur J Clin Invest 1987; 17:117-22.

63. Teixeira SR, Tappenden KA, Erdman JW, Jr. Altering dietary protein type and quantity reduces urinary albumin excretion without affecting plasma glucose concentrations in BKS.cg-m +Lepr db/+Lepr db (db/db) mice. J Nutr 2003; 133:673-8.

64. Tovar AR, Murguia F, Cruz C, Hernandez-Pando R, Aguilar-Salinas CA, Pedraza-Chaverri J, Correa-Rotter R, Torres N. A soy protein diet alters hepatic lipid metabolism gene expression and reduces serum lipids and renal fibrogenic cytokines in rats with chronic nephrotic syndrome. J Nutr 2002; 132:2562-9.

65. Pedraza-Chaverri J, Barrera D, Hernandez-Pando R, Medina-Campos ON, Cruz C, Murguia F, Juarez-Nicolas C, Correa-Rotter R, Torres N, Tovar AR. Soy protein diet ameliorates renal nitrotyrosine formation and chronic nephropathy induced by puromycin aminonucleoside. Life Sci 2004; 74:987-99.

66. Trujillo J, Ramirez V, Perez J, Torre-Villalvazo I, Torres N, Tovar AR, Munoz RM, Uribe N, Gamba G, Bobadilla NA. Renal protection by a soy diet in obese Zucker rats is associated with restoration of nitric oxide generation. Am J Physiol Renal Physiol 2005; 288:F108-16.

67. Fair DE, Ogborn MR, Weiler HA, Bankovic-Calic N, Nitschmann EP, Fitzpatrick-Wong SC, Aukema HM. Dietary soy protein attenuates renal disease progression after 1 and 3 weeks in Han:SPRD-cy weanling rats. J Nutr 2004; 134:1504-7.

68. Aukema HM, Housini I. Dietary soy protein effects on disease and IGF-I in male and female Han:SPRD-cy rats. Kidney Int 2001; 59:52-61.

69. Coresh J, Byrd-Holt D, Astor BC, Briggs JP, Eggers PW, Lacher DA, Hostetter TH. Chronic kidney disease awareness, prevalence, and trends among U.S. adults, 1999 to 2000. J Am Soc Nephrol 2005; 16:180-8.

70. Jovanovic D, Jovovic D, Mihailovic-Stanojevic N, Miloradovic Z, Dimitrijevic J, Maksic N, Djukanovic L. Influence of carvedilol on chronic renal failure progression in spontaneously hypertensive rats with adriamycin nephropathy. Clin Nephrol 2005; 63:446-53.

71. Fujihara CK, Antunes GR, Mattar AL, Andreoli N, Malheiros DM, Noronha IL, Zatz R. Cyclooxygenase-2 (COX-2) inhibition limits abnormal COX-2 expression and progressive injury in the remnant kidney. Kidney Int 2003; 64:2172-81.

72. Goncalves AR, Fujihara CK, Mattar AL, Malheiros DM, Noronha Ide L, de Nucci G, Zatz R. Renal expression of COX-2, ANG II, and AT1 receptor in remnant kidney:strong renoprotection by therapy with losartan and a nonsteroidal anti-inflammatory. Am J Physiol Renal Physiol 2004; 286:F945-54.

73. Ogborn MR, Sareen S. Amelioration of polycystic kidney disease by modification of dietary protein intake in the rat. J Am Soc Nephrol 1995; 6:1649-54.

74. Teixeira SR, Tappenden KA, Carson L, Jones R, Prabhudesai M, Marshall WP, Erdman JW, Jr. Isolated soy protein consumption reduces urinary albumin excretion and improves the serum lipid profile in men with type 2 diabetes mellitus and nephropathy. J Nutr 2004; 134:1874-80.

75. Cupisti A, D'Alessandro C, Ghiadoni L, Morelli E, Panichi V, Barsotti G. Effect of a soy protein diet on serum lipids of renal transplant patients. J Ren Nutr 2004; 14:31-5.

76. Breyer M, Badr K (1996) Arachidonic acid metabolites and the kidney. In:The Kidney, 5 ed. (Brenner, B., ed.), pp. 754-88. W.B. Saunders Co.

77. Warford-Woolgar L, Peng CY, Shuhyta J, Wakefield A, Sankaran D, Ogborn M, Aukema HM. Selectivity of cyclooxygenase (COX) isoform activity and prostanoid production in normal and diseased Han:SPRD-*cy* rat kidneys. Am J Physiol Renal Physiol 2006; 290:F897-904.

78. Aukema HM, Adolphe J, Mishra S, Jiang J, Cuozzo FP, Ogborn MR. Alterations in renal cytosolic phospholipase A_2 and cyclooxygenases in polycystic kidney disease. Faseb J 2003; 17:298-300.

79. Murakami M, Masuda S, Kudo I. Arachidonate release and prostaglandin production by group IVC phospholipase A_2 (cytosolic phospholipase A_2 gamma). Biochem J 2003; 372:695-702.

80. Hack N, Tay A, Schultz A, Muzin N, Clayman P, Egan S, Skorecki KL. Regulation of rat kidney mesangial cell phospholipase A_2. Clin Exp Pharmacol Physiol 1996; 23:71-5.

81. Vane JR, Bakhle YS, Botting RM. Cyclooxygenases 1 and 2. Annu Rev Pharmacol Toxicol 1998; 38:97-120.

82. Chandrasekharan NV, Dai H, Roos KL, Evanson NK, Tomsik J, Elton TS, Simmons DL. COX-3, a cyclooxygenase-1 variant inhibited by acetaminophen and other analgesic/antipyretic drugs:cloning, structure, and expression. Proc Natl Acad Sci U S A 2002; 99:13926-31.

83. Davies NM, Good RL, Roupe KA, Yanez JA. Cyclooxygenase-3:axiom, dogma, anomaly, enigma or splice error?--Not as easy as 1, 2, 3. J Pharm Pharm Sci 2004; 7:217-26.

84. Harris RC, McKanna JA, Akai Y, Jacobson HR, Dubois RN, Breyer MD. Cyclooxygenase-2 is associated with the macula densa of rat kidney and increases with salt restriction. J Clin Invest 1994; 94:2504-10.

85. Morham SG, Langenbach R, Loftin CD, Tiano HF, Vouloumanos N, Jennette JC, Mahler JF, Kluckman KD, Ledford A, Lee CA, Smithies O. Prostaglandin synthase 2 gene disruption causes severe renal pathology in the mouse. Cell 1995; 83:473-82.

86. Nantel F, Meadows E, Denis D, Connolly B, Metters KM, Giaid A. Immunolocalization of cyclooxygenase-2 in the macula densa of human elderly. FEBS Lett 1999; 457:475-7.

87. Simmons DL, Botting RM, Hla T. Cyclooxygenase isozymes:the biology of prostaglandin synthesis and inhibition. Pharmacol Rev 2004; 56:387-437.

88. Serhan CN, Levy B. Novel pathways and endogenous mediators in anti-inflammation and resolution. Chem Immunol Allergy 2003; 83:115-45.

89. Sprecher H. Metabolism of highly unsaturated n-3 and n-6 fatty acids. Biochim Biophys Acta 2000; 1486:219-31.

90. Horrobin DF. The relationship between schizophrenia and essential fatty acid and eicosanoid metabolism. Prostaglandins Leukot Essent Fatty Acids 1992; 46:71-7.

91. Persson AE, Salomonsson M, Westerlund P, Greger R, Schlatter E, Gonzalez E. Macula densa cell function. Kidney Int Suppl 1991; 32:S39-44.

92. Schnermann J, Traynor T, Yang T, Arend L, Huang YG, Smart A, Briggs JP. Tubuloglomerular feedback:new concepts and developments. Kidney Int Suppl 1998; 67:S40-5.

93. Wang JL, Cheng HF, Harris RC. Cyclooxygenase-2 inhibition decreases renin content and lowers blood pressure in a model of renovascular hypertension. Hypertension 1999; 34:96-101.

94. Cheng HF, Wang JL, Zhang MZ, Miyazaki Y, Ichikawa I, McKanna JA, Harris RC. Angiotensin II attenuates renal cortical cyclooxygenase-2 expression. J Clin Invest 1999; 103:953-61.

95. Jensen BL, Kurtz A. Differential regulation of renal cyclooxygenase mRNA by dietary salt intake. Kidney Int 1997; 52:1242-9.

96. Yang T, Singh I, Pham H, Sun D, Smart A, Schnermann JB, Briggs JP. Regulation of cyclooxygenase expression in the kidney by dietary salt intake. Am J Physiol 1998; 274:F481-9.

97. Wolf K, Castrop H, Hartner A, Goppelt-Strube M, Hilgers KF, Kurtz A. Inhibition of the renin-angiotensin system upregulates cyclooxygenase-2 expression in the macula densa. Hypertension 1999; 34:503-7.

98. Harding P, Carretero OA, Beierwaltes WH. Chronic cyclooxygenase-2 inhibition blunts low sodium-stimulated renin without changing renal haemodynamics. J Hypertens 2000; 18:1107-13.

99. Kammerl MC, Nusing RM, Seyberth HW, Riegger GA, Kurtz A, Kramer BK. Inhibition of cyclooxygenase-2 attenuates urinary prostanoid excretion without affecting renal renin expression. Pflugers Arch 2001; 442:842-7.

100. Yang T, Endo Y, Huang YG, Smart A, Briggs JP, Schnermann J. Renin expression in COX-2-knockout mice on normal or low-salt diets. Am J Physiol Renal Physiol 2000; 279:F819-25.

101. Hocherl K, Kammerl MC, Schumacher K, Endemann D, Grobecker HF, Kurtz A. Role of prostanoids in regulation of the renin-angiotensin-aldosterone system by salt intake. Am J Physiol Renal Physiol 2002; 283:F294-301.

102. Stichtenoth DO, Wagner B, Frolich JC. Effect of selective inhibition of the inducible cyclooxygenase on renin release in healthy volunteers. J Investig Med 1998; 46:290-6.

103. Kurumbail RG, Stevens AM, Gierse JK, McDonald JJ, Stegeman RA, Pak JY, Gildehaus D, Miyashiro JM, Penning TD, Seibert K, Isakson PC, Stallings WC. Structural basis for selective inhibition of cyclooxygenase-2 by anti-inflammatory agents. Nature 1996; 384:644-8.

104. Wu KK, Liou JY. Cellular and molecular biology of prostacyclin synthase. Biochem Biophys Res Commun 2005; 338:45-52.

105. Kashfi K, Rigas B. Is COX-2 a 'collateral' target in cancer prevention? Biochem Soc Trans 2005; 33:724-7.

106. Hirose S, Yamamoto T, Feng L, Yaoita E, Kawasaki K, Goto S, Fujinaka H, Wilson CB, Arakawa M, Kihara I. Expression and localization of cyclooxygenase isoforms and cytosolic phospholipase A2 in anti-Thy-1 glomerulonephritis. J Am Soc Nephrol 1998; 9:408-16.

107. Takano T, Cybulsky AV. Complement C5b-9-mediated arachidonic acid metabolism in glomerular epithelial cells :role of cyclooxygenase-1 and -2. Am J Pathol 2000; 156:2091-101.

108. Weichert W, Paliege A, Provoost AP, Bachmann S. Upregulation of juxtaglomerular NOS1 and COX-2 precedes glomerulosclerosis in fawn-hooded hypertensive rats. Am J Physiol Renal Physiol 2001; 280:F706-14.

109. Wang JL, Cheng HF, Zhang MZ, McKanna JA, Harris RC. Selective increase of cyclooxygenase-2 expression in a model of renal ablation. Am J Physiol 1998; 275:F613-22.

110. Yang P, Chan D, Felix E, Cartwright C, Menter DG, Madden T, Klein RD, Fischer SM, Newman RA. Formation and antiproliferative effect of prostaglandin E(3) from eicosapentaenoic acid in human lung cancer cells. J Lipid Res 2004; 45:1030-9.

111. Calviello G, Di Nicuolo F, Gragnoli S, Piccioni E, Serini S, Maggiano N, Tringali G, Navarra P, Ranelletti FO, Palozza P. n-3 PUFAs reduce VEGF expression in human colon cancer cells modulating the COX-2/PGE2 induced ERK-1 and -2 and HIF-1alpha induction pathway. Carcinogenesis 2004; 25:2303-10.

112. Vecchini A, Ceccarelli V, Susta F, Caligiana P, Orvietani P, Binaglia L, Nocentini G, Riccardi C, Calviello G, Palozza P, Maggiano N, Di Nardo P. Dietary alpha-linolenic acid reduces COX-2 expression and induces apoptosis of hepatoma cells. J Lipid Res 2004; 45:308-16.

113. Rao CV, Hirose Y, Indranie C, Reddy BS. Modulation of experimental colon tumorigenesis by types and amounts of dietary fatty acids. Cancer Res 2001; 61:1927-33.

114. Denkins Y, Kempf D, Ferniz M, Nileshwar S, Marchetti D. Role of omega-3 polyunsaturated fatty acids on cyclooxygenase-2 metabolism in brain-metastatic melanoma. J Lipid Res 2005; 46:1278-84.

115. Horia E, Watkins BA. Comparison of stearidonic acid and alpha-linolenic acid on PGE2 production and COX-2 protein levels in MDA-MB-231 breast cancer cell cultures. J Nutr Biochem 2005; 16:184-92.

116. Dommels YE, Haring MM, Keestra NG, Alink GM, van Bladeren PJ, van Ommen B. The role of cyclooxygenase in n-6 and n-3 polyunsaturated fatty acid mediated effects on cell proliferation, $PGE(_2)$ synthesis and cytotoxicity in human colorectal carcinoma cell lines. Carcinogenesis 2003; 24:385-92.

117. Jia Q, Zhou HR, Bennink M, Pestka JJ. Docosahexaenoic acid attenuates mycotoxin-induced immunoglobulin a nephropathy, interleukin-6 transcription, and mitogen-activated protein kinase phosphorylation in mice. J Nutr 2004; 134:3343-9.

118. Moon Y, Pestka JJ. Deoxynivalenol-induced mitogen-activated protein kinase phosphorylation and IL-6 expression in mice suppressed by fish oil. J Nutr Biochem 2003; 14:717-26.

119. Du C, Fujii Y, Ito M, Harada M, Moriyama E, Shimada R, Ikemoto A, Okuyama H. Dietary polyunsaturated fatty acids suppress acute hepatitis, alter gene expression and prolong survival of female Long-Evans Cinnamon rats, a model of Wilson disease. J Nutr Biochem 2004; 15:273-80.

120. Horiba N, Kumano E, Watanabe T, Shinkura H, Sugimoto T, Inoue M. Subtotal nephrectomy stimulates cyclooxygenase 2 expression and prostacyclin synthesis in the rat remnant kidney. Nephron 2002; 91:134-41.

121. Komers R, Lindsley JN, Oyama TT, Schutzer WE, Reed JF, Mader SL, Anderson S. Immunohistochemical and functional correlations of renal cyclooxygenase-2 in experimental diabetes. J Clin Invest 2001; 107:889-98.

122. Komers R, Zdychova J, Cahova M, Kazdova L, Lindsley JN, Anderson S. Renal cyclooxygenase-2 in obese Zucker (fatty) rats. Kidney Int 2005; 67:2151-8.

123. Wang JL, Cheng HF, Shappell S, Harris RC. A selective cyclooxygenase-2 inhibitor decreases proteinuria and retards progressive renal injury in rats. Kidney Int 2000; 57:2334-42.

124. Blume C, Heise G, Muhlfeld A, Bach D, Schror K, Gerhardz CD, Grabensee B, Heering P. Effect of flosulide, a selective cyclooxygenase 2 inhibitor, on passive heymann nephritis in the rat. Kidney Int 1999; 56:1770-8.

125. Cheng HF, Wang CJ, Moeckel GW, Zhang MZ, McKanna JA, Harris RC. Cyclooxygenase-2 inhibitor blocks expression of mediators of renal injury in a model of diabetes and hypertension. Kidney Int 2002; 62:929-39.

126. Cheng H, Zhang M, Moeckel GW, Zhao Y, Wang S, Qi Z, Breyer MD, Harris RC. Expression of mediators of renal injury in the remnant kidney of ROP mice is attenuated by cyclooxygenase-2 inhibition. Nephron Exp Nephrol 2005; 101:e75-85.

127. Dey A, Maric C, Kaesemeyer WH, Zaharis CZ, Stewart J, Pollock JS, Imig JD. Rofecoxib decreases renal injury in obese Zucker rats. Clin Sci (Lond) 2004; 107:561-70.

128. Sanchez PL, Salgado LM, Ferreri NR, Escalante B. Effect of cyclooxygenase-2 inhibition on renal function after renal ablation. Hypertension 1999; 34:848-53.

129. Tomasoni S, Noris M, Zappella S, Gotti E, Casiraghi F, Bonazzola S, Benigni A, Remuzzi G. Upregulation of renal and systemic cyclooxygenase-2 in patients with active lupus nephritis. J Am Soc Nephrol 1998; 9:1202-12.

130. Kitahara M, Eitner F, Ostendorf T, Kunter U, Janssen U, Westenfeld R, Matsui K, Kerjaschki D, Floege J. Selective cyclooxygenase-2 inhibition impairs glomerular

capillary healing in experimental glomerulonephritis. J Am Soc Nephrol 2002; 13:1261-70.

131. Rossat J, Maillard M, Nussberger J, Brunner HR, Burnier M. Renal effects of selective cyclooxygenase-2 inhibition in normotensive salt-depleted subjects. Clin Pharmacol Ther 1999; 66:76-84.

132. Swan SK, Rudy DW, Lasseter KC, Ryan CF, Buechel KL, Lambrecht LJ, Pinto MB, Dilzer SC, Obrda O, Sundblad KJ, Gumbs CP, Ebel DL, Quan H, Larson PJ, Schwartz JI, Musliner TA, Gertz BJ, Brater DC, Yao SL. Effect of cyclooxygenase-2 inhibition on renal function in elderly persons receiving a low-salt diet. A randomized, controlled trial. Ann Intern Med 2000; 133:1-9.

2. MODULATION OF RENAL INJURY IN *pcy* MICE BY DIETARY FAT CONTAINING (N-3) FATTY ACIDS DEPENDS ON LEVEL AND TYPE OF FAT.

Reproduced with permission from

Sankaran D, Lu J, Bankovic-Calic N, Ogborn MR, Aukema HM.

Modulation of renal injury in pcy mice by dietary fat containing n-3 fatty acids depends on the level and type of fat. Lipids. 2004. 39(3): 207-214.

© Copyright of the American Oil Chemists' Society Press

2.1 Abstract

Low fat diets and diets containing (n-3) fatty acids slow the progression of renal injury in the male Han:SPRD-*cy* rat model of polycystic kidney disease (PKD). To determine whether these dietary fat effects are similar in females and in another model of renal cystic disease, in this study we used both male and female *pcy* mice to examine effects of fat level and type on disease progression. Adult *pcy* mice were fed 4g, 10g or 20g soybean oil/100g diet for 130 d in study 1. In study 2, weanling *pcy* mice were fed high or low levels of fat rich in 18:2n-6 (corn oil, CO), 18:3n-3 (flaxseed oil/corn oil 4:1g/g, FO) or 22:6n-3 (algal oil/corn oil 4:1g/g, DO) for 8 weeks. In adult *pcy* mice, low compared to high fat diets lowered kidney weights (2.4 ± 0.2 vs. 3.1 ± 0.2 g/100g body weight, P=0.006) and serum urea nitrogen (9.6 ± 0.6 vs. 11.9 ± 0.6 mmol/L, P=0.009), while in young *pcy* mice it reduced renal fibrosis volumes (0.44± 0.04 vs. 0.62 ± 0.04 ml/kg body wt, P<0.0001). FO feeding in young *pcy* mice mitigated the detrimental effects of high fat on fibrosis, while not altering kidney size, function and oxidative damage when compared to the CO fed mice. In contrast, DO compared to CO fed mice had higher kidney weights (2.64 ± 0.07 vs. 2.24 ± 0.08 g/100g body weight, P=0.005), SUN (9.4 ± 0.57 vs. 7.0 ± 0.62 mmol/L, P<0.0001), cyst volumes (7.9 ± 0.28 vs. 6.2 ± 0.30 mL/kg body wt, P<0.0001) and similar levels of oxidative damage and fibrosis. The fatty acid compositions of the diets were reflected in the kidneys: 18:2n-6, 18:3n-3 and 22:6n-3 were the highest in the CO, FO and DO diets, respectively. Dietary effects on kidney disease progression were similar in males and females. A low fat diet slows progression of renal injury in male and female *pcy* mice, consistent with findings in the male Han:SPRD-*cy* rat. Dietary fat type also influences renal injury, with flaxseed oil

diets rich in 18:3n-3 slowing early fibrosis progression compared to diets rich in 18:2n-6 or in 22:6n-3.

2.2 Introduction

Polycystic kidney disease (PKD) is the fourth most common cause of end stage renal disease, affecting over 12 million worldwide, and is primarily caused by mutations in one of two genes, PKD1 and PKD2 (1,2). Treatment of PKD patients involves alleviation of associated secondary disorders, but there currently are no strategies to combat disease progression itself. A number of studies involving dietary interventions using animal models of renal cystic diseases, however, have obtained promising results in retarding disease progression. In these models, disease progression is retarded by reduction of dietary protein to a low yet growth-maintaining level, substitution of soy protein for casein, supplementation with a saponin-enriched alcohol extract from soy protein isolate, and adding flax or fish oil to the diet, with some of these interventions having been shown to prolong life (3-11).

In male Han:SPRD-*cy* rats with PKD, low fat compared to high fat feeding is beneficial, resulting in less histological damage, lower serum creatinine and improved creatinine clearance (11,12). Although the disease progresses at a much slower rate in female Han:SPRD-*cy* rats, dietary fat restriction also is beneficial to a lesser extent (12). The relevance of animal models and of gender to human disease is always an issue, necessitating the use of multiple models of the disease and the inclusion of both genders to examine intervention effects. The *pcy* mouse has a form of renal cystic disease with progressive renal failure and has been used as a model of human autosomal dominant PKD (13-15), although synteny of the *pcy* gene with the NPH3 gene has been observed (16). The NPH3 protein is mutated in adolescent nephronophthisis, another type of renal cystic disease (16). Phenotypically, this model exhibits several characteristics of both of

these forms of renal cystic disease (16,17). All renal cystic diseases involve disturbances of regeneration and repair with different components predominating in different models.

In the *pcy* mouse model gender differences in response to varying fat type and protein source have been observed (3,18). Therefore in the first study presented herein, we examined the effects of feeding differing fat levels on the progression of disease in male and female *pcy* mice in order to determine whether the beneficial effects of fat restriction observed in the Han:SPRD-*cy* rat extend to this model of renal cystic disease. In contrast to the first part of this study as well as previous *pcy* studies in which adult *pcy* mice have been used, the benefits of dietary interventions on renal injury have been observed in young Han:SPRD-*cy* rats (11,12). Therefore, in the second study, we examined whether dietary fat level would have the same effect in weanling *pcy* mice. In this study the type of fat also was altered in order to determine whether fat type would influence fat level effects on disease progression in these mice. In Han:SPRD-*cy* rats, both fish oil [rich in 20:5n-3 and 22:6n-3] and flax oil [rich in 18:3n-3] compared to oils rich in 18:2n-6 slow disease progression (10,11). Furthermore, a fish oil diet mitigates the detrimental effects of a high fat diet rich in (n-6) fatty acids in weanling Han:SPRD-*cy* rats (11).

However, compared to this rat model, the effects of dietary oil rich in (n-3) fatty acids are unresolved in studies using adult pcy mice given a moderate level of dietary fat. In the long-term fish oil appears to be detrimental (18), while in the short-term it appears to be beneficial (19). Therefore, to differentiate between possible effects of oils containing distinct (n-3) fatty acids, in the second study weanling pcy mice were fed diets containing high and low levels of corn oil [rich in 18:2n-6] compared to flax oil [rich in

18:3n-3] or a novel algal oil [rich in 22:6n-3] in order to determine whether fat level effects are influenced by fat type in this model of renal disease.

2.3 Materials and Methods

Animals

CD1-pcy/pcy (pcy) mice were obtained from our breeding colony that was established from mice provided to us by V.H. Gattone II, University of Kansas Medical Center. The animal experimental protocols were in accordance with the guidelines of National Institutes of Health Guide for the Care and Use of Laboratory Animals. All mice were housed in individual cages under temperature, humidity and light-controlled conditions. All diet ingredients, with the exception of flax and algal oils, were purchased from Dyets Inc. (Bethlehem, PA) or Harlan Teklad (Madison, WI). Flax oil (FO) was a generous gift from Bioriginal Food and Science Corporation (Saskatoon, SK) and algal oil (DO) from Martek Biosciences Corporation (Winchester, KY).

Diets and Experimental Protocol

Study 1 had three dietary treatments and two genders in a 3 x 2 design, with each group having eight mice. Adult male and female mice, at 70 d of age, were randomly assigned to one of three diets containing fat at either a low (4%, 4g/100g diet), medium (10%, 10g/100g diet) or high level (20%, 20g/100g diet). These diets were based on the AIN-93M diet for adult rodents, which uses soybean oil as the lipid source (20), and differed only in fat level. This diet contains 8g 18:3n-3 and 53g 18:2n-6 per 100g of total fatty acids present (11). Energy from fat and carbohydrate were substituted for each other and other ingredients were adjusted to maintain a constant nutrient-to-energy ratio in these diets. All mice were fed the experimental diets for 130 d.

In study 2, male and female mice were randomly assigned to one of six experimental diets at weaning (4 wk of age, n=8/diet group). The diets contained three types of dietary

oils, namely corn [rich in 18:2n-6], flaxseed [rich in 18:3n-3], and DHASCO [algal oil rich in 22:6n-3], at high (20%) and low (7%) levels, providing 20g and 7g of fat/100g diet, respectively, in a 2 x 2 x 3 design. To compensate for a potential essential fatty deficiency in the DHASCO oil diet, corn oil was added at the ratio of 4:1 (4g of DHASCO oil, 1g of corn oil). The flaxseed oil diet was treated in a similar fashion. Diets are indicated as CO, containing corn oil, DO, containing DHASCO/corn oil (4:1, g/g) and FO, containing flaxseed/corn oil (4:1, g/g). The fatty acid compositions of these diets are shown in Table 2-1. Since these are growing mice, the level of fat in the low fat diet was 7g/100g diet as prescribed in the AIN-93G diet (compared to 4g fat /100g diet in the maintenance diet fed to the adult mice in study 1). Although study 2 was designed as a longer feeding trial, the study was shortened since two males from the high DO group and one male from the low DO group died of renal failure by 8 wk of feeding. Mice were added to the study as they became available from the breeding colony and fed for an 8 wk period. This allowed us to allocate additional mice to the groups in which mice died along with littermates placed on the other diets, thus restoring an n=8 for all groups at the end of the study for analyses. In addition to the 3 mice that died of renal failure, some mice did not maintain fluid volume in the last weeks of the study and had to be rehydrated with 0.9% physiologic saline (administered subcutaneously). Weight loss and failure of a portion of the skin raised by "tenting" to resume its normal shape were used to determine whether rehydration was necessary. The average number of treatments per mouse was two, and the volume of saline used was determined based on the extent of weight loss. No animals were dehydrated at termination.

Mice were weighed weekly and at the end of the feeding period were killed and trunk blood was collected to obtain serum. Livers and right kidneys were removed, weighed and frozen in liquid nitrogen. Left kidneys were removed, weighed and fixed in 10% buffered formalin for morphological and histological analyses.

Histology and Immunohistochemistry

The left kidney was embedded in paraffin and sectioned at 5 microns. Sections for cyst area measurement were stained with hematoxylin and eosin and those for quantitative analysis of fibrosis with aniline blue (in adaptation of Masson's trichrome stain) that permits image analysis measurement using a standard incandescent microscope light source. This adaptation demonstrates perfect concordance of staining with an immunofluorescent detection of collagen type III (7,11,21).

As a measure of renal injury, detection of oxidized modifications of LDL (ox-LDL, including Cu^{2+}- ox-LDL and malondialdehyde-LDL) was carried out using a 1:50 dilution of rabbit anti-Cu^{2+}-ox-LDL polyclonal antibody for 30 min (AB3230, Chemicon International, Temecula, CA) (10). Secondary detection was done using Dako EnVision Plus system (K4008, Dako Corporation, CA). Sections were counterstained with hematoxylin (Dako Mayer's hematoxylin, S3309, Dako Corporation, Carpinteria, CA).

Image Analysis

An imaging system comprising of a Spot Junior CCD camera mounted on an Olympus BX60 microscope was used for image analysis. After being captured using the SPOT software (version 3.10), images were analyzed as described previously (7,10,11) using the Image Pro Plus (version 4.10, Media Cybernetics, Silverspring, MD) software for cyst area, renal fibrosis and ox-LDL. Briefly, the portion of tissue section occupied by

tubular lumen or cyst was measured through a series of images at 10X objective starting from a random field of tissue section until 25 measurements from 3-5 whole kidney cross sections were collected. All measurements were carried out in a blinded fashion. Identification of tubular lumen or cyst was performed by automated measurements using hue and intensity characteristics. Renal fibrosis ratio was determined using a 20X objective and using the proportion of section areas that had taken up aniline blue stain. Cyst area ratio and renal fibrosis ratio were determined in this manner and expressed relative to left kidney and body weight to yield cyst or fibrosis volume (assuming 1g =1mL) as described previously (7,10,11). Areas positive for fibrosis and ox-LDL were expressed as the fraction of solid tissue area, thereby correcting for the extent of cystic change in each kidney. Cyst and fibrosis volume reflect renal cyst growth and fibrosis, respectively.

Biochemistry

Serum urea nitrogen (SUN) was determined spectrophotometrically using reagents from Sigma kit 640-A (Sigma Chemical Co., MO).

For analyses of dietary fat, two grams of diet were homogenized in chloroform/methanol (2:1 , by vol) and filtered. After the addition of water, separation of the organic and aqueous phases was facilitated by letting the mixture sit overnight at room temperature. The organic phase was drawn off, evaporated to dryness at 50-70 °C and resuspended in 1 ml of toluene. The fatty acids were methylated using 3N methanolic HCl at 80 °C for 1 h. Fatty acid methyl esters were extracted in hexane and analyzed by gas chromatography.

For kidney fatty acid analyses lipids were extracted from the right kidneys of four mice, randomly selected from each group. Ten mg of lyophilized kidney was homogenized in chloroform/methanol (2:1 , by vol) containing 0.01% butylated hydroxytoluene. After centrifugation at 1500xg for 15 min, the supernatant was treated with 0.73% NaCl and was recentrifuged. The aqueous phase was discarded and the organic phase was washed twice with theoretical upper phase containing chloroform/methanol/water (3:48:47, by vol). The organic layer was transferred to a clean glass tube, dried under nitrogen and resuspended in 0.6 mL of toluene. The lipid extracts were transmethylated using 3N methanolic HCl at 80°C for 2 h. After washing twice with water and centrifuging, the organic phase was dried under nitrogen and resuspended in 50 μL of hexane. Both diet and kidney fatty acid methyl esters were separated by gas liquid chromatography on a Varian Star 3400 (Varian Inc, ON), using a 30m capillary column, with an internal diameter of 0.25 mm and a 0.25 μm thick film (Agilent Technologies, ON).

For conjugated diene analyses, lipids were extracted from livers in the same way as from kidneys, and the conjugated diene concentration was determined spectrophotometrically using the American Oil Chemists' Society Official Method Ti la-64 (22). The lipid extracts were diluted in isooctane and absorbance of samples at 233 nm was measured. Using oxidized oil with a known conjugated diene concentration as a reference, the detection limit was determined to be 17ng of conjugated dienes.

Statistical Analyses

Data were analyzed using 2-way (study 1) and 3-way (study 2) ANOVA, with litter included as a random effect, using SAS software (SAS, Cary, NC). Normality of the

data was tested using a plot of residuals vs. predicted and the Shapiro-Wilk's W statistic. Data were normalized by logarithmic transformation if necessary. Differences between means were tested using post-hoc t-tests (simple contrasts). Post-hoc t-tests were performed only if the overall main or interaction effect was significant at $P<0.05$. Main and interaction effects were considered significant at $P<0.05$. In several cases interactions of type or level with gender were present ; in these cases male and female data were analyzed separately. In some cases, specific fatty acids were present in trace amounts (<0.1mol/100mol total fatty acids) ; for these fatty acids, only the groups that had >0.1mol/100mol of total fatty acids were included in the analyses.

Chi-square analyses were performed on the number of mice requiring rehydration in study 2. Simple effects of fat type, fat level and gender were compared by this test.

2.4 Results

Fat Level Effects

In adult *pcy* mice, high compared to low fat diets resulted in higher kidney weights and SUN concentrations (Table 2-2). Renal cystic growth and fibrosis were extensive and were not affected by fat level in these animals at 200 d of age. In the early stages of renal disease, as observed in study 2, fat level effects were observed in renal fibrosis (Table 2-3), the number of healthy mice (see below) and some renal fatty acid levels (Table 2-4). Renal fibrosis was reduced in low fat compared to high fat fed mice in all diets (Table 2-3), but the detrimental effects of high fat were mitigated by FO, with fibrosis in the high fat fed FO group being similar to that in the low fat CO and DO groups (Table 2-3).

In addition to the 3 mice that died of renal failure in study 2 (2 on high DO and 1 on low DO diet), some mice could not maintain fluid volume in the last weeks of the study and had to be rehydrated with physiologic saline. The number of animals that had to be treated in this way included 7 high DO fed males, 2 high DO fed females, 2 high FO fed males, 1 high CO fed male and 1 low DO fed male. Chi-square analyses of fat level effects (within each fat type) revealed that significantly more mice in the high fat DO group required rehydration than in the low fat DO group.

Fat Type Effects

In study 2, after 8 weeks of feeding, kidney weights of DO fed mice were higher than those of CO fed mice, and SUN concentrations and cyst volumes were higher in DO compared with both CO and FO fed mice (Table 2-3). Body weights were lower in high fat DO fed male mice, compared to other male mice fed high fat diets (Table2- 3). There

was increased fibrosis in the DO and CO fed mice, compared to FO fed mice (Fig. 2-1), and ox-LDL was higher in DO compared to FO fed mice (Table 2-3). Chi-square analyses of fat type effects in mice that required rehydration revealed that mice on the high fat DO diet required rehydration more often those on the high CO or FO diets.

In order to assess whether the higher ox-LDL in DO fed mice was a reflection of systemic oxidative damage due to the higher polyunsaturated fatty acid content of the diet, conjugated dienes were assessed in the liver, a tissue not affected by cystic injury at this age. There was no evidence of peroxidation in the liver, as the level of conjugated dienes was below the detection limit of 17 ng, which represented less than 0.003% of total lipid (data not shown).

Renal fatty acid levels reflected the fatty acid compositions of the diets and as a result, 18:2n-6, 18:3n-3 and 22:6n-3 were the highest in the CO, FO and DO diets respectively (Table 2-4). Although the level of 18:2n-6 provided in the FO compared to DO diets was only 2-fold higher, the levels of 20:4n-6 in the kidneys of FO fed mice were 7-12 fold higher. Compared to the kidneys of CO fed mice, the levels of 20:4n-6 were 13-15 fold lower in kidneys of DO fed mice and 2 fold lower in kidneys of FO fed mice.

Gender Effects

Several markers of renal injury and function indicated a lesser degree of renal injury in females. However, the dietary fat level and type effects in females were not different from those in males. A few interactions between gender and fat level and type on body weight and kidney weight respectively indicated that dietary effects on these were not as great in females compared to males.

Table 2-1. Fatty Acid Composition of the Experimental Diets (Study 2).

	CO	DO	FO
10:0	-[a]	0.89±0.02[b]	-
12:0	-	3.36±0.07	-
14:0	-	12.67±0.26	-
16:0	10.91±0.01	14.67±0.16	6.54±0.07
16:1n-7	0.11±0.00	1.15±0.02	-
18:0	2.08±0.03	1.14±0.00	3.21±0.01
18:1n-7	0.54±0.01	0.12±0.00	0.63±0.00
18:1n-9	26.63±0.26	19.92±0.06	19.16±0.00
18:2 n-6	57.3±0.29	13.1±0.08	23.48±0.23
18:3n-3	0.94±0.07	0.23±0.00	45.43±0.32
22:5 n-3	-	-	-
22:6n-3	-	31.36±0.33	-

[a]<0.1g/100g total fatty acids.

[b]Values represent means±SEM of two determinations of the major fatty acids (≥ 0.5g/ 100g total fatty acids present in any diet).

Table 2-2. Body and kidney weights and renal disease markers in male and female pcy mice fed 4g, 10g or 20g of soybean oil per 100g diet for 130 days (study 1).

Fat level (g/100g diet)	4%	10 %	20%	Pooled SEM	Effects
Body weight (g)					
Male	40.0[a]	38.5	40.5	1.38	G
Female	32.5	32.0	36.9		
Relative Kidney wt (g/100g body wt)					
Male	2.7	3.0	3.5	0.24	G, L[b]
Female	2.2	2.5	2.7		
SUN (mmol/L)					
Male	10.4	12.7	13.4	2.42	G, L[b]
Female	8.9	9.7	10.4		
Cyst Volume (mL/Kg body wt)[c]	10.8	11.5	13.9	1.02	None
Renal Fibrosis (ml/Kg body wt)[c,d]	2.39	1.96	1.60	0.39	None

Abbreviations: CO, corn oil diet ; DO, DHASCO/corn oil (4:1, g/g) diet ; FO, flaxseed/corn oil (4:1, g/g) diet.

[a]Values are Least Square Means (n=8).

[b]P<0.05, high compared to low fat fed mice.

[c]Data from males only.

[d]Corrected for solid tissue area.

Table 2-3. Body and kidney weights and renal disease markers in male and female *pcy* mice fed diets containing corn oil (CO), DHASCO/corn (4:1 g/g, DO) and flaxseed/corn oil (4:1 g/g, FO) diets at 20g or 7g of fat per 100g diet for 8 wk (study 2).

Fat Type	CO		DO		FO		Pooled	Effects
Fat Level (g/100g diet)	7%	20%	7%	20%	7%	20%	SEM	
Body weight (g)[a]								
Male	30.4[b]	32.2	28.0	24.1	31.3	32.1	0.925	T, L×T [c]
Female	23.8	26.5	24.7	25.4	26.1	27.4	1.320	None
Relative Kidney wt (g/100g body wt)[a]								
Male	2.43	2.74	3.24	3.22	2.85	2.94	0.164	T[d]
Female	2.10	1.70	2.31	1.77	2.06	2.06	0.122	None
SUN (mmol/L)								
Male	7.6	7.9	12.1	10.5	7.7	7.4	1.099	G, T[e]
Female	6.0	6.4	6.8	8.1	6.5	6.5		
Renal Fibrosis (mL/Kg body wt)[f]								
Male	0.54	0.84	0.51	0.77	0.28	0.48	0.077	G, T[g], L
Female	0.46	0.54	0.58	0.76	0.28	0.35		
Cyst Volume (mL/Kg body wt)								
Male	6.6	7.7	8.5	8.7	7.1	7.8	0.546	G, T[e]
Female	5.6	4.9	6.2	8.1	5.1	5.4		
Oxidized LDL (cells/high power field)[f]								
Male	0.47	0.59	0.62	0.67	0.41	0.49	0.076	T[h]
Female	0.41	0.40	0.45	0.71	0.35	0.36		

Abbreviations used: SUN, serum urea nitrogen ; G, gender ; L, level.

[a]Interactions with gender were present ; therefore data were analyzed separately for male and female mice.

[b]Values are Least Square Means (n=8).

[c]Interaction between fat level and type. The only significant simple fat level or type effects was observed in the high fat DO males, which had significantly lower body weights than males in all the other groups.

[d]$P<0.05$, DO>CO.

[e]$P<0.01$, DO>CO, FO.

[f]Corrected for solid tissue area.

[g]$P<0.0001$, FO<CO, DO.

[h]$P<0.005$, DO>FO.

Table 2-4. Kidney fatty acid composition (mol/100mol of total fatty acids) in male and female *pcy* mice given CO, DO and FO diets at 20g or 7g of fat per 100g diet.

Fatty Acid	Gender	CO		DO		FO		Effect
		20%	7%	20%	7%	20%	7%	
C14:0	Male	0.48±0.06[a]	0.87±0.05	2.57±0.52	1.52±0.18	0.52±0.03	0.89±0.23	T, L×T
	Female	0.42±0.03	0.97±0.05	3.21±0.67	1.82±0.20	0.63±0.10	0.94±0.15	
C16:0	Male	20.11±0.31	22.41± 0.21	24.00±1.11	25.84±0.86	18.05±0.13	23.57±1.65	G, L,T
	Female	20.61±0.42	25.06±0.25	22.93±0.56	27.58±0.39	19.71±0.22	23.97±0.30	
C18:0	Male	14.60±0.28	13.29±0.18	14.82±1.03	15.36±0.47	15.66±0.40	13.76±1.77	L
	Female	15.47±0.50	13.65±0.34	15.44±1.24	13.22±1.00	15.73±1.36	13.82±0.81	
C16:1n-7	Male	0.43±0.04	2.05±0.05	0.70±0.11	1.72±0.29	0.46±0.03	2.71±0.70	L
	Female	0.44±0.02	2.32±0.17	0.91±0.19	2.64±0.32	0.91±0.17	3.05±0.64	
C18:1n-7[b]	Male	1.34±0.06	2.69±0.11	0.68±0.05	1.23±0.03	1.04±0.03	2.27±0.20	L,T, L×T
	Female	1.36±0.03	2.28±0.11	0.63±0.02	1.76±0.04	1.05±0.04	2.22±0.06	L,T

C18:1n-9	Male	9.79±0.63	13.54±1.17	11.44±1.24	12.57±0.76	11.13±0.61	15.23±2.80	G, L
	Female	10.85±0.78	16.61±0.76	12.27±1.56	16.27±1.05	12.85±1.72	16.88±2.44	
C18:2n-6[b]	Male	19.56±1.11	11.95±0.42	12.63±0.54	8.47±0.21	16.62±0.37	10.65±0.61	L,T, L×T
	Female	21.11±1.34	13.91±0.38	11.08±0.47	9.27±0.46	17.90±0.55	10.51±0.47	L,T, L×T
C18:3n-3[d]	Male	0.14±0.01)	-[c]	-	-	6.90±0.78	2.91±0.75	L
	Female	0.20±0.02	0.10±0.01	-	-	7.62±1.69	2.60±0.19	
C20:2n-6	Male	1.03±0.04	0.56±0.07	0.25±0.03	0.23±0.01	0.43±0.04	0.40±0.05	G, L, T, L×T
	Female	1.04±0.03	0.53±0.06	0.17±0.01	0.19±0.004	0.35±0.03	0.22±0.01	
C20:4n-6[b]	Male	13.95±0.43	13.68±0.84	0.55±0.04	1.09±0.03	6.76±0.38	7.21±1.06	T
	Female	16.64±0.82	15.79±0.47	0.53±0.03	1.43±0.04	8.87±1.09	9.11±0.61	T
C20:5n-3[d]	Male	-	-	8.24±0.60	7.23±0.52	2.04±0.07	2.71±0.41	T, L×T
	Female	-	-	9.76±1.06	6.95±0.46	2.71±0.32	3.35±0.48	
C22:5n-6[d]	Male	4.44±0.50	6.76±0.31	-	-	-	-	G, L, G×L
	Female	1.48±0.04	1.86±0.11	-	-	-	-	
C22:6n-3	Male	9.36±1.16	7.23±0.25	20.54±0.58	20.77±0.91	15.61±0.85	11.60±4.44	T

Female	5.54±0.23	4.49±0.15	19.47±0.85	14.81±0.73	6.87±0.87	8.19±0.96

Abbreviations used: G, gender, T, type and L, level.

[a] Values expressed as Means±SEM of fatty acids present at a level of > 1 mol/100 mol total fatty acids in kidneys of at least one diet group.

[b] Interactions with gender were present ; therefore data were analyzed separately for male and female mice.

[c] Less than 0.1moles/100 moles total fatty acids.

[d] Statistical analyses performed only on groups having >0.1mol/100mol of total fatty acids.

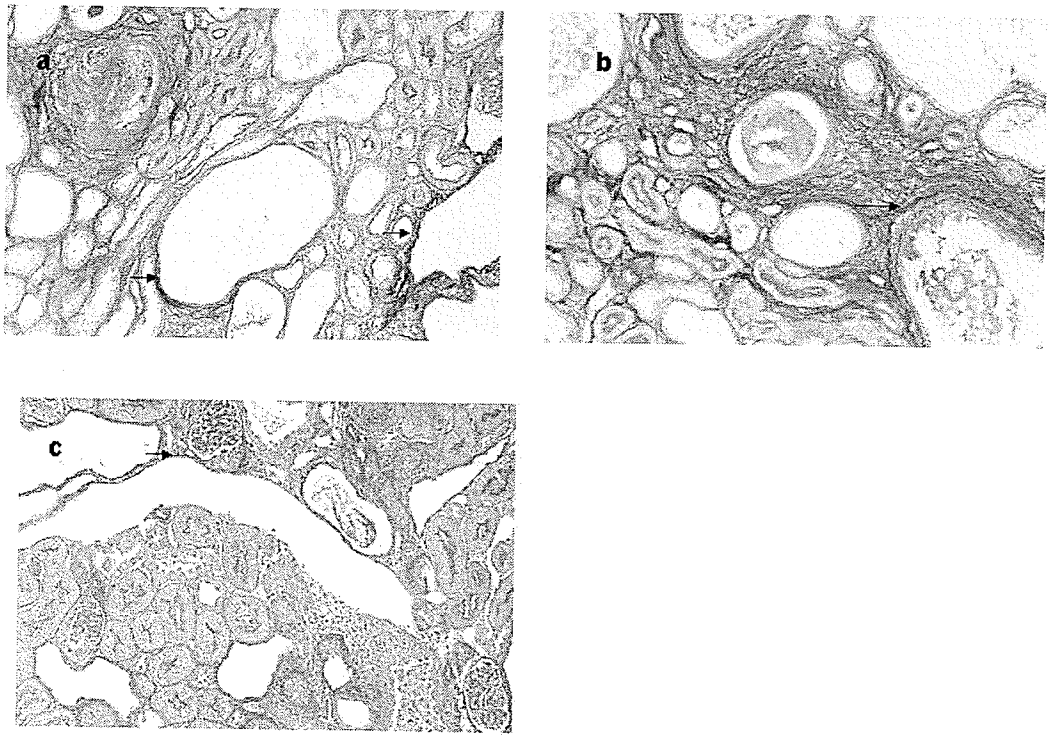

Figure 2-1. Renal fibrosis in male *pcy* mice fed high fat diets (20g of fat/100g diet) (a) containing corn oil (CO), (b) DHASCO/corn oil (4:1 g/g, DO) or (c) flaxseed/corn oil (4:1 g/g, FO) oil. Aniline blue stain, magnification 40X. Arrows point to areas of increased renal fibrosis identified by darkly stained collagen deposits in interstitial spaces, especially around periphery of cysts.

2.5 Discussion

A high fat diet worsens renal disease progression in *pcy* mice, with a significant increase in renal fibrosis manifested early in the disease process, and elevated SUN and kidney size observed in the older animals. There was a 3-fold increase in renal fibrosis levels in 200-day-old adult *pcy* mice compared to 84-day-old younger mice. This change is similar in magnitude with previously reported renal fibrotic damage in *pcy* mice, which becomes progressively more severe with age (23). The extensive level of renal fibrosis in the older animals may have obscured the changes observed in the younger mice, but the effect on function, as indicated by elevated SUN levels, suggests that the early changes did have long term effects. These findings in the *pcy* mouse are consistent with previous studies which demonstrated that a high fat diet accelerates renal disease progression in the Han:SPRD-*cy* rat (11,12). It also further extends those studies to demonstrate that the benefits of a low fat diet are also present in female *pcy* mice. Notably, reducing the dietary fat level slows renal disease progression, yet maintains normal body growth.

The most notable fat type effect on disease progression was observed in the markedly reduced renal fibrosis in the FO compared to CO and DO fed mice. In addition, the FO diet mitigated the negative effect of high fat feeding on fibrosis with the high FO fed mice having renal fibrosis similar to the low fat fed mice on the other diets. The beneficial effect of FO herein is consistent with the demonstrated beneficial effect of oils with (n-3) fatty acids on renal injury in the weanling Han:SPRD-*cy* rat (10,11). In contrast to the beneficial effects of FO, mice fed DO compared to CO diets failed to thrive, had lower body weights, increased cystic growth and impaired kidney function (higher SUN concentrations). This is reminiscent of previous findings of reduced survival

in adult *pcy* mice fed a fish oil diet containing (n-3) fatty acids (14). Studies that have exhibited a beneficial effect of dietary (n-3) fatty acids on renal injury in the Han:SPRD-*cy* rat model have been short-term supplementation studies in weanling rats and there is currently no documentation of the long-term effects of dietary (n-3) supplementation in this model. Therefore, the possibility that short-term benefits of (n-3) fatty acids do not persist in the long-term cannot be overlooked. It is, therefore, imperative to exercise caution in extrapolating the apparent benefits of diets containing (n-3) fatty acids in early renal injury to potential benefits in later stages of disease progression.

The greater amount of renal inflammation in the early stages of renal injury in the Han:SPRD-*cy* rat model compared to the *pcy* mouse may help explain why (n-3) fatty acids are beneficial in early stages of disease progression in the Han:SPRD-*cy* rat, while having lesser benefits in the *pcy* mouse. Supplementing the diet with (n-3) fatty acids causes a shift in eicosanoid production, with 20:5n-3 inhibiting the metabolism of 20:4n-6 to the more inflammatory eicosanoids, thereby exerting an anti-inflammatory effect in renal disease (24). Thus, the beneficial effects of (n-3) fatty acids in early renal disease could be due to a reduction in renal inflammation by altering the renal eicosanoid profile.

Although the DO diet also may have been expected to reduce renal inflammation because of its high (n-3) fatty acid content, the reduction in eicosanoid precursor may have been excessive in these mice. While overproduction of eicosanoids may increase inflammation, normal levels of eicosanoids play important roles in the maintenance of kidney functions, including blood flow, glomerular filtration rate, urine concentration and renin release (25,26). Although there was increased 20:5n-3 in the kidneys of DO fed mice, the level of 20:4n-6 was markedly reduced, perhaps resulting in a deficiency of

critical eicosanoids in these kidneys. Competition for the delta-6 desaturase enzyme at the 18-carbon fatty acid level by (n-6) and (n-3) fatty acids has been documented (27), and feeding formulas rich in 22:6n-3 and 20:5n-3 and lacking in 20:4n-6 results in reduced growth of pre-term infants (28,29). It is of interest to determine whether the inclusion of 20:4n-6 in the DO diet would have been beneficial, as is the case with infant formulas. In the previous studies in which a diet containing (n-3) fatty acids slowed the progression of renal injury, 20:4n-6 levels were maintained at levels similar to those in the FO fed mice in the current study (8,11). Thus the adverse effects of the high DO diet may have been due to the marked suppression of 20:4n-6, resulting in a greater reduction of critical eicosanoid formation.

Lesser magnitude of renal injury observed in females is consistent with well-documented findings of gender-associated dimorphism in human and animal PKD. The average age of renal failure is about 5 years earlier in men than in women with PKD (30,31) and disease progression is more aggressive in male Han:SPRD-*cy* rats than in the females (32). However, dietary fat effects were similar in female and male *pcy* mice, demonstrating the relevance of dietary fat restriction in females in addition to the previously studied males (11,12).

Renal ox-LDL formation is negligible in normal kidneys, but increases with extent of injury in the kidneys of the Han:SPRD-*cy* rat (10). This is consistent with other studies in which ox-LDL was immunohistochemically demonstrated in glomeruli of rats and humans with glomerulosclerosis (33,34), and in various immune and non-immune mediated renal injuries, including PKD in which oxidized products accumulate (35-37). Compromised resistance to oxidant injury due to the depletion of renal antioxidant

enzymes (38) is observed in the Han:SPRD-*cy* rat. We also found the highest levels of ox-LDL in the DO fed mice, which had the greatest development of renal injury. Although an enrichment of 22:6n-3 in tissue membranes increases their susceptibility to lipid peroxidation (39), the lack of significant accumulation of conjugated dienes in the unaffected livers in our study suggests that the increased renal expression of ox-LDL in mice fed DO is not simply due to an increase in peroxidation of the higher levels of (n-3) polyunsaturated fatty acids. In fact, both DO and FO fed mice have similar amounts of renal (n-3) polyunsaturated fatty acids compared to the CO fed mice, but differing levels of ox-LDL, as well as other markers of renal injury. However, the possibility that injured kidneys are more susceptible to fatty acid peroxidation cannot be ruled out.

Our results demonstrate that dietary fat alters disease progression in both male and female *pcy* mice. Low fat slows the development of renal injury and flax oil containing 18:3n-3 reduces early renal disease progression. However, caution is warranted in the use of (n-3) fatty acids as potential therapeutic agents in this form of renal injury, as very high levels of 20 and 22 carbon (n-3) fatty acids without adequate 20:4n-6 appear to be detrimental.

2.6 References

1. Sutters M, Germino GG. Autosomal dominant polycystic kidney disease: molecular genetics and pathophysiology. J Lab Clin Med. 2003 ;141:91-101.

2. Igarashi P, Somlo S. Genetics and pathogenesis of polycystic kidney disease. J Am Soc Nephrol 2002 ; 13:2384-2398.

3. Aukema HM, Housini I, Rawling JM. Dietary soy protein effects on inherited polycystic kidney disease are influenced by gender and protein level. J Am Soc Nephrol 1999 ; 10:300-308.

4. Keith DS, Torres VE, Johnson CM, Holley KE. Effect of sodium chloride, enalapril, and losartan on the development of polycystic kidney disease in Han:SPRD rats. Am J Kidney Dis 1994 ; 24:491-498.

5. Tomobe K, Philbrick D, Aukema HM, Clark WF, Ogborn MR, Parbtani A, Takahashi H, Holub BJ. Early dietary protein restriction slows disease progression and lengthens survival in mice with polycystic kidney disease. J Am Soc Nephrol 1994 ; 5: 1355-1360.

6. Torres VE, Mujwid DK, Wilson DM, Holley KH. Renal cystic disease and ammoniagenesis in Han:SPRD rats. J Am Soc Nephrol 1994 ; 5:1193-1200.

7. Ogborn MR, Bankovic-Calic N, Shoesmith C, Buist R, Peeling J. Soy protein modification of rat polycystic kidney disease. Am J Physiol 1998 ; 274: F541-549.

8. Ogborn MR, Nitschmann E, Weiler H, Leswick D, Bankovic-Calic N. Flaxseed ameliorates interstitial nephritis in rat polycystic kidney disease. Kidney Int 1999 ; 55:417-423.

9. Philbrick DJ, Bureau DP, Collins FW, Holub BJ. Evidence that soyasaponin Bb retards disease progression in a murine model of polycystic kidney disease. Kidney Int. 2003 ; 63:1230-1239.

10. Ogborn MR, Nitschmann E, Bankovic-Calic N, Weiler HA, Aukema HM. Dietary flax oil reduces renal injury, oxidized LDL content, and tissue n-6/n-3 FA ratio in experimental polycystic kidney disease. Lipids. 2002 ; 37:1059-1065.

11. Lu J, Bankovic-Calic N, Ogborn M, Saboorian MH, Aukema HM. Detrimental effects of a high fat diet in early renal injury are ameliorated by fish oil in Han:SPRD-cy rats. J Nutr. 2003 ; 133:180-186.

12. Jayapalan S, Saboorian MH, Edmunds JW, Aukema HM. High dietary fat intake increases renal cyst disease progression in Han:SPRD-cy rats. J Nutr. 2000 ; 130:2356-2360.

13. Takahashi H, Calvet JP, Dittemore-Hoover D, Yoshida K, Grantham JJ, Gattone V H, 2nd. A hereditary model of slowly progressive polycystic kidney disease in the mouse. J Am Soc Nephrol. 1991 ; 1: 980-989.

14. Aukema HM, Ogborn MR, Tomobe K, Takahashi H, Hibino T, Holub BJ. Effects of dietary protein restriction and oil type on the early progression of murine polycystic kidney disease. Kidney Int. 1992 ; 42:837-842.

15. Gattone VH 2nd, Kuenstler KA, Lindemann GW, Lu X, Cowley BD Jr, Rankin CA, Calvet JP. Renal expression of a transforming growth factor-alpha transgene accelerates the progression of inherited, slowly progressive polycystic kidney disease in the mouse. J Lab Clin Med. 1996 ; 127:214-222.

16. Omran H, Haffner K, Burth S, Fernandez C, Fargier B, Villaquiran A, Nothwang HG, Schnittger S, Lehrach H, Woo D, Brandis M, Sudbrak R, Hildebrandt F. Human adolescent nephronophthisis: gene locus synteny with polycystic kidney disease in pcy mice. J Am Soc Nephrol. 2001 ; 12:107-113.

17. Guay-Woodford LM. Murine models of polycystic kidney disease: molecular and therapeutic insights. Am J Physiol Renal Physiol. 2003 ; 285:F1034-1049.

18. Aukema HM, Yamaguchi T, Takahashi H, Philbrick DJ, Holub BJ Effects of dietary fish oil on survival and renal fatty acid composition in murine polycystic kidney disease. Nutr Res. 1992 ; 12:1383-1392.

19. Yamaguchi T, Valli VE, Philbrick D, Holub B, Yoshida K, Takahashi H. Effects of dietary supplementation with n-3 fatty acids on kidney morphology and the fatty acid composition of phospholipids and triglycerides from mice with polycystic kidney disease. Res Commun Chem Pathol Pharmacol. 1990 ; 69:335-351.

20. Reeves PG, Nielsen FH, Fahey GC Jr. AIN-93 purified diets for laboratory rodents: final report of the American Institute of Nutrition ad hoc writing committee on the reformulation of the AIN-76A rodent diet. J Nutr. 1993 ; 123:1939-1951.

21. Cohen AH. Masson's trichrome stain in the evaluation of renal biopsies. Am J Clin Pathol. 1975 ; 65:631-643.

22. AOCS Official Method Ti-1a-64, Spectrophotometric determination of conjugated dienoic acid. In Official Methods and Recommended Practices of the American Oil Chemists' Society. Fourth ed. American Oil Chemists' society, Champaign, Ill. 1989

23. Okada H, Ban S, Nagao S, Takahashi H, Suzuki H, Neilson EG. Progressive renal fibrosis in murine polycystic kidney disease: an immunohistochemical observation. Kidney Int. 2000 ; 58:587-597.

24. Lefkowith JB, Klahr S. Polyunsaturated fatty acids and renal disease. Proc Soc Exp Biol Med. 1996 ; 213:13-23.

25. Breyer M, Badr K. Arachidonic acid metabolites and the kidney. In B. Brenner, editor. The Kidney 5 ed. W.B. Saunders Co ; 1996

26. Imig JD. Eicosanoid regulation of the renal vasculature, Am J Physiol Renal Physiol. 2000 ; 279:F965-981.

27. Sprecher H. Metabolism of highly unsaturated n-3 and n-6 fatty acids. Biochim Biophys Acta. 2000 ; 1486:219-231.

28. Carlson SE,Werkman SH. A randomized trial of visual attention of preterm infants fed docosahexaenoic acid until two months. Lipids. 1996 ; 31:85-90.

29. Lapillonne A, Carlson SE. Polyunsaturated fatty acids and infant growth. Lipids. 2001 ; 36:901-911.

30. Gabow PA, Johnson AM, Kaehny WD, Kimberling WJ, Lezotte DC, Duley IT, Jones RH. Factors affecting the progression of renal disease in autosomal- dominant polycystic kidney disease. Kidney Int. 1992 ; 41:1311-1319.

31. Choukroun G, Itakura Y, Albouze G, Christophe JL, Man NK, Grunfeld JP, Jungers P. Factors influencing progression of renal failure in autosomal dominant polycystic kidney disease. J Am Soc Nephrol. 1995 ; 6:1634-1642.

32. Cowley BD Jr, Rupp JC, Muessel MJ, Gattone VH 2nd. Gender and the effect of gonadal hormones on the progression of inherited polycystic kidney disease in rats. Am J Kidney Dis. 1997 ; 29:265-272.

33. Lee HS, Kim YS. Identification of oxidized low density lipoprotein in human renal biopsies. Kidney Int. 1998 ; 54:848-856.

34. Magil AB, Frohlich JJ, Innis SM, Steinbrecher UP. Oxidized low-density lipoprotein in experimental focal glomerulosclerosis. Kidney Int. 1993 ; 43:1243-1250.

35. Baud L, Ardaillou R. Involvement of reactive oxygen species in kidney damage. Br Med Bull. 1993 ; 49:621-629.

36. Torres VE, Bengal RJ, Litwiller RD, Wilson DM. Aggravation of polycystic kidney disease in Han:SPRD rats by buthionine sulfoximine. J Am Soc Nephrol. 1997 ; 8:1283-1291.

37. Diamond JR, Karnovsky MJ. A putative role of hypercholesterolemia in progressive glomerular injury. Annu Rev Med. 1992 ; 43:83-92.

38. Maser RL, Vassmer D, Magenheimer BS, Calvet JP. Oxidant stress and reduced antioxidant enzyme protection in polycystic kidney disease. J Am Soc Nephrol. 2002 ; 13:991-999.

39. Song JH, Miyazawa T. Enhanced level of n-3 fatty acid in membrane phospholipids induces lipid peroxidation in rats fed dietary docosahexaenoic acid oil. Atherosclerosis. 2001 ; 155:9-18.

3. DIETARY FLAX OIL DURING PREGNANCY AND LACTATION RETARDS DISEASE PROGRESSION IN RAT OFFSPRING WITH INHERITED KIDNEY DISEASE

Reproduced with permission from

Sankaran D, Bankovic-Calic N, Peng CY, Ogborn MR, Aukema HM. Pediatric Research. 2006

© Lipincott Williams and Wilkins with the assistance of HighWire Press ®

3.1 Abstract

Dietary flax oil (FO) retards disease progression in growing or adult animal models of kidney disease. To determine whether dietary flax oil during the perinatal period would alter renal disease progression in offspring, Han-SPRD-*cy* rats with inherited cystic kidney disease were given diets with either 7% FO or corn oil (CO), throughout pregnancy and lactation. At 3 wk of age, offspring were then given either the same or the alternate diet for 7 weeks. Rats given FO during the maternal period had 15% less renal cyst growth compared to rats given no FO or FO only in the post-weaning period. Dietary FO, compared to CO, in the maternal period also resulted in 12% lower cell proliferation and 15% less oxidant injury in diseased kidneys of offspring. Including FO in both the maternal and post-weaning period resulted in 29-34% less renal interstitial fibrosis and 22-23% lower glomerular hypertrophy. Along with improved histology, these rats exhibited 13% less proteinuria and 30% lower creatinine clearance when dietary FO was given in the maternal period. The potential for dietary FO during pregnancy and lactation to positively modulate adult renal disease has significant implications for the 1 in 1000 individuals with congenital cystic kidney disease.

3.2 Introduction

Chronic kidney disease is a gradual irreversible loss of kidney function which usually leads to end-stage renal disease and the need for expensive renal replacement therapies. Its increasing prevalence (>50% rise in 10 years in the U.S and a 19% rise in 5 years in Canada) (1, 2) and staggering healthcare costs warrant further inquiry into treatment options that slow or prevent its progression. Dietary interventions such as altering dietary fat sources slow the progression of chronic renal disease. Dietary n-3 fatty acids from fish and flax sources have been shown to be reno-protective, particularly in renal injury that has an immune and/or inflammatory component (3-7). These protective effects of n-3 fatty acids on renal disease progression in humans or animal models have been demonstrated in adult or weanling animals.

The fetal programming hypothesis suggests that the "first" environment, the intrauterine, also influences the risk of chronic diseases in adult life (8). For example, higher maternal saturated fat intake has been linked to hyperinsulinemic, hyperglycemic, pro-atherogenic and hypertensive phenotypes in offspring (9-11), while a study with high maternal n-3 fatty acids intake failed to show such deleterious fetal programming effects (12). Impaired fetal nephrogenesis and reduced nephron number can result from maternal malnutrition and are associated with adult hypertension in humans (13) as well as experimental models of developmental programming (14-16). These reports indicate that renal organogenesis is susceptible to changes in the fetal environment which can modulate development of chronic diseases later in life.

The Han:SPRD-*cy* rat is an established model of autosomal dominant polycystic kidney disease (PKD) in which heterozygotes develop progressive cystic expansion, renal

interstitial fibrosis, inflammation and oxidative damage, as well as hypertension and uremia in adult life (17). Dietary flax (rich in n-3 fatty acids) reduces renal interstitial fibrosis, cystic growth and renal macrophage infiltration in this model of hereditary kidney disease when given in the post-weaning period of life (7, 18). The aim of the current study was to determine whether flax oil supplementation during pregnancy and lactation would slow the progression of renal disease in offspring of Han:SPRD-*cy* rats. To further delineate the effects of maternal dietary flax oil supplementation on renal injury, a group of animals that were given flax oil during both the maternal and post-weaning periods as well as a group of animals that were fed flax oil only in the post-weaning period were included.

3.3 Materials and Methods

Animals

All animal procedures were approved by the University of Manitoba Committee on Animal Care and were in accordance with the guidelines of the Canadian Council on Animal Care. Breeder Han:SPRD-*cy* rats [also known as PKD/Mhm (*cy*/+) rats] were derived from our breeding colony, which originated from the colony of Dr. Benjamin Cowley, University of Kansas Medical Center, Kansas City (17). They were randomly assigned to either a flax oil diet (FO, 7% oil, rich in 18:3n-3) or a corn oil control diet (CO, 7% oil, rich in linoleic acid, 18:2n-6) two weeks prior to mating and throughout pregnancy and lactation. Male offspring from both groups were weaned at three weeks of age and were given either the same maternal diet or the alternate diet for another seven weeks. Diet ingredients, with the exception of flax oil, were purchased from Dyets Inc. (Bethlehem, PA) or Harlan Teklad (Madison, WI). Flax oil (FO) was a generous gift from Bioriginal Food and Science Corporation (Saskatoon, SK). Diets were based on the AIN93G guidelines for rodent diets for optimal growth and adequate nutrition (19, 20). Hence the diets were identical (including calorie, carbohydrate, protein, mineral and vitamin content) except for the fat source.

Rats were weighed weekly and placed in metabolic cages for urine collection a week before termination. At the end of the feeding period, rats were anesthetized with CO_2 over-exposure, decapitated and trunk blood was collected to obtain serum. Left kidneys were removed and weighed. The left kidney was sectioned in half longitudinally across the hilum, and one half of wet kidney tissue was fixed in 10% buffered formalin for morphological and histological analyses.

Renal Biochemistry

Serum urea was determined spectrophotometrically using reagents from Sigma kit 640-A (Sigma Chemical Co., MO). Serum creatinine and urinary creatinine were measured using a method developed by Heingard and Tiderstrom and adapted for a micro-assay procedure using 96-well plates. Urinary protein was measured using the Bradford method for total protein.

Histology and Immunohistochemistry

The formalin-fixed left kidney was embedded in paraffin, sectioned at 5 microns and was processed using our previously described methods for histological and immunohistochemical analyses (7, 19). Transverse tissue sections (including cortex, medulla and papilla) were stained with hematoxylin and eosin for cyst area measurement and those for quantitative analysis of fibrosis with Sirius red (in adaptation of Masson's trichrome stain) which permits image analysis measurement using a standard incandescent microscope light source. Renal cell proliferation was assessed using a 1:50 dilution of an anti-mouse proliferating cell nuclear antigen (PCNA) antibody (M0879, Dako Corporation, Carpinteria, CA). Renal inflammation and oxidant injury were detected using 1:50 dilutions of a mouse anti-rat monocytes/macrophages monoclonal antibody (MAB 1435, Chemicon International, Temecula, CA) and a rabbit anti-Cu 2+-oxidized LDL polyclonal antibody (AB3230, Chemicon International, Temecula, CA), respectively. The Dako EnVision Plus system (K4008, Dako Corporation, Carpinteria, CA) was used for secondary detection. Animals were classified as affected by an experienced, blinded observer (NBC) on the basis of cyst growth and pathology that is characteristic of the disease.

Image Analysis

After being captured using a SPOT junior CCD camera by random stage movement through the sections, images were analyzed using the Image Pro version 4.5 package (Media Cybernetics, Silverspring, MD) as described previously (7, 19). An average of 25 measurements starting from a random field of tissue section from kidney cross sections were collected for all histomorphometric analyses. All measurements were carried out in a blinded fashion. The portion of tissue section occupied by tubular lumen or cyst was determined for cyst area measurements. Renal interstitial fibrosis and oxidant injury were measured by densitometry, while the number of cells stained positive for PCNA as well as macrophages were counted using the Image Pro version 4.5 package (Media Cybernetics, Silverspring, MD) as described previously (7, 19). Renal cyst area measurements were expressed relative to kidney weight-to-body weight ratios. PCNA positive cells in tubular epithelial cells were counted as these are the base cell type of cysts. Measurements of fibrosis, oxidized LDL and other cellular markers were corrected to solid tissue areas of sections to avoid underestimation of these variables due to empty cystic areas in these sections.

Using standard sterological techniques developed by Weibel (21), mean glomerular volume (MGV) was determined by measuring glomerular diameters of 30 randomly chosen glomeruli per kidney by light microscopy using hematoxylin and eosin stained sections. Using the aforementioned imaging system and a 20X calibration grid, the maximum diameter of each glomerulus was measured and converted to an estimate of glomerular volume using the following formula: mean glomerular area (MGA) was calculated as $MGA=\pi r^2$. MGV was calculated as $MGV=1.25(MGA)^{3/2}$. The value of

1.25 is derived from β/K, which are co-efficients based on assumptions made for the maximum diameter of spheres (β=1.38) and the distribution bias of section location (K= 1.10) (22).

Statistical Analyses

Data were analyzed using a general linear model ANOVA followed by post-hoc t-tests when interactions were present, using SAS software (SAS, Cary, NC). Normality of the data was tested using a plot of actual vs. predicted residuals and the Shapiro-Wilk's W statistic on the residuals. Data were normalized by logarithmic transformation if necessary. Post-hoc t-tests were performed only if the main or interaction effects were significant at $P<0.05$ or $P<0.1$ respectively.

3.4 Results

During the study period, all animals thrived on the diets. The diets given during the maternal period did not affect either body weights at weaning (pups given CO= 55.5g ± 1.1g and pups given FO=56.7g ± 1.1g) or litter size (mean litter size= 8.3 ± 0.7 for female breeders given CO and FO).

Dietary FO compared to CO in the maternal period improved renal histology and function in diseased offspring. The primary defect in Han:SPRD-*cy* rats is the growth and development of renal cysts that disrupt normal renal architecture, eventually causing structural damage leading to pathology. Dietary FO in the maternal period, alone or in combination with FO in the post-weaning period, resulted in 15-28 % less in cyst growth when compared to rats given FO only in the post-weaning period (Fig. 3-1). Less cyst growth resulted in smaller kidneys in these rats, whether expressed as unadjusted weights, relative to body weight (Table 3-1) or relative to liver weight (data not shown), thus supporting the cyst expansion data. This data indicates that the dietary FO in the maternal period had disease mitigating effects on the primary defect in this model of kidney disease.

Dietary FO in the maternal period also resulted in 14% fewer PCNA positive cells, reflecting less cell proliferation (Fig. 3-2). This protective effect of dietary FO in the maternal period was as effective as dietary FO in the post-weaning period. When FO was given in both time periods, no further benefit on cell proliferation was observed. A similar pattern was observed for oxidant injury (Fig. 3-3). Dietary FO in the maternal and post-weaning periods independently resulted in less staining for oxidized LDL (33% and 45% less respectively, compared to rats given CO in both feeding periods). Combining

the dietary FO treatments in both feeding periods did not enhance the effect of FO in the post-weaning period alone. Renal inflammation was not significantly altered by dietary FO in the maternal period, but was 21% lower with FO in the post-weaning period (Fig.3-4).

With respect to renal function, diseased rats compared to normal rats had worsened renal function as indicated by blood and urine parameters (Table 3-1). Concurrent with its beneficial effects on histology, dietary FO given during the maternal period resulted in less proteinuria (P=0.0125) and lower creatinine clearance (P=0.0001). This reduction in creatinine clearance was associated with higher levels of serum urea (P= 0.0039) and creatinine (P=0.0307).

To further probe glomerular and interstitial changes associated with reduced proteinuria in rats given FO during the maternal period, an examination of mean glomerular volumes and renal interstitial fibrosis was undertaken. Glomerular hypertrophy (Fig.3-5) and renal interstitial fibrosis (Fig.3-6) and were altered by dietary FO when given in the maternal period. However, in order to manifest this effect, dietary FO also had to be included in the post-weaning period. When dietary FO was given in both feeding periods, glomerular hypertrophy was lower by 22-23% (Fig.3-5) and interstitial fibrosis was 19-30% less (Fig.3-6), compared to any treatment that included dietary CO in either feeding period.

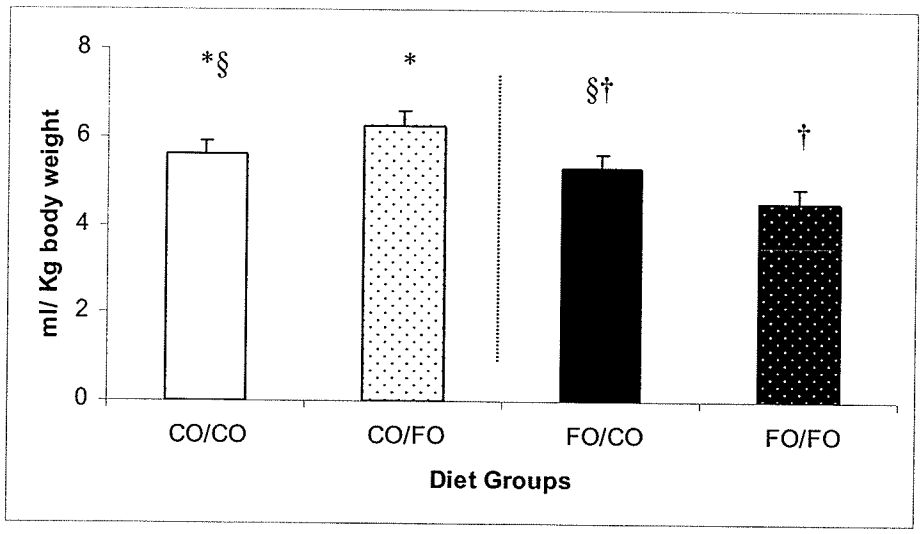

Figure 3-1. Renal cystic change in Han:SPRD-*cy* rats given dietary FO compared to CO diets in the maternal and/or post-weaning periods. Values are means ± SEM. Maternal x post-weaning period interaction (P=0.0255). Means with different symbols denote significant differences (P<0.05).

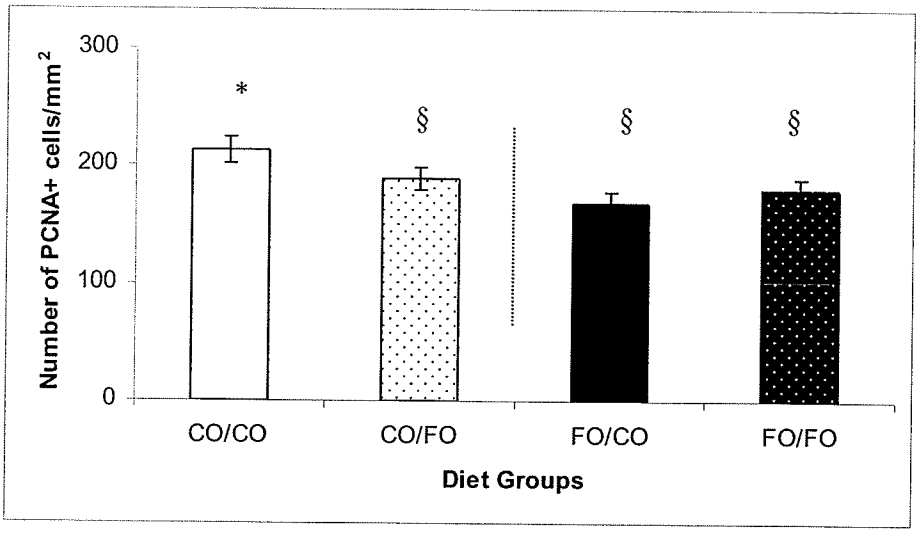

Figure 3-2. Renal cells positive for PCNA in Han:SPRD-*cy* rats given dietary FO compared to CO in the maternal and/or post-weaning periods. Values are means ± SEM. Maternal X post-weaning period interaction (P=0.0291). Means with different symbols denote significant differences (P<0.05).

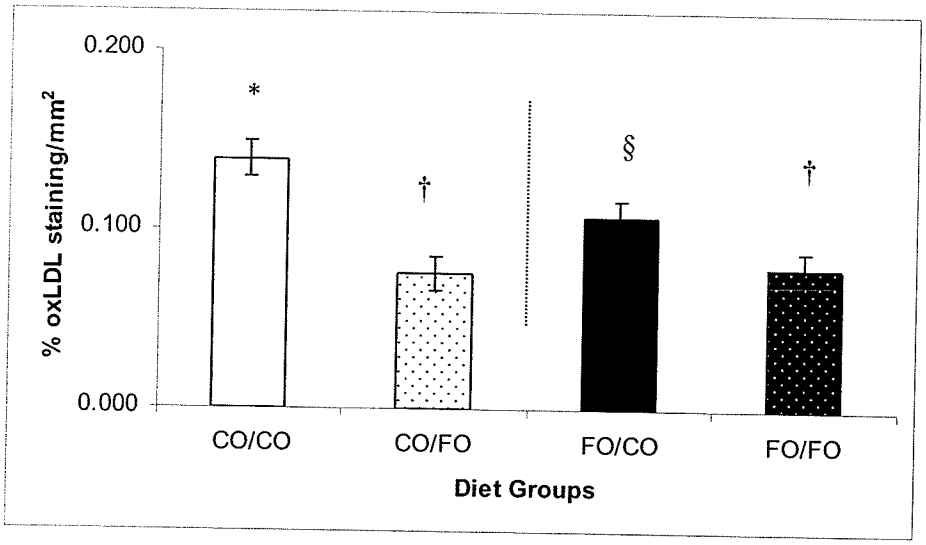

Figure 3-3. Renal oxidized-LDL staining in Han:SPRD-*cy* rats given dietary FO compared to CO in the maternal and/or post-weaning periods. Values are means ± SEM. Maternal X post-weaning period interaction (P=0.0816). Means with different symbols denote significant differences (P<0.05).

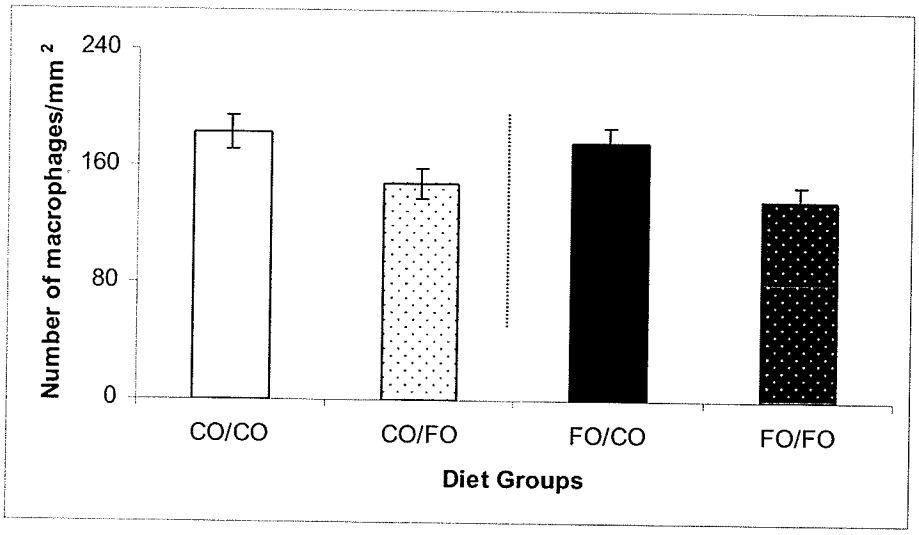

Figure 3-4. Renal macrophage count in Han:SPRD-*cy* rats given dietary FO compared to CO in the maternal and/or post-weaning periods. Values are means ± SEM. Post-weaning period (P=0.0007, FO<CO).

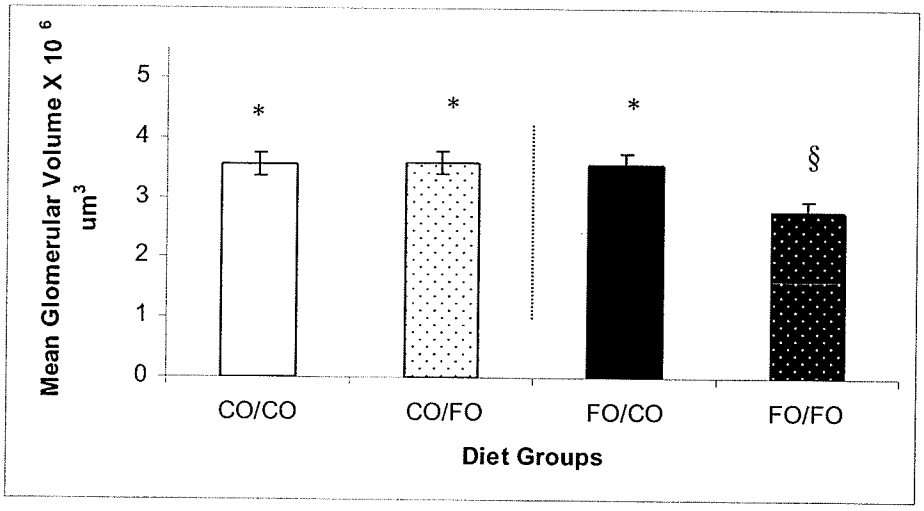

Figure 3-5. Mean glomerular volume in Han:SPRD-*cy* rats given dietary FO compared to CO in the maternal and/or post-weaning periods. Values are means ± SEM. Maternal X post-weaning period interaction P=0.0160). Means with different symbols denote significant differences (P<0.05).

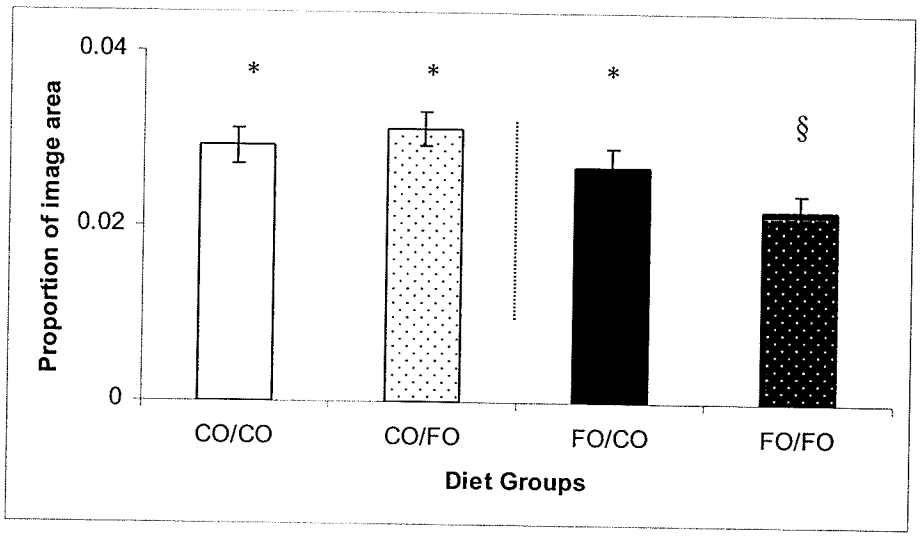

Figure 3-6. Renal interstitial fibrosis in Han:SPRD-*cy* rats given dietary FO compared to CO in the maternal and/or post-weaning periods. Values are means ± SEM. Maternal X post-weaning period interaction (P=0.0378). Means with different symbols denote significant differences (P<0.05).

Table 3-1. Kidney weights, serum and urine biochemistry in diseased (*cy/+*) and normal (+/+) Han:SPRD-cy rats given dietary FO and CO in the maternal and/or post-weaning periods.

Maternal/Post weaning Period	CO/CO	CO/FO	FO/CO	FO/FO	Significant Effects *P*
***cy/+* Rats**	**N=15**	**N=18**	**N=19**	**N=19**	
Body Weight (g)[§]	333 ± 5.6[¶]	328 ± 5.1[¶]	332 ± 5.1[¶]	306 ± 4.8[†]	Interaction (*P*=0.0515)
Kidney Weight (g/100g body weight)	2.44 ± 0.1[¶]	2.62 ±0.1[*]	2.29 ±0.1[¶]	2.00 ± 0.1[†]	Interaction (*P*=0.0104)
Kidney Weight (g)	8.14±0.3[¶*]	8.58±0.3[*]	7.44±0.3[¶]	6.15±0.3[†]	Interaction (*P*=0.0044)
Serum Creatinine (µmol/L)	76.4±4.3	67.6±3.8	81.7±3.6	79.3±3.7	Maternal Period (*P*=0.0307)
Serum Urea (mmol/L)	33.9±2.2	28.9±2.0	36.8±1.9	38.1±1.9	Maternal Period (*P*=0.0039)
Creatinine Clearance (ml/min/100g body weight)	0.22±0.02	0.27±0.02	0.18±0.02	0.17±0.02	Maternal Period (*P*=0.0031)
Urinary Protein (mg/24 hr)	12.1±0.9	11.8±0.7	11.0±0.8	9.1±0.7	Maternal Period (*P*=0.0176)
+/+ Rats	**N=13**	**N=9**	**N=8**	**N=8**	
Body weight (g)	350 ± 6.0	342 ± 7.9	357 ± 9.1	355 ± 7.9	None
Kidney Weight (g/100g body weight)	0.76 ± 0.02	0.73± 0.03	0.73± 0.03	0.69± 0.03	None
Kidney Weight (g)	2.58±0.1	2.50±0.1	2.63±0.1	2.47±0.1	None
Serum Creatinine (µmol/L)	42.2±1.7	37.0±2.2	39.2±2.3	39.5±2.3	None
Serum Urea (mmol/L)	8.7±0.5	9.0±0.7	7.2±0.8	9.0±0.8	None
Creatinine clearance (ml/min/100g body weight)	0.44±0.02	0.48±0.03	0.49±0.02	0.45±0.02	None
Urinary Protein (mg/24 hr)	10.0±0.9	10.4±1.2	10.5±1.1	10.0±1.1	None

[§] Data are expressed as least squares means. Means with different superscripts are significantly different ($P<0.05$)

3.5 Discussion

This study demonstrates that dietary supplementation with FO initiated during pregnancy and lactation reduces histologic renal injury in offspring of Han:SPRD-*cy* rats. Dietary FO given in the maternal period alleviated increases in cyst expansion, kidney size, renal cell proliferation, oxidant damage, interstitial fibrosis, glomerular hypertrophy and proteinuria. The concept that the events encountered in fetal life can have life-long consequences and affect adult health is rapidly gaining acceptance. There is growing evidence that maternal nutritional status can alter the state of the fetal genome and program gene expression in normal embryonic kidney development (16). The current study further extends the above observations that maternal nutrition also can have long term effects on the postnatal kidney afflicted by a hereditary disease. Autosomal dominant PKD is a developmental disorder, affecting 1 in 400 to 1 in 1000 people and, is the most common genetic cause of renal failure in humans (23). Localization of the PKD1 and PKD2 genes has made it possible to use genetic markers to determine the status of asymptomatic individuals from families with a history of PKD, even as early as prenatally (23). This ability for early identification of PKD allows for subsequent preventative therapy such as dietary intervention during the maternal period as demonstrated in the current study.

The beneficial effects of flax oil given maternally are consistent with previous studies that reported amelioration of renal injury when flax oil intervention was introduced in the adult or post-weaning stages (6, 7, 19). In cystic kidney diseases, recent evidence suggests that cyst expansion precedes the changes in function and is associated with the initiation of inflammation, fibrosis and other secondary changes (24). Thus,

therapeutic interventions that reduce the rate of cystic growth will ameliorate development of late-onset renal insufficiency (24). Dietary FO in the maternal period not only reduced cyst expansion and kidney size in diseased rat offspring but also resulted in improvements in other histological parameters and function (proteinuria). Proteinuria is not only a marker of compromised kidney function, but it also is a key indicator of prognosis and therapy of chronic renal injury (25).

Although the reduction in creatinine clearance may appear to be contradictory to the observed benefits on cyst expansion and renal histology, a decrease in GFR is not always associated with worsening of disease. In the Modification of Diet in Renal Disease study, low protein diets had seemingly contrasting short- and long-term effects on GFR. In this study, adults with moderate renal injury in the low compared to normal protein diet group had an initial faster mean decline in GFR but a slower mean decline in GFR thereafter (26). This initial decrease in GFR followed by long-term reduction in disease progression by dietary protein restriction also has been demonstrated in an animal model (27). Thus, it is possible that an initial short-term reduction in creatinine clearance with dietary FO in the maternal period is followed by a slower decline in GFR in the long term. We speculate that resistance to glomerular hypertrophy is linked to the reduced proteinuria we have observed ; in turn the lower proteinuria may explain the reduced interstitial fibrosis we have demonstrated in animals given dietary FO. A longer term study that examines the effects of dietary FO in the maternal period on GFR and the ultimate outcome of renal disease is needed to definitively address this issue.

Glomerular hypertrophy and other glomerular abnormalities have been reported in human PKD kidneys (28) as well as in 6-month-old cystic rat kidneys (29). The

glomerulus is often ignored in PKD, probably because the tubular cystic changes are more dramatic. However, although glomerular changes occur later in the disease process, these changes are important since it is the failure of glomerular filtration that eventually leads to end stage renal failure. The current study is the first to demonstrate a dietary effect on mean glomerular volume in cystic kidney disease, demonstrating the potential for dietary interventions during the maternal period to counter the glomerular abnormalities in this disorder.

Dietary supplementation of flaxseed or FO in rat dams increases 18:3n-3 (α-linolenic acid) and reduces 20:4n-6 (arachidonic acid) in the milk as well as in the tissues of offspring (30, 31) confirming that there is both placental and milk transfer of these fatty acids. The high α-linolenic acid content in FO may contribute to the reno-protective effects observed in the current study. FO compared to CO supplementation in Han:SPRD-*cy* rat and *pcy* mouse models of cystic kidney disease leads to an enrichment of renal α-linolenic acid and 20:5n-3 (eicosapentaenoic acid), and a reduction of linoleic acid (18:2n-6) and arachidonic acid (7, 19) . These studies demonstrate that α-linolenic acid is converted to longer chain n-3 fatty acids, and inhibits conversion of linoleic acid to arachidonic acid. Since arachidonic acid and eicosapentaenoic acid compete for the same metabolic enzymes, supplementing the diet with n-3 fatty acids may cause a shift in eicosanoid production, with eicosapentaenoic acid competitively inhibiting the metabolism of arachidonic acid to the more detrimental 2 series eicosanoids (32). Not only is the rate of conversion of eicosapentaenoic acid to thromboxane A_3 lower than that of arachidonic acid to thromboxane A_2 (33), but the vasoconstrictor potency of thromboxane A_3 is also significantly lower than that of its 2 series counterpart (34). N-3

fatty acid enrichment with FO also has been associated with anti-proliferative effects in renal injury in weanling Han:SPRD-*cy* rats (7) as well as in cancer models (35-37). These reported anti-proliferative effects are similar to those observed in the current study, suggesting that altered eicosanoid during the maternal period could attenuate the increased cell proliferation observed in diseased kidneys.

Autosomal dominant PKD is a slowly progressing chronic kidney disease that begins *in utero* (23). The results from the present study demonstrate that initiating dietary interventions *in utero* can reduce the progression of this genetically determined kidney disease. The findings may be relevant to other juvenile genetic/inherited cystic renal diseases such as autosomal recessive PKD and juvenile nephronophthisis as well as other renal disorders with a genetic basis such as IgA nephropathy, Alport syndrome and congenital nephrotic syndrome.

3.6 References

1. Coresh J, Byrd-Holt D, Astor BC, Briggs JP, Eggers PW, Lacher DA, Hostetter TH. Chronic kidney disease awareness, prevalence, and trends among U.S. adults, 1999 to 2000. J Am Soc Nephrol. 2005 ;16:180-188
2. Chauhan T. End-stage renal disease patients up nearly 19%. CMAJ. 2004 ;170:1087
3. Donadio JV. The emerging role of omega-3 polyunsaturated fatty acids in the management of patients with IgA nephropathy. J Ren Nutr. 2001 ;11:122-128
4. Lu J, Bankovic-Calic N, Ogborn M, Saboorian MH, Aukema HM. Detrimental effects of a high fat diet in early renal injury are ameliorated by fish oil in Han:SPRD-cy rats. J Nutr. 2003 ;133:180-186
5. Hall AV, Parbtani A, Clark WF, Spanner E, Keeney M, Chin-Yee I, Philbrick DJ, Holub BJ. Abrogation of MRL/lpr lupus nephritis by dietary flaxseed. Am J Kidney Dis. 1993 ;22:326-332
6. Ingram AJ, Parbtani A, Clark WF, Spanner E, Huff MW, Philbrick DJ, Holub BJ. Effects of flaxseed and flax oil diets in a rat-5/6 renal ablation model. Am J Kidney Dis. 1995 ;25:320-329
7. Ogborn MR, Nitschmann E, Bankovic-Calic N, Weiler HA, Aukema H. Dietary flax oil reduces renal injury, oxidized LDL content, and tissue n-6/n-3 FA ratio in experimental polycystic kidney disease. Lipids. 2002 ;37:1059-1065
8. Barker DJ. The fetal and infant origins of disease. Eur J Clin Invest. 1995 ;25:457-463

9. Taylor PD, McConnell J, Khan IY, Holemans K, Lawrence KM, Asare-Anane H, Persaud SJ, Jones PM, Petrie L, Hanson MA, Poston L. Impaired glucose homeostasis and mitochondrial abnormalities in offspring of rats fed a fat-rich diet in pregnancy. Am J Physiol Regul Integr Comp Physiol. 2005 ;288:R134-R139

10. Khan IY, Dekou V, Douglas G, Jensen R, Hanson MA, Poston L, Taylor PD. A high-fat diet during rat pregnancy or suckling induces cardiovascular dysfunction in adult offspring. Am J Physiol Regul Integr Comp Physiol. 2005 ;288:R127-R133

11. Palinski W, D'Armiento FP, Witztum JL, de Nigris F, Casanada F, Condorelli M, Silvestre M, Napoli C. Maternal hypercholesterolemia and treatment during pregnancy influence the long-term progression of atherosclerosis in offspring of rabbits. Circ Res. 2001 ;89:991-996

12. Siemelink M, Verhoef A, Dormans JA, Span PN, Piersma AH. Dietary fatty acid composition during pregnancy and lactation in the rat programs growth and glucose metabolism in the offspring. Diabetologia. 2002 ;45:1397-1403

13. Keller G, Zimmer G, Mall G, Ritz E, Amann K. Nephron number in patients with primary hypertension. N Engl J Med. 2003 ;348:101-108

14. Woods LL, Weeks DA, Rasch R. Programming of adult blood pressure by maternal protein restriction: role of nephrogenesis. Kidney Int. 2004 ;65:1339-1348

15. Langley-Evans SC, Langley-Evans AJ, Marchand MC. Nutritional programming of blood pressure and renal morphology. Arch Physiol Biochem. 2003 ;111:8-16

16. Welham SJ, Riley PR, Wade A, Hubank M, Woolf AS. Maternal diet programs embryonic kidney gene expression. Physiol Genomics. 2005 ;22:48-56

17. Cowley BD Jr, Gudapaty S, Kraybill AL, Barash BD, Harding MA, Calvet JP, Gattone VH 2nd. Autosomal-dominant polycystic kidney disease in the rat. Kidney Int. 1993 ;43:522-534

18. Ogborn MR, Nitschmann E, Weiler H, Leswick D, Bankovic-Calic N. Flaxseed ameliorates interstitial nephritis in rat polycystic kidney disease. Kidney Int. 1999 ;55:417-423

19. Sankaran D, Lu J, Bankovic-Calic N, Ogborn MR, Aukema HM. Modulation of renal injury in pcy mice by dietary fat containing n-3 fatty acids depends on the level and type of fat. Lipids. 2004 ;39:207-214

20. Reeves PG, Nielsen FH, Fahey GC Jr. AIN-93 purified diets for laboratory rodents: final report of the American Institute of Nutrition ad hoc writing committee on the reformulation of the AIN-76A rodent diet. J Nutr. 1993 ;123:1939-1951

21. Weibel E. Practical Methods for Biological Morphometry. In: Stereological Methods. Academic Press, London, p 40–45. 1979.

22. Hirose K, Osterby R, Nozawa M, Gundersen HJ. Development of glomerular lesions in experimental long-term diabetes in the rat. Kidney Int. 1982 ;21:689-695

23. Wilson PD. Polycystic kidney disease. N Engl J Med. 2004 ;350:151-164

24. Grantham JJ, Torres VE, Chapman AB, Guay-Woodford LM, Bae KT, King BF Jr, Wetzel LH, Baumgarten DA, Kenney PJ, Harris PC, Klahr S, Bennett WM,

Hirschman GN, Meyers CM, Zhang X, Zhu F, Miller JP. Volume progression in polycystic kidney disease. N Engl J Med. 2006 ;354:2122-2130

25. 2002 K/DOQI clinical practice guidelines for chronic kidney disease: evaluation, classification, and stratification. Am J Kidney Dis 2002 ;39:S1-S266

26. Levey AS, Greene T, Beck GJ, Caggiula AW, Kusek JW, Hunsicker LG, Klahr S. Dietary protein restriction and the progression of chronic renal disease: what have all of the results of the MDRD study shown? Modification of Diet in Renal Disease Study group. J Am Soc Nephrol. 1999 ;10:2426-2439

27. De Keijzer MH, Provoost AP. Effects of dietary protein on the progression of renal failure in the Fawn-Hooded rat. Nephron. 1990 ;55:203-209

28. Zeier M, Fehrenbach P, Geberth S, Mohring K, Waldherr R, Ritz E. Renal histology in polycystic kidney disease with incipient and advanced renal failure. Kidney Int. 1992 ;42:1259-1265

29. Tanner GA, Tielker MA, Connors BA, Phillips CL, Tanner JA, Evan AP. Atubular glomeruli in a rat model of polycystic kidney disease. Kidney Int 2002 ;62:1947-1957

30. Korotkova M, Gabrielsson BG, Holmang A, Larsson BM, Hanson LA, Strandvik B. Gender-related long-term effects in adult rats by perinatal dietary ratio of n-6/n-3 fatty acids. Am J Physiol Regul Integr Comp Physiol. 2005 ;288:R575-R579

31. Wiesenfeld PW, Babu US, Collins TF, Sprando R, O'Donnell MW, Flynn TJ, Black T, Olejnik N. Flaxseed increased alpha-linolenic and eicosapentaenoic acid

and decreased arachidonic acid in serum and tissues of rat dams and offspring. Food Chem Toxicol. 2003 ;41:841-855

32. Lefkowith JB, Klahr S. Polyunsaturated fatty acids and renal disease. Proc Soc Exp Biol Med. 1996 ;213:13-23

33. Needleman P, Raz A, Minkes MS, Ferrendelli JA, Sprecher H. Triene prostaglandins: prostacyclin and thromboxane biosynthesis and unique biological properties. Proc Natl Acad Sci U S A. 1979 ;76:944-948

34. Grimminger F, Mayer K, Kramer HJ, Stevens J, Walmrath D, Seeger W. Differential vasoconstrictor potencies of free fatty acids in the lung vasculature: 2-versus 3-series prostanoid generation. J Pharmacol Exp Ther. 1993 ;267:259-265

35. Wang L, Chen J, Thompson LU. The inhibitory effect of flaxseed on the growth and metastasis of estrogen receptor negative human breast cancer xenograftsis attributed to both its lignan and oil components. Int J Cancer. 2005 ;116:793-798

36. Chen J, Wang L, Thompson LU. Flaxseed and its components reduce metastasis after surgical excision of solid human breast tumor in nude mice. Cancer Lett. 2005 ;234:168-175

37. Fritsche KL, Johnston PV. Effect of dietary alpha-linolenic acid on growth, metastasis, fatty acid profile and prostaglandin production of two murine mammary adenocarcinomas. J Nutr. 1990 ;120:1601-1609

4. LATE DIETARY INTERVENTION LIMITS BENEFITS OF SOY PROTEIN OR FLAX OIL IN EXPERIMENTAL POLYCYSTIC KIDNEY DISEASE

Sankaran D, Bankovic-Calic N, Cahill L, Peng CY, Ogborn MR, Aukema HM

4.1 Abstract

Dietary soy protein and flax oil retard kidney disease progression when initiated in the early stages of disease in several experimental models, including the Han:SPRD-*cy* rat. However, individuals with kidney disease often do not become aware of their condition until injury to the kidney is extensive. The objective of this study was to determine whether initiating these interventions in established disease would alter further progression of renal injury. Two month old adult male Han:SPRD-*cy* rats were given either a flax oil diet (7% flax oil), a soy protein diet (20% soy protein) or a control diet (7% corn oil, 20% casein) for 4 months. Renal disease progression was assessed by examining morphological, immunohistochemical, and biochemical parameters. Compared to controls, there was 21-24% less staining of proliferating cells, 21-24% less oxidative damage and 13-15% less renal inflammation in kidneys from rats given dietary soy protein and flax oil. Renal cystic growth and fibrosis and serum creatinine levels were not altered by these dietary treatments. Late intervention with dietary soy protein and flax oil reduces some disease-associated pathologies in established renal disease in Han:SPRD-*cy* rats. The potential benefits of the anti-oxidant and anti-inflammatory effects on ultimate renal disease outcome in the long term needs to be determined.

4.2 Introduction

Chronic kidney disease (CKD), a gradual irreversible loss of kidney function eventually leading to end-stage renal disease and the need for expensive renal replacement therapies, is now recognized as a worldwide pandemic. The increasing prevalence and healthcare costs of end-stage renal disease warrant further inquiry into treatment options that slow or prevent the progression of CKD. Current therapeutic strategies to slow the progression of CKD are based primarily on antagonism of angiotensin II and dietary protein restriction (1).

The importance of examining the effects of specific food ingredients, and not just macronutrient proportions, on chronic renal disease has been confirmed by a number of studies. Dietary soy protein has been associated with reno-protective effects in several models of early CKD, including rats with chronic nephritic syndrome (2), rats with early diabetic nephropathy (3) and rat and mouse models of polycystic kidney disease (PKD) (4-7). Flax oil-based diets also are beneficial in ameliorating early kidney disease in rats and mice with PKD (8, 9). These studies have established that dietary soy protein and flax oil reduce renal injury when initiated at the early stages of deterioration of renal function. However, individuals with CKD often do not become aware of their condition, until injury to the kidney is extensive (10). Therefore, most individuals diagnosed with CKD are not likely to consider a change in diet until histologic injury is already well advanced. In animal models of advanced renal injury caused by renal ablation, dietary interventions such as soy protein (11) and flaxseed and flax oil (12) are beneficial in retarding renal disease progression. Similar protective effects of dietary soy protein (13, 14) also have been suggested in humans with advanced nephropathies.

The Han:SPRD-*cy* rat is a model of genetically determined chronic kidney disease in which heterozygotes develop PKD and associated renal interstitial fibrosis, inflammation and oxidative damage, as well as hypertension and uraemia in adult life (15). Since there are no studies that have examined the effects of dietary intervention of dietary soy protein and flax oil in adult Han:SPRD-*cy* rats with established renal disease, the aim of this study to determine whether dietary soy protein or flax oil supplementation could alter further progression of renal injury in Han:SPRD-*cy* rats with advanced PKD. In addition to assessing disease progression using biochemical, morphological and immunohistochemical parameters, we also examined renal fatty acid concentrations to provide insight into whether soy protein or flax oil diets alter fatty acid profiles in advanced renal injury, similar to the alterations previously reported in early renal disease (4, 5, 8, 9).

4.3 Materials and Methods

Animals

All animal procedures were approved by the University of Manitoba Committee on Animal Use and were in accordance with the guidelines of the Canadian Council on Animal Care. Han:SPRD-cy [also known as PKD/Mhm (cy/+)] rats were derived from our breeding colony, which originated from the colony of Dr. Benjamin Cowley, University of Kansas Medical Center, Kansas City (15). The stage of disease in rats at two months of age is analogous to stage 3 CKD, in which there is a moderate decrease in kidney function and GFR (16). Two month old adult male Han:SPRD-cy heterozygotes were randomly assigned to either a flax oil diet (7% flax oil, rich in 18:3n-3 and 20% casein), a soy protein diet (containing 20% soy protein isolate and 7% corn oil) or a control diet (containing 7% corn oil, rich in 18:2n-6 and 20% casein as the protein source). The nitrogen content of the protein sources was identical, resulting in equivalent levels of protein in all diets. Other than these changes in protein and lipid sources, diets were based on the AIN93 guidelines for rodent diets. All diet ingredients, with the exception of flax oil, were purchased from Dyets Inc. (Bethlehem, PA) or Harlan Teklad (Madison, WI). Flax oil (FO) was a gift from Bioriginal Food and Science Corporation (Saskatoon, SK, Canada).

Animals were given the diets for four months, weighed weekly and at the end of the feeding period were killed and trunk blood was collected to obtain serum. Right and left kidneys were removed, weighed and used for fatty acid analysis and for morphological and histological analyses, respectively.

Histology and Immunohistochemistry

Left kidneys, fixed in 10% buffered formalin, were embedded in paraffin, sectioned at 5 microns and processed using our previously described methods for histological and immunohistochemical analyses (4, 5, 8, 9). Sections for cyst area measurement were stained with haematoxylin and eosin and those for quantitative analysis of fibrosis with Sirius red which permits image analysis measurement using a standard incandescent microscope light source. Renal cell proliferation was assessed using a 1:50 dilution of an anti-mouse proliferating cell nuclear antigen (PCNA) antibody (M0879, Dako Corporation, Carpinteria, CA). Renal inflammation and oxidant injury were detected using 1:50 dilution of a mouse anti-rat monocytes/macrophages monoclonal antibody (MAB1435, Chemicon International, Temecula, CA) and a rabbit anti-Cu 2+-oxidized LDL polyclonal antibody (AB3230, Chemicon International, Temecula, CA), respectively. The Dako EnVision Plus system (K4008, Dako Corporation, Carpinteria, CA) was used for secondary detection.

Image Analysis and morphometric assessment

Quantitative histological analysis of the left kidney was performed using our previously described methods (4, 5, 8, 9). Briefly, 25-30 images captured by a Spot Junior CCD camera by random stage movement through the sections were subsequently analyzed using Image Pro version 4.5 Package (Media Cybernetics). Renal cyst area measurements were expressed relative to kidney weight-over-body weight ratios. In addition, fibrosis, oxidized LDL and other cellular markers were corrected to solid tissue areas of sections to avoid underestimation of these variables due to empty cystic areas in these sections.

Gas Chromatography and Serum Biochemistry

Lipids from a portion of the right kidney (snap frozen in liquid nitrogen and stored at -80°C) were solvent extracted and fatty acids were analyzed as methyl esters by gas chromatography as described (4, 5, 8). Serum urea nitrogen was determined spectrophotometrically using reagents and standards from the Sigma Chemical Company (MO, USA). Serum creatinine was measured using a modified Jaffe method.

Statistical Analyses

Data were analyzed using a general linear model one-way ANOVA followed by post-hoc t-tests, using SAS software (SAS, Cary, NC). Normality of the data was tested using a plot of actual residuals vs. predicted residuals and the Shapiro-Wilk's W statistic. Data were normalized by logarithmic transformation if necessary. Post-hoc t-tests were performed only if the F test was significant at $P<0.05$.

4.4 Results

Renal epithelial cell proliferation was lower with dietary treatment (P=0.0001) (Table 4-1). The number of PCNA positive cells was 21% lower in kidney sections of rats given soy protein and 24% lower in kidney sections of rats given flax oil, compared to the control diet. Renal oxidative damage was reduced by a similar magnitude as proliferation (P=0.0105) (Table 4-1), with 21% and 24% less oxidized LDL staining in renal sections from rats given soy protein and flax oil diets, respectively. Rats given flax oil and soy protein also had less macrophage infiltration in their kidneys compared to those of control fed rats (P=0.0113) (Table 4-1). Macrophage numbers were reduced by 13% and 15% with soy protein and flax oil feeding respectively. Cystic growth and renal interstitial fibrosis, tended to be lower with dietary treatment, but were not significantly different than controls (Table 4-1).

Rats in all three groups thrived and grew equally well, as evidenced by similar body weights at the end of the study (Table 4-2). Relative kidney weights, on the other hand, were reduced in rats given soy protein, compared to those given control or flax oil diets (Table 4-2). Diet also differentially affected serum biochemistry (Table 4-2). While serum creatinine concentrations were not affected by dietary intervention, animals given soy protein diets had significantly lower serum urea levels compared to those given control and flax oil diets.

Soy protein and flax oil diets affected renal fatty acid proportions differently (Table 4-3). Rats given flax oil diets had the lowest total n-6 polyunsaturated fatty acid levels (reflected in the reduced amounts of 18 and 20 carbon n-6 fatty acids) and the highest total n-3 polyunsaturated fatty acid levels in the kidney (reflected in the elevated

levels of 18, 20 and 22 carbon n-3 fatty acids), compared to those given soy protein and control diets.

Table 4-1. Renal disease markers in adult Han:SPRD-*cy* rats given control, flax oil and soy protein diets for four months.

Parameter	Control N=19	Flax Oil N=11	Soy N=11	Effects P
Cyst volume (mL/g left kidney weight)	0.84 ± 0.06[†]	0.80 ± 0.08	0.75± 0.08	NS[¶]
Cyst volume (mL/kg body weight)	1.49 ± 0.1	1.45 ± 0.14	1.27 ± 0.13	NS
Renal Interstitial Fibrosis (fraction of solid tissue area)	0.018 ± 0.001	0.016 ± 0.002	0.015 ± 0.002	NS
Macrophage count (cells/high power field)	23.8 ± 0.94[a]	20.2 ± 1.30[b]	20.8 ± 1.30[b]	0.0113
PCNA count (cells/high power field)	30.9 ± 0.96[a]	23.3 ± 1.32[b]	24.4 ± 1.32[b]	0.0001
Oxidized LDL (fraction of solid tissue area)	0.029 ± 0.001[a]	0.022 ± 0.002[b]	0.023 ± 0.002[b]	0.0105

[†]Values are least square means ± SEM

[¶]NS= Not Significant

[a]Means with different superscripts are significantly different ($P<0.05$)

Table 4-2. Body & kidney weights and serum chemistry of adult Han:SPRD-*cy* rats given control, flax oil and soy protein diets for four months.

Parameter	Control N=19	Flax Oil N=11	Soy N=11	Effects P
Body Weight (g)	564.9 ± 8.6[†]	571.6 ± 10.9	593.5 ± 11.9	NS[¶]
Kidney Weight (g/100g body wt)	0.85 ± 0.02[a]	0.86 ± 0.03[a]	0.74 ± 0.03[b]	0.0193
Serum Creatinine (μmol/L)	79.1 ± 3.3	76.3 ± 4.2	79.5 ± 4.6	NS
Serum Urea Nitrogen (mmol/L)	27.4 ± 1.7[a]	25.6 ± 2.3[a]	17.4 ± 2.3[b]	0.0032

[†]Values are least square means ± SEM

[¶]NS= Not Significant

[a]Means with different superscripts are significantly different ($P<0.05$)

Table 4-3. Kidney fatty acid proportions of total fatty acids and select n-6/n-3 fatty acids in adult Han:SPRD-*cy* rats given control, flax oil or soy protein diets for four months.

Parameter	*Kidney Fatty Acids (g/100g)*			
	Control N=6	*Flax Oil N=6*	*Soy N=6*	*Effect P*
18:2n-6	20.2 ± 1.15[†,a]	14.0 ± 1.15[b]	20.8 ± 1.15[a]	0.001
18:3n-3	0.11 ± 1.12[a]	7.63 ± 1.12[b]	0.19 ± 1.12[a]	0.003
20:4n-6	17.7 ± 1.53[a]	11.4 ± 1.53[b]	19.0 ± 1.53[a]	0.0105
20:5n-3	-[#,a]	3.97 ± 0.29[b]	-[a]	<0.0001
22:6n-3	0.50 ± 0.11[a]	1.16 ± 0.11[b]	0.67 ± 0.11[a]	0.0016
Total Saturated Fatty Acids	37.4 ± 1.2	39.0 ± 1.2	38.0 ± 1.2	NS[¶]
Total Mono-Unsaturated Fatty Acids	21.1 ± 1.7	19.6 ± 1.7	18.3 ± 1.7	NS
Total n-6 Poly-Unsaturated Fatty Acids	38.4 ± 0.99[a]	25.9 ± 0.99[b]	40.3 ± 0.99[a]	<0.0001
Total n-3 Poly-Unsaturated Fatty Acids	0.63 ± 0.74[a]	18.03 ± 0.74[b]	0.87 ± 0.74[a]	<0.0001

[†]Values are least square means of fatty acids ± SEM

[#] Less than 0.1g/100g of total fatty acids

[¶] NS=Not significant

[a] Means with different superscripts are significantly different ($P<0.05$)

4.5 Discussion

Consistent with previously reported beneficial effects of soy protein and flax oil in animal models of early (2-9) as well as advanced renal disease (11, 12) the current study demonstrates that these dietary interventions retard some of the pathologies associated with renal injury when introduced in established kidney disease. Renal disease in the two month old rats at the beginning of the dietary intervention in this study was analogous to stage 3 CKD. In these rats, renal epithelial cell proliferation, oxidant injury and inflammation were lower in both soy protein and flax oil supplemented rats compared to the rats given control diets. Hence, in addition to the previously demonstrated preventative effects of these dietary interventions in the early stages of renal disease in this experimental model, the current study demonstrates changes in the disease-associated pathologies when dietary intervention is initiated at a later stage of disease. However, the protective effects on renal injury were not reflected in a significant amelioration of disease (cyst growth, fibrosis) or renal function (serum creatinine), as is the case with early dietary intervention in the Han:SPRD-*cy* rat (4, 5, 8). The lack of dietary effects on these parameters may reflect the fact that cyst expansion is a less integral part of renal injury in the six month old Han:SPRD-*cy* rat (15). Therefore, while later intervention reduces certain disease-associated inflammatory changes, a preventative approach utilizing an earlier intervention strategy likely would be more effective in the long-term.

CKD is associated with recurrent cardiovascular disease (17) and high cardiovascular disease-related mortality is prevalent in end-stage renal disease patients (18). Indeed, individuals with CKD are more likely to die of adverse cardiovascular

events than to reach ESRD (17). Chronic inflammation has been identified as a major risk factor for increased cardiovascular disease risk in progressive CKD. Since inflammation and oxidative stress are linked to one another as well as to poor CKD prognosis (18, 19), treatment modalities that focus on anti-oxidant and anti-inflammatory approaches have the potential to improve poor patient outcomes. The benefits of dietary soy protein and flax oil on renal inflammation, cell proliferation and oxidant injury as observed in the current study therefore is of interest. Survival studies using these dietary interventions initiated at different stages of disease are needed to determine whether the benefits on disease-associated pathologies would ultimately translate into improved survival.

Although the effects of dietary soy protein and flax oil on renal injury were similar, it is unlikely that they mediate these effects via the same mechanisms. The flax oil diet resulted in a marked change in fatty acid composition of the kidney, while the soy protein diet did not effect these changes. N-3 fatty acids compete with arachidonic acid for incorporation into cell membranes and as cyclooxygenase substrates, resulting in the synthesis of 3-series eicosanoids in a number of tissues, including the kidney (20). Concurrent with previous studies in younger rats (8, 9), the highest renal enrichment of n-3 fatty acids and lowest levels of n-6 polyunsaturated fatty acids were observed in the flax oil fed rats, thus reducing the availability of arachidonic acid and potentially shifting the balance towards production of less inflammatory eicosanoids. Anti-inflammatory as well as anti-proliferative effects of flax oil have been demonstrated not only in early renal injury (8) but also in cancer models (21, 22).

In addition to the similar effects of dietary soy protein on renal histology, dietary soy protein compared to flax oil also resulted in smaller kidney size and reduced serum urea levels. Reduced serum urea levels with soy protein feeding in the current study, however, likely does not reflect a change in disease status since serum creatinine values were not altered. Also, it is known that dietary soy protein compared to casein results in lower serum urea levels independent of disease; this has been demonstrated in the Han:SPRD-*cy* rat model (6). Nevertheless, this modest reduction in urea by merely changing the source of dietary protein may be beneficial in patients suffering from the side effects of uraemia and represents a potential treatment in this regard. The unique amino acid profile of soy protein (enrichment of L-arginine, a nitric oxide precursor, and glycine, a vasodilatory amino acid) may be responsible for some of the beneficial effects of soy. Dietary soy protein ameliorated renal disease progression in Zucker fatty rats by restoring renal nitric oxide production and renal nitric oxide synthase alterations (3), indicating that this may be one of the potential mechanisms of action of soy protein. Altered nitric oxide synthesis also appears to play a role in the progression of other chronic kidney diseases, including PKD (23, 24).

Isoflavones (25) and soysaponins (26) also have been implicated as the active ingredients in soy responsible for its beneficial effects on renal disease. In a recent study, an eight week regimen of purified dietary genistein (the major soy isoflavone) reduced renal inflammation and oxidant damage in the Han:SPRD-*cy* rat (27). Interestingly, genistein failed to show an effect on serum creatinine and cystic growth, similar to the effects of soy protein in the current study. The possibility that genistein mediates the effects of soy protein is further supported by the evidence that genistein inhibits several

enzymes involved in cell proliferation such as protein tyrosine kinases and DNA topoisomerases in vitro (28). The inhibitory effect of dietary soy protein on cell proliferation, as observed in this study also could be due to the oestrogen receptor binding ability of genistein and other soy isoflavones (28).

In conclusion, soy protein and flax oil supplementation confer protection on disease-related pathologies in established CKD, with the modes of action likely being different for each intervention. As such, the examination of potentially additive and/or synergistic effects of a combination of soy protein and flax oil interventions in renal disease would be of great interest. However, although the results of the current study suggest that although some benefits on pathological events associated with renal disease would be expected if initiated in the later stages of renal injury, renal function is not affected under the conditions studied. It is likely that maximum benefits on slowing disease progression would be observed if late dietary interventions were combined with a preventative approach that initiated these y interventions in the early stages of renal disease. Future long term studies in cohorts identified early by imaging, genomic or other methods with disorders such as Alport's, PKD, and diabetes mellitus are needed to truly evaluate the role of nutrition in the prevention of chronic renal failure.

4.6 References

1. Zandi-Nejad K, Brenner BM. Primary and secondary prevention of chronic kidney disease. J Hypertens. 2005 ; 23:1771-1776.
2. Pedraza-Chaverri J, Barrera D, Hernandez-Pando R, Medina-Campos ON, Cruz C, Murguia F, Juarez-Nicolas C, Correa-Rotter R, Torres N, Tovar AR. Soy protein diet ameliorates renal nitrotyrosine formation and chronic nephropathy induced by puromycin aminonucleoside. Life Sci 2004 ; 74:987-999.
3. Trujillo J, Ramirez V, Perez J, Torre-Villalvazo I, Torres N, Tovar AR, Munoz RM, Uribe N, Gamba G, Bobadilla NA. Renal protection by a soy diet in obese Zucker rats is associated with restoration of nitric oxide generation. Am J Physiol Renal Physiol 2005 ; 288:F108-116.
4. Ogborn MR, Nitschmann E, Weiler HA, Bankovic-Calic N. Modification of polycystic kidney disease and fatty acid status by soy protein diet. Kidney Int 2000 ; 57:159-166.
5. Fair DE, Ogborn MR, Weiler HA, Bankovic-Calic N, Nitschmann EP, Fitzpatrick-Wong SC, Aukema HM. Dietary soy protein attenuates renal disease progression after 1 and 3 weeks in Han:SPRD-cy weanling rats. J Nutr 2004 ; 134:1504-1507.
6. Aukema HM, Housini I. Dietary soy protein effects on disease and IGF-I in male and female Han:SPRD-cy rats. Kidney Int 2001 ; 59:52-61.
7. Tomobe K, Philbrick DJ, Ogborn MR, Takahashi H, Holub BJ. Effect of dietary soy protein and genistein on disease progression in mice with polycystic kidney disease. Am J Kidney Dis 1998 ; 31:55-61.

8. Ogborn MR, Nitschmann E, Bankovic-Calic N, Weiler HA, Aukema H. Dietary flax oil reduces renal injury, oxidized LDL content, and tissue n-6/n-3 FA ratio in experimental polycystic kidney disease. Lipids. 2002 ;37:1059-1065.

9. Sankaran D, Lu J, Bankovic-Calic N, Ogborn MR, Aukema HM. Modulation of renal injury in pcy mice by dietary fat containing n-3 fatty acids depends on the level and type of fat. Lipids. 2004 ;39:207-214.

10. Coresh J, Byrd-Holt D, Astor BC, Briggs JP, Eggers PW, Lacher DA, Hostetter TH, Chronic kidney disease awareness, prevalence, and trends among U.S. adults, 1999 to 2000. J Am Soc Nephrol. 2005 ;16:180-188.

11. Williams AJ, Walls J. Metabolic consequences of differing protein diets in experimental renal disease. Eur J Clin Invest. 1987 ;17:117-122.

12. Ingram AJ, Parbtani A, Clark WF, Spanner E, Huff MW, Philbrick DJ, Holub BJ. Effects of flaxseed and flax oil diets in a rat-5/6 renal ablation model. Am J Kidney Dis 1995 ;25:320-329.

13. Teixeira SR, Tappenden KA, Carson L, Jones R, Prabhudesai M, Marshall WP, Erdman JW, Jr. Isolated soy protein consumption reduces urinary albumin excretion and improves the serum lipid profile in men with type 2 diabetes mellitus and nephropathy. J Nutr. 2004 ;134:1874-1880.

14. Stephenson TJ, Setchell KD, Kendall CW, Jenkins DJ, Anderson JW, Fanti P. Effect of soy protein-rich diet on renal function in young adults with insulin-dependent diabetes mellitus. Clin Nephrol. 2005 ;64:1-11.

15. Cowley BD Jr., Gudapaty S, Kraybill AL, Barash BD, Harding MA, Calvet JP, Gattone VH 2nd. Autosomal-dominant polycystic kidney disease in the rat. Kidney Int. 1993 ;43:522-534.

16. K/DOQI clinical practice guidelines for chronic kidney disease. evaluation, classification, and stratification. Am J Kidney Dis. 2002 ;39:S1-266.

17. Weiner DE, Tighiouart H, Stark PC, Amin MG, MacLeod B, Griffith JL, Salem DN, Levey AS, Sarnak MJ. Kidney disease as a risk factor for recurrent cardiovascular disease and mortality. Am J Kidney Dis. 2004 ;44:198-206.

18. Stenvinkel P. Inflammation in end-stage renal disease--a fire that burns within. Contrib Nephrol. 2005 ;149:185-199.

19. Locatelli F, Canaud B, Eckardt KU, Stenvinkel P, Wanner C, Zoccali C. Oxidative stress in end-stage renal disease: an emerging threat to patient outcome. Nephrol Dial Transplant. 2003 ;18:1272-1280.

20. Gallon LS, Barcelli UO. Measurement of prostaglandin E3 and other eicosanoids in biologic samples using high pressure liquid chromatography and radioimmunoassay. Prostaglandins. 1986 ;31:217-225.

21. Chen J, Wang L, Thompson LU. Flaxseed and its components reduce metastasis after surgical excision of solid human breast tumor in nude mice. Cancer Lett 2005 ;234:168-175.

22. Fritsche KL, Johnston PV. Effect of dietary alpha-linolenic acid on growth, metastasis, fatty acid profile and prostaglandin production of two murine mammary adenocarcinomas. J Nutr. 1990 ;120:1601-1609.

23. Al-Nimri MA, Komers R, Oyama TT, Subramanya AR, Lindsley JN, Anderson S. Endothelial-derived vasoactive mediators in polycystic kidney disease. Kidney Int 2003 ;63:1776-1784.

24. Wang D, Braendstrup O, Larsen S, Horn T, Strandgaard S. The expression and activity of renal nitric oxide synthase and circulating nitric oxide in polycystic kidney disease rats. Apmis. 2004 ;112:358-368.

25. Velasquez MT, Bhathena SJ. Dietary phytoestrogens: a possible role in renal disease protection. Am J Kidney Dis. 2001 ;37:1056-1068.

26. Philbrick DJ, Bureau DP, Collins FW, Holub BJ. Evidence that soyasaponin Bb retards disease progression in a murine model of polycystic kidney disease. Kidney Int. 2003 ;63:1230-1239.

27. Ogborn MR, Nitschmann E, Bankovic-Calic N, Weiler H, Aukema HM: Flax and soy phytoestrogen effects on renal injury and lipid content in experimental polycystic kidney disease. J Am Nutraceut Assoc. 2005 ;8:26-32.

28. Magee PJ, Rowland IR. Phyto-oestrogens, their mechanism of action: current evidence for a role in breast and prostate cancer. Br J Nutr. 2004 ;91:513-531.

5. COX-2 EXPRESSION IN CYSTIC KIDNEYS IS DEPENDENT ON DIETARY N-3 FATTY ACID COMPOSITION

Sankaran D, Lu J, Ogborn MR, and Aukema HM

5.1 Abstract

Dietary n-3 fatty acids generally attenuate elevated cyclooxygenase-2 (COX-2) levels in disease states. However, models of renal cyst disease (RCD) exhibit reduced renal COX-2 expression. Therefore, the *in vivo* regulation of COX-2 expression by dietary n-3 fatty acids was examined. In archived tissues from dietary studies COX-2 protein and gene expression was up-regulated in diseased *pcy* mouse and Han:SPRD-*cy* rat kidneys when given diets containing EPA (eicosapentaenoic acid) and/or DHA (docosahexaenoic acid), but not those containing ALA (α-linolenic acid), compared to control diets with LA (linoleic acid). The presence of disease was necessary to elicit these effects as COX-2 expression was unaltered by diet in normal kidneys. The effects were specific for COX-2, since COX-1 levels were unaltered by these dietary manipulations in either model. Thus in RCD, diets containing EPA and DHA but not ALA appear to specifically up-regulate renal COX-2 gene and protein levels *in vivo*.

5.2 Introduction

Cyclooxygenase (COX) -2 is one of the COX isoforms involved in the conversion of 20-carbon polyunsaturated fatty acids to physiologically active prostanoids. COX-1 and COX-2 have similar structures but distinct physiologic functions (1). Initially, COX-1 was considered to be constitutively expressed and have general "housekeeping" functions, while COX-2 was believed to be inducible and involved in inflammatory responses. However, evidence of both constitutive and inductive roles for both isoforms have been observed in the kidney (2).

The role of n-3 fatty acids in the modulation of COX-2 expression *in vivo* as well as *in vitro* has been studied in a number of experimental models of disease. Both long chain (alpha-linolenic acid, ALA, 18:3 n-3) and very long chain (eicosapentaenoic acid, EPA, 20:5 n-3 and docosahexaenoic acid, DHA, 22:6 n-3) n-3 fatty acids attenuate elevated COX-2 levels and activity in various cancer cell-lines as well as animal models (3-9), in mice with mycotoxin-induced IgA nephropathy (10, 11) and in Long-Evans Cinnamon rats with acute hepatitis (12). In these models, attenuation of the disease-induced COX-2 elevation by n-3 fatty acids is associated with slower disease progression.

COX-2 expression is generally up-regulated with disease, as seen in inflammatory conditions, cancer and some nephritic models. However, in models of renal cystic disease (RCD), COX-2 levels are either down-regulated or not increased with renal disease (13, 14). RCD is the most frequently inherited nephropathy affecting approximately 1 in 1000 people (15) and is characterized by abnormal cyst growth and renal interstitial inflammation and fibrosis which eventually lead to renal failure. Animal models of RCD

are useful as experimental models of chronic kidney disease because they exhibit the pathology of chronic renal disease without the metabolic, autoimmune or endocrine alterations present in other models of renal disease. In addition, the effects of dietary n-3 fatty acids on disease progression in models of RCD vary according to the type of n-3 fatty acid and the model. Therefore, since RCD models exhibit reduced COX-2 expression with disease and distinct effects of diets containing different fatty acids, these models provide a unique opportunity to examine the regulation of COX-2 expression by dietary n-3 fatty acids *in vivo*.

5.3 Materials and Methods

For this study, archived tissues from several previous studies conducted in our laboratory were utilized. The animal and experimental protocols were in accordance with the standards of the Canadian Council on Animal Care and the National Institutes of Health Guide for the Care and Use of Laboratory Animals and were approved by the institutional Committees on Animal Care and Ethics. All animals were housed under temperature, humidity and light-controlled conditions. Diet ingredients, with the exception of flax (Omega Nutrition, Vancouver, BC) and algal oils, were purchased from Dyets Inc. (Bethlehem, PA) and Harlan Teklad (Madison, WI). Algal oil was a generous gift from Martek Biosciences Corporation (Winchester, KY). All diets were based on AIN 93 guidelines for rodent diets and varied only in fat source and level in each study. The protocols of these studies are briefly described below.

Study 1

Weanling CD1-*pcy/pcy* (*pcy)* mice were obtained from our breeding colony that was established from mice provided to us by V.H. Gattone II (16). *pcy* mice were randomly assigned to one of six experimental diets (4 wk of age, n=8/diet group) for 8 weeks as described (17). The diets contained three types of dietary oils, namely corn (rich in n-6 LA), flaxseed (rich in n-3 ALA), and DHASCO (algal oil rich in n-3 DHA), at high (20g of fat/100g diet) and low (7g of fat/100g diet) levels in a 2 x 3 design. Diets are indicated as CO, containing corn oil, FO, containing flaxseed/corn oil (4:1, g/g) and DO, containing DHASCO/corn oil (4:1, g/g). The FO diet contained 45g of ALA while the DO diet contained 0.23g of ALA and 31g of DHA per 100g of total fat. The CO diet contained 0.9g of ALA and no EPA or DHA per 100g of total dietary fat.

Study 2

Weanling Han:SPRD-*cy* rats [also known as PKD/Mhm (*cy*/+) rats) were obtained from our breeding colony that was established from rats provided to us by Dr. B.D. Cowley (18). Rats were randomly assigned to either a high or a low fat diet containing 20 or 5 g of fat/100 g of diet using cottonseed oil (CSO, rich in n-6 LA) and menhaden oil + soybean oil (4:1, g/g) (MO, rich in n-3 EPA and DHA) for 6 weeks as described (19). The n-3 fatty acid composition of the MO diet was as follows: 2.1g of ALA, 13g of EPA and 4.2g of DHA per 100g of total dietary fat. The CSO diet contained 0.5g of ALA and no EPA or DHA per 100g of total dietary fat.

Study 3

Weanling male Han:SPRD-*cy* rats were given either a 7% corn oil diet (CO, rich in n-6 LA) or a 7% flax oil diet (FO, rich in n-3 ALA) for 12 weeks. The FO diet contained 52.3g compared to 0.9g of ALA in the CO diet per 100g of total dietary fat (20).

In all three studies, kidneys were removed, weighed, snap frozen in liquid nitrogen and stored at -80°c until mRNA and protein analyses.

Immunoblotting

Half of the kidney was lyophilized and homogenized in ice-cold homogenization buffer containing protease inhibitors as described (13, 14). After centrifugation of the kidney homogenate, the resulting pellet was re-suspended in buffer containing 1% TritonX-100 and re-centrifuged. The resulting supernatant contains the COX proteins. Protein concentrations of these fractions were determined using the Bradford method. After SDS-PAGE, detection of COX-1 and COX-2 was carried out with primary

antibodies (1:250 dilution, Cayman Chemical, Ann Arbor, Michigan) followed by incubation with a peroxidase-conjugated secondary antibody. ChemiGlow^{TM} (Alpha Innotech, San Leandro, California) substrate was used to visualize the immunoreactive bands which were then analyzed and quantified on the Fluorchem^{TM} FC digital imaging system (Alpha Innotech Corporation, San Leandro, California).

Quantitative RT-PCR

Total RNA was extracted from 10-20 mg of lyophilized kidneys using TRIzol as described (14). DNA was removed by treatment with DNase I (Invitrogen, Carlsbad, CA) for 15 min at room temperature. One-step RT-PCR was performed on 0.5 μg of total RNA using the QuantiTect® SYBR® Green RT-PCR kit (Qiagen, Mississauga, Canada). PCR primers were chosen using Primer 3 software (Rosen and Skaletsky). Oligonucleotide sequences for the rat COX-1 and -2 primers have been described (14). Mouse primers for COX-1 and -2 were as follows: COX-1 sense 5'-CACAACACTTCACCCACCAG-3', COX-1 antisense 5'-AGAGCCGCAGGTGATACTGT-3', COX-2 sense 5'-GCTGTACAAGCAGTGGCAAA-3', COX-2 antisense 5'-TTCTGCAGCCATTTCCTTCT-3'. Quantitative, real-time RT-PCR was performed on a Cepheid SmartCycler II (Cepheid, Sunnyvale, CA) using the following protocol: reverse transcription at 50°C for 30 min, PCR activation at 95°C for 15 min, 40 PCR cycles at 94°C for 15s, 55°C for 30s and 72°C for 30s. Relative amounts of mRNA were determined by comparing cycle threshold (CT) numbers for equal amounts of RNA subjected to RT-PCR and calculating differences in gene expression using the formula $2^{\Delta CT}$ as described (14).

Statistical Analysis

Data were analyzed using a general linear model ANOVA using SAS software (SAS, Cary, NC). Normality of the data was assessed using a plot of actual residuals vs. predicted residuals and the Shapiro-Wilk's W statistic and data were normalized by logarithmic transformation if necessary. Post-hoc t-tests were performed only if the overall main or interaction effect was significant at $P<0.05$.

5.4 Results

Effect of diets rich in DHA and ALA on renal COX-2 protein and gene expression in pcy mice

To examine the effect of different types of dietary n-3 PUFA on the renal COX isoforms in the *pcy* mouse model of renal cystic disease, mRNA and protein expression of these isoforms were determined in *pcy* mice given high and low CO, FO and DO. Mice given high DO diets (rich in DHA) had approximately 4.3 times more renal COX-2 protein than mice fed high FO and CO diets (Fig. 5-1A). Also, low DO fed mice had nearly twice as much renal COX-2 protein than their low FO and CO fed counterparts (Fig. 5-1A). The main effect of fat level on COX-2 protein did not attain statistical significance (P=0.0690). However, since the P value was almost significant, and because the pattern of protein expression was similar to the gene expression in which there was a significant fat level effect in the DO fed mice, post-hoc analyses were performed on these groups of mice. The analyses revealed that high DO fed mice had 143% more COX-2 immunoreactive bands (P<0.05) compared to those fed low DO (Fig. 5-1A). Neither level of dietary FO (rich in ALA), compared to CO, altered renal COX-2 gene expression (Fig. 5-1B). The relative increases in COX-2 protein in the (high) DO group were reflected in the COX-2 mRNA levels (Fig.5-1B). Kidneys from mice fed a high level of DO had up to 200% higher COX-2 mRNA levels than kidneys from mice in any of the other diet groups (Fig. 5-1B). In contrast, neither fat level nor type altered protein and gene levels of renal COX-1 (Table 5-1).

Effect of diets rich in EPA+DHA and ALA on renal COX-2 protein and gene expression in Han:SPRD-cy rats

To further probe this regulatory effect of very long chain n-3 fatty acid diets on COX-2 *in vivo*, we examined COX protein expression in Han:SPRD-*cy* rats fed high or low MO or CSO diets. Diseased rats given high MO diets (rich in EPA and DHA) had nearly 5 times more (Fig. 5-2A), while those on low MO diets had 1.2 times more COX-2 protein levels (Fig. 5-2A), compared to their counterparts given high and low CSO diets respectively. However, this effect of dietary fat type was only observed in diseased and not normal kidneys (Fig.5-2B). Similar to the effects of dietary very long chain n-3 PUFA in the *pcy* mice, dietary MO did not significantly alter COX-1 enzyme levels in the Han:SPRD-*cy* rats (Figs. 5-3A and B).

Rats given low fat diets had 2-10 times more renal COX-2 immunoreactive protein levels compared to their high fat fed counterparts in both genotypes, indicating that this effect is independent of disease (Figs.2A and B). On the other hand, high fat diets resulted in greater renal COX-1 immunoreactivity in diseased rats (Fig.5-3B) compared to normal rats (Fig.5-3A). Gel analyses revealed that the quality of the mRNA from these archived tissues was compromised, precluding its use for determination of gene expression (Data not shown).

The expression of these enzymes in Han:SPRD-*cy* rats given FO compared to CO diets also was examined to determine whether dietary FO (rich in ALA) affected COX isoform expression in this model. In contrast to the effects of MO on COX-2 in this model shown in study 2, FO diets did not alter COX-2 protein or gene expression (Table 5-2). Renal COX-1 protein and gene expression also remained unaltered by FO diets, consistent with the observed lack of an effect of n-3 fatty acids on COX-1 expression in studies 1 and 2 (Table 5-2).

(A)

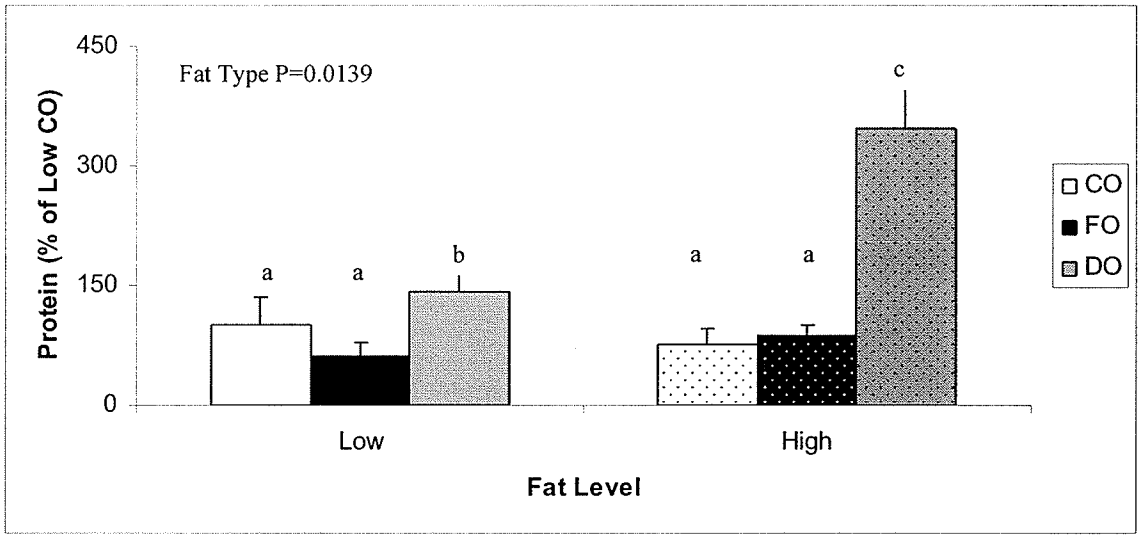

(B)

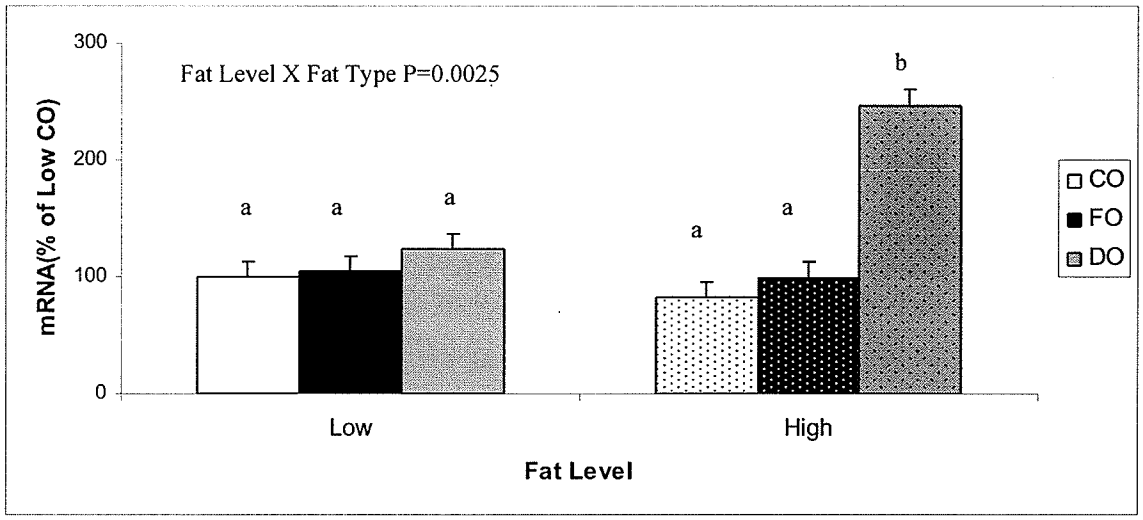

Figure 5-1. Relative renal COX-2 protein (A) and mRNA (B) levels in *pcy* mice given low (7g fat/100g diet) and high (20g fat/100g diet) corn oil (CO), flax oil (FO) and DHASCO (DO) diets for 8 weeks (n=5-6). Values are means (as percentage of Low CO) + SEM. Means with different alphabets denote significant differences ($p<0.05$).

Table 5-1. Renal COX-1 protein and mRNA levels in *pcy* mice fed low (7g fat/100g diet) and high (20g fat/100g diet) corn oil (CO), flax oil (FO) and DHASCO oil (DO) diets for 8 weeks (n=5-6).

Fat Level	Low			High			Significant Effects
Fat Type	CO	FO	DO	CO	FO	DO	
COX-1 Protein	100±12	111.2±13.2	81.6±9.2	107.1±21	79.8±13.9	108.1±8.8	None
COX-1 mRNA	100±19.0	117±19.0	106±19.0	75±20.4	90±20.4	147±20.4	None

Values are means (as percentage of Low CO) ± SEM.

(A)

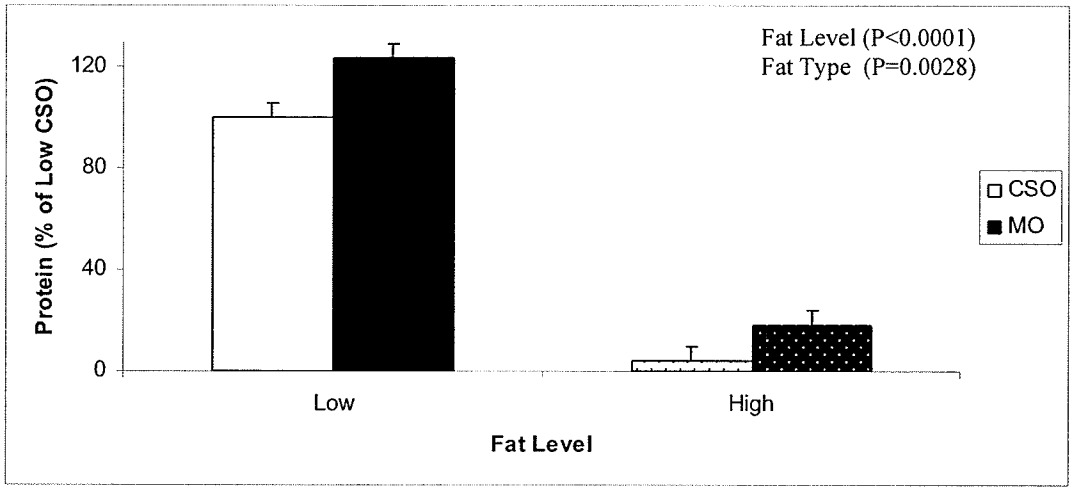

(B)

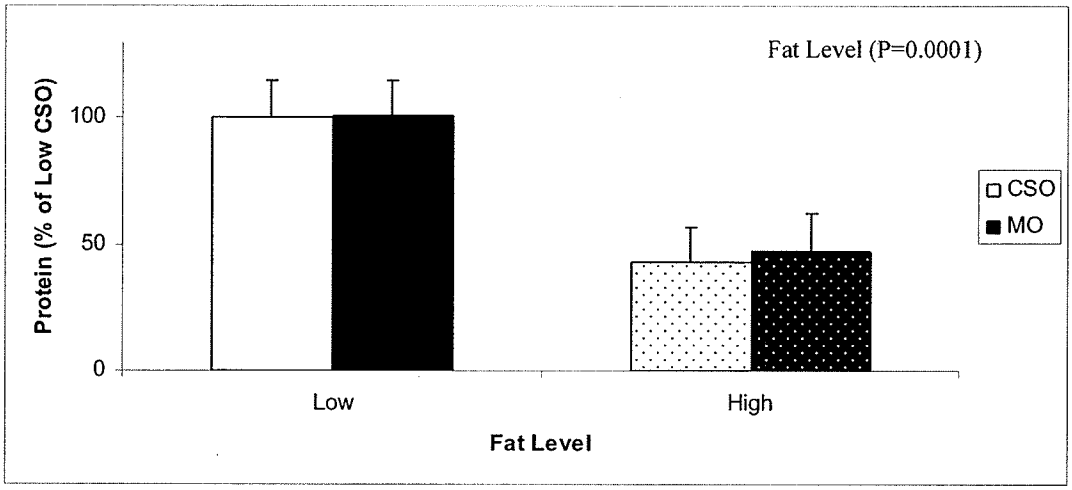

Figure 5-2. Relative renal COX-2 protein levels in diseased (A) and in normal (B) Han:SPRD-*cy* rats given low (5g fat/100g diet) and high (20g fat/100g diet) cottonseed oil (CSO) and menhaden oil (MO) diets (n=9-12). Values are means (as percentage of Low CSO) + SEM.

(A)

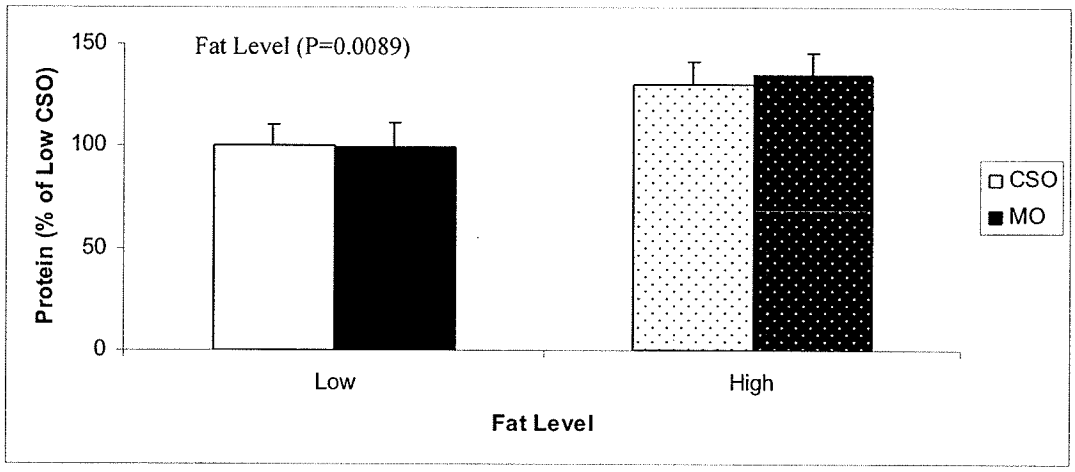

(B)

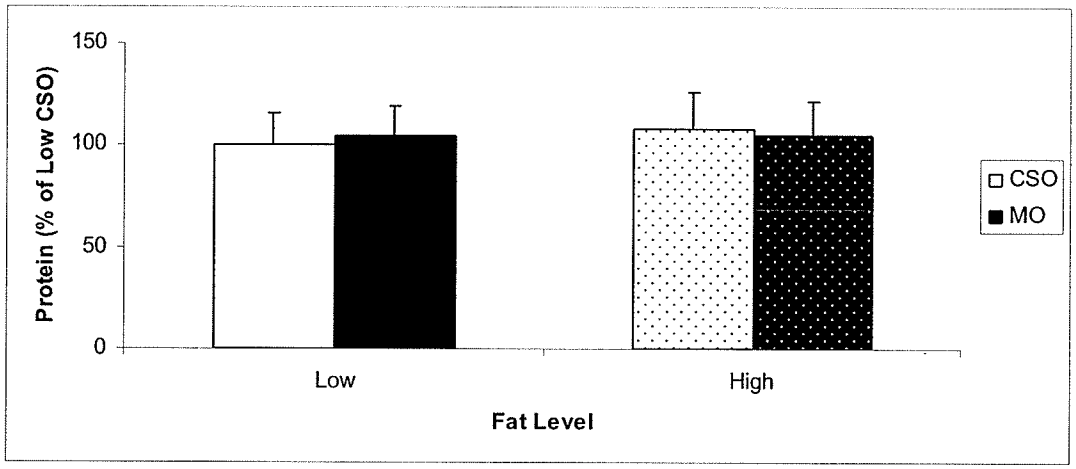

Figure 5-3. Renal COX-1 protein expression in diseased (A) and in normal (B) Han:SPRD-*cy* rats given low (5g fat/100g diet) and high (20g fat/100g diet) cottonseed oil (CSO) and menhaden oil (MO) diets for 8 weeks (n=9-12). Values are means (as a percentage of Low CSO) ± SEM.

Table 5-2. Renal COX-1 and COX-2 protein and mRNA expression in diseased Han:SPRD-*cy* rats given corn oil (CO) and flax oil (FO) diets for 12 weeks (n=9-12).

Fat Type	CO	FO	Significant Effects
COX-1 Protein	100±9.2	98±9.6	None
COX-1mRNA	100±24.2	127±22.5	None
COX-2 Protein	100±13.4	79.8±13.4	None
COX-2 mRNA	100±14.0	112±13.1	None

Values are means (as a percentage of CO) ± SEM

5.5 Discussion

The current study provides evidence that dietary oils enriched in the very-long chain n-3 fatty acids, EPA and DHA, specifically up-regulate COX-2 mRNA and protein levels in diseased kidneys. In contrast, dietary oils enriched in the long chain n-3 fatty acid, ALA, do not exert this effect. The highly unsaturated n-3 fatty acids, EPA and DHA, alter COX-2 expression at the gene and protein level in *in vitro* as well as in some *in vivo* feeding studies (6, 7, 10, 11, 21-23). Dietary enrichment with 18:3n-3 ALA alters COX-2 mRNA levels in a mouse hepatoma model (5). However, ALA did not alter COX-2 protein levels in a breast cancer cell line while stearidonic acid (18:4n-3) significantly reduced COX-2 expression even at low concentrations (8), indicating that regulation of COX-2 expression by n-3 fatty acids appears to be dependent on the degree of unsaturation in some cases. Therefore, the observation in the current study that diets containing EPA and DHA or DHA alone up-regulate, while those containing ALA do not alter COX-2 expression in both rodent models of inherited chronic kidney disease supports the premise that COX-2 regulatory effect of n-3 fatty acids depends on the number of double bonds in the fatty acid chain.

Interestingly, although the n-3 fatty acid containing diets elicit similar responses in COX-2 in both rodent models of RCD, their effects on renal disease progression in these models are not similar. In *pcy* mice, the FO diet (rich in ALA) compared to the n-6-enriched CO diet had beneficial effects on renal injury, while the DO diet (containing DHA) worsened renal injury (17). The detrimental effect of dietary oils containing very long chain n-3 fatty acids is supported by the results of a previous study in which *pcy* mice given dietary fish oil compared to an LA-enriched diet had lower survival rates and

exhibited worsened renal function as well as a deterioration of renal architecture (24). On the contrary, in diseased Han:SPRD-*cy* rats both ALA-enriched FO and EPA- and DHA-enriched MO diets, compared to diets rich in n-6 fatty acids, significantly attenuated markers of renal injury such as cyst expansion, renal fibrosis and inflammation (19, 20). Therefore, it is likely that in these models of RCD, dietary n-3 fatty acids alter COX-2 expression independent of their effects on renal disease progression. However, the presence of kidney disease is important, as COX-2 expression was not altered by dietary MO in normal rats. Thus, the induction of COX-2 by diets containing EPA and DHA or DHA alone appears to be independent of their effects on disease progression, although the presence of disease appears to be necessary to elicit these effects.

COX-2 expression has been shown to be modulated by a number of transcription factors which appear to be cell-specific. For example, COX-2 expression in the liver (5) and in macrophages (25) is tightly regulated by members of CCAAT enhancer binding proteins (C/EBP), while in cultured glomerular (including mesangial) cells nuclear factor (NF) κB modulates transcriptional regulation of COX-2 (26, 27). Supplementation with n-3 fatty acids have been shown to mitigate induction of COX-2 mRNA and protein levels in a number of inflammatory and cancer models (5-8, 10-12, 21, 22). One of the mechanisms by which n-3 fatty acids mediate their effects on COX-2 expression is likely via transcriptional regulation of COX-2 since n-3 fatty acids have been shown to alter NFκB and C/EBP β (5, 8, 22, 28-30). Thus, in the current study, modulation of transcription factors that regulate COX-2 expression is a potential mechanism by which diets containing EPA and DHA or DHA alone exert their effects on renal COX-2 levels.

Notably, n-3 fatty acids did not alter COX-1 expression in both *pcy* mice as well as Han:SPRD-*cy* rats, although expression of this enzyme was modulated by the presence of renal disease and by fat level (13, 14). This is consistent with the fact that *in vitro* COX-2 metabolizes a wider range of fatty acids as substrates and oxygenates EPA and ALA more efficiently than COX-1 (1, 31).

In a number of models of chronic renal disease, renal injury increases the expression of COX protein and mRNA and this parallels increased enzyme activity (32-36). However, in models of RCD, the presence of renal disease results in reduced COX-2 expression (13, 14). In addition, this reduction in COX-2 levels is inversely related to COX-2 enzyme activity (14). Thus, in the current study the increase in renal COX-2 expression with diets containing EPA and DHA or DHA alone may reflect a decrease in renal COX-2 activity. This premise is supported by a number of *in vivo* and *in vitro* studies that demonstrate a decrease in COX-2 activity after supplementation with EPA and/or DHA (4, 9, 28, 37, 38).

The results of the current study indicate that the level of fat in the diet modulates the effect of n-3 fatty acid on COX-2 expression. Diets containing high levels of n-3 fatty acids appear to exaggerate the effect of the n-3 fatty acids on renal COX-2 expression. *pcy* mice given high DO diets had a greater elevation in renal COX-2 expression compared to mice given low DO diets. Although fat level effects in Han:SPRD-*cy* rats were such that high fat fed rats had lesser renal COX-2 immunoreactivity compared to those given low fat diets, this effect was mitigated to a greater extent in diseased rats given a high level of MO in the diet.

In conclusion, the *in vivo* modulation of renal COX-2 expression in diseased kidneys by diets containing n-3 fatty acids appears to be dependent on the chain length of the fatty acid. In murine models of RCD, diets containing oils rich in EPA and DHA up-regulate COX-2 expression, while diets containing oils rich in ALA do not alter COX-2 *in vivo*.

5.6 References

1. Vane JR, Bakhle YS, Botting RM. Cyclooxygenases 1 and 2. Annu Rev Pharmacol Toxicol. 1998 ;38:97-120.

2. Breyer MD, Harris RC. Cyclooxygenase 2 and the kidney. Curr Opin Nephrol Hypertens. 2001 ;10:89-98.

3. Yang P, Chan D, Felix E, Cartwright C, Menter DG, Madden T, Klein RD, Fischer SM, Newman RA. Formation and antiproliferative effect of prostaglandin E(3) from eicosapentaenoic acid in human lung cancer cells. J Lipid Res. 2004 ;45:1030-9.

4. Calviello G, Di Nicuolo F, Gragnoli S, Piccioni E, Serini S, Maggiano N, Tringali G, Navarra P, Ranelletti FO, Palozza P. n-3 PUFAs reduce VEGF expression in human colon cancer cells modulating the COX-2/PGE2 induced ERK-1 and -2 and HIF-1alpha induction pathway. Carcinogenesis. 2004 ;25:2303-10.

5. Vecchini A, Ceccarelli V, Susta F, Caligiana P, Orvietani P, Binaglia L, Nocentini G, Riccardi C, Calviello G, Palozza P, Maggiano N, Di Nardo P. Dietary alpha-linolenic acid reduces COX-2 expression and induces apoptosis of hepatoma cells. J Lipid Res. 2004 ;45:308-16.

6. Rao CV, Hirose Y, Indranie C, Reddy BS. Modulation of experimental colon tumorigenesis by types and amounts of dietary fatty acids. Cancer Res. 2001 ;61:1927-33.

7. Denkins Y, Kempf D, Ferniz M, Nileshwar S, Marchetti D. Role of omega-3 polyunsaturated fatty acids on cyclooxygenase-2 metabolism in brain-metastatic melanoma. J Lipid Res. 2005 ;46:1278-84.

8. Horia E, Watkins BA. Comparison of stearidonic acid and alpha-linolenic acid on PGE_2 production and COX-2 protein levels in MDA-MB-231 breast cancer cell cultures. J Nutr Biochem. 2005 ;16:184-92.

9. Dommels YE, Haring MM, Keestra NG, Alink GM, van Bladeren PJ, van Ommen B. The role of cyclooxygenase in n-6 and n-3 polyunsaturated fatty acid mediated effects on cell proliferation, PGE(2) synthesis and cytotoxicity in human colorectal carcinoma cell lines. Carcinogenesis. 2003 ;24:385-92.

10. Jia Q, Zhou HR, Bennink M, Pestka JJ. Docosahexaenoic acid attenuates mycotoxin-induced immunoglobulin a nephropathy, interleukin-6 transcription, and mitogen-activated protein kinase phosphorylation in mice. J Nutr. 2004 ;134:3343-9.

11. Moon Y, Pestka JJ. Deoxynivalenol-induced mitogen-activated protein kinase phosphorylation and IL-6 expression in mice suppressed by fish oil. J Nutr Biochem. 2003 ;14:717-26.

12. Du C, Fujii Y, Ito M, Harada M, Moriyama E, Shimada R, Ikemoto A, Okuyama H. Dietary polyunsaturated fatty acids suppress acute hepatitis, alter gene expression and prolong survival of female Long-Evans Cinnamon rats, a model of Wilson disease. J Nutr Biochem. 2004 ;15:273-80.

13. Aukema HM, Adolphe J, Mishra S, Jiang J, Cuozzo FP, Ogborn MR. Alterations in renal cytosolic phospholipase A2 and cyclooxygenases in polycystic kidney disease. Faseb J. 2003 ;17:298-300.

14. Warford-Woolgar L, Peng CY, Shuhyta J, Wakefield A, Sankaran D, Ogborn MR, Aukema HM. Selectivity of cyclooxygenase (COX) isoform activity and prostanoid

production in normal and diseased Han:SPRD-*cy* rat kidneys. Am J Physiol Renal Physiol. 2006 ;290:F897-904.

15. Iglesias CG, Torres VE, Offord KP, Holley KE, Beard CM, Kurland LT. Epidemiology of adult polycystic kidney disease, Olmsted County, Minnesota: 1935-1980. Am J Kidney Dis. 1983 ;2:630-9.

16. Takahashi H, Calvet JP, Dittemore-Hoover D, Yoshida K, Grantham JJ, Gattone VH 2nd. A hereditary model of slowly progressive polycystic kidney disease in the mouse. J Am Soc Nephrol. 1991 ;1:980-9.

17. Sankaran D, Lu J, Bankovic-Calic N, Ogborn MR, Aukema HM. Modulation of renal injury in pcy mice by dietary fat containing n-3 fatty acids depends on the level and type of fat. Lipids. 2004 ;39:207-14.

18.Cowley BD Jr, Gudapaty S, Kraybill AL, Barash BD, Harding MA, Calvet JP, Gattone VH 2nd. Autosomal-dominant polycystic kidney disease in the rat. Kidney Int. 1993 ;43:522-34.

19. Lu J, Bankovic-Calic N, Ogborn M, Saboorian MH, Aukema HM. Detrimental effects of a high fat diet in early renal injury are ameliorated by fish oil in Han:SPRD-cy rats. J Nutr. 2003 ;133:180-6.

20. Ogborn MR, Nitschmann E, Bankovic-Calic N, Weiler HA, Aukema H. Dietary flax oil reduces renal injury, oxidized LDL content, and tissue n-6/n-3 FA ratio in experimental polycystic kidney disease. Lipids. 2002 ;37:1059-65.

21. Singh J, Hamid R, Reddy BS. Dietary fat and colon cancer: modulation of cyclooxygenase-2 by types and amount of dietary fat during the postinitiation stage of colon carcinogenesis. Cancer Res. 1997 ;57:3465-70.

22. Lee JY, Plakidas A, Lee WH, Heikkinen A, Chanmugam P, Bray G, Hwang DH. Differential modulation of Toll-like receptors by fatty acids: preferential inhibition by n-3 polyunsaturated fatty acids. J Lipid Res. 2003 ;44:479-86.

23. Lo CJ, Chiu KC, Fu M, Lo R, Helton S. Fish oil augments macrophage cyclooxygenase II (COX-2) gene expression induced by endotoxin. J Surg Res. 1999 ;86: 103-7.

24. Aukema HM, Yamaguchi T, Takahashi H, Philbrick DJ, Holub BJ. Effects of dietary fish oil on survival and renal fatty acid composition in murine polycystic kidney disease. Nutrition Research. 1992 ;12:1383-92.

25. Gorgoni B, Caivano M, Arizmendi C, Poli V. The transcription factor C/EBPbeta is essential for inducible expression of the cox-2 gene in macrophages but not in fibroblasts. J Biol Chem. 2001 ;276:40769-77.

26. Tak PP, Firestein GS. NF-kappaB: a key role in inflammatory diseases. J Clin Invest. 2001 ;107:7-11.

27. Sheu ML, Chao KF, Sung YJ, Lin WW, Lin-Shiau SY, Liu SH. Activation of phosphoinositide 3-kinase in response to inflammation and nitric oxide leads to the up-regulation of cyclooxygenase-2 expression and subsequent cell proliferation in mesangial cells. Cell Signal. 2005 ;17:975-84.

28. Bousserouel S, Brouillet A, Bereziat G, Raymondjean M, Andreani M. Different effects of n-6 and n-3 polyunsaturated fatty acids on the activation of rat smooth muscle cells by interleukin-1 beta. J Lipid Res. 2003 ;44:601-11.

29. Calder PC. Dietary modification of inflammation with lipids. Proc Nutr Soc. 2002 ;61: 345-58.

30. Babcock TA, Helton WS, Anwar KN, Zhao YY, Espat NJ. Synergistic anti-inflammatory activity of omega-3 lipid and rofecoxib pretreatment on macrophage proinflammatory cytokine production occurs via divergent NF-kappaB activation. J Parenter Enteral Nutr. 2004 ;28: 232-9.

31. Laneuville O, Breuer DK, Xu N, Huang ZH, Gage DA, Watson JT, Lagarde M, DeWitt DL, Smith WL. Fatty acid substrate specificities of human prostaglandin-endoperoxide H synthase-1 and -2. Formation of 12-hydroxy-(9Z, 13E/Z, 15Z)-octadecatrienoic acids from alpha-linolenic acid. J Biol Chem. 1995 ;270:19330-6.

32. Horiba N, Kumano E, Watanabe T, Shinkura H, Sugimoto T, Inoue M. Subtotal nephrectomy stimulates cyclooxygenase 2 expression and prostacyclin synthesis in the rat remnant kidney. Nephron. 2002 ;91:134-41.

33. Hirose S, Yamamoto T, Feng L, Yaoita E, Kawasaki K, Goto S, Fujinaka H, Wilson CB, Arakawa M, Kihara I. Expression and localization of cyclooxygenase isoforms and cytosolic phospholipase A2 in anti-Thy-1 glomerulonephritis. J Am Soc Nephrol. 1998 ;9: 408-16.

34. Komers R, Lindsley JN, Oyama TT, Schutzer WE, Reed JF, Mader SL, Anderson S. Immunohistochemical and functional correlations of renal cyclooxygenase-2 in experimental diabetes. J Clin Invest. 2001 ;107:889-98.

35. Wang JL, Cheng HF, Harris RC. Cyclooxygenase-2 inhibition decreases renin content and lowers blood pressure in a model of renovascular hypertension. Hypertension. 1999 ;34:96-101.

36. Wang JL, Cheng HF, Shappell S, Harris RC. A selective cyclooxygenase-2 inhibitor decreases proteinuria and retards progressive renal injury in rats. Kidney Int. 2000 ;57:2334-42.

37. Rao CV, Reddy BS. Modulating effect of amount and types of dietary fat on ornithine decarboxylase, tyrosine protein kinase and prostaglandins production during colon carcinogenesis in male F344 rats. Carcinogenesis. 1993 ;14:1327-33.

38. Takahashi M, Fukutake M, Isoi T, Fukuda K, Sato H, Yazawa K, Sugimura T Wakabayashi K. Suppression of azoxymethane-induced rat colon carcinoma development by a fish oil component, docosahexaenoic acid (DHA). Carcinogenesis. 1997 ;18:1337-42.

6. SELECTIVE COX-2 INHIBITION MARKEDLY SLOWS DISEASE PROGRESSION AND ATTENUATES ALTERED PROSTANOID PRODUCTION IN HAN:SPRD-*cy* RATS WITH INHERITED KIDNEY DISEASE

Sankaran D, Bankovic-Calic N, Ogborn MR, Crow G, Aukema HM

6.1 Abstract

Selective cyclooxygenase -2 (COX-2) inhibitors appear to have beneficial reno-protective effects in most, but not all, renal disease conditions. The objective of our study was to examine the effects of COX-2 inhibition in a rat model of polycystic kidney disease. Four week old Han:SPRD-cy rats were given either a standard rodent diet containing 3mg NS398 kg body weight^{-1} day^{-1} or a control diet with no drug for 7 weeks. In diseased rats, selective COX-2 inhibition resulted in an 18% and 67% reduction in cystic expansion and interstitial fibrosis respectively without altering renal function. Disease-associated pathologies such as renal inflammation, cell proliferation, and oxidant injury also were ameliorated (by 33, 38 and 59% respectively) with NS398 treatment. Kidney disease was associated with elevated renal COX-1 and -2 enzyme activities and treatment with NS398 blunted the increase in COX-2 enzyme activity (as indicated by 21% and 28% lower renal thromboxane B_2 and prostaglandin E_2 levels, respectively). Urinary excretion of prostanoid metabolites in diseased rats was further reduced with NS398. In summary, COX-2 inhibition attenuated renal injury, reduced the elevated renal COX-2 activity and ameliorated disease-related alterations in prostanoid production in this rat model of chronic renal disease.

6.2 Introduction

Cyclooxygenase (COX) exists as 2 major isoforms, COX-1 and COX-2. Previously, COX-1 was considered to be constitutively expressed and have general "housekeeping" functions, while COX-2 was believed to be inducible and involved in inflammatory responses (1). However, it is now known that COX-2 also is constitutively expressed in the mammalian kidney and that its metabolites play an integral role in the regulation of renal hemodynamics, the renin-angiotensin system, nephronogenesis and in renal pathogenesis (1).

Elevated COX-2 enzyme activity has been reported in a number of renal disorders and nephritic models (2-6), including the rat model of polycystic kidney disease (PKD) (7). In animal models of renal disease as well as in humans with elevated COX-2 activity, COX-2 inhibition often has beneficial effects (3, 8-15). However, pharmacologic blockade of COX-2 decreased GFR in salt-depleted and elderly subjects (16, 17) and was detrimental in a rat model of glomerulonephritis (18). However, the effect of selectively blocking COX-2 in cystic kidneys has not been ascertained.

The Han:SPRD-*cy* rat is an established model of autosomal dominant PKD in which heterozygotes develop progressive cystic change, renal interstitial fibrosis, inflammation, oxidative damage as well as hypertension and uremia in adult life (19). We have recently demonstrated that renal disease selectively alters the prostanoid profile and ratios in the Han:SPRD-*cy* rat (7). In diseased kidneys, the thromboxane B_2 (TXB_2) to prostaglandin (PG) ratios were higher than in normals, suggesting that the presence of cystic kidney disease shifts the balance towards a greater vasoconstrictive effect which may contribute to disease progression. In addition, among the vasodilatory prostanoids,

prostacyclin was altered to a greater extent than PGE_2 by renal disease. Although both renal COX-1 and COX-2 activities were elevated in diseased rats, the COX-2 activity was the predominant COX activity in both normal and diseased Han:SPRD-*cy* rats. The study indicated that there were no specific prostanoids associated with these isoforms. Thus, we undertook the current study to determine whether administering a selective COX-2 inhibitor *in vivo* would ameliorate renal cystic disease progression as well as disease-associated alterations in renal tissue injury and prostanoid production in these rats. This study also elucidates further the role of COX-2 and its metabolites in the pathogenesis of disease in the Han:SPRD-*cy* rat model of PKD.

6.3 Materials and Methods

Animals.

All animal procedures were examined by the University of Manitoba Protocol Management and Review committee and were in accordance with the guidelines of the Canadian Council on Animal Care. Han:SPRD-*cy* [also known as PKD/Mhm (*cy*/+)] rats were derived from our breeding colony, which originated from the colony of Dr. Benjamin Cowley (University of Kansas Medical Center, Kansas City, KS) (19). Weanling male Han:SPRD-*cy* heterozygotes were randomly assigned to either a control diet consisting of the AIN93G rodent diet (20) or the same diet with NS398 added. NS398 selectively inhibits rodent COX-2 (IC50=30nM), while not affecting COX-1 dependent prostanoid production (IC50 >100μM) (21, 22). It inhibits COX-1 activity only minimally even at doses >200mg/kg body weight (23). NS398 was mixed with the diet to achieve a dose of 3mg kg body weight^{-1}day^{-1}. In order to achieve this dose and based on previously determined food intake data, weanling rats were given 25mg NS-398 kg diet^{-1} for the first 2 weeks of the study and then switched to 36mg NS-398 kg diet^{-1} for the remainder of the study. Food intake (by routinely weighing food cups) and weekly body weight measurements were taken for all rats to ensure adequate dosage. The dosage of NS398 used in this study was based on previous studies that showed effective inhibition of COX-2 in the rat for up to 24 hours using a similar dose (24, 25). Diet ingredients, with the exception of NS398 (Cayman Chemical, Ann Arbor, Michigan, USA), were purchased from Dyets Inc.(Bethlehem, PA) or Harlan Teklad (Madison, WI).

Animals were fed the control and experimental diets for 7 weeks (ie until they were 10 weeks of age). At 9 weeks of age, rats were placed in metabolic cages for the

collection of metabolic data and after an acclimatization period of 2 days, 24h food and water intakes were measured. Urine was collected and stored at -80 °C for later analyses. At the end of the feeding period, rats were killed and trunk blood was collected to obtain serum. Left kidneys were removed, weighed and sectioned in half longitudinally across the hilum. One half of wet kidney tissue was fixed in 10% buffered formalin for morphological and histological analyses. The other half of the left kidney and the right kidneys were snap frozen in liquid nitrogen and stored at -80°C for later analyses.

Histology and Immunohistochemistry.

The left kidney was embedded in paraffin, sectioned at 5 microns and was processed using our previously described methods for histologic and immunohistochemical analyses (26). Sections for cyst area measurement were stained with hematoxylin and eosin and those for quantitative analysis of fibrosis with Sirius red (in adaptation of Masson's trichrome stain) which permits image analysis measurement using a standard incandescent microscope light source. Renal cell proliferation, inflammation and oxidant injury were assessed using 1:50 dilutions of an anti-mouse proliferating cell nuclear antigen (PCNA) antibody (M0879, Dako Corporation, Carpinteria, CA), a mouse anti-rat monocytes/macrophages monoclonal antibody (MAB 1435, Chemicon International, Temecula, CA) and a rabbit anti-Cu 2+-oxidized LDL polyclonal antibody (AB3230, Chemicon International, Temecula, CA) respectively. Dako EnVision Plus system (K4008, Dako Corporation, Carpinteria, CA) was used for secondary detection. Omission of the incubation step with primary antibody was used as a negative control for all antigens.

Image Analysis and morphometric assessment.

Quantitative histologic analysis of the left kidney was performed using our previously described methods (26, 27). Briefly, after being captured using a SPOT junior CCD camera by random stage movement through the sections, images were analyzed using the Image Pro version 4.5 package (Media Cybernetics, Silverspring, MD). An average of 25 measurements, starting from a random field of tissue section from kidney cross sections, were collected for all histomorphometric analyses. All measurements were carried out in a blinded fashion. The portion of tissue section occupied by tubular lumen or cyst was determined for cyst area measurements. Renal interstitial fibrosis and oxidant injury were measured by densitometry, while the number of cells stained positive for PCNA as well as macrophages were counted using the Image Pro version 4.5 package (Media Cybernetics, Silverspring, MD) as described previously (26, 27). Renal cyst area measurements were expressed relative to kidney weight-to-body weight ratios. PCNA positive cells in tubular epithelial cells were counted as these are the base cell type of cysts. Measurements of fibrosis, oxidized LDL and other cellular markers were corrected to solid tissue areas of sections to avoid underestimation of these variables due to empty cystic areas in these sections.

Immunoblotting.

Half of the left kidney was lyophilized and 30 mg were homogenized in ice-cold homogenization buffer containing protease inhibitors and 1% Triton X-100 as described (7, 28). After centrifugation of the kidney homogenate, the resulting pellet was re-suspended in buffer containing 1% Triton X-100 and re-centrifuged. The resulting supernatant contains COX-2 protein. Protein concentrations of these fractions were determined using the Bradford method. After SDS-PAGE, detection of COX-2 was

carried out with a 1:250 dilution of the primary antibody (160106, Cayman Chemical, Ann Arbor, Michigan) followed by incubation with a peroxidase-conjugated secondary antibody at a dilution of 1:20,000. ChemiGlow™ (Alpha Innotech, San Leandro, California) substrate was used to visualize the immunoreactive bands which were then analyzed and quantified on the Fluorchem™ FC digital imaging system (Alpha Innotech Corporation, San Leandro, California) (7, 28).

Real-time RT-PCR.

Total RNA was extracted from 10-20 mg of lyophilized kidneys using TRIzol as described (7). DNA was removed by DNase treatment with DNase I (Invitrogen, Carlsbad, CA) for 15 min at room temperature. One-step RT-PCR was performed on 0.5□g of total RNA using the QuantiTect® SYBR® Green RT-PCR kit (Qiagen, Mississauga, Canada). Oligonucleotide sequences for the rat COX-1 and -2 primers, generated using the Primer 3 software, have been described (7). Real-time RT-PCR was performed on a Cepheid SmartCycler II (Cepheid, Sunnyvale, CA) with the following protocol:reverse transcription at 50°C for 30 min, PCR activation at 95°C for 15 min, 40 PCR cycles at 94°C for 15 s, 55°C for 30 s and 72°C for 30 s. Relative amounts of mRNA were determined by comparing cycle threshold (CT) numbers for equal amounts of RNA subjected to RT-PCR and calculating differences in gene expression using the formula $2^{\Delta CT}$ as described (7).

Prostanoid Production and COX Activity.

Tissue processing for the determination of prostanoids has been described (7). Briefly, 60 mg of lyophilized tissue from the right kidney was homogenized with ice-cold fresh Tyrodes buffer. Protein concentrations of all fractions were determined using the

Bradford method. For determination of endogenous prostanoid levels, steady state prostanoid production in vitro and potential COX activity, aliquots were incubated under the following times and conditions:1) 0 min for determination of endogenous levels of prostanoids and background levels for conditions 2-4; 2) 60 min at 37°C for determination of steady-state in vitro prostanoid production; 3) 10 min at 37°C for determination of prostanoid production by total COX activity; 4) 10 min at 37°C with 0.1 μM SC560, a selective COX-1 inhibitor (Cayman, Ann Arbor, Michigan) for determination of prostanoid production by COX-2 activity. COX-1 activity was determined by the difference between total COX (condition 3) and COX-2 (condition 4) activity. Criteria for selection of incubation times and level of inhibitor have been published (7). At the end of all incubation periods, reactions were stopped with fresh ice-cold acetylsalicylic acid (5mmol/L final concentration). Samples were centrifuged and the supernatant was collected and stored at -80°C for the determination of PGE_2 and the stable metabolites of PGI_2 (6-keto-$PGF_{1\alpha}$) and TXA_2 (TXB_2) using commercial enzyme immunoassay (EIA) kits (Cayman Chemical, Ann Arbor, Michigan).

Urinary TXB_2, 6-keto-$PGF_{1\alpha}$ and PGEM (stable urinary metabolite of PGE_2) were also analyzed using EIA kits (Cayman Chemicals, Ann Arbor, MI, USA) according to the manufacturer's instructions.

Statistical Analyses.

Data were analysed using SAS software (SAS Inc., Cary, NC) as a completely randomized design with a 2x2 factorial set of treatments [2 genetic groups, (+/+ and *Cy*/+) and two diets (Control and NS398)]. Diagnostic tests were performed to evaluate assumptions about the residuals, in particular normality and the uniformity of their

variance across treatment groups. Data were normalized using a logarithmic transformation where necessary. Where variance was unequal across treatment groups, the SAS Mixed procedure was used to accomodate this. Post-hoc t-tests were performed if the interaction effect was significant at $P<0.10$. A P value of <0.05 was used to determine significance of main or treatment effects.

6.4 Results

Selective COX-2 inhibition with NS398 ameliorates indices of renal injury, but does not alter renal function, in diseased Han:SPRD-cy rats. During the study period, all animals thrived on the diets and displayed normal growth patterns including a slight growth depression (7%) associated with disease (Table 6-1). Food intake data indicated that rats treated with NS398 were ingesting between 3-5 mg NS398 kg body $wt^{-1}day^{-1}$ (data not shown). NS398 administration resulted in reduced urinary excretion and renal production of prostanoids (see below) indicating the dose of NS398 was effective in inhibiting COX-2 activity *in vivo*.

The effect of selective COX-2 inhibition with NS398 on parameters of renal injury was determined morphologically and immunohistochemically. Cystic expansion, the primary defect in Han:SPRD-*cy* rats, was 18% lower with drug treatment for 7 weeks (Fig. 6-1). Interstitial fibrosis was reduced by 67% in kidneys of NS398 treated rats (Figs. 6-2A and B). Disease-associated pathologies such as renal inflammation, cell proliferation and oxidant injury also were ameliorated with selective COX-2 blockade. Renal macrophage infiltration, a marker of inflammation, was 33% lower in diseased rats given NS398 than those given no drug (Figs. 6-3A and B). Selective COX-2 inhibitor treatment also resulted in a reduction in renal cell proliferation, with 38% fewer PCNA positive cells in kidney sections of rats given NS398 compared to those given the control diet (Figs. 6-4A and B). Further, compared to rats given NS398-free diets, oxidative damage (as determined by the presence of oxidized LDL) was reduced by 59% in the kidneys of NS398 treated rats (Figs. 6-5A and B).

At the end of the study period, rats with renal disease had larger kidneys, lower creatinine clearance rates and overall worsened renal function compared to their normal counterparts (Table 6-1). The reduction in creatinine clearance was associated with elevated serum creatinine and urea levels (Table 6-1). In contrast to the effects on renal injury, worsened renal function in diseased Han:SPRD-*cy* rats was not attenuated by NS398 treatment. Neither genotype nor selective COX-2 inhibition significantly affected proteinuria (Table 6-1).

COX-2 inhibition results in elevated COX-2 gene and protein expression in Han:SPRD-cy rats. Consistent with previously reported COX-2 mRNA expression in Han:SPRD-*cy* rat kidneys (7), diseased rat kidneys had 80-86% lower COX-2 mRNA levels compared to their normal unaffected counterparts (Table 6-2). NS398 treatment partially reversed these changes by increasing renal COX-2 gene expression by 14-66% in normal and diseased rats. Renal COX-2 protein levels, as measured by western immunoblotting analyses, reflected the relative COX-2 gene levels. Diseased rat kidneys had a 92% reduction in COX-2 enzyme levels compared to normal rat kidneys. As with gene expression, selective COX-2 inhibition with NS398 upregulated immunoreactive protein expression of COX-2 in normal and diseased kidneys by 84 and 64% respectively.

Selective COX-2 inhibition attenuates disease-associated increases in endogenous renal prostanoids. In normal kidneys, the vasodilatory PGE_2 and 6-keto-$PGF_{1\alpha}$ were the predominant prostanoids, accounting for nearly 93% of the endogenous and the in vitro steady-state prostanoid levels, while the vasoconstrictory TXB_2 accounted for 7% (Table 6-3). Endogenous and in vitro steady state levels of all three prostanoids were

significantly higher in diseased compared to normal kidneys. In diseased kidneys, the vasodilatory prostanoids constituted 87-89% of the total endogenous and steady-state prostanoid levels and TXB_2 accounted for 11-13%.

Selective COX-2 inhibition with NS398 blunted the disease-associated elevation in endogenous prostanoid levels, with the effect being significant for PGE_2, TXB_2 and total prostanoid levels (Table 6-3). In diseased rats, NS398 treated vs untreated rats had 21% lower renal TXB_2 levels, 28% less PGE_2 and overall 29% less total prostanoids. Though NS398 did not significantly alter in-vitro steady state levels of the prostanoids (Table 6-3), its effect on these levels followed a trend similar to that of the endogenous prostanoid concentrations.

Selective COX-2 inhibition attenuates disease-associated increases in COX activities and prostanoid production. COX activities in normal and diseased kidneys mirrored the endogenous prostanoid levels. Total COX, COX-1 and COX-2 (Table 6-4) activities were significantly higher in kidneys from diseased rats compared to those from normal rats, irrespective of the prostanoid measured. NS398 treatment of diseased rats attenuated this disease-induced increase in total COX and COX-2 activities as measured by total prostanoid production as well as TXB_2 and PGE_2 (Table 6-4). Consistent with selectivity of the drug, NS398 did not have a significant effect on renal COX-1 activity (Table 6-4).

PGE_2 and 6-keto-$PGF_{1\alpha}$ have vasodilatory effects in the kidney, while TXB_2 is vasoconstrictory; hence, the balance between their relative amounts is crucial for maintenance of normal renal function. Thus, the TXB_2 to PG ratios for all conditions (except COX-1 activity, in which the presence of very low values precludes these ratios in being meaningful) were calculated to determine which prostanoid exhibited the

greatest relative difference between diseased and normal rats. TXB_2/PGE_2 was higher in diseased compared to normal rat kidneys when calculated by any of the conditions (Fig. 6-6A). TXB_2/6-keto-$PGF_{1\alpha}$ (Fig. 6-6B) also was elevated by disease, but the relative increase was significant ($P<0.05$) only for prostanoids resulting from COX-2 activity. 6-keto-$PGF_{1\alpha}/PGE_2$ (Fig. 6-6C) was higher in diseased rats compared to normal rats when measured by all conditions. Thus, the change in the relative levels of prostanoids in diseased kidneys is in the order of TXB_2 > 6-keto-$PGF_{1\alpha}$ > PGE_2. The ratios of the vasodilatory and vasoconstrictory prostanoids in rats given NS398 and control diets also were calculated to determine selective prostanoid production by COX isoforms. Interestingly, selective COX-2 inhibition with NS398 did not significantly alter relative renal prostanoid ratios (Figs. 6-6 A-C).

Selective COX-2 inhibition decreases urinary prostanoid metabolite excretion even further in Han:SPRD-cy rat. Similar to the renal prostanoid profile, urinary PGEM and 6-keto-$PGF_{1\alpha}$ were the predominant prostanoids excreted by both normal and diseased rats (92-96% in normals and 86-89% in PKD rats) (Table 6-5). Urinary levels of TXB_2 accounted for 4-8% of total prostanoids in normal compared to 11-14% in PKD animals (Table 6-5).

Diseased rats had significantly lower urinary prostanoid levels compared to their normal counterparts, ranging from a 2 fold (TXB_2 and PGEM) to a 7 fold decrease (6-keto-$PGF_{1\alpha}$) in urinary prostanoid excretion. Preferential COX-2 inhibition resulted in a further reduction of urinary vasodilatory prostanoid excretion in both normal and diseased rats. NS398 treatment resulted in 31-58% less PGEM and 31-48% less 6-keto-

$PGF_{1\alpha}$ levels in the urine (Table 6-5). NS398 treatment did not alter urinary TXB_2 levels, although they tended to be lower in treated diseased rats.

Table 6-1. Body weights, kidney weights and renal function parameters in normal (+/+) and diseased (*Cy/+*) Han:SPRD-*cy* rats given NS398 in the diet for 7 weeks.

	Control		NS398		Effects
	+/+	Cy/+	+/+	Cy/+	P value
	N = 13	n = 12	n = 9	n = 16	
Body Weight (g)	385 ± 4	362 ± 4	387 ± 5	355 ± 4	Genotype(P<0.0001)
Kidney Weight (g/100g body weight)	0.73 ± 0.1	2.50 ± 0.1	0.77 ± 0.1	2.30 ± 0.1	Genotype(P<0.0001)
Serum Creatinine (µmol/L)	54.6 ± 3.5	101.9 ± 3.5	50.8 ± 4.2	103.5 ± 3.5	Genotype(P<0.0001)
Serum Urea Nitrogen (mmol/L)	4.2 ± 1.3	28.5 ± 1.4	3.7 ± 1.5	29.0 ± 1.2	Genotype(P<0.0001)
Creatinine Clearance (ml/min/100g body weight)	0.34 ± 0.02	0.16 ± 0.03	0.41 ± 0.03	0.18 ± 0.02	Genotype(P<0.0001)
Urinary protein (mg/24hr)	5.7 ± 0.5	5.7 ± 0.5	4.4 ± 0.8	6.0 ± 0.4	None

Values are means ± SE.

Table 6-2. Relative renal COX-2 mRNA and protein expression in Han:SPRD-cy rats given NS398 in the diet for 7 weeks.

	Control		NS398		Effects
	+/+	Cy/+	+/+	Cy/+	P value
	n = 9	n = 9	n = 9	n =9	
COX-2 mRNA	100 ± 11.1	13.6 ± 14.2	113.6 ± 15.3	22.5 ± 11.5	Genotype(P<0.0001), Drug (P=0.0246)
COX-2 Protein	100 ± 12.3[a]	8.2 ± 1.4[b]	184.4 ± 21.0[c]	13.5 ± 1.1[d]	Interaction (P=0.0116)

Values are means (as percentage of control normal) ± SE. Means with different superscripts are significantly different (P<0.05).

Table 6-3. Endogenous (0 min) and in vitro steady-state (60 min) prostanoid levels in normal (+/+) and diseased (Cy/+) Han:SPRD-cy rats given NS398 in the diet for 7 weeks.

	Control		NS398		Effects
	+/+	Cy/+	+/+	Cy/+	P value
	n = 9	n = 9	n = 8	n = 9	
	Endogenous Levels				
TXB_2	0.10 ± 0.04^a	0.66 ± 0.04^b	0.12 ± 0.04^a	0.52 ± 0.04^c	Interaction (P=0.0544)
PGE_2	0.75 ± 0.21^a	2.28 ± 0.22^b	0.96 ± 0.22^a	1.64 ± 0.21^c	Interaction (P=0.0607)
6-keto-$PGF_{1\alpha}$	0.59 ± 0.28	2.69 ± 0.28	0.56 ± 0.30	2.01 ± 0.28	Genotype (P<0.0001)
Total	1.44 ± 0.45^a	5.91 ± 0.48^b	1.64 ± 0.48^a	4.18 ± 0.45^c	Interaction (P=0.0474)
	In vitro Steady-State Levels				
TXB_2	0.43 ± 0.54	6.28 ± 0.54	0.50 ± 0.57	5.16 ± 0.54	Genotype (P<0.0001)
PGE_2	1.91 ± 0.45	5.82 ± 0.47	2.54 ± 0.47	5.47 ± 0.45	Genotype (P<0.0001)

6-keto-$PGF_{1\alpha}$	4.17 ± 3.27	38.03 ± 3.27	3.72 ± 3.47	32.73 ± 3.27	Genotype (P<0.0001)
Total	6.51 ± 3.86	50.19 ± 4.09	6.76 ± 4.09	43.35 ± 3.86	Genotype (P<0.0001)

Values are means ± SE. Means with different superscripts are significantly different (P<0.05).

Table 6-4. Renal COX, COX-1 and COX-2 activities (ng/mg protein/min) as determined by PGE_2, 6-keto-PGF_{1a}, TXB_2 and total prostanoid production in normal (+/+) and diseased (Cy/+) rat kidneys given NS398 in the diet for 7 weeks.

	Control		NS398		Effects
	+/+	Cy/+	+/+	Cy/+	P value
	n = 9	n = 9	n = 8	n = 9	
			COX Activity		
TXB_2	0.03 ± 0.03	0.46 ± 0.03	0.03 ± 0.04	0.38 ± 0.03	Genotype (P<0.0001)
PGE_2	0.10 ± 0.02[a]	0.33 ± 0.02[b]	0.12 ± 0.02[a]	0.25 ± 0.02[c]	Interaction (P=0.0379)
6-keto-$PGF_{1\alpha}$	0.20 ± 0.16	2.28 ± 0.16	0.20 ± 0.17	1.93 ± 0.16	Genotype (P<0.0001)
Total	0.33 ± 0.18[a]	3.10 ± 0.19[b]	0.36 ± 0.19[a]	2.56 ± 0.18[c]	Interaction (P=0.0719)
			COX-1 Activity		
TXB_2	0.00 ± 0.00	0.03 ± 0.01	0.00 ± 0.00	0.05 ± 0.02	Genotype (P=0.0180)
PGE_2	0.00 ± 0.00	0.06 ± 0.02	0.01 ± 0.00	0.03 ± 0.00	Genotype (P=0.0037)

6-keto-$PGF_{1\alpha}$	0.02 ± 0.01	0.19 ± 0.12	0.01 ± 0.00	0.23 ±0.06	Genotype (P=0.0173)
Total	0.02 ± 0.01	0.30 ± 0.14	0.02 ± 0.01	0.31 ± 0.07	Genotype (P=0.0041)
			COX-2 Activity		
TXB_2	0.03 ± 0.03^a	0.44 ± 0.03^b	0.04 ± 0.03^a	0.34 ± 0.03^c	Interaction (P=0.0330)
PGE_2	0.10 ± 0.02^a	0.28 ± 0.02^b	0.12 ± 0.02^a	0.20 ± 0.02^c	Interaction (P=0.0158)
6-keto-$PGF_{1\alpha}$	0.23 ± 0.17	2.16 ± 0.17	0.23 ± 0.18	1.70 ± 0.17	Genotype (P<0.0001)
Total	0.36 ± 0.19^a	2.96 ± 0.21^b	0.38 ± 0.21^a	2.27 ± 0.19^c	Interaction (P=0.0801)

Values are means ± SE. Means with different superscripts are significantly different (P<0.05).

Table 6-5. Urinary prostanoid excretion (ng/24hr) in normal (+/+) and diseased (Cy/+) rat kidneys given NS398 in the diet for 7 weeks.

	Control		NS398		Effects
	+/+	*Cy*/+	+/+	*Cy*/+	P value
	$n = 13$	$n = 12$	$n = 9$	$n = 16$	
Urinary TXB_2	4.24 ± 0.59	2.78 ± 0.51	5.01 ± 0.59	1.82 ± 0.46	Genotype ($P<0.0001$)
Urinary PGEM	11.16 ± 0.48	7.04 ± 0.52	7.66 ± 0.61	2.97 ± 0.45	Genotype($P<0.0001$), Drug ($P<0.0001$)
Urinary 6-keto $PGF_{1\alpha}$	83.36 ± 4.44	13.02 ± 4.62	57.22 ± 6.05	6.76 ± 4.00	Genotype($P<0.0001$), Drug ($P<0.0001$)

Values are means ± SE.

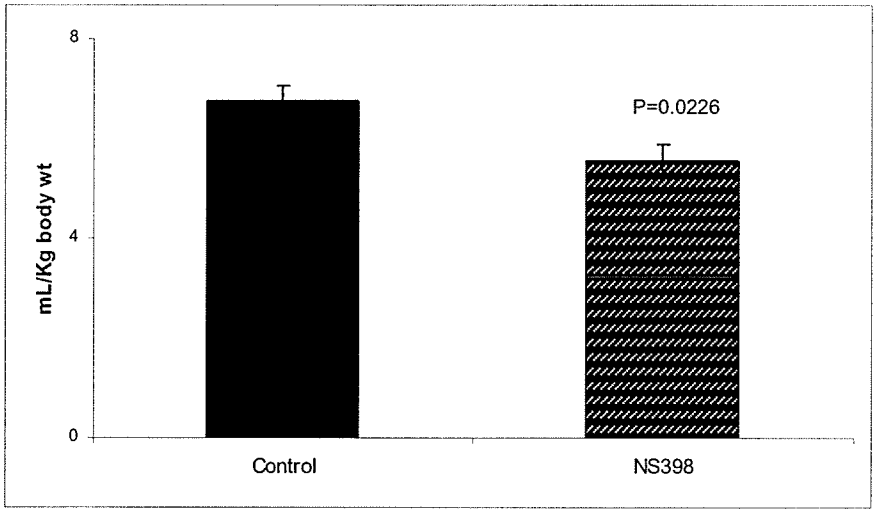

Figure 6-1. Renal cystic change in diseased Han:SPRD-*cy* (*Cy*/+) rats given NS398 in the diet for 7 weeks. Values are means + SE (n = 12-16).

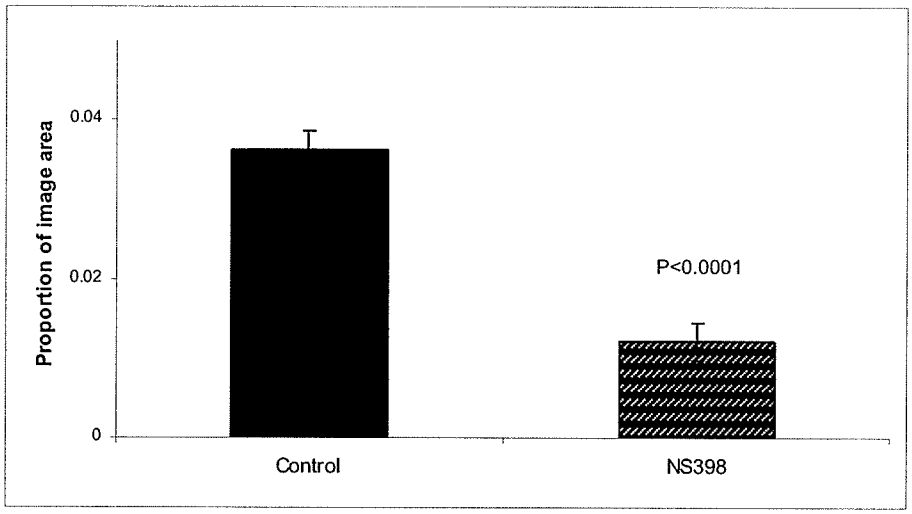

Figure 6-2A. Renal interstitial fibrosis in diseased Han:SPRD-*cy* (*Cy*/+) rats given NS398 in the diet for 7 weeks. Values are means + SE (n = 12-16).

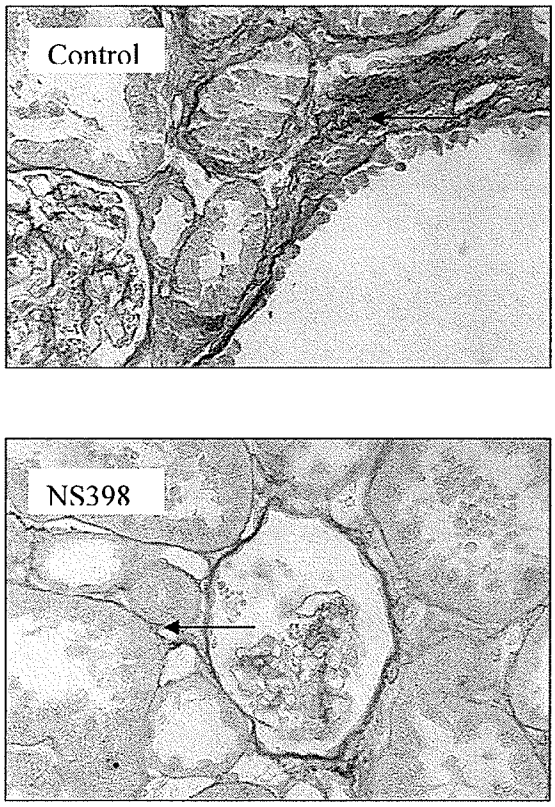

Figure 6-2B. Renal interstitial fibrosis in diseased (*Cy*/+) Han:SPRD-*cy* rats given NS398 in the diet for 7 weeks. Sirius red stain, magnification 40X. Arrows point to areas of increased renal fibrosis identified by darkly stained collagen deposits in interstitial spaces, especially around periphery of cysts.

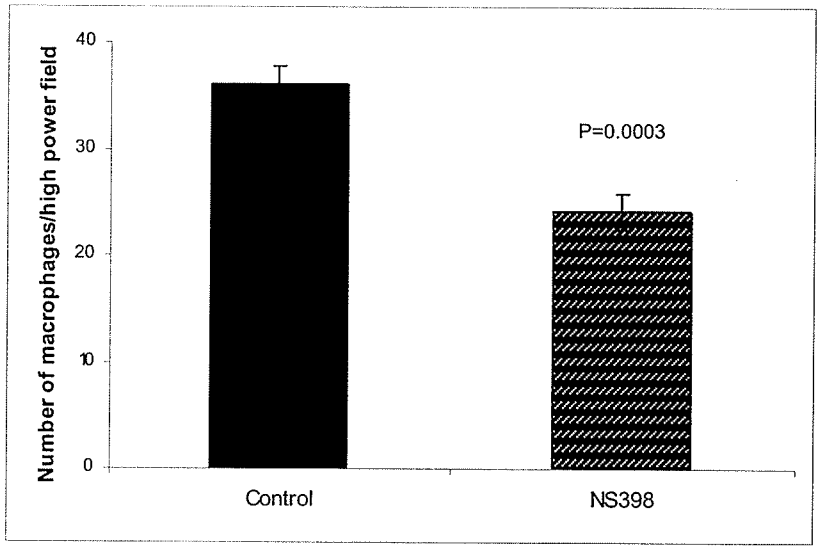

Figure 6-3A. Renal macrophage count in diseased Han:SPRD-*cy* (*Cy*/+) rats given NS398 in the diet for 7 weeks. Values are means + SE (n = 12-16).

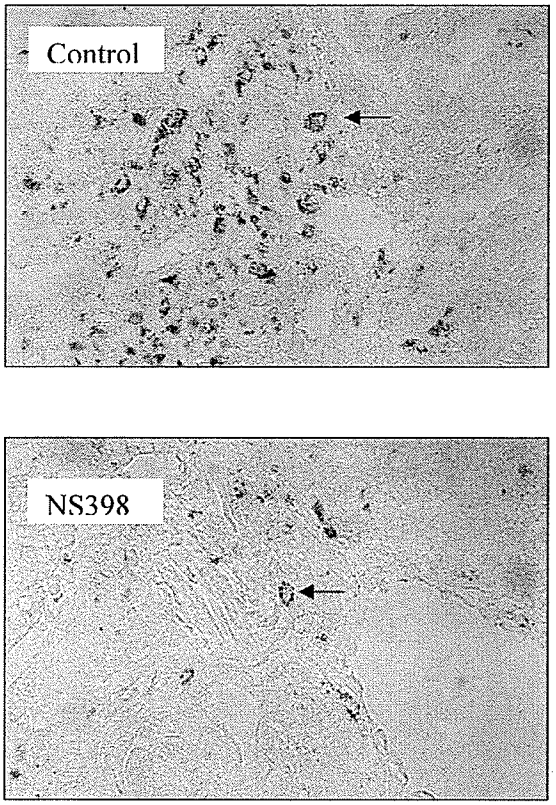

Figure 6-3B. Renal macrophage infiltration in diseased (*Cy*/+) Han:SPRD-*cy* rats given NS398 in the diet for 7 weeks. Magnification 20X. Arrows point to areas of spherical, dark brown-ringed ED1+ macrophages in renal interstitium.

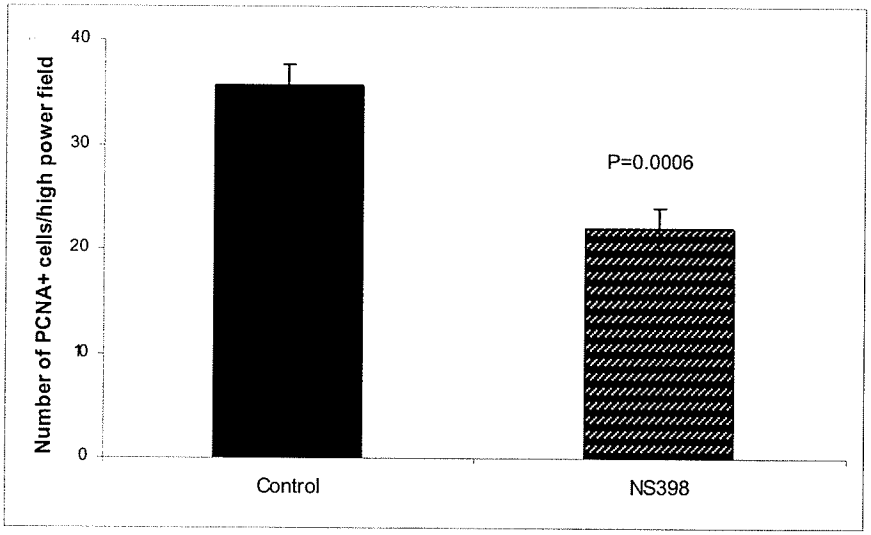

Figure 6-4A. Renal cells positive for PCNA in diseased Han:SPRD-*cy* (*Cy*/+) rats given NS398 in the diet for 7 weeks. Values are means + SE (n = 12-16).

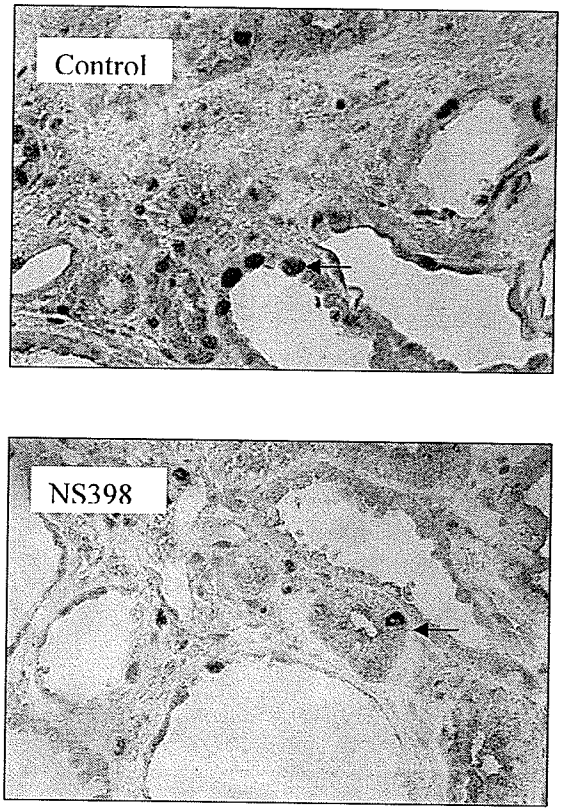

Figure 6-4B. Renal PCNA + epithelial cells in diseased (*Cy*/+) Han:SPRD-*cy* rats given NS398 in the diet for 7 weeks. Magnification 20X. Arrows point to areas of spherical, dark brown PCNA + cells in tubular epithelial cells.

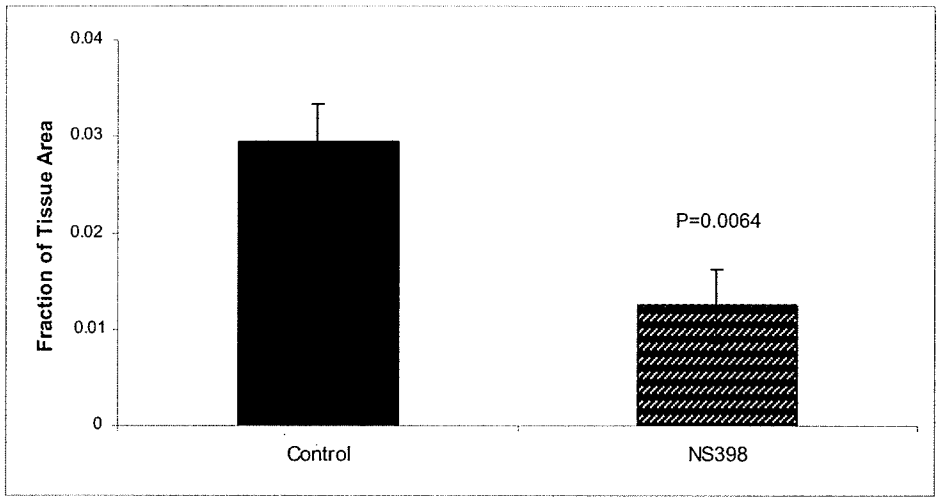

Figure 6-5A. Renal oxidized LDL staining in diseased Han:SPRD-*cy* (*Cy*/+) rats given NS398 in the diet for 7 weeks. Values are means + SE (n = 12-16).

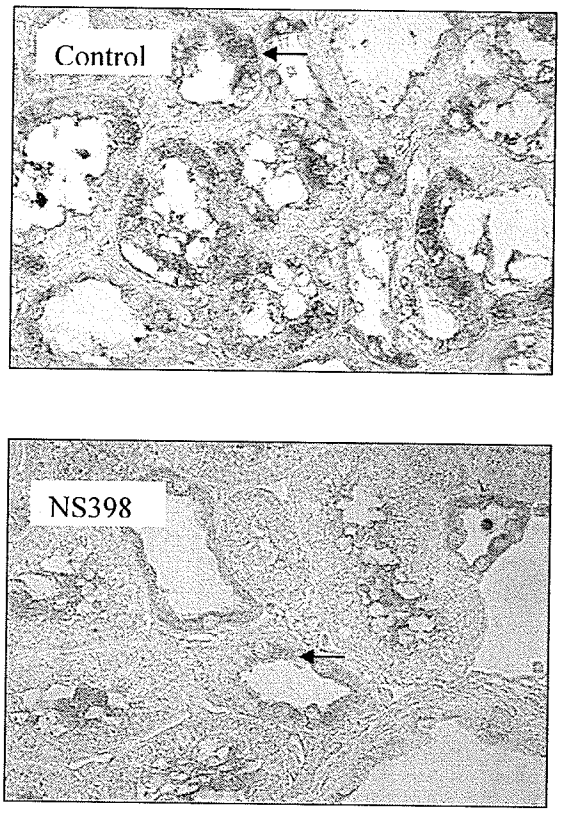

Figure 6-5B. Renal oxLDL staining in diseased (*Cy*/+) Han:SPRD-*cy* rats given NS398 in the diet for 7 weeks. Magnification 20X. Arrows point to areas of intense pink Cu2+- oxLDL staining especially around periphery of cysts.

A

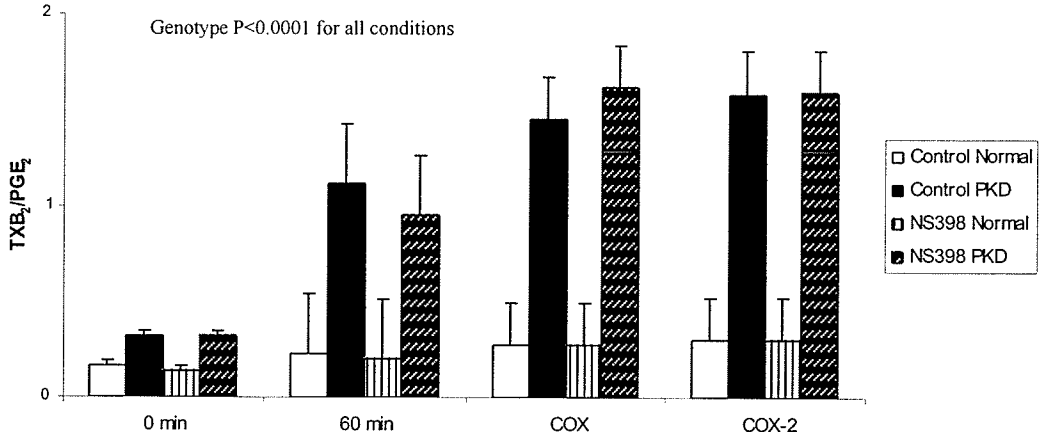
Genotype P<0.0001 for all conditions
TXB2/PGE2
2
1
0
0 min
60 min
COX
COX-2
Control Normal
Control PKD
NS398 Normal
NS398 PKD

B

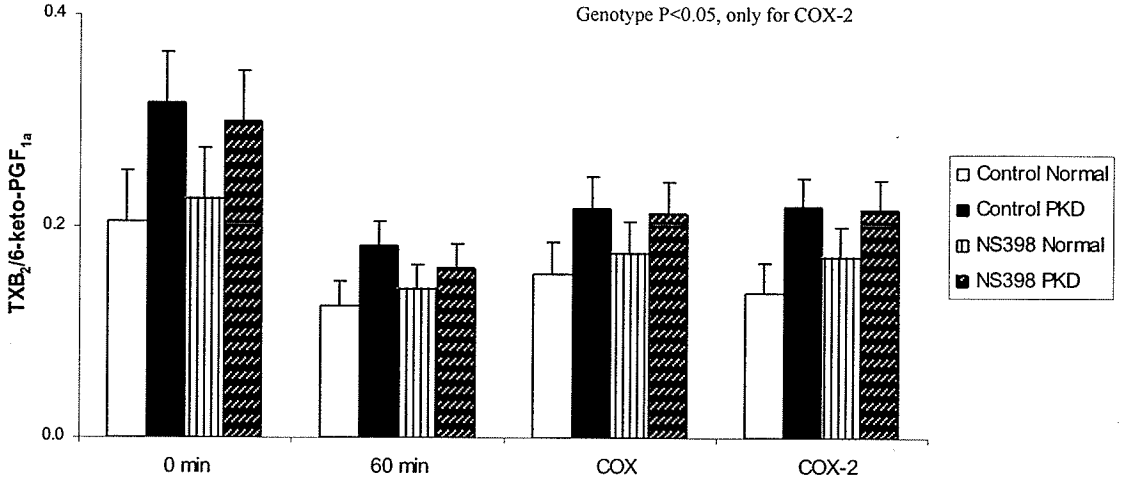
Genotype P<0.05, only for COX-2
TXB2/6-keto-PGF1a
0.4
0.2
0.0
0 min
60 min
COX
COX-2
Control Normal
Control PKD
NS398 Normal
NS398 PKD

C

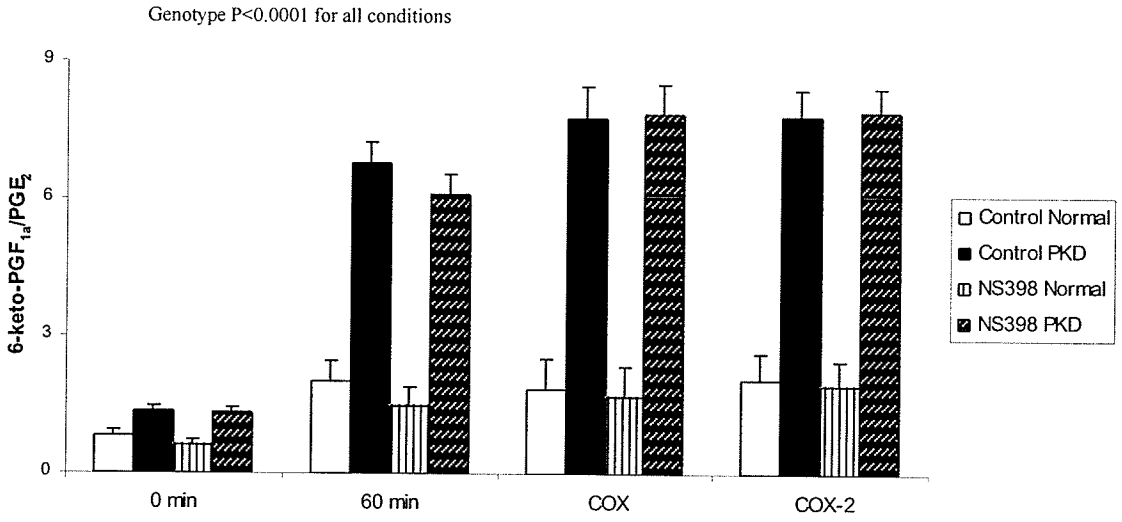

Figure 6-6. (A) TXB_2/PGE_2, (B) TXB_2/6-keto-$PGF_{1\alpha}$ and (C) 6-keto-$PGF_{1\alpha}/PGE_2$ ratios in normal (+/+) and diseased (*Cy*/+) kidneys from Han:SPRD-*cy* rats given NS398 or control diets in the following conditions:0 min (endogenous levels), 60 min (steady-state in vitro levels), COX activity and COX-2 activity. Values are means + SE (n = 8-9).

6.5 Discussion

Selective COX-2 inhibition by NS398 significantly ameliorated renal injury in Han:SPRD-*cy* rats with inherited cystic kidney disease. Treatment with NS398 resulted in lower cyst growth and interstitial fibrosis as well as fewer PCNA positive cells, decreased macrophage counts and less oxidant injury in the kidneys of diseased rats, indicating that COX-2 plays a significant role in the pathology and progression of chronic renal injury in Han:SPRD-*cy* rats. These observations are consistent with the previously reported reno-protective effects of selective COX-2 inhibitors in other forms of chronic renal injury (3, 8-14). Moreover, the attenuation of inflammatory and proliferative components of this renal disease by NS398 is concurrent with the established anti-inflammatory effects of COX-2 inhibition as well as previously reported anti-proliferative (29-31) and anti-fibrotic benefits of NS398 (32).

Despite the lack of an effect on renal function, these histological changes are likely to have long term beneficial effects on disease progression. Cyst expansion is a sensitive marker of disease progression, precedes the changes in function and is associated with the initiation of inflammation, fibrosis and other secondary changes (33). Hence, the mitigating effects of NS398 on cyst growth and other disease-associated pathologies, despite not being reflected in renal function parameters, would likely ameliorate the development of late-onset renal insufficiency. These results compel further investigation into the effects of different doses and longer term effects of selective COX-2 inhibitors on cystic renal disease progression.

The results of the current study demonstrate that COX-2 is primarily responsible for the increased COX activity in the diseased Han:SPRD-*cy* rat kidney. The elevated

COX-2 activity in these diseased kidneys is associated with higher TXB_2 to PG ratios (compared to normal kidneys), suggesting that the prostanoid balance shifts towards a greater vasoconstrictory effect in diseased kidneys. Indeed, earlier studies have demonstrated that inhibition of TXA_2 synthase ameliorates renal injury, proteinuria and glomerulosclerosis in the remnant kidney (34, 35). Interestingly, selective COX-2 inhibition did not significantly alter TXB_2 to PG ratios suggesting that NS398 treatment reduced both vasoconstrictory and vasodilatory prostanoids to a similar extent. These results confirm and extend our previous findings (7) of a lack of isoform specificity in prostanoid production in the rat kidney.

In the current study, COX-2 inhibition in normal rats did not alter renal PGE_2 levels. This is consistent with earlier studies in animals (36) as well as humans (37-39) that show a similar PGE_2 sparing effect of selective COX-2 inhibitors in normal kidneys. This PGE_2-sparing effect of COX-2 inhibitors has been interpreted as indirect evidence that under normal conditions the majority of renal PGE_2 is produced by COX-1 activity. However, the current direct analyses of renal COX-1 and -2 activities demonstrate that while COX-2 inhibition does not reduce PGE_2 production in normal rat kidneys, the predominant COX activity in the kidney is due to the COX-2 isoform. This premise is consistent with findings from a recent study (40) in which renal PGE_2 production in normal Sprague-Dawley rat kidneys was found to be predominantly COX-2 dependent. The current study shows that this PGE_2 pool is resistant to inhibition by COX-2 selective inhibitors in the normal kidney. In contrast, in kidneys of diseased rats, selective COX-2 inhibition resulted in a reduction of renal PGE_2 levels, consistent with previous findings (3, 14, 41). Taken together, this suggests that renal PGE_2 production induced by disease

is susceptible to COX-2 inhibition while PGE_2 produced in the normal physiologic state is resistant to such pharmacologic inhibition.

The effect of selective COX-2 inhibition on prostacyclin and thromboxane production was determined by measuring renal 6-ketoPGF$_{1\alpha}$ and TXB_2 levels, respectively. Similar to the effect of COX-2 inhibition on PGE_2 levels, NS398 did not alter renal 6-ketoPGF$_{1\alpha}$ or TXB_2 levels in normal rats, but resulted in decreased 6-ketoPGF$_{1\alpha}$ and TXB_2 levels in diseased rat kidneys. Taken together with the finding that renal COX-2 activity is the predominant COX isoform activity, these results suggest that, similar to renal PGE_2, renal synthesis of 6-ketoPGF$_{1\alpha}$ and TXB_2 is primarily COX-2-dependent and that prostanoid pools resistant to COX-2 inhibition are present in normal kidneys, while those susceptible to COX-2 inhibition are present in diseased kidneys. This inference is consistent with studies that demonstrated the efficacy of COX-2 inhibitors for prostanoids synthesized by inflamed tissue compared to those produced by normal tissue (24, 25).

In contrast to renal prostanoid production, whole body synthesis of prostanoids can be reduced by selective COX-2 antagonism in normal rats as shown by reduced urinary excretion of PGEM and 6-ketoPGF$_{1\alpha}$. Urinary excretion of PGEM reflects whole body synthesis of PGE_2 (45), while urinary excretion of 6-ketoPGF$_{1\alpha}$ reflects systemic as well as renal production of prostacylin (46). The inhibitory effect of NS398 on PGEM and 6-ketoPGF$_{1\alpha}$ excretion confirms the well-characterized inhibitory effects of specific COX-2 inhibitors on whole body prostacyclin synthesis (37, 42, 47, 48). By comparison, urinary excretion of TXB_2 has been shown to reflect intra-renal synthesis of TXB_2 (44),

and the lack of an NS398 treatment effect on TXB_2 excretion in normal rats is consistent with the data on renal TXB_2 production.

The primary feature of PKD is tubular cystic expansion associated with abnormal proliferation of renal tubular epithelial cells. Cyst epithelia are hyperproliferative and lose polarized cell architecture (49). In vitro studies in cyst epithelial cells demonstrate a significant role for adenosine 3' 5'-cyclic monophosphate (cAMP) in the proliferation of cyst mural cells as well as in cyst fluid secretion (50-52). In addition, elevated renal and urine levels of cAMP have been reported in the animal models of PKD (53, 54). Consistent with the premise that adenylyl cyclase agonists have the potential to accelerate cyst growth in PKD, studies using agents that block adenylyl cyclase activation resulted in a dramatic reduction in cyst formation and growth in animal models of inherited renal cystic disorders (53). PGI_2 and PGE_2 are adenylyl cyclase agonists that result in elevated intracellular cAMP levels in the kidney (52, 55, 56). Thus, it is possible that the reduction of endogenous renal levels of PGI_2 and PGE_2 by NS398 in PKD rats leads to a decrease in adenylyl cyclase activation and reduced cAMP levels, thereby abrogating cyst expansion and ameliorating disease-associated pathologies.

In diseased compared to normal kidneys, COX-2 gene and protein expression were markedly reduced but the activity of COX-2 was higher, consistent with previous findings (7). The findings of the current study corroborate and extend these observations to the effects mediated by NS398. Selective inhibition of COX-2 activity resulted in an induction of COX-2 mRNA as well as protein expression in diseased and normal rat kidneys. The inverse relationship between renal COX-2 enzyme levels and renal COX-2 activity in Han:SPRD-*cy* rats is likely due to a negative feedback mechanism and may be

one of the regulatory mechanisms controlling the protein levels of COX-2. This finding is at odds with reports that suggest a positive feedback loop where the presence of renal disease increases both COX-2 expression and activity in concert (2, 3, 5, 9, 57). However, this premise is corroborated by reports that show chronic pharmacologic blockade of COX-2 activity induces renal COX-2 expression (13, 58, 59).

In conclusion, our study provides clear evidence of a role for COX-2 aberrations in the pathology and progression of renal disease in the Han:SPRD-*cy* rat. Selective COX-2 inhibition significantly ameliorates characteristic features of cystic renal disease (ie. cystic growth and interstitial fibrosis) as well as disease-associated pathologies (such as inflammation, oxidant injury and cell proliferation), without adversely affecting renal function. Further studies on the dose, potential risks and long-term effects of COX-2 inhibition in this disorder are warranted.

6.6 References

1. Cheng HF and Harris RC. Renal effects of non-steroidal anti-inflammatory drugs and selective cyclooxygenase-2 inhibitors. Curr Pharm Des. 2005; 11:1795-1804.

2. Hirose S, Yamamoto T, Feng L, Yaoita E, Kawasaki K, Goto S, Fujinaka H, Wilson CB, Arakawa M, and Kihara I. Expression and localization of cyclooxygenase isoforms and cytosolic phospholipase A2 in anti-Thy-1 glomerulonephritis. J Am Soc Nephrol. 1998; 9:408-416.

3. Komers R, Lindsley JN, Oyama TT, Schutzer WE, Reed JF, Mader SL, and Anderson S. Immunohistochemical and functional correlations of renal cyclooxygenase-2 in experimental diabetes. J Clin Invest. 2001; 107:889-898.

4. Komers R, Zdychova J, Cahova M, Kazdova L, Lindsley JN, and Anderson S. Renal cyclooxygenase-2 in obese Zucker (fatty) rats. Kidney Int. 2005; 67:2151-2158.

5. Wang JL, Cheng HF, Zhang MZ, McKanna JA, and Harris RC. Selective increase of cyclooxygenase-2 expression in a model of renal ablation. Am J Physiol. 1998; 275:F613-622.

6. Wang JL, Cheng HF, and Harris RC. Cyclooxygenase-2 inhibition decreases renin content and lowers blood pressure in a model of renovascular hypertension. Hypertension. 1999; 34:96-101.

7. Warford-Woolgar L, Peng CY, Shuhyta J, Wakefield A, Sankaran D, Ogborn M, and Aukema HM. Selectivity of cyclooxygenase (COX) isoform activity and prostanoid production in normal and diseased Han:SPRD-cy rat kidneys. Am J Physiol Renal Physiol. 2006; 290:F897-904.

8. Blume C, Heise G, Muhlfeld A, Bach D, Schror K, Gerhardz CD, Grabensee B, and Heering P. Effect of flosulide, a selective cyclooxygenase 2 inhibitor, on passive heymann nephritis in the rat. Kidney Int. 1999; 56:1770-1778.

9. Wang JL, Cheng HF, Shappell S, and Harris RC. A selective cyclooxygenase-2 inhibitor decreases proteinuria and retards progressive renal injury in rats. Kidney Int. 2000; 57:2334-2342.

10. Cheng HF, Wang CJ, Moeckel GW, Zhang MZ, McKanna JA, and Harris RC. Cyclooxygenase-2 inhibitor blocks expression of mediators of renal injury in a model of diabetes and hypertension. Kidney Int. 2002; 62:929-939.

11. Cheng H, Zhang M, Moeckel GW, Zhao Y, Wang S, Qi Z, Breyer MD, and Harris RC. Expression of mediators of renal injury in the remnant kidney of ROP mice is attenuated by cyclooxygenase-2 inhibition. Nephron Exp Nephrol. 2005; 101:e75-85.

12. Dey A, Maric C, Kaesemeyer WH, Zaharis CZ, Stewart J, Pollock JS, and Imig JD. Rofecoxib decreases renal injury in obese Zucker rats. Clin Sci (Lond). 2004; 107:561-570.

13. Fujihara CK, Antunes GR, Mattar AL, Andreoli N, Malheiros DM, Noronha IL, and Zatz R. Cyclooxygenase-2 (COX-2) inhibition limits abnormal COX-2 expression and progressive injury in the remnant kidney. Kidney Int. 2003; 64:2172-2181.

14. Sanchez PL, Salgado LM, Ferreri NR, and Escalante B. Effect of cyclooxygenase-2 inhibition on renal function after renal ablation. Hypertension. 1999; 34:848-853.

15. Tomasoni S, Noris M, Zappella S, Gotti E, Casiraghi F, Bonazzola S, Benigni A, and Remuzzi G. Upregulation of renal and systemic cyclooxygenase-2 in patients with active lupus nephritis. J Am Soc Nephrol. 1998; 9:1202-1212.

16. Rossat J, Maillard M, Nussberger J, Brunner HR, and Burnier M. Renal effects of selective cyclooxygenase-2 inhibition in normotensive salt-depleted subjects. Clin Pharmacol Ther. 1999; 66:76-84.

17. Swan SK, Rudy DW, Lasseter KC, Ryan CF, Buechel KL, Lambrecht LJ, Pinto MB, Dilzer SC, Obrda O, Sundblad KJ, Gumbs CP, Ebel DL, Quan H, Larson PJ, Schwartz JI, Musliner TA, Gertz BJ, Brater DC, and Yao SL. Effect of cyclooxygenase-2 inhibition on renal function in elderly persons receiving a low-salt diet. A randomized, controlled trial. Ann Intern Med. 2000; 133:1-9.

18. Kitahara M, Eitner F, Ostendorf T, Kunter U, Janssen U, Westenfeld R, Matsui K, Kerjaschki D, and Floege J. Selective cyclooxygenase-2 inhibition impairs glomerular capillary healing in experimental glomerulonephritis. J Am Soc Nephrol. 2002; 13:1261-1270.

19.Cowley BD, Jr., Gudapaty S, Kraybill AL, Barash BD, Harding MA, Calvet JP, and Gattone VH, 2nd. Autosomal-dominant polycystic kidney disease in the rat. Kidney Int. 1993; 43:522-534.

20. Reeves PG, Nielsen FH, and Fahey GC, Jr. AIN-93 purified diets for laboratory rodents:final report of the American Institute of Nutrition ad hoc writing committee on the reformulation of the AIN-76A rodent diet. J Nutr. 1993; 123:1939-1951.

21. Futaki N, Takahashi S, Yokoyama M, Arai I, Higuchi S, and Otomo S. NS-398, a new anti-inflammatory agent, selectively inhibits prostaglandin G/H synthase/cyclooxygenase (COX-2) activity in vitro. Prostaglandins. 1994; 47:55-59.

22. Gierse JK, Hauser SD, Creely DP, Koboldt C, Rangwala SH, Isakson PC, and Seibert K. Expression and selective inhibition of the constitutive and inducible forms of human cyclo-oxygenase. Biochem J. 1995; 305:479-484.

23. Futaki N, Arai I, Hamasaka Y, Takahashi S, Higuchi S, and Otomo S. Selective inhibition of NS-398 on prostanoid production in inflamed tissue in rat carrageenan-air-pouch inflammation. J Pharm Pharmacol. 1993; 45:753-755.

24. Masferrer JL, Zweifel BS, Manning PT, Hauser SD, Leahy KM, Smith WG, Isakson PC, and Seibert K. Selective inhibition of inducible cyclooxygenase 2 in vivo is antiinflammatory and nonulcerogenic. Proc Natl Acad Sci U S A. 1994; 91:3228-3232.

25. Futaki N, Takahashi S, Kitagawa T, Yamakawa Y, Tanaka M, and Higuchi S. Selective inhibition of cyclooxygenase-2 by NS-398 in endotoxin shock rats in vivo. Inflamm Res. 1997; 46:496-502.

26. Ogborn MR, Nitschmann E, Bankovic-Calic N, Weiler HA, and Aukema H. Dietary flax oil reduces renal injury, oxidized LDL content, and tissue n-6/n-3 FA ratio in experimental polycystic kidney disease. Lipids. 2002; 37:1059-1065.

27. Sankaran D, Lu J, Bankovic-Calic N, Ogborn MR, and Aukema HM. Modulation of renal injury in pcy mice by dietary fat containing n-3 fatty acids depends on the level and type of fat. Lipids. 2004; 39:207-214.

28. Aukema HM, Adolphe J, Mishra S, Jiang J, Cuozzo FP, and Ogborn MR. Alterations in renal cytosolic phospholipase A2 and cyclooxygenases in polycystic kidney disease. Faseb J. 2003; 17:298-300.

29. Yao M, Song DH, Rana B, and Wolfe MM. COX-2 selective inhibition reverses the trophic properties of gastrin in colorectal cancer. Br J Cancer. 2002; 87:574-579.

30. Wu G, Luo J, Rana JS, Laham R, Sellke FW, and Li J. Involvement of COX-2 in VEGF-induced angiogenesis via P38 and JNK pathways in vascular endothelial cells. Cardiovasc Res. 2006; 69:512-519.

31. Buecher B, Broquet A, Bouancheau D, Heymann MF, Jany A, Denis MG, Bonnet C, Galmiche JP, and Blottiere HM. Molecular mechanisms involved in the antiproliferative effect of two COX-2 inhibitors, nimesulide and NS-398, on colorectal cancer cell lines. Dig Liver Dis. 2003; 35:557-565.

32. Harding P, Glass WF, 2nd, and Scherer SD. COX-2 inhibition potentiates the antiproteinuric effect of enalapril in uninephrectomized SHR. Prostaglandins Leukot Essent Fatty Acids. 2003; 68:17-25.

33. Grantham JJ, Torres VE, Chapman AB, Guay-Woodford LM, Bae KT, King BF, Jr., Wetzel LH, Baumgarten DA, Kenney PJ, Harris PC, Klahr S, Bennett WM, Hirschman GN, Meyers CM, Zhang X, Zhu F, and Miller JP. Volume progression in polycystic kidney disease. N Engl J Med. 2006; 354:2122-2130.

34. Stahl RA, Thaiss F, Wenzel U, Schoeppe W, and Helmchen U. A rat model of progressive chronic glomerular sclerosis:the role of thromboxane inhibition. J Am Soc Nephrol. 1992; 2:1568-1577.

35. Schmitz PG, Krupa SM, Lane PH, Reddington JC, and Salinas-Madrigal L. Acquired essential fatty acid depletion in the remnant kidney:amelioration with U-63557A. Kidney Int. 1994; 46:1184-1191.

36. Seibert K, Masferrer JL, Needleman P, and Salvemini D. Pharmacological manipulation of cyclo-oxygenase-2 in the inflamed hydronephrotic kidney. Br J Pharmacol. 1996; 117:1016-1020.

37. Stichtenoth DO, Marhauer V, Tsikas D, Gutzki FM, and Frolich JC. Effects of specific COX-2-inhibition on renin release and renal and systemic prostanoid synthesis in healthy volunteers. Kidney Int. 2005; 68:2197-2207.

38. Stichtenoth DO, Wagner B, and Frolich JC. Effect of selective inhibition of the inducible cyclooxygenase on renin release in healthy volunteers. J Investig Med. 1998; 46:290-296.

39. Stichtenoth DO, Wagner B, and Frolich JC. Effects of meloxicam and indomethacin on cyclooxygenase pathways in healthy volunteers. J Investig Med. 1997; 45:44-49.

40. Hetu PO and Riendeau D. Cyclo-oxygenase-2 contributes to constitutive prostanoid production in rat kidney and brain. Biochem J. 2005; 391:561-566.

41. Takano T, Cybulsky AV, Cupples WA, Ajikobi DO, Papillon J, and Aoudjit L. Inhibition of cyclooxygenases reduces complement-induced glomerular epithelial cell injury and proteinuria in passive Heymann nephritis. J Pharmacol Exp Ther. 2003; 305:240-249.

42. Dilger K, Herrlinger C, Peters J, Seyberth HW, Schweer H, and Klotz U. Effects of celecoxib and diclofenac on blood pressure, renal function, and vasoactive prostanoids in young and elderly subjects. J Clin Pharmacol. 2002; 42:985-994.

43. Murphey LJ, Williams MK, Sanchez SC, Byrne LM, Csiki I, Oates JA, Johnson DH, and Morrow JD. Quantification of the major urinary metabolite of PGE2 by a liquid chromatographic/mass spectrometric assay:determination of cyclooxygenase-specific PGE2 synthesis in healthy humans and those with lung cancer. Anal Biochem. 2004; 334:266-275.

44. Patrono C, Ciabattoni G, Patrignani P, Filabozzi P, Pinca E, Satta MA, van Dorne D, Cinotti GA, Pugliese F, Pierucci A, and Simonetti BM. Evidence for a renal origin of urinary thromboxane B2 in health and disease. Adv Prostaglandin Thromboxane Leukot Res. 1983; 11:493-498.

45. Seyberth HW, Sweetman BJ, Frolich JC, and Oates JA. Quantifications of the major urinary metabolite of the E prostaglandins by mass spectrometry:evaluation of the method's application to clinical studies. Prostaglandins. 1976; 11:381-397.

46. Rosenkranz B, Kitajima W, and Frolich JC. Relevance of urinary 6-keto-prostaglandin F1 alpha determination. Kidney Int. 1981; 19:755-759.

47. Catella-Lawson F, McAdam B, Morrison BW, Kapoor S, Kujubu D, Antes L, Lasseter KC, Quan H, Gertz BJ, and FitzGerald GA. Effects of specific inhibition of cyclooxygenase-2 on sodium balance, hemodynamics, and vasoactive eicosanoids. J Pharmacol Exp Ther. 1999; 289:735-741.

48. McAdam BF, Catella-Lawson F, Mardini IA, Kapoor S, Lawson JA, and FitzGerald GA. Systemic biosynthesis of prostacyclin by cyclooxygenase (COX)-2:the human pharmacology of a selective inhibitor of COX-2. Proc Natl Acad Sci U S A. 1999; 96:272-277.

49. Wilson PD. Polycystic kidney disease. N Engl J Med. 2004; 350:151-164.

50. Yamaguchi T, Pelling JC, Ramaswamy NT, Eppler JW, Wallace DP, Nagao S, Rome LA, Sullivan LP, and Grantham JJ. cAMP stimulates the in vitro proliferation of renal cyst epithelial cells by activating the extracellular signal-regulated kinase pathway. Kidney Int. 2000; 57:1460-1471.

51. Hanaoka K and Guggino WB. cAMP regulates cell proliferation and cyst formation in autosomal polycystic kidney disease cells. J Am Soc Nephrol. 2000; 11:1179-1187.

52. Belibi FA, Reif G, Wallace DP, Yamaguchi T, Olsen L, Li H, Helmkamp GM, Jr., and Grantham JJ. Cyclic AMP promotes growth and secretion in human polycystic kidney epithelial cells. Kidney Int. 2004; 66:964-973.

53. Gattone VH, 2nd, Wang X, Harris PC, and Torres VE. Inhibition of renal cystic disease development and progression by a vasopressin V2 receptor antagonist. Nat Med. 2003; 9:1323-1326.

54. Yamaguchi T, Nagao S, Kasahara M, Takahashi H, and Grantham JJ. Renal accumulation and excretion of cyclic adenosine monophosphate in a murine model of slowly progressive polycystic kidney disease. Am J Kidney Dis. 1997; 30:703-709.

55. Breyer MD and Breyer RM. G protein-coupled prostanoid receptors and the kidney. Annu Rev Physiol. 2001; 63:579-605.

56. Nasrallah R and Hebert RL. Prostacyclin signaling in the kidney:implications for health and disease. Am J Physiol Renal Physiol. 2005; 289:F235-246.

57. Wang D and Strandgaard S. The pathogenesis of hypertension in autosomal dominant polycystic kidney disease. J Hypertens. 1997; 15:925-933.

58. Hocherl K, Kammerl MC, Schumacher K, Endemann D, Grobecker HF, and Kurtz A. Role of prostanoids in regulation of the renin-angiotensin-aldosterone system by salt intake. Am J Physiol Renal Physiol. 2002; 283:F294-301.

59. Ferguson S, Hebert RL, and Laneuville O. NS-398 upregulates constitutive cyclooxygenase-2 expression in the M-1 cortical collecting duct cell line. J Am Soc Nephrol. 1999; 10:2261-2271.

7. DISCUSSION

The main findings of this research are 1) dietary FO rich in 18:3n-3, ALA slows early renal disease progression in weanling *pcy* mice with PKD, concurrent with previous studies using the Han:SPRD-*cy* rat model, 2) prenatal exposure to FO-based diets attenuates renal histologic injury in Han:SPRD-*cy* rat offspring, 3) FO diets retard further pathologies associated with renal injury when introduced in adult Han:SPRD-*cy* rats with advanced kidney disease, 4) dietary oils rich in 20:5n-3 EPA and 22:6n-3 DHA, specifically up-regulate COX-2 mRNA and protein levels in diseased rodent kidneys with PKD, while those rich in ALA do not exert this effect and 5) selective COX-2 inhibition by NS398 significantly ameliorates renal injury and disease-associated elevations in prostanoid production in Han:SPRD-*cy* rats.

This research provides a unique comprehensive overview of the effects of dietary FO on different stages of the progression of inherited renal cystic disease. The results from this research demonstrate that dietary FO ameliorates early renal histologic injury in weanling animals, in those given FO prenatally as well as in animals with established kidney disease. The beneficial effect of FO on early renal disease progression is consistent with the previously demonstrated beneficial effect of oils with n-3 fatty acids on renal injury in weanling Han:SPRD-*cy* rats. In the current research, dietary FO given during the maternal period ameliorated renal histologic parameters as well as proteinuria in rat offspring with PKD. These findings give credence to the 'fetal programming of adult disease' theory and contribute to the mounting evidence in support of the developmental plasticity of the kidney in response to maternal nutritional status. To our

knowledge, this research provides the first piece of evidence to demonstrate maternal FO also can have long term effects on the postnatal kidney afflicted by a hereditary disease.

In addition to providing evidence for the reno-protective effects of dietary FO in early stages of renal disease, the current research also demonstrates beneficial effects of FO diets when initiated at a later stage of disease. FO supplementation lowered renal epithelial cell proliferation, oxidant injury and inflammation in adult Han:SPRD-*cy* rats with advanced renal injury. However, the protective effects of dietary FO on renal injury were not reflected in a significant amelioration of cyst growth, fibrosis or renal function, as is the case with early dietary intervention in the Han:SPRD-*cy* rat. A plausible explanation for the lack of dietary effects on these parameters could be the fact that cyst expansion is a less integral part of renal injury in the six month old Han:SPRD-*cy* rat (1). The significance of these results can be appreciated when considered in the context of chronic inflammation being a major risk factor for increased cardiovascular disease risk in progressive CKD. Thus, therapeutic interventions that demonstrate anti-oxidant and anti-inflammatory effects have the potential to improve poor patient outcomes. To determine whether benefits on disease-associated pathologies would ultimately translate into improved survival, survival studies using dietary FO intervention initiated at different stages of CKD are needed.

Hence, the results of the current research suggest that although some benefits on pathological events associated with renal disease would be expected if FO diets are initiated in the later stages of renal injury, maximum benefits on slowing disease progression would be observed if combined with a preventative approach that introduces dietary FO in the early stages of renal disease, perhaps even as early as *in utero*.

Moreover, these intriguing results compel further investigation into the mechanisms of this unique dietary effect of maternal FO, using classical fetal programming parameters such as nephron number and blood pressure as well as an evaluation of the genetic and epigenetic modulation of inherited renal disease by FO in the maternal diet. Of note, in Han:SPRD-*cy* rats, some genes such *glypican3* and *fibronectin 1* are upregulated in early stages of the disease, before the appearance of cysts and/or onset of renal failure (2). These genes have been linked to early embryonic cell migration and renal development and upregulation of these genes could be an early event linked to cyst formation. These genes may thus be good candidates to study genetic and epigenetic changes that occur early in the progression of PKD in response to maternal FO.

Despite increasing evidence of the reno-protective effects of oils containing n-3 fatty acids, little is known regarding their mechanisms of action. Renal pathogenic mechanisms that may be affected by dietary n-3 fatty acids include cell proliferation, infiltration of inflammatory cells, and production of inflammatory mediators. Accumulation of extracellular matrix proteins in the renal interstitium is a consistent feature of a number of chronic renal diseases, including PKD (3). Indeed, recent transcriptome analysis of the Han:SPRD *Cy/Cy* rat with a severe PKD phenotype identified nearly 30 genes involved in extracellular matrix metabolism that were significantly up-regulated with renal disease (2). Increasing evidence suggests that chemotactic chemokines such as monocyte chemoattractant protein (MCP-1) may play a critical role in the regulation of interstitial inflammation and other processes related to fibrotic injury. In the kidney, the proinflammatory transcription factor NFκB regulates

production of MCP-1, adhesion molecules (intracellular adhesion molecule-1, ICAM-1), cytokines [interleukin (IL)-1 and tumor necrosis factor-α (TNF-α)] as well as expression of genes such as COX-2 (4). Recent evidence suggests that both EPA and DHA inhibit MCP-1 production and mRNA expression as well as NFκB activation *in vitro* (5) and *in vivo* in renal cells (6). Renal NFκB inhibition by n-3 fatty acids is likely mediated via peroxisome proliferator-activated receptor (PPAR) γ activation (5). It is possible that FO supplementation (rich in ALA) in animal models of PKD also exerts its reno-protective effects in a similar fashion since dietary FO leads to an enrichment of ALA, EPA and DHA in the cystic kidney (7,8) demonstrating that ALA is converted to longer chain n-3 fatty acids.

It is well-established that AA and EPA compete for the same metabolic enzymes. In addition to the AA-derived COX prostanoids, the LOX as well as CYP450 monoxygenase products also play crucial roles in the maintenance of renal function and hemodynamics (9,10). For example, 20-HETE is an endogenous vasoconstrictor and its inhibition reduces blood pressure in spontaneously hypertensive rats as well as DOCA-salt treated rats (11,12). On the other hand, EETs are potent vasodilators and exhibit anti-inflammatory effects (13). Interestingly, EPA appears to be the preferred substrate for AA-metabolizing CYP450 monoxygenases (14), and results in the synthesis of epoxy EETs which also function as potent vasodilators. A recent study by Theuer and colleagues (6) demonstrated that dietary EPA protected affected rat kidneys from renal damage and this effect was associated with increased epoxy EET synthesis. Hence, in general, supplementing the diet with n-3 fatty acids may either cause a reduction of AA-derived eicosanoids or an increase in n-3 fatty acid-derived eicosanoids, thereby reducing

glomerular and interstitial inflammation, mesangial cell contractility, platelet aggregation, and vasoconstriction in response to renal injury. However, the physiologic relevance of n-3 fatty acid-derived eicosanoids produced via the renal COX, LOX and CYP450 monoxygenase pathways in PKD is yet to be determined. Thus, the questions that remain unanswered are 1) whether synthesis of trienoic prostanoids in n-3 fatty acid-enriched renal tissue, in this model of inherited cystic disease, does occur and 2) whether this shift in prostanoid synthesis directly affects disease progression in PKD.

The current research provides evidence that dietary oils rich in n-3 fatty acids modulate renal COX-2 mRNA and protein levels in the *pcy* mouse model as well as in the Han:SPRD-*cy* rat and this effect is dependent on the degree of unsaturation of the n-3 fatty acids. The results from chapter 5 demonstrate that while dietary oils rich in 20:5n-3 (EPA) and 22:6n-3 (DHA) specifically up-regulated COX-2 mRNA and protein levels in diseased kidneys, those enriched in 18:3n-3 (ALA) did not exert this effect. One of the mechanisms by which n-3 fatty acids mediate their effects on COX-2 expression is likely via transcriptional regulation of COX-2 since n-3 fatty acids have been shown to alter NFκB. However, modulation of transcription factors that regulate COX-2 expression was not examined in the current research. Future studies should explore the effects of dietary n-3 fatty acids on COX-2 transcriptional regulation in order delineate the mechanism(s) by which diets containing n-3 fatty acids exert their effects on renal COX-2 levels. In addition, insight into the steady-state transcriptional regulation of COX-2 in animal models of renal cystic disease would also aid in defining the role of COX-2 in PKD. Changes in gene and protein expression of an enzyme do not always reflect a change in enzyme activity, particularly in the Han:SPRD-*cy* rat in which COX-2 activity and

expression are inversely related. An important limitation of the dietary intervention studies in this research is that renal COX-2 activity following dietary n-3 fatty acid intervention was not addressed due to lack of a reproducible method (unsuccessful derivatization for mass spectroscopic analyses) at the time.

The finding that selective COX-2 inhibition by NS398 significantly ameliorated renal injury in the Han:SPRD-*cy* rats with PKD is an important contribution of this research. Treatment with NS398 resulted in lower cyst growth and interstitial fibrosis as well as fewer number of PCNA positive cells, decreased macrophage count and less oxidant injury in the kidneys of diseased rats indicating that COX-2 plays a significant role in the pathology and progression of chronic renal injury in Han:SPRD-*cy* rats. The modulation of renal injury in PKD by prostanoids is likely mediated by their effects on the adenylyl cyclase-cAMP pathway, since PGs are potent adenylyl cyclase agonists and increase intracellular cAMP levels in the kidney. Prostanoids orchestrate their effects on renal function via a number of membrane bound G-protein coupled-receptor pathways that are specific to the individual prostanoids. Four of the receptor subtypes bind PGE_2 (EP1–EP4); two bind PGD_2 (DP1 and DP2) and the FP, IP, and TP receptors bind $PGF_{2\alpha}$, PGI_2, and TXA_2, respectively. IP, DP1, EP2, and EP4 are "stimulatory" receptors that signal through Gs-mediated increases in intracellular cAMP. EP1, FP and TP are also "stimulatory" but signal through Gq-mediated increases in intracellular calcium. EP3 is considered as an "inhibitory" receptor which couples to Gi to decrease cAMP formation (15). *In vitro* studies in cyst epithelial cells demonstrate a significant role for cAMP in the proliferation of cyst mural cells as well as in transepithelial fluid secretion. In addition, elevated renal and urine levels of cAMP have been reported in the animal models of

PKD. Thus, it is possible that the reduction of endogenous renal levels of PGI_2 and PGE_2 by NS398 in PKD rats leads to a decrease in adenylyl cyclase activation and reduced cAMP levels via receptor mediated signaling, thereby abrogating cyst expansion and ameliorating disease-associated pathologies.

The association between prostanoids (comprising of PGs and TXs) and renal cystic disease pathology is a common thread that runs through this research. Our findings demonstrate that dietary and pharmacologic modulation of the COX pathway (may potentially) result in aberrations in prostanoid synthesis. It is possible that n-3 fatty acid diets/COX-2 inhibitors, in addition to modulating COX, also affect the expression and activity of the terminal prostanoid synthases (such as PGI synthase, TXA synthase and PGE sythase, Fig.1-1). However, the current research failed to examine prostanoid signaling downstream of COXs. Aside from their ligand-receptor binding at the plasma membrane, other mechanisms have been implicated in prostanoid signaling. EP3 and EP4 receptors can be internalized into the nucleus and can regulate gene transcription by modulating intracellular calcium release (15). Also, PGI_2 and PGJ_2 (PGD_2 metabolite) have been shown to bind $PPAR_\delta$ and $PPAR\gamma$, respectively for direct activation of transcriptional targets (15). Taken together with the fact that renal $NF_\kappa B$ inhibition by n-3 fatty acids is likely mediated via $PPAR\gamma$ activation, the effect of dietary n-3 fatty acids as well as selective COX-2 inhibitors on downstream prostanoid signaling in cystic rat kidneys needs to be further elucidated.

Overall, this research has established a positive modulatory effect of dietary FO on various stages of inherited kidney disease, from as early as prenatal to advanced PKD. This research also provides clear evidence that pathology and progression of renal disease

in the Han:SPRD-*cy* rat are at least partly controlled by aberrations in COX-2 metabolism. The findings of this research may impact treatment options, both dietary and pharmaceutical, in those afflicted with PKD as well as other chronic renal diseases and contribute to the current knowledge of pathogenesis of this inherited cystic disease.

7.1 References

1. Cowley BD, Jr., Gudapaty S, Kraybill AL, Barash BD, Harding MA, Calvet JP, Gattone VH, 2nd. Autosomal-dominant polycystic kidney disease in the rat. Kidney Int 1993; 43:522-34.

2. Riera M, Burtey S, Fontes M. Transcriptome analysis of a rat PKD model:Importance of genes involved in extracellular matrix metabolism. Kidney Int 2006; 69:1558-63.

3. Eddy AA. Progression in chronic kidney disease. Adv Chronic Kidney Dis 2005; 12:353-65.

4. Viedt C, Dechend R, Fei J, Hansch GM, Kreuzer J, Orth SR. MCP-1 induces inflammatory activation of human tubular epithelial cells:involvement of the transcription factors, nuclear factor-kappaB and activating protein-1. J Am Soc Nephrol 2002; 13:1534-47.

5. Li H, Ruan XZ, Powis SH, Fernando R, Mon WY, Wheeler DC, Moorhead JF, Varghese Z. EPA and DHA reduce LPS-induced inflammation responses in HK-2 cells:evidence for a PPAR-gamma-dependent mechanism. Kidney Int 2005; 67:867-74.

6. Theuer J, Shagdarsuren E, Muller DN, Kaergel E, Honeck H, Park JK, Fiebeler A, Dechend R, Haller H, Luft FC, Schunck WH. Inducible NOS inhibition, eicosapentaenoic acid supplementation, and angiotensin II-induced renal damage. Kidney Int 2005; 67:248-58.

7. Ogborn MR, Nitschmann E, Bankovic-Calic N, Weiler HA, Aukema H. Dietary flax oil reduces renal injury, oxidized LDL content, and tissue n-6/n-3 FA ratio in experimental polycystic kidney disease. Lipids 2002; 37:1059-65.

8. Sankaran D, Lu J, Bankovic-Calic N, Ogborn MR, Aukema HM. Modulation of renal injury in pcy mice by dietary fat containing n-3 fatty acids depends on the level and type of fat. Lipids 2004; 39:207-14.

9. Badr KF. Sepsis-associated renal vasoconstriction:potential targets for future therapy. Am J Kidney Dis 1992; 20:207-13.

10. Badr KF. Five-lipoxygenase products in glomerular immune injury. J Am Soc Nephrol 1992; 3:907-15.

11. Su P, Kaushal KM, Kroetz DL. Inhibition of renal arachidonic acid omega-hydroxylase activity with ABT reduces blood pressure in the SHR. Am J Physiol 1998; 275:R426-38.

12. Oyekan AO, McAward K, Conetta J, Rosenfeld L, McGiff JC. Endothelin-1 and CYP450 arachidonate metabolites interact to promote tissue injury in DOCA-salt hypertension. Am J Physiol 1999; 276:R766-75.

13. Node K, Ruan XL, Dai J, Yang SX, Graham L, Zeldin DC, Liao JK. Activation of Galpha s mediates induction of tissue-type plasminogen activator gene transcription by epoxyeicosatrienoic acids. J Biol Chem 2001; 276:15983-9.

14. Lauterbach B, Barbosa-Sicard E, Wang MH, Honeck H, Kargel E, Theuer J, Schwartzman ML, Haller H, Luft FC, Gollasch M, Schunck WH. Cytochrome P450-dependent eicosapentaenoic acid metabolites are novel BK channel activators. Hypertension 2002; 39:609-13.

15. Cha YI, Solnica-Krezel L, DuBois RN. Fishing for prostanoids:deciphering the developmental functions of cyclooxygenase-derived prostaglandins. Dev Biol 2006; 289:263-72.

APPENDIX A: METHOD DETAILS

IMMUNOHISTOCHEMISTRY STAINING PROTOCOL (FOR RAT PCNA AND MACROPHAGES)

Preparation of working solutions:

Blocking Serum : Mix 5000 uL of 1x PBS with 75 uL of normal horse serum (S2000, Vector Labs). Vortex for ~ 30 seconds.

Secondary Antibody: Mix 5000 uL of 1x PBS with 75 uL of biotinylated horse anti-mouse IgG (BA2000, included in VECTASTAIN ABC kit, Vector Labs). Vortex for ~30 seconds.

ABC substrate (Peroxidase Solution): Mix 5000 uL of 1x PBS with 2 drops of reagent A and 2 drops of reagent B (from the VECTASTAIN ABC kit). Vortex for ~30 seconds. Allow mixture to sit for ~30 minutes before use to enable chelation.

Primary antibody solution
All primary antibody dilutions are made using 1X PBS. You need ~100uL of diluted antibody for each slide

Antibody	Dilution
Mouse anti-rat monocytes/macrophages monoclonal antibody (MAB1435, Chemicon Intl, Temecula, CA)	1:50
Mouse anti-rat monoclonal anti-PCNA antibody (M0879, Dako Intl, Carpinteria, CA)	1:50

Prepare glass staining jars containing the following solutions:

Jar #1: 100% Xylol
Jar #2: 100% Xylol
Jar #3: 100% Anhydrous Ethanol (anhy. EtOH)
Jar #4: 100% Anhy. EtOH
Jar #5: 95% Ethanol (95 ml anhy. EtOH +5 ml of ddH_20)
Jar #6: 90% Ethanol (90 ml anhy. EtOH +10 ml of ddH_20)
Jar #7: 80% Ethanol (80 ml anhy. EtOH +20 ml of ddH_20)
Jar #8: 50% Ethanol (50 ml anhy. EtOH +50 ml of ddH_20)
Jar #9: 100 ml ddH_2O
Jar #10: Methanolic hydrogen peroxide solution (100 mL methanol + 1000 uL 30% H_2O_2)

DAB solution (3,3'-di-amino benzidine tablets, Sigma-Aldrich, D4293, to make 5 ml solution):

Do this after the primary antibody step so that the solution has time to sit for awhile. Place 5ml of ddH_2O in a test tube. Add one urea (silver) and one DAB (gold) tablet to the ddH_2O. Vortex until the tablets have dissolved in the water.

Staining Protocol:

1. Dewaxing Step: Place slides in each of the following solutions for the times specified:

XYLOL I: 10 MINUTES
XYLOL II: 8 MINUTES (increase Xylol II time from 5min to 8 min if the tissue section is bigger)

2. Dehydration steps : Place slides in each of the following solutions for the times specified

100% Anhy. EtOH I: 5 MINUTES
100% Anhy. EtOH II: 5 MINUTES
95% EtOH: 5 MINUTES
90% EtOH: 5 MINUTES
80% EtOH: 5 MINUTES
50% EtOH: 5 MINUTES
H_2O: 5 MINUTES

3. Blocking endenous peroxidase activity step
Place slides in jar containing methanolic H_2O_2 solution for 30 minutes at room temperature.
Wash slides in ddH_2O for 5 minutes.

(For detection of PCNA + cells- Include an antigen retrieval step at this stage. Microwave slides for 15 min in coplin jars filled with 10mM citric acid buffer. Cool at room temperature for 1 hour.)
(Note: antigen retrieval is to break down any bonds that may have been formed during fixing. So, using acidic pH ie citrate and heat ie microwave helps liberate the antigens so that they can successfully bind to the antibodies)

4. Blocking step
Shake any excess liquid off the slides.
Place slides in a petri dish facing upward.
Scrape off half the lower portion of the kidney especially if tissue section is too big)
Wipe around the edges of the remaining kidney section so as to remove any excess fluid that may dilute the solution-to-be-added. Blot on top of the kidney section as well, if needed.
Cover tissue with a few drops of diluted normal horse serum.
Cover the tissue with cover slips to prevent dehydration.
Incubate the slides at room temperature for 30 minutes.

5. **Primary Antibody**

Take the cover slips off the slides.
Wash slides in 1x PBS.
Shake any excess liquid off the slides.
Place slides in a petri dish facing upward.
Wipe around the edges of the remaining kidney section so as to remove any excess fluid that may dilute the solution-to-be-added. Blot on top of the kidney section as well, if needed.
Cover tissue with 100 uL of diluted primary antibody (or more if bigger chunk).
Cover the tissue with cover slips to prevent dehydration.
Incubate the slides for 1h at room temperature.

6. Secondary Antibody
Take the cover slips off of the slides.
Wash slides in 1x PBS.
Shake any excess liquid off the slides.
Place slides in a petri dish facing upward.
Wipe around the edges of the remaining kidney section so as to remove any excess fluid that may dilute the solution-to-be-added. Blot on top of the kidney section as well, if needed.
Cover tissue with a few drops of diluted secondary antibody.
Cover the tissue with cover slips to prevent dehydration.
Incubate the slides at room temperature for 30-45 min.

7. Peroxidase Step
Take the cover slips off of the slides.
Wash slides in 1x PBS.
Shake any excess liquid off the slides.
Place slides in a petri dish facing upward.
Wipe around the edges of the remaining kidney section so as to remove any excess fluid that may dilute the solution-to-be-added. Blot on top of the kidney section as well, if needed.
Cover tissue with a few drops of ABC substrate solution.
Cover the tissue with cover slips to prevent dehydration.
Incubate the slides at room temperature for 30 minutes.

8. DAB Step
Take the cover slips off of the slides.
Wash slides in 1x PBS.
Shake any excess liquid off the slides.
Place slides in a petri dish facing upward.
Wipe around the edges of the remaining kidney section so as to remove any excess fluid that may dilute the solution-to-be-added. Blot on top of the kidney section as well, if needed.
Cover tissue with a few drops of DAB solution.
Leave DAB on tissue for 5-10 min.
Wash the slides in ddH_2O

9. Mounting
Shake any excess liquid off of the slides.
Place a drop of Immunon Geltol mounting medium on a new coverslip.
Place the coverslip over the tissue ensuring that there are no air bubbles.

NOTE: Macrophage and PCNA staining can also be carried out using the DAKO EnVision + kit (see below for details).

IMMUNOSTAINING FOR OXLDL-USING DAKO EnVision+ System

Can do 16 slides/day. Put slides in glass holder to enable easier immersion in solutions. Prepare all solutions before starting.

Name of kit: DAKOCytomation, EnVision+R System-HRP (ACE), For use with Rabbit Primary Antibodies (kit contains 3 bottles: Peroxidase Block, Labelled Polymer-HRP Anti-Rabbit, and ACE+ Substrate Chromogen) (K4008, Dako Cytomation Inc, CA)

Before starting experiment:
Bring Peroxidase Block and Labelled Polymer to room temperature. For convenience, AEC+ substrate chromogen can be used straight from the fridge (2-4°C)

Primary Antibody: Make a 1:100 dilution of the primary OxLDL antibody (Rabbit anti-Cu2+ oxLDL polyclonal antibody, AB3230, Chemicon Intl, CA) using DAKO antibody diluent (S0809).

I Dewaxing and Dehydration

Xylol I - 10min
Xylol II - 5 min
100% Ethanol I - 5 min
100% Ethanol II - 5 min
95% Ethanol - 5 min
80% Ethanol - 5 min
50% Ethanol – 5 min
ddH20- 5min

II Blocking endogenous peroxidases
Incubate slides with DAKO peroxidase block (provided in kit, DAKO Envision™ + System- HRP [AEC], K4008) for 5 min.
Wash in ddH20 for 5 min.

III Primary Antibody step
Apply about 100uL diluted primary antibody for oxLDL (.....) to all slides and cover with long coverslip. Incubate for 30min.
Wash with ddH20 from squirt bottle.
Dry slides with kimwipe and place face-up in Petri dish.

IV Peroxidase-Labelled Polymer step
Apply few drops of peroxidase-labelled polymer to all slides and incubate for 30 min.
Wash with ddH20 from squirt bottle.
Dry slides with kimwipe and place face-up in Petri dish.

V Substrate Chromogen step
Apply few drops of AEC+ substrate chromogen to all slides and incubate for 5-10 min (depends on color development).
Wash with ddH20 from squirt bottle.
Dry slides with kimwipe and place face-up in Petri dish.

VI Hematoxylin counterstain step
Immerse slides in DAKO hematoxylin solution (S3309, Dako cytomation Inc. , CA) for 30 seconds.
Wash with ddH20 from squirt bottle.
Dip slides 10 times into a bath of 0. 037mol/L ammonia or similar bluing agent.
Wash with ddH20 from squirt bottle.

VII Mounting slides
Shake any excess liquid off of the slides.
Place a drop of Immunon Geltol mounting medium on a new coverslip.
Place the coverslip over the tissue ensuring that there are no air bubbles.

MEAN GLOMERULAR VOLUME MEASUREMENT

I Taking Pictures of Glomeruli (capturing) using SPOT ADVANCED

1. Turn camera on (Spot Diagnostics Instruments, Inc).
2. Turn computer on.
3. Turn microscope on (bottom right), press "preset" to ensure that lights are only half way up the scale.
4. Ensure microscope is on the 20X lens.
5. Put slide on microscope table with the labeled end of the slide on the left.
6. Focus on a section of the kidney that contains glomeruli, using ONLY the focus knob of the microscope. The knobs to move the slidetable are located on the right side of the table.
7. Double click on SPOT ADVANCED.
8. Click on "Camera" and select "compute exposure" from the drop down list. It should say "Factory Default". Click OK.
9. Click on Camera icon (top right) and take a picture. This takes care of the background. This only needs to be done once each day. Close the image without saving it.
10. Take another picture of a glomerulus using the camera (top right). If the image is not clear, click on the "focus" icon (third one down the right). Click "begin" and use the fine focus on the microscope until the image appears focused. Close the "focus" window and take another picture.
11. Click on the word "camera" at the top of the window. Select "Get Sequential Image" from drop down menu. Type in the number of images (30). The time interval between images needs to be set (start higher to begin with until you get used to finding glomeruli). You need to type in what number to start saving at (i. e 1). D:\Deepaglom\B1\B1 Make sure overwrite is marked and click begin.

    NB: Save each kidney slide as a separate folder by changing the slide number for every new slide.

II Measuring glomerular size using IMAGEPRO

1. Double click on "IMAGE PRO".

2. Click on "FILE" and go to S:\ drive (nephrology drive). Click on BLYDT-HANSEN and then AR DIABETES. This is where you'll find the 20X calibration grid that we use. Make sure the yellow line is on the grid.

3. Open your file " D:\Deepaglom\Slide\Slide01)

4. Click on "Measure" and then select "MEASUREMENTS". Click on "ADVANCED OPTIONS". Click on the "\" line tool . This is used to measure the glomerular diameter. In order to be consistent, measure the largest diameter.

5. Draw a line across the glom that represents the diameter.

6. Click on "INPUT/OUTPUT" (Meaurements-Length) and click on "DDE-to-EXCEL" to ensure that the data will go to an EXCEL file under your name.

7. Click "INPUT/OUTPUT" .... EXPORT NOW.

8. The data will be saved in EXCEL which you can save under your name in the D:\ drive.

9. The glomerular diameter will be measured in um.

This diameter is converted into an estimate of glomerular volume using the following formulae:

Mean Glomerular Area (MGA) = πr^2

Mean Glomerular Volume = 1. 25 $(MGA)^{3/2}$

The value of 1. 25 is derived from β/K , which are co-efficients based on assumptions made for maximum diameter of spheres (β= 1. 38) and the distribution bias of section location (K=1. 10).

SERUM AND URINARY CREATININE ASSAY

Principle of the assay

Creatinine is a metabolite of phospho-Creatine (p-Creatine), a molecule used as a store for high-energy phosphate that can be utilized by tissues for the production of ATP. The source of Creatine may vary between species. Dietary intake may be accompanied by de novosynthesis from the amino acids arginine, glycine, and methionine. This occurs in stepwise fashion primarily in the kidneys and liver, although other organ systems may be involved and species-specific differences may exist. The vast majority of Creatine (> 90%) is found in muscle, as well as other tissues including heart, brain, photo-receptors, and testes. Creatine and p-Creatine are converted non-enzymatically to the metabolite Creatinine, which diffuses into the blood and is excreted by the kidneys. In vivo, this conversion appears to be irreversible and in vitro it is favored by higher temperatures and lower pH. Some Creatinine may form via p-Creatinine as well. Under normal conditions, its formation occurs at a rate that is relatively constant. For instance, in humans approximately 2% of the Creatine/p-Creatine pool is converted to Creatinine daily. This predictability makes Creatinine a useful tool for normalizing the levels of other molecules found in urine. In addition, altered Creatinine levels can be used as an indicator of kidney dysfunction, or may be associated with other conditions that result in decreased renal blood flow.

In the Jaffe reaction, creatinine is treated with an alkaline picrate solution to yield a bright orange-red complex. Diluted samples are added to a microplate, and alkaline picrate reagent is added and incubated at room temperature for 30 minutes. Intensity of the color at 490/500 nm corresponds to the concentration of creatinine in the sample. Unfortunately, the Jaffe reaction is not specific and a number of substances including proteins in body fluids will interfere.

Thus, we used a modified Jaffe method developed by Heinegard and Tiderstrom, where the color derived from creatinine is destroyed at acid pH. The advantage of this method over the Jaffe reaction, is that the creatinine-picrate color fades faster than the interfering chromogens at acidic pH. The difference in color intensity measured at or near 500nm before and after acidification is proportional to creatinine concentration.

Reference: Heinegard D, Tiderstrom G. 1973 Determination of serum creatinine by a direct colorimetric method. Clinica Chimica Acta 43: 305-310.

SOLUTIONS

(a) 0. 05 M Sodium Phosphate and 0. 05 M Sodium Borate:

- Add 13. 40 g of $Na_2HPO_4 \cdot 7H_20$ (sodium phosphate) and 6. 9 g of $BNaO_2 \cdot 4H_20$ (sodium borate) to 900 mL of distilled water
- Add sodium hydroxide pellets to reach a pH of 12. 7
- Top up solution with distilled water to 1 L

*Keep solution refrigerated

(sodium phosphate 268. 07 g = 1 mole
13. 4035 g = 0. 05 mole)

(sodium borate 137. 9 g = 1 mole
6. 895 g = 0. 05 mole)

(b) 4% aqueous SDS

- Add 40 g SDS to 1 L distilled water

*Keep solution at room temperature

(c) Picric Acid 1. 3% (Sigma, cat. # P6744-1GA)

(d) 60% Acetic Acid solution

- 60 mL concentrated Acetic Acid + 40 mL distilled water

(e) 15% Acetic Acid solution

- Prepare using a 1:4 dilution
- 1 mL 60% Acetic Acid + 3 mL Picric solution (see reagent on p. 2)

PROCEDURE

Step 1: Prepare standards, samples, and reagent
Standards:
Use standard set from Sigma, cat. # C3613

Urine – use standard concentrations of 0 mg/dl, 1 mg/dl, 3 mg/dl, 6 mg/dl, 10mg/dl
To prepare standard concentration of 6 mg/dl: 60 µl of 10mg/dl standard + 40 µl ddH_20

Serum – use standard concentrations of 0 mg/dl, 0. 25 mg/dl, 0. 50 mg/dl, 1 mg/dl, 3 mg/dl
To prepare standard concentration of 0. 25 mg/dl: 20 µl of 1 mg/dl + 80 µl ddH_20
To prepare standard concentration of 0. 50 mg/dl: 50 µl of 1 mg/dl + 100 µl ddH_20

Samples:
Urine – 10-fold dilution (some samples will require 20-fold dilution)
For example: 20 µl urine sample + 180 µl distilled water
Range of results for urine creatinine concentration for rat:
Normal 10 wk: 40-100 mg/dl
PKD 10 wk: 15-110 mg/dl
Normal 7 months: 30-60 mg/dl
PKD 7 months: 30-70 mg/dl

Serum – no dilution
Range of results for serum creatinine concentration for rat:
Normal 10 wk: 0. 4-0. 7 mg/dl
PKD 10 wk: 0. 5-1. 0 mg/dl
PKD 6 months: 0. 7-1. 2 mg/dl
Normal 7 months: 0. 5-0. 6 mg/dl
PKD 7 months – 0. 9-1. 4 mg/dl

Reagent:
Picric solution (mix daily in amount required), **Combine in proportions of 2:2:1
2 volumes 0. 05 M Sodium Phosphate and 0. 05 M Sodium Borate solution (a)
2 volumes of 4% aqueous SDS (b)
1 volume Picric Acid (c)

For example: To make 20 mL of Picric solution:
8 ml 0. 05 M Sodium Phosphate and 0. 05 M Sodium Borate solution (a)
8 ml 4% aqueous SDS (b)
4 ml Picric Acid (c)

Step 2: Add 20 µl of blank, standards, and samples (urine samples diluted) to wells of 96 well-plate (Fisher, cat # 07-200-641). Make duplicates of each.

Step 3: Add 200 µl of Picric solution to each well using a multi-tip pipet (make sure pipet tips touch the bottom of each well) and mix by filling and expelling the tip three times.

Step 4: Cover well-plate with well cover sheet (Cayman, cat # 400012) and incubate at room temperature for 45 minutes (begin timing as soon as Picric solution is added to the last row of wells). To ensure adequate mixing, place well-plate on the orbital shaker at 140 rpm. After 40 minutes, remove well cover sheet (this will cause all the bubbles to disappear) and place well-plate on the microplate reader and shake every 15-20 seconds for 5 seconds for the last 3-4 minutes.

Step 5: Read 96 well-plate at 500 nm on microplate reader.

Step 6: Add 20 µl of 15% Acetic Acid solution using a multi-tip pipet (make sure pipet tips touch the bottom of each well) and mix by filling and expelling the tip three times.

Step 7: Incubate at room temperature for 6 minutes (begin timing as soon as 15% Acetic Acid solution is added to the last row of wells). To ensure adequate mixing, place well-plate on the microplate reader and shake every 15-20 seconds for 5 seconds for the last 3-4 minutes.

NOTE: Timing should begin immediately after the 15% Acetic Acid solution is added to the last row of wells as this ensures all standards have been incubated for at least 6

minutes. After 6 minutes, the absorbance does not change ; therefore, even if the first row of samples is incubated for 8 minutes this will not affect the absorbance. Whereas if timing were to begin after the 15% Acetic Acid solution was added to the first row of wells, the last row of wells would only be incubated in the Acetic Acid for 4 minutes and there is a greater change in the absorbance when samples are incubated at 4 minutes compared to 6 minutes.

Step 8: Read well-plate at 500 nm on microplate reader.

Step 9: Calculations
a) To find the final absorbance of standards and samples:

Final absorbance = pre-acid absorbance – post-acid absorbance

b) Take average of duplicates. (duplicates should be $\leq$5% difference. Repeat any samples that are >5%).

c) Using Microsoft Excel, construct a standard curve with absorbance on the x-axis and concentration on the y-axis. Using the equation given, calculate the concentration of creatinine in urine and/or serum. For urine, multiply concentration by the dilution factor.

SERUM UREA NITROGEN ASSAY

Principle of the Assay

Urea is the major end product of protein nitrogen metabolism. It is synthesized in the liver from ammonia which is produced by amino acid domination. The determination of serum urea nitrogen is an important index of kidney function. Impaired renal function or increased tissue protein breakdown are associated with increased urea nitrogen levels whereas liver damage or pregnancy are associated with decreased levels.

The Bertelot reaction has long been used for the measurement of urea and ammonia. The present method is a modified Bertelot.

$$\text{Urea} + H_2O \xrightarrow{\text{Urease}} 2\,NH_3 + CO_2$$

$$NH_3 + \text{Salicylate} + \text{Hypochlorite} \longrightarrow \text{2,2- Dicarboxyindophenol (blue green color)}$$

The BUN colorimetric procedure is a modification of the Bertelot reaction. Urea is converted to ammonium by the use of urease. Ammonium ion then reacts with a mixture of salicylate, sodium nitroprusside, and hypochlorite to yield a blue-green chromophore. The intensity of the color formed is proportional to the urea concentration in the sample.

Stock Reagents:

1) Urea Nitrogen (BUN) Reagent Set (Colometric Method), Teco Diagnostics Cat. #B551-132

Set Includes: 2 x Enzyme Reagent
2 x Colour Developer
*Urea Nitrogen (BUN) Standard (20mg/dL)

2) 40% Urea Solution
Cat. #200-315-5

General Instructions:

Step 1)

Prepare a 15x dilution of the stock 40% Urea Solution to use as a "working stock".

- This needs to be prepared because nitrogen's concentration in a 40% urea solution equals 1864mg/dL (Calculations below). If one were to prepare standards from this high of a concentration, there would be an extremely large room for error.

Calculations to determine Nitrogen's concentration in 40% Urea:

40% Urea Nitrogen = 40g of Urea/100mL
Urea's Molar Mass = 60
Nitrogen's Molar Mass = 14

- There are 2 Nitrogen molecules / 1 urea molecule, therefore the mass of nitrogen in a 40% urea solution = 28

28 g/mol nitrogen / 60 g/mol urea = 46. 6

- Thus, urea is composed of 46. 6% Nitrogen

40g Urea/dL of 40% Urea Solution x 46. 6% N = 18. 64g/dL of nitrogen in 40% Urea Solution

18. 64g/dL nitrogen x 1dL/100mL = 1864mg/dL of N

- The concentration of nitrogen in the 40% Urea Solution is 1864mg/dL.

Calculations to prepare working stock:

1864mg/dL nitrogen / 15 = 1242. 67mg/mL of nitrogen in a 15x dilution of a 40% Urea

Ex. To make 1. 5mL of working stock:

1242. 67mg/dL "Working Stock" = 100uL of 40% urea stock
1400uL of Deionized water

- Keep extra working stock at 4°C

Step2) Reconstitute the BUN Enzyme Reagent

Add 100mL of Deionized Water
Swirl to dissolve (the solution can because very bubbly)

Step 3) Pipette 120uL of the BUN Enzyme Reagent, using a 200uL multi-channel micropipette, into wells of 96 well-plate (Fisher, cat #07-200-641).

Cover plate with cover Sheet (Cayman, cat#400012)
Allow to equilibrate to room temperature (Approx. 15min)

Step 4) Meanwhile, prepare standards and samples

** Standards:

Prepare from Working Stock ranging in concentration from 10mg/dL –100mg/dL (Eg. 10mg/dL, 20,g/dL, 30mg/dL, 50mg/dL, and 100mg/dL)
(Urea Nitrogen is linear up to 100mg/dL)

Samples:

Undiluted (May be necessary to prepare 2. 5x dilutions.)

Step 5) After Enzyme Reagent has reach room temperature, pipette 8uL of Ddeionized water (blank), standards, samples, and 20mg/dL control into their respective wells.

Plate triplicates of each, re-cover, and place on Orbital Shaker for 10 minutes at approx. 50rpm.

Step 6) Add 120uL of the Colour Developer to each well using the 200 uL multi-channel micropipette.

Place on Orbital Shaker for 10 minutes at approx. 50rpm.

Step 7) Set up Template on spectrometer and read at 630nm

*The 20mg/dL control is used to check the accuracy of the standards. When plating, treat as an unknown.

** If standards of lower concentration are needed, prepare them using the 20mg/dL control for better accuracy.

HOMOGENIZATION OF LYOPHILIZED KIDNEY TISSUE FOR EIA EICOSANOID ANALYSIS

STEP1: Prepare list of conditions

Condition	Treatment	Incubation time (in 37°C water bath)
1	180uL homogenate + 20ul 10% ethanol	0 minutes
2	180uL homogenate + 20ul 10% ethanol	0 minutes
3	180uL homogenate + 20ul 10% ethanol	10 minutes
4	180uL homogenate + 20ul 10% ethanol	10 minutes
5	180uL homogenate + 20ul 1uM SC560	10 minutes
6	180uL homogenate + 20ul 1uM SC560	10 minutes
7	180uL homogenate + 20ul 10% ethanol	60 minutes
8	180uL homogenate + 20ul 10% ethanol	60 minutes

NOTE: SC560 is dissolved in 100% ethanol but is diluted to 1uM with a final ethanol concentration of 10%.
Time 0= endogenous production
Time 60= invitro steady state
1uM SC560= inhibits COX-1 selectively

STEP2: Calculate the amount of kidney homogenate

8 conditions X 180 uL homogenate per condition= 1440 uL homogenate reqd.
+ 20 uL for protein assay

1460 uL total
X 1. 1 to allow for error

~1700 uL TOTAL (round off to 1700)

Therefore, need to make 1700 uL of homogenate

Fresh Tyrodes solution is used to homogenize dried kidney tissue

For every 70mg of dried kidney tissue 2 mL of Tyrodes is required.

Therefore, if we need a final 1700 uL homogenate volume it will require 59. 5mg (0. 0595g) of dried kidney tissue and 1700 uL of Tyrodes. ($\frac{70mg}{2\ ml} = \frac{X}{1.7\ ml}$)

The smallest volume of fresh Tyrodes that can be made without having major difficulty with pH adjustments is 100mL.

TO MAKE 100mL of TYRODES

Reconstitute Tyrodes according to instructions in pamphlet (make up the contents of the bottle upto 1L). Cover the stock Tyrodes solution bottle with tin foil and place in 4C fridge until ready to use. To 100ml of stock Tyrodes (without sodium bicarbonate ; found in 4C chrom. fridge) add 100mg(0. 100g) of Sodium bicarbonate. Cover with tin foil to keep solution in the dark and place on ice to chill. Cover with Saran wrap and stir until dissolved (~15 minutes) and then pH to 7. 6.

To stop all reactions a 5mmol FINAL concentration (ie concentration of ASA when mixed with kidney homogenate) of COLD ASA is required. It takes ~1/2 hr for the powdered ASA to dissolve in deionized water at room temperature, therefore, while you are preparing the Tyrodes solution, you can prepare the ASA.

To make Acetyl salicylic acid solution
To 50 ml of deionized water, add 56. 6mg of dry ASA powder. Cover with saran wrap and stir until dissolved (~1/2 hr). Place on ice to chill.

A final concentration of 0. 01% Triton is required in the homogenate to breakdown proteins.

Therefore add 17uL of 1% Triton to 1700 uL of kidney homogenate.
(ie. 1% X (x uL) = 0. 01% X (1700 uL)

TO MAKE 1% Triton

Weigh out 0. 02 g of Triton solution in a small glass beaker and add 1. 8 ml of Tyrodes. Cover with saran wrap and mix well. This solution mixes best if fresh Tyrodes is at room temp. Cover this 1% Triton solution with tin foil.

STEP 3: Make inhibitor concentrations.

In this case we need 1uM of SC560 in a 10% ethanol solution. Stock SC560 is made up as 28. 35 mM of SC560 in 100% ethanol. Make 10% ethanol by mixing 0. 5ml of 100% ethanol with 4. 5 ml of Tyrodes.
Therefore.... .

Step A:

1. 5uL of 28. 35 mM stock
13. 5uL Tyrodes + 135uL 10% ethanol = 283uM SC560 in 10% ethanol

Step B:

1uL of 283uM SC560 in 10% ethanol
282 uL of 10% ethanol = 1uM SC560

STEP 4: Homogenizing

Weigh out 59. 5 mg of lyophilized kidney tissue in a 10ml glass test tube and keep tube on ice and cover top with saran wrap.

Add 1700 uL of chilled Tyrodes.

Note: Make sure that rotor on homogenizer is clean and dry.

Place test tube containing lyophilized kidney tissue in a small glass beaker containing ice. Insert rotor into test tube and homogenize at speed 15 for 30 seconds. Stop and check that all kidney tissue is at the bottom of the tube. If not, use rotor tip to push everything to the bottom of the test tube. Homogenize again for another 30 seconds.

Add the 17uL of 1% Triton of kidney homogenate. Vortex for 10 seconds. Let homogenate sit on ice for 30 seconds (cover top with saran wrap) and vortex every 10 minutes for 10 seconds (therefore vortex 2 more times). While this sits on ice you can label 8 1. 5 ml microcentrifuge tubes and add the appropriate condition. Place the microcentrifuge tubes on ice.

After homogenate has sat on ice for ½ hour, aliquot 180uL of homogenate to clean 1. 5 ml microcentrifuge tubes containing the appropriate condition. Vortex samples for 10 seconds and let sit on ice for another ½ hour. Aliquot 20uL of homogenate for protein assay.

After samples have sat on ice for ½ hour, place the appropriate conditions in the water bath for 10 minutes @ 37C as well as conditions 7 and 8 for 60 minutes.

After the second ½ period, to the time 0 samples, add 800uL of chilled ASA and vortex for 5 seconds to mix. Next centrifuge samples @ 12,000 g (11400 rpm) for 4C for 5 minutes. Remove samples and draw off supernatant and place it in a clean labelled 1. 5 ml microcentrifuge tube.

Once the 10 minute and 60 minute incubations are over, add 800 uL of chilled ASA and vortex for 5 seconds to mix. Next centrifuge samples @ 12,000 g (11400 rpm) for 4C for 5 minutes. Remove samples and draw off supernatant and place it in a clean labelled 1. 5ml microcentrifuge tube.

Samples can then be stored in the -80°C freezer.

6-KETO-PROSTAGLANDIN $F_{1\alpha}$ EIA KIT (CAYMAN CHEMICALS, CAT. NO. 515211)

PGI_2 is non-enzymatically dehydrated to 6-keto-$PGF_{1\alpha}$ ($t_{1/2}$= 2-3 minutes) and then to its major metabolite 2,3-dinor-6-keto-$PGF_{1\alpha}$ ($t_{1/2}$= 30 minutes).

Principle of the Assay

The assay is based on the competition between 6-keto-$PGF_{1\alpha}$ and a 6-keto-$PGF_{1\alpha}$ acetylecholinesterase (AChE) conjugate (6-keto-$PGF_{1\alpha}$ tracer) for a limited number of 6-keto-$PGF_{1\alpha}$- specific rabbit antiserum binding sites. Because the concentration of the tracer is held constant while the concentration of 6-keto-$PGF_{1\alpha}$ varies, the amount of tracer is able to bind to the rabbit antiserum will be inversely proportional to the concentration of 6-keto-$PGF_{1\alpha}$ in the well. This rabbit antiserum 6-keto-$PGF_{1\alpha}$ (either free or tracer) complex binds to the mouse monoclonal anti-rabbit IgG that has been previously attached to the well. The plate is washed to remove any unbound reagents and then Ellman's reagent (containing the substrate to AChE) is added to the well. The product of this enzymatic reaction has a distinct yellow color and absorbs strongly at 412 nm. The intensity of this color, determined spectrophotometrically is proportional to the amount of 6-keto-$PGF_{1\alpha}$ tracer bound to the well, which is inversely proportional to the amount of free 6-keto-$PGF_{1\alpha}$ present in the well during the incubation.

Definition of terms

Blank: background absorbance caused by Ellman's reagent. This background absorbance is subtracted from the absorbance readings of all other wells.

Total activity (TA): total enzymatic activity of the AChE-linked tracer.

Non-specific binding (NSB): non-immunological binding of the tracer to the well.

Maximum binding (B_0) : maximum amount of the tracer that the antiserum can bind in the absence of free analyte

% Bound/Maximum Bound (% B/B_0) : ratio of the absorbance of a particular sample or standard well to that of the maximum binding (B_0) well.

Standard Curve: a plot of the % B/B_0 values versus concentration of a series of wells containing known amounts of analyte.

Assay Procedure

1. EIA buffer: Add 100 uL EIA buffer to NSB wells. Add 50 uL EIA buffer to B0 wells.
2. 6-keto-$PGF_{1\alpha}$ standard: Add 50 uL of standards to respective standard wells in duplicate (S1-S8). Before pipetting each standard, make sure to equilibrate tip in that standard.

3. Sample: Pipet 50uL sample per well. Each sample is assayed in duplicate.
4. 6-keto-$PGF_{1\alpha}$ tracer : Add 50 uL tracer to all wells except TA and Blank wells.
5. 6-keto-$PGF_{1\alpha}$ antiserum: Add 50 ul antiserum to all wells except TA, NSB and the Blank wells.
6. Incubate the plate: Cover each plate with plastic film and incubate for 18h at 4°C.
7. Develop the plate: When ready to develop the plate, reconstitute Ellman's reagent as per kit instructions. Reconstituted Ellman's is only stable for a day and should be protected from light at all times. Empty the wells and rinse wells five times with wash buffer (provided in the kit). Add 200 uL Ellman's reagent to each well and 5uL tracer to the TA wells. Cover plate with plastic film and develop plate for in the dark on an orbital shaker for 90-120 minutes.
8. Read the plate: Read the plate at 412 nm using the SpectraMax 340 (Molecular Devices Corporation, SpectraMax 340, Sunnyville, California). The SOFTmax Pro software was used to calculate the absorbance values using the 4-parameter option. Before reading the plate, wipe the bottom of the plate with a Kimwipe to remove dust, fingerprints etc. The plate should be read when the B0 absorbance is between 0. 3-0. 8 AU. If the absorbance is > 1. 5, wash the plate, add fresh Ellman's and develop again.

PROSTAGLANDIN E_2 MONOCLONAL EIA KIT (CAYMAN CHEMICALS, CAT NO. 514010)

In vivo, PGE_2 is rapidly converted to an inactive metabolite (13,14-dihydro-15-keto-PGE_2) by the prostaglandin 15-dehydrogenase pathway ($t_{1/2}$ in plasma=30 seconds).

Principle of the Assay

The assay is based on the competition between PGE_2 and a PGE_2 acetylecholinesterase (AChE) conjugate (PGE_2 tracer) for a limited number of PGE_2 monoclonal antibody. Because the concentration of the tracer is held constant while the concentration of PGE_2 varies, the amount of tracer is able to bind to PGE_2 monoclonal antibody will be inversely proportional to the concentration of PGE_2 in the well. This antibody- PGE_2 (either free or tracer) complex binds to goat polyclonal anti-mouse IgG that has been previously attached to the well. The plate is washed to remove any unbound reagents and then Ellman's reagent (containing the substrate to AChE) is added to the well. The product of this enzymatic reaction has a distinct yellow color and absorbs strongly at 412 nm. The intensity of this color, determined spectrophotometrically is proportional to the amount of PGE_2 tracer bound to the well, which is inversely proportional to the amount of free PGE_2 present in the well during the incubation.

Definition of terms

Blank: background absorbance caused by Ellman's reagent. This background absorbance is subtracted from the absorbance readings of all other wells.

Total activity (TA): total enzymatic activity of the AChE-linked tracer.

Non-specific binding (NSB): non-immunological binding of the tracer to the well.

Maximum binding (B_0) : maximum amount of the tracer that the antiserum can bind in the absence of free analyte

% Bound/Maximum Bound (% B/B_0) : ratio of the absorbance of a particular sample or standard well to that of the maximum binding (B_0) well.

Standard Curve: a plot of the % B/B_0 values versus concentration of a series of wells containing known amounts of analyte.

Assay Procedure

1. EIA buffer: Add 100 uL EIA buffer to NSB wells. Add 50 uL EIA buffer to B_0 wells.
2. PGE_2 standard: Add 50 uL of standards to respective standard wells in duplicate (S1-S8). Before pipetting each standard, make sure to equilibrate tip in that standard.
3. Sample: Pipet 50uL sample per well. Each sample is assayed in duplicate.

4. PGE_2 tracer : Add 50 uL tracer to all wells except TA and Blank wells.
5. PGE_2 antibody: Add 50 ul antibody to all wells except TA, NSB and the Blank wells.
6. Incubate the plate: Cover each plate with plastic film and incubate for 18h at 4°C.
7. Develop the plate: When ready to develop the plate, reconstitute Ellman's reagent as per kit instructions. Reconstituted Ellman's is only stable for a day and should be protected from light at all times. Empty the wells and rinse wells five times with wash buffer (provided in the kit). Add 200 uL Ellman's reagent to each well and 5uL tracer to the TA wells. Cover plate with plastic film and develop plate for in the dark on an orbital shaker for 60-90 minutes.
8. Read the plate: Read Read the plate at 412 nm using the SpectraMax 340 microplate reader (Molecular Devices Corporation, SpectraMax 340, Sunnyville, California). The SOFTmax Pro software is used to calculate absorbance values using the 4-parameter option. Before reading the plate, wipe the bottom of the plate with a Kimwipe to remove dust, fingerprints etc. The plate should be read when the B0 absorbance is between 0. 3-0. 8 AU. If the absorbance is > 1. 5, wash the plate, add fresh Ellman's and develop again.

THROMBOXANE B_2 EIA KIT (CAYMAN CHEMICALS, CAT NO. 519031)

TXA_2 is rapidly hydrolyzed non-enzymatically converted to TXB_2, which is then metabolized to urinary metabolites for clearance by the kidneys.

Principle of the Assay

The assay is based on the competition between TXB_2 and a TXB_2 acetylecholinesterase (AChE) conjugate (TXB_2 tracer) for a limited number of TXB_2 specific rabbit antiserum binding sites. Because the concentration of the tracer is held constant while the concentration of TXB_2 varies, the amount of tracer is able to bind to the rabbit antiserum will be inversely proportional to the concentration of TXB_2 in the well. This rabbit antiserum TXB_2 (either free or tracer) complex binds to the mouse monoclonal anti-rabbit IgG that has been previously attached to the well. The plate is washed to remove any unbound reagents and then Ellman's reagent (containing the substrate to AChE) is added to the well. The product of this enzymatic reaction has a distinct yellow color and absorbs strongly at 412 nm. The intensity of this color, determined spectrophotometrically is proportional to the amount of TXB_2 tracer bound to the well, which is inversely proportional to the amount of free TXB_2 present in the well during the incubation.

Definition of terms

Blank: background absorbance caused by Ellman's reagent. This background absorbance is subtracted from the absorbance readings of all other wells.

Total activity (TA): total enzymatic activity of the AChE-linked tracer.

Non-specific binding (NSB): non-immunological binding of the tracer to the well.

Maximum binding (B_0) : maximum amount of the tracer that the antiserum can bind in the absence of free analyte

% Bound/Maximum Bound (% B/B_0) : ratio of the absorbance of a particular sample or standard well to that of the maximum binding (B_0) well.

Standard Curve: a plot of the % B/B_0 values versus concentration of a series of wells containing known amounts of analyte.

Assay Procedure

1. EIA buffer: Add 100 uL EIA buffer to NSB wells. Add 50 uL EIA buffer to B_0 wells.
2. TXB_2 standard: Add 50 uL of standards to respective standard wells in duplicate (S1-S8). Before pipetting each standard, make sure to equilibrate tip in that standard.
3. Sample: Pipet 50uL sample per well. Each sample is assayed in duplicate.
4. TXB_2 tracer : Add 50 uL tracer to all wells except TA and Blank wells.

5. TXB_2 antiserum: Add 50 ul antiserum to all wells except TA, NSB and Blank wells.
6. Incubate the plate: Cover each plate with plastic film and incubate for 18h at room temperature.
7. Develop the plate: When ready to develop the plate, reconstitute Ellman's reagent as per kit instructions. Reconstituted Ellman's is only stable for a day and should be protected from light at all times. Empty the wells and rinse wells five times with wash buffer (provided in the kit). Add 200 uL Ellman's reagent to each well and 5uL tracer to the TA wells. Cover plate with plastic film and develop plate for in the dark on an orbital shaker for 60 minutes.
8. Read the plate: Read the plate at 412 nm using the SpectraMax 340 microplate reader. The SOFTmax Pro software is used to calculate the absorbance values using the 4-parameter option. Before reading the plate, wipe the bottom of the plate with a Kimwipe to remove dust, fingerprints etc. The plate should be read when the B_0 absorbance is between 0. 3-0. 8 AU. If the absorbance is > 1. 5, wash the plate, add fresh Ellman's and develop again.

PROSTAGLANDIN E METABOLITE EIA KIT (CAYMAN CHEMICALS, CAT NO. 514010)

In vivo, PGE_2 is rapidly converted to an inactive metabolite (13,14-dihydro-15-keto-PGE_2) by the prostaglandin 15-dehydrogenase pathway ($t_{1/2}$ in plasma=30 seconds). But blood, urine and other samples often contain very little intact PGE_2, and measurement of metabolites is essential to provide a reliable estimate of PGE_2 production. The PGEM assay was developed to convert all immediate PGE_2 metabolites into a single, stable derivative quantifiable by EIA.

Principle of the Assay
The assay is based on the competition between PGEM and a PGEM acetylecholinesterase (AChE) conjugate (PGEM tracer) a limited number of PGEM specific rabbit antiserum binding sites. Because the concentration of the tracer is held constant while the concentration of PGEM varies, the amount of tracer is able to bind to the rabbit antiserum will be inversely proportional to the concentration of PGEM in the well. This rabbit antiserum PGEM (either free or tracer) complex binds to the mouse monoclonal anti-rabbit IgG that has been previously attached to the well. The plate is washed to remove any unbound reagents and then Ellman's reagent (containing the substrate to AChE) is added to the well. The product of this enzymatic reaction has a distinct yellow color and absorbs strongly at 412 nm. The intensity of this color, determined spectrophotometrically is proportional to the amount of PGEM tracer bound to the well, which is inversely proportional to the amount of free PGEM present in the well during the incubation

Definition of terms

Blank: background absorbance caused by Ellman's reagent. This background absorbance is subtracted from the absorbance readings of all other wells.

Total activity (TA): total enzymatic activity of the AChE-linked tracer.

Non-specific binding (NSB): non-immunological binding of the tracer to the well.

Maximum binding (B_0) : maximum amount of the tracer that the antiserum can bind in the absence of free analyte

% Bound/Maximum Bound (% B/B_0) : ratio of the absorbance of a particular sample or standard well to that of the maximum binding (B_0) well.

Standard Curve: a plot of the % B/B_0 values versus concentration of a series of wells containing known amounts of analyte.

Derivatization of Standards
Using an equilibrated pipet tip (equilibrated in ethanol) transfer 100uL of PGEM standard

into a clean 2ml eppendorf tube and dilute with 900uL dd H20. The concentration of this standard is 40 ng/ml.
Aliquot 50uL of this standard into another clean 2ml eppendorf tube and then dilute to a total volume of 1ml with EIA buffer (ie 950ul EIA buffer). Add 300 uL carbonate buffer and incubate overnight at 37°C. Then add 400uL phosphate buffer and 300uL of EIA buffer. This solution is 1000 pg/ml.

Derivatization of samples
Aliquot 500uL of each sample into a clean 2 mL eppendorf tube. Add 150uL Carbonate buffer and incubate overnight at 37°C. Then add 200uL Phosphate buffer and 159uL EIA buffer. If needed, samples can be diluted further with PGEM buffer.

Assay Procedure

1. PGEM buffer: Add 50 uL EIA and 50 uL PGEM buffer to NSB wells. Add 50 uL PGEM buffer to B_0 wells.
2. PGEM standard: Add 50 uL of derivatized standards to respective standard wells in duplicate (S1-S8). Before pipetting each standard, make sure to equilibrate tip in that standard.
3. Sample: Pipet 50uL derivatized sample per well. Each sample is assayed in duplicate.
4. PGEM tracer : Add 50 uL tracer to all wells except TA and Blank wells.
5. PGEM antiserum: Add 50 ul antiserum to all wells except TA, NSB and the Blank wells.
6. Incubate the plate: Cover each plate with plastic film and incubate for 18h at room temperature.
7. Develop the plate: When ready to develop the plate, reconstitute Ellman's reagent as per kit instructions. Reconstituted Ellman's is only stable for a day and should be protected from light at all times. Empty the wells and rinse wells five times with wash buffer (provided in the kit). Add 200 uL Ellman's reagent to each well and 5uL tracer to the TA wells. Cover plate with plastic film and develop plate for in the dark on an orbital shaker for 60-90 minutes.
8. Read the plate: Read the plate at 412 nm using the SpectraMax 340 microplate reader (Molecular Devices Corporation, SpectraMax 340, Sunnyville, California). The SOFTmax Pro software is used to calculate absorbance values using the 4-parameter option. Before reading the plate, wipe the bottom of the plate with a Kimwipe to remove dust, fingerprints etc. The plate should be read when the B0 absorbance is between 0. 3-0. 8 AU. If the absorbance is > 1. 5, wash the plate, add fresh Ellman's and develop again.

SUMMARY OF STEPS REQUIRED TO CARRY OUT REAL TIME RT-PCR USING QIAGEN"S QUANTITECT SYBR GREEN RT-PCR KIT SYSTEM

I) RNA ISOLATION PROTOCOL

-For use with Invitrogen's TRIzol Regent Cat. No. 15596-018
-TRIzol is store at 4°C, and is **extremely toxic** to skin and eyes, **THEREFORE ALL WORK MUST BE CARRIED OUT IN A FUME HOOD.**
-Homogenization is carried out at room temperature in fume hood, as must steps 1-3

1. HOMOGENIZATION

All tissues should be freeze dried and stored in -80°C to preserve RNA from degrading. Tissues are then removed from -80°C one at a time and weighed into glass centrifuge tubes. For whole tissues use approximately 50-100mg of sample, for dried samples use 20-30mg of sample. After samples are weighed go to fume hood and add 1 ml of TRIzol per 50-100mg of tissue weighed.

Homogenize tissue/TRIzol mixture using Heidolph Diax 900 with probe TYP10F ; ensure probe is clean, autoclave if necessary. Homogenize for 20 sec interval and stop, allow 10 sec bake period. Repeat this 20 sec homogenize/ 10 sec bake, 5 times to ensure homogenous mixture. Transfer the 1ml of homogenate to a 1. 5ml micro centrifuge tube, and let incubate at room temperature for 5 minutes.

2. SEPARATION

Now add . 2ml of Chloroform to each tube and cap tightly. Invert tubes by hand 50 times, jut simply back and forth will do, to ensure even mixture of Chloroform and Homogenate, then let incubate at room temp for 3 minutes. Place tubes into Eppendorf centrifuge 5417C (in 4°C fridge) and centrifuge at 10,000 RPM for 15 minutes. Remove tubes and return to fume hood, RNA is collected in the upper clear aqueous phase.

3. PRECIPITATION

Using 100µl pipette transfer as much of the upper aqueous phase as possible to a new set of 1. 5ml micro centrifuge tubes. Now add 0. 5ml of Isopropanol per 1ml of TRIzol to tubes. Once again invert tubes by hand 30 times to ensure even mixture. Let incubate at room temperature for 10 minutes. Now centrifuge using Eppendorf centrifuge 5417C (in 4°C fridge), at 10,000 RPM for 20 minutes.

NOTE YOU CAN NOW SAFELY WORK WITH SAMPLES OUTSIDE OF FUME HOOD

4. RNA WASH

Dump out supernatant and confirm presence of RNA pellet on the base of tube, it should appear as a white pellet. Now add 1ml of 75% Ethanol to each tube, vortex, and once again centrifuge at 10,000 RPM for 10 minutes.

5. REDISSOLVING THE RNA

Now dump out ethanol from tubes by inverting the tube, while inverted place a Kimwipe against the inside of the tube to remove any Ethanol droplets. Allow tubes to rest inverted for 12-15 minutes to allow any still present Ethanol to air dry, **DO NOT EXCEED THIS DRY TIME**, as a completely dried RNA pellet will lose its solubility in re-suspension. During this 12-15 minute period preheat oven to 55°C and start up Pharmacia Biotech Ultrospec 4000 (UV/Visible spectrophotometer). Once the pellet is dry, re-suspend it in 100µl of Nuclease-free water by passing the solution up and down through the pipette 50 times, using 100µl aerosol tips. . Now place tubes in 55°C oven for 10 minutes, **DO NOT EXCEED THIS TIME.** Once 10-minute heating period is complete, vortex samples briefly.

6. SPECTROPHOTOMETER / CALCULATIONS

Using a new set of 1. 5ml micro centrifuge tubes prepare samples for spectrophotometer readings. Each sample is represented by 996µl Deionized water + 4. 4µl (4µl + 10% for pipette error) of sample (taken from previously heated sample tubes above). Also, create a 1ml blank that will be used to reference the machine. At spectrophotometer terminal open Swift II Instrument Control Program ; program will then register the 6-cell changer attached. Now click on the white box, located next to the red box, the spectrophotometer will recalibrate and the box will turn blue after a brief period. Now click on the absorbance window and adjust to A260. Place the 1ml of water into the cuvette and click reference on the screen, the spectrophotometer will now be zeroed and ready to use for samples. Put the 1ml H2O blank back into the 1. 5ml micro centrifuge tube and now read the samples by placing each into the cuvette one at a time. Once all samples have been read, repeat the above procedure for A280. **NOTE A260/A280 ratio should be approximately 1. 7 in range.**

NOTE ALL ISOLATED RNA SAMPLES SHOULD VERIFED BY GEL ELECTROPHORESIS

Calculation for concentration of RNA in stock is as follows:

Note: An absorbance of 1 unit at 260 nm corresponds to 40µg of RNA per ml (A260 = 1 => 40µg/ml).

Volume of RNA sample = 100µl
Dilution = 4µl of RNA sample + 996µl deionized water (1/250 dilution).
Measure absorbance of diluted sample in a 1 ml cuvette.

A260 = 0. 75

Concentration of RNA sample = 40 x A_{260} x dilution factor
= 40 x 0. 75 x 250
= 7500µg/ml
= 7. 5µg/µl

Note: above equation sums up to- A260 x 10 = Xµg/µl

Total yield = concentration x volume of sample in microlitres
= 7. 5µg/µl x 100µl
= 750µg RNA

II) RNA ELECTROPHORESIS PROTOCOL

1. 1% AGAROSE GEL PREPARATION

Make up 1X TAE Buffer as per buffer sheet included section VII. Now weigh out 1g of GIBCOBRL Ultra Pure Agarose, cat #15510-019 and add to 100 ml of 1X TAE Buffer. Melt the gel in microwave on high just until boil, ensure that the agarose has melted completely by gently swirling the flask, and also look for the presence of any undissolved beads of Agarose. Pour gel into either the large or small casting apparatus (Life Technologies- Horizon 58 or Horizon 11-14), using the black separators for edges. While the gel is still liquid, quickly insert the comb(s) into the gel ; allow gel to set for 20 minutes at room temperature.

2. SAMPLE PREPARATION

Each sample will be made up to 12. 1µl total volume, consisting of 8µl RNase-free water + 3µl 4X RNA Loading buffer + 0. 1µl Ethidium Bromide + 1µl RNA in sequence, master mixes can be prepared when using multiple samples. Sample must be prepared on ice to prevent RNA degradation, and should be vortexed to ensure a homogenous mixture to load gel with. **ETHIDIUM BROMIDE IS EXTREMELY TOXIC AND MUST BE HANDLED WITH CARE.**

3. LOAD THE GEL

Once the gel has set remove the black separators and fill the reservoir with 1X TAE buffer, either used or new and buffer must cover gel and electrodes. Now with even pressure pull out the comb, exposing the developed wells within the gel. Load 12µl of sample into desired well using the 20µl pipette.

4. RUNNING THE GEL

Connect gel apparatus to power supply (Amersham Pharmacia Biotech Electrophoresis Power Supply EPS301) using designated leads, ensure correct polarity

connections. Run gel at 30mA for approximately 20 minutes until blue indicator band has moved across approximately 1/4 of the gel.

5. DEVELOPING THE GEL

Once finished remove leads and carefully cut off excess gel past blue indicator bands, which can be re-used. Take remaining gel out and transfer to the Alpha Innotech Corporation Fluorchem Hood, place gel on black base within the hood (white screen may have to be lifted if in place). Turn on the UV button on the base panel and close the door. Open the Fluorchem 8000 program on the desktop, and then click on Acquire. Once the acquire window has opened, select Filter Wheel Position 2, and Reflective UV and the gel should become visible. Now adjust the light, zoom and focus so that bands within the gel are clear and focused. Once adjusted click on the High Sensitivity tab and then on the Acquire button. The image can now be adjusted using the Gamma Settings, such that bands can be lightened and the background darkened. The gel picture can now be saved and/or printed.

III) PRIMER DESIGN PROTOCOL

Custom primers are designed using internet based software, and all primers are ordered through Invitrogen Corporation. Primers are designed using the following steps:

1- Go to the Entrez PubMed web site, link- (http://www. ncbi. nlm. nih. gov. proxy2. lib. umanitoba. ca/entrez/query. fcgi?db=PubMed)
Then click on the Nucleotide tab located at the top of the page.
2- Now enter the gene of interest and do a search. When the results list appears, find the gene name and ensure that it states 'mRNA, complete cds' in the title.
3- Click on the GI number and highlight the DNA sequence located after the title- Origin, and copy the sequence (highlighting and copying the numbers on the left is fine, they will be automatically removed later).
4- With the sequence copied, go to the Primer 3 Input website located at- (http://frodo. wi. mit. edu/cgi-bin/primer3/primer3_www. cgi) and paste the sequence into the input box.
5- There are many options on this page, but only the following items need to be adjusted:
- **Sequence Id**: input the name you wish to call the primer
- **Product Size Range**: type in 100-150
- **Primer Size**: Min:19 Opt:20 Max:21
- **Primer Tm**: Min:60 Opt:60 Max:60
- **Primer GC%**: Min:40 Opt:50 Max:60

6- Now click on the Pick Primers button, and the software will design primers as per your conditions. The output will give you five possible primer combinations, with all information indicated such as exact size, temperature, GC%, and product size, and of which any can be used.
7- Use primer order sheets and fill in desired primer sequences, then select 50nm as the selected concentration.

PRIMER RECONSTITUTION:

- Once primers have arrived, they must be reconstituted as follows:
    - Briefly centrifuge the vial in a pulse manner to bring primer to base of the tube.
    - Add 100µl of Nuclease-free water to the vial.
    - Let mixture sit for 2 minutes to allow re-hydration of primer into water
    - Finally vortex to ensure homogenous mixture

PRIMER CALCULATIONS:

- Desired primer concentration for both RT-PCR and Real Time PCR is 1µM ; therefore, working primer concentrations are made from stock vial as follows:

Primers comes as X number of nanomoles, for example a primer that is ordered comes as 59. 6nm, using the following formula one can determine the amount of stock needed to make a work solution-

$$\frac{.05\text{nm} \times 100\mu\text{l}}{59.6\text{nm}} = 0.08389\mu\text{l}$$

In addition, as per protocol a volume of 2µl per primer is required for the master mix, therefore-

2µl / . 08389µl = 23. 84µl - 1µl primer = 22. 84µl nuclease-free water

Therefore, if we want 2µl of 1µM primer to add to our master mix, the working solution should be 1µl primer and 22. 84µl nuclease-free water for a primer with a concentration of 59. 6nm. It is generally useful to make 5X volume of all primers ; therefore, one would make up 5µl primer and 114. 2µl nuclease-free water

Primers are store in -20°C and are generally good for a year.

IV) DEOXYRIBONUCLEASE I PROTOCOL

All isolated RNA samples must be DNase treated to remove any sources of DNA that may have been carried over during isolation. Deoxyribonuclease I treatment digests both single and double-stranded DNA into random oligodeoxy-ribonucleotides, such that they will not be amplified during PCR and will not interfere with the desired product.

1. KIT INFORMATION

- For use with Invitrogen's Deoxyribonuclease I, Amplification Grade Cat. No 18068-015
- Kit contains- 18068-015 DNase I, Amp Grade
    - Y02340 10X DNase I Reaction Buffer
    - 25mM EDTA pH 8. 0
- Kit is stored at -20°C

2. DNase PROTOCOL

All samples are prepared in Costar PCR Tubes 0. 2ml Cat No. 07-200-493 and are kept on ice. All sample preparation is as follows:

- 1µg RNA sample
- 1µl 10X DNase I Reaction Buffer
- 1µl DNase 1, Amp Grade, 1U/µl
- Nuclease free water to 10µl

All reaction values are based on 1µg of RNA ratio for smaller or larger concentrations adjust accordingly. Example: For 0. 5µg of RNA-

- 0. 5µg RNA sample
- 0. 5µl 10X DNase I Reaction Buffer
- 0. 5µl DNase 1, Amp Grade, 1U/µl
- Nuclease free water to 5µl

For multiple samples and primers create a master mix using the above ratio formula to ensure even conditions, and are as follows:

For Access RT-PCR System (For Primer Testing)

Utilizes 1µg RNA sample, concentration calculation example using **three** samples and **four** primers would be as follows:

Sample	Conc. Desired (1µg RNA / X Conc.)	X # of Primers = + NF H20 = 10µl*
N2	1. 7 1 / 1. 7 = 0. 58µl	X 4 primers = 2. 35µl+ 7. 65µl = 10µl

N3 4. 12 1 / 4. 12 = 0. 24µl X 4 primers = 0. 97µl+ 9. 03µl = 10µl
PKD3 1 1 / 1 = 1µl X 4 primers = 4µl+ 6µl = 10µl

*All tubes are made up to 10µl sample and nuclease free water so that each tube will receive an equal volume of Master Mix.

Master Mix for **three** samples and **four** primers would be as follows:

X # of Primers X # of Samples + 10%
Sample and H2O - 8µlX 4 primers = 32µl - 10µl** = 22µl X 3. 3 = 72. 6µl
1µl 10X DNase I Reaction Buffer - 1µlX 4 primers = 4µl X 3. 3 = 13. 2µl
1µl DNase 1, Amp Grade, 1U/µl - 1µl X 4 primers = 4µl X 3. 3 = 13. 2µl .
99µl

** - 10µl is subtracted from the Sample and H2O value here as we have already prepared the mixtures of 10µl Sample and H2O previously, as indicated by *.

From the 99µl, 10% is extra, so the volume is considered to be 90µl. Now the 90µl is divided over the 3 tubes made above (i. e. N2, N3, and PKD3 each get 30µl). This brings the final volume in each tube to 40µl (10µl of sample and NF H20 + the 30µl Master Mix).

To confirm the volume in each tube is calculated correctly, RT-PCR DNase tubes will **always** work out to be 10µl X the number of primers, so in this example- 10µl X 4 primers would equal 40µl and that is what we have.

For QuantiTect SYBR Green RT-PCR Kit System (For Real Time RT-PCR)

Utilizes 0. 5µg RNA sample, concentration calculation example using **three** samples and **four** primers would be as follows:

Sample	Conc.	Desired (0. 5µg RNA / X Conc.)	X # of Primers = + NF H20 = 5µl*
N2	1. 7	0. 5 / 1. 7 = 0. 29µl X 4 primers =	1. 16µl+ 3. 84µl = 5µl
N3	4. 12	0. 5 / 4. 12 = 0. 12µl X 4 primers =	0. 48µl+ 4. 52µl = 5µl
PKD3	1	0. 5 / 1 = 0. 5µl X 4 primers =	2µl+ 3µl = 5µl

*All tubes are made up to 5µl sample and nuclease free water so that each tube will receive an equal volume of Master Mix.

Master Mix for **three** samples and **four** primers would be as follows:

	X # of Primers =	X # of Samples + 10%
Sample and H2O -4µl	X 4 primers = 16µl - 5µl** = 11µl	X 3. 3 = 36. 3µl
1µl 10X DNase I Reaction Buffer - 0. 5µl	X 4 primers = 2µl	X 3. 3 = 6. 6µl
1µl DNase 1, Amp Grade, 1U/µl - 0. 5µl	X 4 primers = 2µl	X 3. 3 = 6. 6µl
		49. 5µl

** - 5µl is subtracted from the Sample and H2O value here as we have already prepared the mixtures of 5µl Sample and H2O previously, as indicated by *.

From the 49. 5µl, 10% is extra, so the volume is considered to be 45µl. Now the 45µl is divided over the 3 tubes made above (i. e. N2, N3, and PKD3 each get 15µl). This brings the final volume in each tube to 20µl (5µl of sample and NF H20 + the 15µl Master Mix).

To confirm the volume in each tube is calculated correctly, QuantiTect SYBR Green RT-PCR Kit DNase tubes will **always** work out to be 5µl X the number of primers, so in this example- 5µl X 4 primers would equal 20µl and that is what we have.

3. THERMOCYCLER PROTOCOL

Once all Sample/Costar PCR Tubes are prepared, the tubes are loaded into the Techne Genius Thermocycler and are incubated as follows:

- 15 minutes at 21°C (Program 7)
- After the program has ended, EDTA is then added to the tubes to inactivate the DNase enzyme. For the Access RT-PCR System 1µl of EDTA **per** primer is added (example from above - 4 primers were used, therefore 4µl of EDTA is added to each tube). For the QuantiTect SYBR Green RT-PCR Kit System 0. 5µl

of EDTA **per** primer is added (example from above - 4 primers were used, therefore 2µl of EDTA is added)
- 10 minutes at 65°C (Program 8)
- Thermocycler will then cycle to Program 9, which holds at 4°C until stopped by the user.

Samples can now be used for the Access RT-PCR System or QuantiTect SYBR Green RT-PCR Kit System depending on preparation above.

V) ACCESS RT-PCR PROTOCOL FOR PRIMER TESTING

This is a general use protocol for running standard reverse transcription polymerase chain reactions. The process will utilize isolated RNA, which will then be reverse transcribed into cDNA ; this cDNA is then amplified exponentially to yield a large fold product that can then be separated and viewed using an agarose gel. This protocol is for use with Promega's Access RT-PCR System Cat. #AC250 revision 7/04, and can be ordered through Fisher Scientific. All RNA samples must previously be DNase treated as per protocol to ensure RNA is of pure yield. Samples are kept on ice at all times to prevent degradation or premature enzyme activity. Samples are prepared in Costar PCR Tubes . 2ml Cat No. 07-200-493. When new primers are ordered it is recommended that a RT-PCR be carried out and products ran on a gel to confirm the presence of a single band of correct base pair size.

1. TUBE PREPARATION

All regents are prepared in Master Mixes to ensure homogenous mixtures, and therefore even enzyme activity. One Master Mix is prepared per primer set (forward and reverse primer make one set) ; therefore, if for example COX1, and COX2 are the genes of interest, one Master Mix must be made up for each of the two set of primers. Each Master Mix contains the following reagents-

	Volume	Final Concentration
Nuclease-Free Water-	21µl	
AMV/Tfl 5X Reaction Buffer-	10µl	1X
dNTP Mix-	1µl	0. 2mM
Forward Primer-	2µl	1µM
Reverse Primer-	2µl	1µM
25mM MgSO4-	2µl	1mM
----------Stop and Vortex to evenly distribute MgSO4---------		
AMV Reverse Transcriptase-	1µl	0. 1u/µl
Tfl DNA Polymerase-	1µl	0. 1u/µl
RNA sample template-	10µl	1µg
	50µl total	

These values are then multiplied for the number of samples in which you wish to look at. For example if you are looking at COX1 and COX2, and want to use three samples, say N1, N2, and N3 then you will end up preparing **SIX** tubes total, each with 50µl -

	Sample		
	N1	N2	N3
Primers			
COX1	X	X	X
COX2	X	X	X

To carry out preparation two Master Mixes will need to be made, one for COX1 and one for COX2, each multiplied by the total number of samples

A) COX1 X the number of samples (here the example uses 3 samples, plus 10% for pipette error)

Nuclease-Free Water- 21µl X 3. 3 = 69. 3µl
AMV/Tfl 5X Reaction Buffer- 10µl X 3. 3 = 33µl
dNTP Mix- 1µl X 3. 3 = 3. 3µl
COX1 Forward Primer- 2µl X 3. 3 = 6. 6µl
COX1 Reverse Primer- 2µl X 3. 3 = 6. 6µl
25mM MgSO4- 2µl X 3. 3 = 6. 6µl
----------Stop and Vortex to evenly distribute MgSO4---------
AMV Reverse Transcriptase- 1µl X 3. 3 = 3. 3µl
Tfl DNA Polymerase- 1µl X 3. 3 = 3. 3µl
Total = 40µl X 3. 3 = 132µl

From the 132µl, 10% is extra, so the volume is considered to be 120µl. This COX1 master is then divide into 3 tubes, such that each tube has 40µl of reagents –

	Sample		
	N1	N2	N3
Primers			
COX1	40µl	40µl	40µl

B) COX2 X the number of samples (plus 10% for pipette error)

Nuclease-Free Water- 21µl X 3. 3 = 69. 3µl
AMV/Tfl 5X Reaction Buffer- 10µl X 3. 3 = 33µl
dNTP Mix- 1µl X 3. 3 = 3. 3µl
COX2 Forward Primer- 2µl X 3. 3 = 6. 6µl
COX2 Reverse Primer- 2µl X 3. 3 = 6. 6µl
25mM MgSO4- 2µl X 3. 3 = 6. 6µl
----------Stop and Vortex to evenly distribute MgSO4---------
AMV Reverse Transcriptase- 1µl X 3. 3 = 3. 3µl
Tfl DNA Polymerase- 1µl X 3. 3 = 3. 3µl
Total = 40µl X 3. 3 = 132µl

From the 132µl, 10% is extra, so the volume is considered to be 120µl. This COX2 master is then divide into 3 tubes, such that each tube has 40µl of reagents

	Sample		
	N1	N2	N3
Primers			
COX2	40µl	40µl	40µl

Once Master Mixes have been evenly distributed to corresponding tubes, DNase treated samples can then be added to each of the tubes. As per DNase treatment protocol add 10µl of treated RNA sample to 40µl of Master Mix, total volume per Promega's Access RT-PCR System protocol is 50µl.

	Sample		
	N1	N2	N3
Primers			
COX1	40µl/10µl	40µl/10µl	40µl/10µl
COX2	40µl/10µl	40µl/10µl	40µl/10µl

2. THERMOCYCLER PROTOCOL

Protocol is designed to work with Techne Genius Thermocycler - Block C, using Costar PCR Tubes . 2ml. Thermocycler is already pre-programmed with the following protocol –

Activity	Program Number	Temperature / Time
- Reverse Transcription enzyme activation and cDNA synthesis	1	45°C / 45 Minutes
- AMV RT inactivation and RNA/cDNA/primer denaturation	2	94°C / 2 Minutes
- Denaturation of cDNA	3*	94°C / 30 Seconds
- Annealing of primers	3*	55°C / 1 Minutes
- Extension of newly synthesized cDNA	3*	68°C / 2 Minutes
- Final extension of new products	4	68°C / 7 Minutes
- Hold / Prevent DNA degradation	5	4°C

* - Note that Program Number 3 will cycle 32 times before moving on to Program Number 4.

Once program is complete the products will remain held in program 5, which they can remain at since the temperature is 4°C. For longer storage put tubes in -20°C freezer.

3. DNA GEL ELECTROPHORESIS

A) 2. 5% AGAROSE GEL PREPARATION

For running RT-PCR cDNA products use a 2. 5% agarose gel, which is made up of 2. 5g of GIBCOBRL Ultra Pure Agarose, cat #15510-019 and add to 100 ml of 1X TBE Buffer (see BUFFERS AND OTHER WORK SOLUTIONS, Section VII). Melt the gel in the microwave on high just until boil, ensure that the agarose has melted completely by gently swirling the flask, and also look for the presence of any undissolved beads of Agarose ; they appear as 'fish eyes'. Place black separators in to either the large or small casting apparatus (Life Technologies- Horizon 58 or Horizon 11-14), and pour gel in once the bottle is just warm, do not pour when still hot, as the excess heat will deform the plastic apparatus. While the gel is still liquid, quickly insert the comb(s) into the gel ; allow gel to set for 20 minutes at room temperature.

B) SAMPLE PREPARATION

cDNA produced by Promega's Access RT-PCR System is run on an agarose gel using Vista Green Nucleic Acid Stain (GE Healthcare, Cat. #RPN5786) as the indicator dye. Vista Green stain binds non-specifically to double strand DNA and will fluoresce when bound and exposed to the UV light produced by the Fluorchem hood. Vista Green is **EXTREMELY LIGHT SENSITIVE**, so always work in low light settings, for example a dark room or under 'candle' light, when preparing Vista Green (see BUFFERS AND OTHER WORK SOLUTIONS), samples **AND** running the gel.

Each sample will be made up to 12µl total volume, consisting of:

- 9µl cDNA amplified product
- 1µl Vista Green

----------**Stop and allow 15 minute incubation**----------

- 2µl of 6XDNA loading buffer (see BUFFERS AND OTHER WORK SOLUTIONS)

Samples must be prepared on ice to prevent cDNA degradation, and should be vortexed to ensure a homogenous mixture to load gel with.

Along with the samples also prepare a 100 base pair DNA ladder (Invitrogen Cat. # 15628-019) as the standard marker, this will be used to confirm approximate product size. The 100 bp ladder is also prepared to 12µl as follows:

- 8µl Nuclease Free Water
- 1µl 100 bp DNA ladder
- 1µl Vista Green

----------**Stop and allow 15-minute incubation**----------

- 2µl of 6XDNA loading buffer

3. LOAD THE GEL

Once the gel has set remove the black separators and fill the reservoir with 1X TBE buffer (see BUFFERS AND OTHER WORK SOLUTIONS), either used or new and buffer must cover gel and electrodes. Now with even pressure pull out the comb, exposing the developed wells within the gel. Load 12µl of sample into desired well using the 20µl pipette.

4. RUNNING THE GEL

Connect gel apparatus to power supply (Amersham Pharmacia Biotech Electrophoresis Power Supply EPS301) using designated leads, ensure correct polarity connections. Run gel at 50mA for approximately 25 minutes in **LOW LIGHT,** again in a dark room or under 'candle' light, until blue indicator band has moved across approximately 1/5 of the gel.

5. DEVELOPING THE GEL

Once finished remove leads and carefully cut off excess gel passed blue indicator bands, which can be re-used. Take remaining gel out and transfer to the Alpha Innotech Corporation Fluorchem Hood, place gel on black base within the hood (white screen may have to be lifted if in place). Open the Fluorchem 8000 program on the desktop, and then click on Acquire. Once the acquire window has opened select Filter Wheel Position 3, and Reflective UV on both the Acquire screen as well as on the Fluorchem hood itself. When gel becomes visible, adjust light, zoom and focus so that bands within the gel are clear and focused. Once adjusted click on the High Sensitivity tab and then on the Acquire button. The image can now be adjusted using the Gamma Settings, such that bands can be lightened and the background darkened. The gel picture can now be saved and/or printed.

VI) QUANTITECT SYBR GREEN RT-PCR KIT PROTOCOL

This is a general use protocol for running Real-Time SYBR Green Reverse Transcription Polymerase Chain Reactions. The process will utilize isolated RNA, which will then be reverse transcribed into cDNA ; this cDNA is then amplified exponentially to yield a large fold product. As the cDNA begins to amplify, it will integrate with the SYBR Green stain present in the Master
Mix SYBR Green that is bound to double strand DNA will emit light, where free SYBR Green will not, this light is then optically read by the Cepheid Smart Cycler II Thermocycler. Using complex calculation the Smart Cycler II software will eliminate and subtract background noise
from optic readings giving a true detection on amplification. By setting a threshold value the software will determine the first cycle in which there is a significant increase in optical activity and hence the first cycle of true DNA amplification, this value is know as the CT value (Cycle Threshold). By comparing the CT values of different samples, one can determine the expression levels of a particular gene of interest. The lower the CT

value the higher the concentration of that gene's mRNA, and therefore the greater the expression in that sample.

This protocol is designed to work with Qiagen's QuantiTect SYBR Green RT-PCR Kit, Cat. # 204243 and the Cepheid Smart Cycler II Thermocycler.

All RNA samples must previously be DNase treated as per the Deoxyribonuclease I protocol to ensure RNA is of pure yield. Samples are kept on ice at all times to prevent degradation or premature enzyme activity.

1. TUBE PREPARATION

All regents are prepared in Master Mixes to ensure homogenous mixtures, and therefore even enzyme activity. One Master Mix is prepared per primer set (forward and reverse primer make one set) ; therefore, if for example COX1 and COX2 are the genes of interest, one Master Mix must be made up for each of the two set of primers. Each Master Mix contains the following reagents add should be prepared in Fisher brand Premium Plus Flat Top Microcentrifuge tubes 0. 5ml, CAT# 05-408-128-

	Volume	Final Concentration
2X QuantiTect SYBR Green-RT-PCR Master Mix-	12. 5µl	1X
Forward Primer-	2µl	1µM
Reverse Primer-	2µl	1µM
QuantiTect RT Mix-	0. 25µl	0. 25µl
Template RNA-	5µl	0. 5µg
RNase-free water-	3. 25µl	
Total =	25µl	

These values are then multiplied for the number of samples in which you wish to look at. For example if you are looking at COX1 and COX2, and want to use three samples, say N1, N2, and N3 then you will end up preparing **SIX** tubes total, each with 25µl -

	Sample N1	N2	N3
Primers			
COX1	X	X	X
COX2	X	X	X

To carry out preparation two Master Mixes will need to be made, one for COX1 and one for COX2, each multiplied by the total number of samples

A) COX1 X the number of samples (plus 10% for pipette error)

2X QuantiTect SYBR Green RT-PCR Master Mix-	12. 5µl X 3. 3 =	41. 25µl
COX1 Forward Primer-	2µl X 3. 3 =	6. 6µlµl
COX1 Reverse Primer-	2µl X 3. 3 =	6. 6µlµl
QuantiTect RT Mix-	0. 25µl X 3. 3 =	0. 825µl
RNase-free water-	3. 25µl X 3. 3 =	10. 725
Total =	20µl X 3. 3 =	66µl

From the 66µl, 10% is extra, so the volume is considered to be 60µl. This COX1 master is then divide into 3 tubes, such that each tube has 20µl of reagents –

	Sample		
	N1	N2	N3
Primers			
COX1	20µl	20µl	20µl

B) COX2 X the number of samples (plus 10% for pipette error)

2X QuantiTect SYBR Green RT-PCR Master Mix-	12. 5µl X 3. 3 =	41. 25µl
COX2 Forward Primer-	2µl X 3. 3 =	6. 6µl
COX2 Reverse Primer-	2µl X 3. 3 =	6. 6µl
QuantiTect RT Mix-	0. 25µl X 3. 3 =	0. 825µl
RNase-free water-	3. 25µl X 3. 3 =	10. 725
Total =	20µl X 3. 3 =	66µl

From the 66µl, 10% is extra, so the volume is considered to be 60µl. This COX2 master is then divide into 3 tubes, such that each tube has 20µl of reagents –

	Sample		
	N1	N2	N3
Primers			
COX1	20µl	20µl	20µl

Once Master Mixes have been evenly distributed to corresponding tubes, DNase treated samples can then be added to each of the tubes. As per DNase treatment protocol add 5µl of treated RNA sample to 20µl of Master Mix, total volume per Qiagen's QuantiTect SYBR Green RT-PCR Kit System protocol is 25µl.

	Sample		
	N1	N2	N3
Primers			
COX1	20µl5µl	20µl5µl	20µl5µl
COX2	20µl5µl	20µl5µl	20µl5µl

2. CEPHEID SMART CYCLER II THERMOCYCLER PROTOCOL

Once all samples are made up, load the 25µl into the specially designed Cepheid Smart Cycler reaction tubes, Cat #11-400-3. Load tubes using filter barrier tips, place the sample mixture in to the top portion of the tube, a brief centrifuge with the specially fitted rotor (Located beside the Real Time PCR machine in microbiology) will later bring the mixture in to the optic window located in the base of the tube. Place all loaded tubes into the chilled carrier block, always transport tubes in block, and store block at -20°C when not in use.

The Smart Cycler block contains sixteen individual modules, known as ICORE® (Intelligent Cooling/Heating Optical Reaction) modules, each will perform individual from one another to ensure very accurate monitoring of the designed protocol. In addition to amplification readings, the software will also detect the temperature of all sites individually ; as well perform a final melt curve to verify product produced.

SETUP-

Turn on Smart Cycler block ; switch is located on back top of block, next double click on the Smart Cycler icon located on the desktop. Once program has loaded you will be prompted for a user name and password, enter the following- User: **hns** password: **hns**. Once main screen has opened click on **Define Protocols** icon.

Within the protocol window either verify the protocol already saved is sufficient or create a new on via the **New Protocol** button if required. If creating a new protocol enter a unique name for it when prompted. Now enter the desired temperatures and times for each of required stages, also enter the number of cycles for each stage, optics should be on during the extension step and a melt curve should be performed at the end to verify product produced. Finally click the **Save Protocol** button

For most of our RT-PCR reactions the pre-made **Jamie RT-PCR** thermocycle protocol will be sufficient. Select it from the given list to view the set stages for this protocol, Note optics are turned on during the extension step, therefore all readings by the software are taken then.

Once the protocol of interest is entered click on the **Define Graphs** icon. Within the define graph window either verify the required graphs are already saved or create a new one via the **New Graph** button if required, note for our studies all graphs parameters are already saved. To view the specifics of each graph select it from the given list, we will be utilizing the following- SYBR Green 2nd der, SYBR Green, Temperature, and Melt graphs.

Now that the protocol and graphs have all been defined and saved we can now officially set up the run as follows-

Load all centrifuged sample tubes into the Smart Cycler block, tubes should make a small click when inserted fully into the ICORE® modules. Now click on the **Create Run** icon, and enter a unique run name in the **Run Name** box.

Next select SYBR Gr from the **Dye Set** box located on the left, followed by the **Add/Remove** icon. Once the **Add/Remove** window has opened select the protocols stored in the database, followed by the number of sites that you will be running, in other words the number of samples loaded into the block.

Use the arrow icons to select the number of desired sites and then click **OK** when complete. Now back on the main screen enter the Sample IDs into the correct sites, such that they correspond to the samples in the Smart Cycler block.

The setup is now complete- click the **Start Run** button to begin the protocol.
Once the run has started select the Analysis Settings Tab from either the top or bottom window, both display the identical information, and change the **Manual Thres Fluor Units** to 10 (**any** value can be used, **but** the **same** value must be used for **all** samples in that study), then select the **Update Analysis** button at bottom of the screen.

While the run is cycling you can monitor the temperature and optical data in real time by selecting the corresponding tabs, note that no optic data will be displayed until first reading during the extension stage. Once optic readings are being recorded select the **SYBR Green** tab from under **Views** to view the real time amplification of your sample.

Near the end of the **Jamie RT-PCR** protocol the Smart Cycle software will perform a melt curve to determine the melting temperatures of the products produced, these values can then be used to verify that the product is as desired. Select **Melt** from the **Views** column.

Once the protocol is complete the results of the run can be viewed by selecting **Results Table** from under **Views,** all CT values and melting temperatures will be displayed. Results from other pervious runs can also be viewed or compared to any other run by using the corresponding buttons located at the bottom of the screen. Results data can also be printed directly or exported to an excel file, to print any results and/or graphs, right click on the graph and then select the print option, to export the data click on the **Export** button at bottom of screen and then deselect the **Optics** box, then click **OK**. All exported data is saved to the Smart Cycler folder on the desktop, under the Export folder.

VII) BUFFERS AND OTHER SOLUTIONS

1. 50X TAE BUFFER - MAKES 1 LITRE (Use a capped bottle)

- 242g TRIS Base
- 100ml 0. 5M EDTA pH 8. 0
- 57. 1ml Glacial Acetic Acid
- Volume up to 1 litre with Deionized water
- CLOSE AND AUTOCLAVE IT

Dilute 50X TAE BUFFER to work solution of 1X TAE BUFFER as needed (20ml of 50X TAE BUFFER in 980ml Deionized water)

2. 5X TBE BUFFER – MAKES 1 LITER (Use a capped bottle)

- 54g TRIS Base
- 27. 5g Boric Acid
- 20ml . 5M EDTA pH 8. 0
- Volume up to 1 litre with Deionized water
- CLOSE AND AUTOCLAVE IT

Dilute 5X TBE BUFFER to work solution of 1X TBE BUFFER as needed (200ml of 5X TBE BUFFER in 800ml Deionized water)

3. 6X DNA GEL LOADING BUFFER (Store at 4°C)

- Prepared in 15ml Conical Tube
- 25mg Bromophenol Blue
- 25mg Xylene Cyanol
- 3 ml Glycerol
- Volume up to 10ml with Deionized water

4. 4X RNA LOADING BUFFER (Store at 4°C)

- Prepared in 1. 5 Micro centrifuge tube
- 337µl Gibco Formamide
- 108µl Fisher Formaldehyde
- 15µl MOPS 1M PH 7. 4
- 1. 5µl . 5M EDTA pH 8. 0
- 5µl 10% SDS
- 33. 5µl Glycerol
- 2. 5µl 10% Bromophenol Blue
- 2. 5µl 10% Xylene Cyanol

5. 1% AGAROSE GEL FOR RNA

- 1g Agarose
- 100ml 1X TAE Buffer

6. 2. 5% AGAROSE GEL FOR DNA

- 2. 5g Agarose
- 100ml 1X TBE Buffer

7. VISTA GREEN WORK SOLUTION

IS LIGHT SENSITIVE AND MUST BE USED IN LOW LIGHT SETTINGS

- 0. 2µl Vista Green
- 100µl 1X TBE
- Vortex

STEPS FOR WESTERN IMMUNOBLOTTING PROCEDURE FOR PROTEIN ESTIMATION

Lyophilization of Kidneys

The left kidney from each rat was lyophilized in preparation for western immunoblotting. The left kidney was removed from the -80°C freezer and the frozen kidney was cut up into small pieces and placed into a pre-weighed 15 mL disposable sterile centrifuge tube (Fisher Scientific, cat no 05-539-5, Nepean, Ontario) topped with a lid with holes. The tube containing the cut up kidney was weighed again and the initial weight of the frozen kidney was recorded. Tubes were then immersed in liquid nitrogen and placed in a pre-cooled (-40°C) lyophilizer (Labconco, Model No 4451 F, Kansas City, Missouri) so that samples could begin drying. All seals were greased so that a vacuum of less than 10 microns of mercury (Hg) was maintained. The freeze dryer was checked periodically to ensure the machine did not lose its seal. The tubes were removed from the freeze dryer and weighed every few hours or after an overnight drying period. When two consecutive equal tube weights were obtained, the freeze drying process was complete. If the weight was not equal to the last weight obtained, the tube was placed back into liquid nitrogen and was returned to the freeze dryer to continue drying. The final dry kidney weight was recorded. A spatula was used to pulverize the dried kidneys and a lid without holes was used to replace the porous lid. Samples were then stored at -80°C.

Homogenization of Kidneys

Cytosolic and particulate buffers were prepared by first mixing all ingredients and then adding 5 M sodium hydroxide (NaOH salt, Fisher Scientific, s318-500, Napean, Ontario) to the solution to obtain a final pH of 7. 2-7. 4. Cytosolic buffer (2 mL or 100 volumes) was added to 20 mg of lyophilized kidney tissue in a glass, round-bottomed tube submerged on ice. Kidney tissue was homogenized for 2 x 30 seconds with a Polytron homogenizer (Brinkmann Instruments, Type PT 10 20 350D, Rexdale, Ontario) on a speed control setting of 5. Tubes were kept on ice
at all times. Homogenate was poured into ultracentrifuge tubes and balanced before being inserted into a cold rotor (Beckman Coulter, Inc. , model no 50. 3TI, Fullerton, California) and placed in the pre-cooled (4°C) ultracentrifuge (Beckman, model no L8-80). Samples were spun at 100,000 x g for 35 minutes. This precipitated the particulate fraction while the cytosolic fraction remained in the supernatant. A transfer pipette was used to draw off the supernatant and this cytosolic fraction was placed into pre-labeled 2 mL microcentrifuge tubes (Fisher Scientific, cat no 05-408-141, Napean, Ontario) and stored at -80°C. The pellet was re-suspended in 0. 4 mL (20 volumes) of particulate homogenization buffer. The tube was vortexed with a glass rod placed in it to help disperse the pellet in the buffer. After sitting on ice for 10 minutes, it was vortexed a second time. Tubes were once again balanced and spun at 100,000 x g for 35 minutes. The particulate fraction was now suspended in the supernatant and was drawn off and placed into a pre-labeled 2 mL microcentrifuge tube (Fisher Scientific). The samples were stored at –80°C.

Total Protein Determination

Total protein was determined in cytosolic and particulate fractions using the Bradford Method established in 1976. In this method, protein forms a complex with the dye brilliant blue G. The absorption maximum of the dye then shifts from 465 to 595 nm. The amount of absorption is proportional to the total amount of protein present in the sample. A 96-well microplate was used, and wells were identified as blank, standard or sample. Standards were made ranging in concentration from 0. 0625 mg/mL to 1 mg/mL using a 2 mg/mL bovine serum albumin (BSA) stock solution (Sigma, P0834, Oakville, Ontario). Kidney homogenates were diluted 20X with deionized water, and 10 μL of blank, standard or diluted sample was added to identified wells in triplicate. Bradford reagent (200 μL, Sigma, B6916), was added to each well using a multi-channel Eppendorf pipette. The plate was covered with a box and mixed on an orbital shaker (Fisher Scientific, model no 361 Nepean, Ontario) for 15 minutes at room temperature. The plate was read at a wavelength of 595 nm using a microplate reader (Molecular Devices Corporation, SpectraMax 340, Sunnyville, California). SOFTmax Pro software was used to calculate total protein concentrations in the samples. Mean values were multiplied by 20 to obtain the total protein concentration in mg/mL.

Protein Separation by Sodium Dodecyl Sulfate Polyacrylamide Gel Electrophoresis (SDS-PAGE)

As has been previously described (Aukema et al. , 2002), one-dimensional sodium dodecyl sulfate (SDS) gel electrophoresis was used to separate proteins of interest, namely cPLA2, COX-1 and COX-2. In this method, protein separation occurs as proteins migrate in an electrical field through a porous gel. Proteins will migrate down to different levels of the gel depending on their size, shape and charge. The pore size of the gel is also an important determinant in how the proteins will migrate.

Two glass plates were cleaned with methanol and placed with their cleaned sides together, with spacers separating the 2 plates. The plates were lined up and screwed into place on a gel module (Amersham Biosciences, part of Hoefer miniVE vertical electrophoresis system, 80-6418-77, Buckinghamshire, England). Deionized water was poured in between the 2 plates to ensure there were no leaks. The water was then poured out and a 7. 5% separating gel solution containing 2670 μL of deionized water, 1250 μL of 1. 5 M tris (hydroxymethyl) aminomethane-hydrochloric acid (tris-HCL) pH 8. 8 (tris base, Fisher Scientific, BP154-1, Napean, Ontario and HCL, Fisher Scientific, A144 500), 50 μL of 10% (w/v) SDS (Fisher Scientific, BP166-100), 1000 μL of 40% bis-acrylamide (Fisher Scientific, BP1408-1), 25 μL of 10% (w/v) ammonium persulfate (APS, Fisher Scientific, BP179-25) and 5 μL of N,N,N',N',-tetramethylethylenediamine (TEMED, Fisher Scientific, BP150-20) was made and added to the space in between the glass plates using a Pasteur pipette until it reached about ¾ of the way up the plates. Deionized water was then carefully layered on top of the separating gel, and the gel was left to polymerize for 30 minutes. The water was poured off and a 4% stacking gel was then prepared and added on top of the separating gel once again using a Pasteur pipette. The stacking gel solution contained 1625 μL of deionized water, 625 μL of 0. 5 M tris-HCL pH 6. 8, 25 μL of 10% (w/v) SDS, 250 μL of 40% bis-acrylamide, 12. 5 μL of 10% APS and 2. 5 μL of TEMED. A comb was inserted into the stacking gel in order to form lanes in which to load the protein samples. The gel was left to polymerize for 45 minutes.

The bottom of the gel module was then unclipped and placed in a chamber filled with used running buffer. Running buffer could be re-used approximately 10 times. The running buffer was made as 10X running buffer and contained 29. 0 g of tris base, 144. 0 g glycine (Fisher Scientific, BP381-1), 10. 0 g of SDS and was made up to 1 L with deionized water. This was then diluted 10X with deionized water before use. New running buffer was poured into the upper compartment of the gel module and the comb was removed. The wells were washed with 100 µL of new running buffer using an Eppendorf pipette.

The amounts of total protein to be loaded for cytosolic cPLA2, particulate cPLA2 and COX-2 (14 µg of each) were based on dose-response curves (see Figures 2 through 4, respectively) and previous data from our lab (Warford, 2003). A slightly higher amount of COX-1 (20 µg) needed to be loaded as the kidney homogenates seemed to have low levels of this particular protein. Volumes of protein samples to be loaded were calculated based on the total kidney protein concentration determined by the Bradford method. The equation used was as follows for cytosolic cPLA2, particulate cPLA2 and COX-2 to load 14 µg of protein: 14 µL/protein concentration (µg/µL) = volume of sample (µL) and 7 µL - volume of sample (µL) = volume of deionized water (µL). Seven µL of Laemmli 2X sample buffer was added to the protein samples. The 2X sample buffer contained 3800 µL of deionized water, 1000 µL of 0. 5 M tris-HCL pH 6. 8 (tris base, Fisher Scientific, BP154-1, Napean, Ontario and HCL, Fisher Scientific, A144 500), 800 µL of glycerol (Fisher Scientific, BP229-1), 1600 µL of 10% (w/v) SDS (Fisher Scientific, BP166-100), 400 µL of 2-mercaptoethanol (Fisher Scientific, BP176-100) and 400 µL of 1% (w/v) bromophenol blue (Sigma, B-8026, Oakville, Ontario). A total of 20 µg of protein was loaded for COX-1. In order to calculate the amount of sample needed to load 20 µg of protein, a similar calculation to the one above was carried out. When the total protein concentration was less than 2. 0 mg/mL, 6X sample buffer was used. Samples were placed on a heating block (Fisher Scientific, 11-718-2) at 90-100°C for 5 minutes to denature proteins. Samples were cooled on ice for 2 minutes, centrifuged (Eppendorf, Model No 5417C, Hamburg, Germany) at 5000 x g for 1 minute and placed back on ice before being loaded onto the gel.

The protein samples were loaded into the lanes of each gel along with a benchmark pre-stained protein ladder (Invitrogen, cat no 10748-010, Burlington, Ontario) and a standard run in duplicate. The standard was prepared by combining 50 µL of particulate sample from rats in the study (4 rats from each group). The proteins migrated in running buffer in an electrophoretic chamber (Amersham Biosciences, part of Hoefer miniVE vertical electrophoresis system, Amersham Biosciences, 80-6418-77, Buckinghamshire, England) at 200V at room temperature until the dye front just came off the gel (approximately 1 hour and 50 minutes).

Western Immunoblotting

Before the dye front ran off the gels, a hydrophobic polyvinylidene fluoride (PVDF) membrane (Amersham Biosciences, Hybond-P RPN303F, Buckinghamshire, England) was cut to the proper size and labeled. The lower left hand corner of the membrane was cut to indicate the first lane. The membrane was moistened with methanol (Fisher Scientific, A452-4, Napean, Ontario) for 10 seconds and then placed in deionized water on an orbital shaker (Fisher Scientific, model no 361) set at 90 revolutions per minute

(rpm) for 7-8 minutes. The water was replaced with transfer buffer and the membrane was put back on the orbital shaker until the gel was ready for transfer. The transfer buffer was made as 10X transfer buffer and contained 29. 0 g tris base (Fisher Scientific, BP154-1), 144. 0 g glycine (Fisher Scientific, BP381-1), and was made up to 1 L with deionized water. Before use, 100 mL of 10X transfer buffer was mixed with 200 mL methanol (Fisher Scientific, A452-4) and 700 mL deionized water. When the gel was finished running, the gel module was removed from the chamber and the glass plates were separated in order to access the gel. The stacking gel was cut off using the spacer and a small amount was cut off from the bottom of the gel. The bottom corner also was cut off to indicate lane number 1. The gel was then equilibrated in transfer buffer for 5-10 minutes.

The gel was then placed in a blot module (Amersham Biosciences, 80-6418-96, Buckinghamshire, England) against the PVDF membrane, in between two pieces of filter paper with the cut corners matching up and oriented in the upper right hand corner of the apparatus. A sponge was placed on one side of the gel/membrane, and enough sponges were placed on the other side to form a tight fit in the "sandwich". Everything was kept wet with used transfer buffer. Transfer buffer could be reused up to 10 times. The transfer apparatus was placed in a chamber filled with used transfer buffer, and new transfer buffer was added to the upper compartment of the transfer apparatus. The apparatus was connected to the power unit and transferred in the fridge (4°C) for 2 hours at 375 milliamps (mA).

After the transfer, the membrane was placed on a piece of filter paper and cut horizontally with a clean scalpel in between the 2 proteins of interest, using the benchmark ladder as a guide. This was only done if the membrane needed to be blotted with 2 different primary antibodies. The membrane was then "blocked" in order to help minimize non-specific binding of the antibodies. The membrane was placed in a dish and lines from the benchmark ladder were marked with pen to ensure that they remained visible throughout the rest of the immunoblotting procedure. The membrane was then placed on a rocker (Boekel Scientific, rocker II model 260350, Feasterville, Pennsylvania) for 1 hour in a 5% skim milk solution (0. 5 g skim milk powder in 10 mL 0. 1% tris base solution (TBS)/Tween). The TBS/Tween was made as 10X TBS/Tween from 24. 2 g tris base (Fisher Scientific, BP154-1, Napean, Ontario) and 80 g sodium chloride (NaCl, Fisher Scientific, BP358-212). This was made up to 800 mL with deionized water. The pH was then adjusted to 7. 6 using HCl. Ten mL of Tween (Fisher Scientific, BP337-500) was then added to make a 1% Tween solution. This solution was then diluted 10X with deionized water to give a final Tween concentration of 0. 1%. After the 1 hour of blocking, the skim milk solution was poured off the membrane so it could be covered with the primary antibody solution.

The primary antibody was prepared in 2% skim milk solution (0. 2 g skim milk powder in 10 mL TBS/Tween). The primary antibody concentration was 1:250 for all proteins, namely cPLA2 [Santa Cruz Biotechnology, N-216, anti-human rabbit polyclonal immunoglobulin G (IgG), cat no sc-438, Santa Cruz, California, USA], COX-1 (Cayman Chemical Company, anti-ovine mouse monoclonal antibody, cat no 160110, Ann Arbor, Michigan) and COX-2 (Cayman Chemical Company, anti-mouse rabbit polyclonal antibody, cat no 160106). The primary antibody solution was poured onto the membrane and the membrane was covered and placed on a rocker (Sanyo GallenKamp, cat no IH-

370, APP IB1684, Loughborough, Leicestershire, England) in the fridge at 4°C overnight. The next morning the primary antibody was removed and saved in the -20°C freezer. It could be reused up to 5 times. The membrane was then washed 3 times in TBS/Tween by being placed on the orbital shaker (Fisher Scientific, Model No 361, Napean, Ontario) at 90 rpm for a specific length of time that depended on the protein of interest. It was washed for 3 x 5 minutes (total 15 minutes) for cytosolic and particulate cPLA2, and for 3 x 10 minutes (total 30 minutes) for COX-1 and COX-2. The secondary antibody was then prepared in TBS/Tween and added to the membrane. For cytosolic and particulate cPLA2, as well as for COX-2, anti-rabbit IgG was used at a concentration of 1:20,000 (Sigma, cat no A-0545). For COX-1, anti-mouse IgG was used at a concentration of 1:20,000 (Sigma, cat no A-3682). The membrane containing the secondary antibody solution was then placed on a rocker (Boekel Scientific, rocker II model 260350, Feasterville, Pennsylvania) for 1 hour at room temperature. The membrane was washed a second time with TBS/Tween on the orbital shaker (Fisher Scientific, Model No 361) set at 90 rpm. For each protein of interest, the length of time for the second wash was the same as for the first wash. The membrane was then ready to be developed.

Two chemiluminescent substrates (Fisher Scientific, ChemiGlow cat no 2900811, Napean Ontario) were mixed with deionized water in a 1:1:4 ratio 4-5 minutes before it was needed. The membrane was then placed on a piece of plastic wrap and the chemiluminescent mixture was evenly distributed over the entire membrane using a Pasteur pipette. This was left to sit for 5 minutes. The liquid was then drained off and the membrane placed on the top portion of a new piece of plastic wrap. The bottom half of the wrap was then carefully folded over the membrane, so as not to trap any air bubbles. The excess plastic wrap was cut using a scalpel and any air bubbles were removed. The membrane was developed in an imaging system (Alpha Innotech, San Leandro, California) and analyzed using appropriate computer software (AlphaEase FC, version 3. 1. 2 and 4. 0. 0).

The integrated density volume (IDV) was calculated and used as a measure of the intensity of the protein band in pixels on the computer screen. In order to obtain the IDV, an object box was placed around the protein band, large enough to encompass the entire band, but no larger than necessary. A background box was then placed underneath the band and as close to the band as possible, to get a representative section of the background staining surrounding the protein band. These 2 boxes were then linked together so that the background pixels could be subtracted from the protein band pixels, in order to obtain the IDV. The IDV is representative of the amount of the particular protein of interest that was present in the sample. The IDV of the protein sample was then divided by the average IDV of the 2 standards in order to control for gel to gel variation. The IDV was expressed in arbitrary units.

KIDNEY FATTY ACID ANALYSIS (FREEZE-DRIED)

Entire procedure after weighing out the kidney is under a fumehood.

Extraction using a modified Folch method.
Principle: This procedure uses a simple mono-phasic alcoholic solvent system, namely chloroform-methanol-water which rapidly and efficiently extracts lipids. The extract is then diluted with one volume each of chloroform and water to form a 2-phased system, chloform and methanol-water.
Any water-soluble contaminants are thus readily partitioned into the methanol-water phase, leaving the lipids relatively contaminant-free in the chloroform phase.

1. Weigh about 0.020g of lyophilized, ground kidney tissue into a 10ml (15X 100mm) test tube and record exact weight in lab book. (rinse spatula with methanol between samples and wear gloves).
2. Add 2.5 ml of chloroform:methanol (2:1) containing 0.01% BHT to the tube making sure to wash down the sides of the tube.
3. Add 100ul of C17 std (4 mg/ml heptadecanoic acid in chloroform) just above the level of the liquid (can reduce by half and still have enough)
4. Add 0.25ml of deionized water.
5. Homogenize with toothed polytron set between 4 and 5 for 20 seconds. Check rotor for trapped tissue, remove and re-immerse tissue if necessary. Then homogenize for another 25 seconds at same setting.
6. Cover tube and let sit while other samples are being extracted. Clean homogenizer between samples by homogenizing with fresh solvent for about 20 sec and drying with a kimwipe.
7. Add 0.8ml of methanol, cap with plastic caps and vortex for 15sec.
8. Ensure caps are tightly on and centrifuge for 10-15 minutes at 1500rpm in GS-6 centrifuge. (liquid in tube is monophasic with sediments at the very bottom of tube)
9. Pipet solvent layer with a Pasteur glass pipet into a clean glass 10ml screw-top tube (15X 100mm).
10. Add 1.5 ml chloroform and 1.2ml of 0.73% Nacl solution, cap and vortex for 30sec, then centrifuge for about 5 minutes as before.
11. Remove the top layer (completely) and discard into a waste bucket.
12. Rinse down sides of the tube with 1 ml of TUP (chloroform:methanol:water 3:48:47) and then remove and discard top layer. Repeat a second time. There is no need to re-centrifuge as long as bottom layer has not been disturbed.
13. Clean N_2 evaporator needles in water bath with alcohol. Using a Pasteur pipet, transfer the bottom layer to an 8 ml (13X100mm) screw-top tube, making sure that no residual top layer is included. Now, either:
    a) flush with nitrogen and store in freezer for later drying or
    b) Evaporate to dryness under nitrogen in a 30C water bath. Immediately upon removal from water bath, add 0.6ml of toluene. Either cap immediately and store in freezer for later methylation or proceed directly to methylation procedure. **Never leave samples sitting dry at any time**

or lipid will oxidize. Also if storing after addition of toluene, cap immediately to retain nitrogen atmosphere.

Methylation

Principle: Free fatty acids are esterified by heating them with a large excess of anhydrous methanol in the presence of an acid catalyst. The presence of water will prevent the reaction from going to completion.

$$RCOOR' + CH_3OH \xleftrightarrow{H+} RCOOCH_3 + R'\text{-}OH$$

$$RCOOH + CH_3OH \xleftrightarrow{H+} RCOOCH_3 + H_20$$

1. Add 1.2 ml of methanolic HCl to tubes (prior to this, ensure that toluene has been evaporated completely in N2 evaporator), cap tightly and vortex for 30 seconds.
2. Place tubes in a rack in a pre-heated 80C oven for 2 hours.
3. Remove rack from oven and cool for 10-15 minutes.
4. Add 1ml of deionized water to the tubes, cap and vortex for 15 sec. Centrifuge for 15 mins as before.
5. Transfer top layer to clean 8 ml tube.
6. To the bottom layer, add 1 ml of petroleum ether, cap and vortex for 15 sec. Centrifuge for 5 min.
7. Transfer top layer to the previously removed top layer.
8. To the combined layers, add 2ml of de-ionized water, cap and vortex for 15 secs . Centrifuge for 15 min as before.
9. Clean needles in drybath. Transfer the top layer into a conical GC vial making sure that none of the bottom layer is included and dry under nitrogen in a dry bath.
10. Once the solvent has evaporated, immediately add 100ul of hexane to tubes and cap. Analyze immediately or store in solvent freezer until GC analysis.

GC analysis

Principle: Gas chromatography involves a sample being vaporized and injected onto the head of the chromatographic column. The sample is transported through the column by the flow of inert, gaseous mobile phase. The column itself contains a liquid stationary phase which is adsorbed onto the surface of an inert solid.

1. Run samples using the DB225 method.
2. Set GC for a split ratio of 10 and inject 0.8ul.
3. C17 counts should be about 1,000,000. Major peaks, C16:0, C18:0, C18:1, C18:2, C20:4.

APPENDIX B: SUPPLEMENTARY DATA TABLES FOR FIGURES

Chapter 3:

Table B-1. Renal histologic and immunohistochemical markers of renal injury in cystic (cy/+) Han:SPRD-cy rats fed FO and CO in the maternal and/or post-weaning diets. **(Figures 3-1, 3-2, 3-3, 3-4, 3-5, 3-6).**

Chapter 5:

Table B-2 Relative renal COX-2 protein (A) and mRNA (B) levels in *pcy* mice given low (7g fat/100g diet) and high (20g fat/100g diet) corn oil (CO), flax oil (FO) and DHASCO (DO) diets for 8 weeks. (Figure 5-1). Values are means (as percentage of Low CO) + SEM. Means with different alphabets denote significant differences ($p<0.05$) **(Figure 5-1 A and B).**

Table B-3. Renal COX-1 and COX-2 protein expression in normal (+/+, A) and in diseased (Cy/+, B) Han:SPRD-*cy* rats given low (5g fat/100g diet) and high (20g fat/100g diet) cottonseed oil (CSO) and menhaden oil (MO) diets for 8 weeks. **(Figure 5-2 A and B, Figure 5-3 A and B).**

Table B-4. Renal histologic and immunohistochemical parameters in cystic rats given NS398 for 7 weeks. **(Figures 6-1, 6-2A and B, 6-3A and B, 6-4A and B, 6-5A and B)**

Table B-5 Renal TXB_2/PGE_2, TXB_2/6-ketoPGF$_{1a}$ and 6-keto-PGF$_{1a}$/PGE_2 ratios in Han:SPRD-*cy* rats given NS398 for 7 weeks **(Figures 6-6A, B and C)**

Table B-1. Renal histologic and immunohistochemical markers of renal injury in cystic (cy/+) Han:SPRD-cy rats fed FO and CO in the maternal and/or post-weaning diets. (Figures 3-1, 3-2, 3-3, 3-4, 3-5, 3-6)

Parameter	Maternal CO		Maternal FO		Pooled	Effects
	Wean CO	Wean FO	Wean CO	Wean FO	SEM	
Renal cell proliferation (number of PCNA+ cells/ mm^2 tissue)	213.7^{a}	189.2^{b}	167.8^{b}	179.5^{b}	10.3	Mat Diet (P= 0.0155), Interaction(P=0.0291)
Cyst area (mL/Kg body wt)	5.59^{ac}	6.25^{a}	5.30^{bc}	4.50^{b}	0.3181	Mat diet (P=0.0023), Interaction (P=0.0255)
Renal oxidant injury(% oxidized LDL staining/mm^2 tissue)	0.139^{a}	0.076^{c}	0.107^{b}	0.079^{c}	0.009	Wean diet (P<0.0001), Interaction (P=0.0816)
Renal inflammation (number of macrophages /mm^2 tissue)	183.5	148.4	177.2	137.04	10.3	Wean diet (P=0.0007)
Renal interstitial fibrosis (fraction of tissue area)	0.029	0.031	0.027	0.022	0.002	Maternal Diet (P=0.0392), Interaction (P=0.0378)
Mean Glomerular Volume ($\mu m^3 \times 10^6$)	3.55	3.59	3.54	2.78	0.19	Interaction (P=0.0160)

Values not sharing a symbol are significantly different.

Table B-2 Relative renal COX-2 protein and mRNA levels in *pcy* mice given low (7g fat/100g diet) and high (20g fat/100g diet) corn oil (CO), flax oil (FO) and DHASCO (DO) diets for 8 weeks. (Figure 5-1 A and B).

Enzyme	Low fat			High Fat			Significant Effects
	CO	FO	DO	CO	FO	DO	
COX-2 mRNA	100±13.1[a]	105±13.1[a]	124±13.1[a]	82±14[a]	98±14[a]	246±14[b]	Oil (P<0.0001), Level x Oil (P=0.0025)
COX-2 Protein	100±35.4[a]	62.3±15.6[a]	142.4±25.5[b]	75.1±21.5[a]	85.5±14.3[a]	345.5±82.5[c]	Oil (P=0.0139), Level (P=0.0690)

Values are means (as percentage of Low CO) + SEM. Means with different alphabets denote significant differences ($p<0.05$).

Table B-3. Relative renal COX-1 and COX-2 protein levels in normal (A) and in diseased (B) Han:SPRD-cy rats given low (5g fat/100g diet) and high (20g fat/100g diet) cottonseed oil (CSO) and menhaden oil (MO) diets. (Figure 5-2 A and B)

(A) Normal Rats

	CSO		MO		Significant Effect
	High	Low	High	Low	
COX-1 protein	108.2±17.5	100±15.6	104.5±17.5	104.8±14.3	None
COX-2 protein	43.0±13.6	100±15.0	46.9±15.0	101.1±13.6	Level (P=0.0001)

Values are means (as percentage of Low CSO) + SEM.

(B) Diseased Rats

	CSO		MO		Significant Effect
	High	Low	High	Low	
COX-1 protein	130.1±11.2	100±10.2	134.6±11.2	99.9±11.2	Level P=0.0089
COX-2 protein	3.9±5.6	100±5.6	18.3±5.6	123.7±5.6	Type P=0.0028 , Level P<0.0001

Values are means (as percentage of Low CSO) + SEM.

Table B-4. . Renal histologic and immunohistochemical parameters in cystic rats given NS398 for 7 weeks. (Figures 6-1, 6-2A and B, 6-3A and B, 6-4A and B, 6-5A and B)

Parameter	Control PKD N=12	NS398 PKD N=16	Pooled SEM	Effects P value
Macrophage count (cells/high power field)	36.01	24.10	1.69	Drug P=0.0003
Renal cell proliferation (cells/high power field)	35.66	21.96	2.06	Drug P=0.0006
Cyst Volume (mL/Kg body weight)	6.74	5.55	0.33	Drug P=0.0226
Oxidized LDL (fraction of tissue area)	0.029	0.012	0.004	Drug P=0.0064
Renal Interstitial fibrosis (fraction of tissue area)	0.036	0.012	0.002	Drug P<0.0001

Table B-5 Renal TXB2/PGE2, TXB2/6-ketoPGF1a and 6-keto-PGF1a/PGE2 ratios in Han:SPRD-cy rats given NS398 for 7 weeks (Figures 6-6A, B and C)

	Control		NS398		Effects
	+/+	*Cy*/+	+/+	*Cy*/+	P value
	n = 9	*n* = 9	*n* = 8	*n* = 9	
TXB_2/PGE_2					
0 min	0.165	0.319	0.136	0.320	Genotype(p<0.0001)
60 min	0.230	1.115	0.200	0.953	Genotype(p<0.0001)
COX	0.277	1.452	0.270	1.615	Genotype(p<0.0001)
COX-2	0.300	1.583	0.300	1.591	Genotype(p<0.0001)
TXB_2/6-keto-PGF_{1a}					
0 min	0.204	0.317	0.226	0.298	Genotype (p=0.0655)
60 min	0.124	0.182	0.141	0.160	Genotype (p=0.0690)
COX	0.155	0.217	0.175	0.212	Genotype (p=.0728)
COX-2	0.137	0.218	0.171	0.215	Genotype (p=0.0277)
6-ketoPGF$_{1a}$/PGE$_2$					
0 min	0.830	1.350	0.609	1.300	Genotype (p<0.0001)
60 min	2.020	6.787	1.468	6.094	Genotype (p<0.0001)

COX	1.860	7.786	1.680	7.847	Genotype ($p<0.0001$)
COX-2	2.070	7.828	1.920	7.892	Genotype ($p<0.0001$)

APPENDIX C: ADDITIONAL DATA COLLECTED FOR CHAPTERS 2-6

Chapter 5:

Table C-1 Renal $cPLA_2$ mRNA and protein expression in pcy mice fed low (5%) and high (20%) fat corn oil (CO), flax oil (FO) and DHASCO (DO) diets for 8 weeks.

Table C-2. Renal $cPLA_2$ protein expression in normal and diseased Han:SPRD-cy rats fed high (20%) and low (5%) cottonseed oil (CSO) and menhaden oil (MO) diets for 8 weeks.

Table C-3. Renal $cPLA_2$ mRNA levels in normal (+/+) and diseased (Cy/+) Han:SPRD-cy rats fed corn oil (CO) and flax oil (FO) diets for 12 weeks.

Table C-4. Renal $cPLA_2$ protein levels in diseased (Cy/+) Han:SPRD-cy rats fed corn oil (CO) and flax oil (FO) diets for 12 weeks.

Chapter 6:

Table C-5. Heart and left ventricular weights and hemodynamic measurements in normal (+/+) and diseased (Cy/+) Han:SPRD-cy rats given NS398 for 7 weeks.

Table C-1 Renal $cPLA_2$ mRNA and protein expression in *pcy* mice fed low (5%) and high (20%) fat corn oil (CO), flax oil (FO) and DHASCO (DO) diets for 8 weeks.

Enzyme	Low fat			High Fat			Significant Effects
	CO	FO	DO	CO	FO	DO	
$cPLA_2$ mRNA	100±18.0	96±18.0	95±18.0	81±19.3	87±19.3	164±19.3	None
$cPLA_2$ Protein	100±27.4	139.8±49.3	178.9±52.5	187.1±77	147.4±36.1	157.1±43	None

Values are means (as percentage of low CO) ± SEM.

Table C-2. Renal cPLA2 protein expression in normal and diseased Han:SPRD-cy rats fed high (20%) and low (5%) cottonseed oil (CSO) and menhaden oil (MO) diets for 8 weeks.

	CSO				MO				Significant Effects
	+/+		Cy/+		+/+		Cy/+		
	High	Low	High	Low	High	Low	High	Low	
$cPLA_2$	82.9 ±14.8	100 ±16.2	113 ±18.1	150.4 ±14.8	69.9 ±18.1	113.4 ±14.8	113.2 ±14.8	160.4 ±14.8	Genotype (P=0.0005), Level (P=0.0026)

Values are means (as percentage of low CSO) ± SEM.

Table C-3 . Renal $cPLA_2$ mRNA levels in normal (+/+) and diseased (Cy/+) Han:SPRD-*cy* rats fed corn oil (CO) and flax oil (FO) diets for 12 weeks.

Enzyme	CO		FO		Significant
	+/+	Cy/+	+/+	Cy/+	Effects
$cPLA_2$	100± 41.8	50± 14.0	97± 27.0	56± 13.1	Genotype (P=0.0162)

Values are means (as percentage of normal low CO) ± SEM.

Table C-4. Renal $cPLA_2$ protein levels in diseased (Cy/+) Han:SPRD-*cy* rats fed corn oil (CO) and flax oil (FO) diets for 12 weeks.

Enzyme	CO Cy/+	FO Cy/+	Significant Effects
$cPLA_2$	100±7.8	87.6±8.2	None

Values are means (as percentage of low CO) ± SEM.

Table C-5. Heart and left ventricular weights and hemodynamic measurements in normal (+/+) and diseased (Cy/+) Han:SPRD-*cy* rats given NS398 for 7 weeks.

Parameter	Control		NS398		Pooled SEM	Effects P value
	+/+ N=12	Cy/+ N=10	+/+ N=7	Cy/+ N=15		
Heart Weight (g/100g body weight)	0.35[b]	0.41[a]	0.36[b]	0.40[a]	0.0051	Genotype (P>0.0001) Interaction (P=0.0593)
Left Ventricular Weight (g/100g body weight)	0.24[a]	0.29[b]	0.24[a]	0.28[c]	0.0032	Genotype (P>0.0001) Interaction (P=0.0634)
Heart Rate	280.2	279.6	285.4	276.3	8.73	None
Mean Arterial Pressure mmHg	100.2	104.5	99	107.5	5.64	None
Systolic BP mmHg	128.5	148	131	139.5	6.71	None
Diastolic BP mmHg	85.8	85.1	83.4	91.7	5.29	None
+ dp/dt_{max} mmHg/s	4722.1	3296.7	5503.2	5588.4	451.7	Drug (P=0.0031)
- dp/dt_{max} mmHg/s	4109.3	3639.7	5579.2	4954	397.1	Drug (P=0.0024)
LVSP mmHg	117.5	110.8	118.8	114.3	5.24	None
LVEDP mmHg	8.4	4.2	6.7	5.3	1.18	Genotype (P=0.0314)

Values are means. Means with different superscripts are significantly different ($p<0.05$).